UNIVERSIDAD DE NAVARRA

TESIS DOCTORAL

Facultad de Farmacia

Departamento de Farmacia y Tecnología Farmacéutica

Protein nanoparticles for oral delivery of bioactives.

Nanopartículas proteicas para la administración oral de bioactivos.

Trabajo presentado por Dña. Rebeca Peñalva Sobrón para obtener el Grado de Doctor

Fdo. Rebeca Peñalva Sobrón

Pamplona, 2014

El presente trabajo titulado **"Protein nanoparticles for oral delivery of bioactives"**, presentado por Dña. **Rebeca Peñalva Sobrón** para optar al grado de Doctor en Farmacia, ha sido realizado bajo nuestra dirección en el Departamento de Farmacia y Tecnología Farmacéutica de la Universidad de Navarra. Estimamos que puede ser presentado al tribunal que lo ha de juzgar.

Y para que así conste, firman la presente:

Fdo.: Dr. Juan M. Irache Garreta

Fdo.: Irene Esparza Catalán

Esta tesis doctoral se ha llevado a cabo gracias a la ayuda para la formación del personal investigador de la Asociación de Amigos de la Universidad de Navarra.

Las investigaciones realizadas en el presente trabajo se han desarrollado dentro del proyecto financiado por el Gobierno de Navarra (Euroinnova) y por la Dirección General del Ministerio de Ciencia e Innovación (ADICAP, ref IPT-2001-1717-9000 00)

A mis padres y mi hermano

A Pedro

"Caminante no hay camino, se hace camino al andar"

Antonio Machado
(Poeta español. 1875-1939)

"El futuro tiene muchos nombres:
Para los débiles es lo inalcanzable,
para los temerosos lo desconocido,
para los valientes es la oportunidad."

Victor Hugo.
(Poeta, dramaturgo y escritor romántico francés. 1802-1885)

Agradecimientos

¡Y ya han pasado 4 años desde que empecé esta "aventura"!. A lo largo de este tiempo he conocido a muchas personas de las que he aprendido y han hecho que esta etapa sea muy positiva no solo en el ámbito académico o profesional sino también en el personal. Por tanto no quiero cerrar esta etapa sin dar las gracias a todas esas personas.

En primer lugar, me gustaría agradecer a la Universidad de Navarra y al Departamento de Farmacia y Tecnología Farmacéutica por permitirme realizar esta tesis doctoral.

Muy especialmente, quisiera dar las gracias a mis directores, el Dr. Juan M. Irache y la Dra. Irene Esparza. He tenido la gran suerte de tener a los MEJORES. Gracias por dirigirme este trabajo, por vuestra paciencia y por la dedicación para poder sacar este trabajo adelante. Ha sido un privilegio aprender de vosotros y darme la oportunidad de realizar esta tesis doctoral.

A Juanma, por dar respuesta a todas mis dudas, por permitirme "el lujo" de iniciarme en este mundo, por su consejo desinteresado y por todo lo que me ha enseñado. Por su comprensión, su gran optimismo en los momentos difíciles y por haberme animado a enfrentarme a retos que hace unos años eran impensables para mí. ¡Mil gracias por todo Juanma!

A Irene, por su dedicación absoluta y ayuda incondicional su apoyo constante, confianza y comprensión. Por todos los buenos y malos momentos que hemos pasado. Las largas horas que hemos hablado por teléfono resolviendo dudas y corrigiendo capítulos han sido muy fructíferas. Eres una de las mejores personas que he conocido nunca. ¡Mil Gracias Irene!.

¡Si se me ha pegado una nano-parte de vosotros he triunfado!

A los investigadores, profesores y personal del Departamento de Farmacia y Tecnología Farmacéutica, Dña. Carmen Dios, Dña. Maribel Calvo, Dña. Conchita Tros, Dña. María del Mar Goñi, Dña. María Jesús Garrido, D. Iñaki Fdez. de Trocóniz y Dña María Blanco, muchas gracias por toda la ayuda cuando la he necesitado. A todo el personal de la planta piloto, a D. Fernando Martínez, Dña. María Huici y Dña. Noelia Ruiz, muchas gracias por todo. Especialmente, a D. Felix Recarte, con quien he aprendido el funcionamiento de muchos equipos y por toda su ayuda en el bricolaje con los HPLC y demás equipos. ¡Cuánto he aprendido de ti!

A la Dra. Socorro Espuelas, porque siempre que la he necesitado me ha ayudado y por esas preguntas que me hacen plantear cosas que nunca se me hubiesen ocurrido. Gracias por esa visión científica y por enseñarme tanto.

A la "Asociación de Amigos de la Universidad de Navarra", sin su ayuda económica, esta tesis no hubiese sido posible.

Son muchas las personas que a lo largo de estos años han hecho que mi estancia es este departamento haya sido muy especial. Siempre he encontrado una palabra de apoyo, una ayuda, una sonrisa y muchas bromas, por ello no quiero que pase esta etapa sin decir GRACIAS!

Me gustaría agradecer muy especialmente a todos los NANOGALENOS, habéis hecho que me sienta dentro de una familia. Espero haber sido capaz de demostraros que sois muy importantes para mí y que me llevo a grandes amigos. Ahora el grupo se está diversificando por el mundo, pero la amistad que nos ha unido no se separa fácilmente. Muchas gracias chic@s, sois l@s mejores!!!

A Patricia Calleja y Judit, sois dos grandes personas y amigas y sé, que siempre estaréis para lo que necesite. Ha sido un auténtico placer conoceros y poder contar con vosotras dentro y fuera del laboratorio. Mil gracias chicas!! Os echaré mucho de menos.

A Luisa y Maite, porque derrocháis alegría y entusiasmo. He aprendido mucho de vosotras y de vuestra positividad y siempre me habéis sacado una sonrisa. Muchas gracias!

A Eneko, por ser auténtico, por enseñarme tanto, por tu paciencia y por dar ese "buen rollo en el grupo". Te mereces lo mejor porque eres una gran persona y un gran científico!

A Nekane y Esther, "pin y pon", sois auténticas, perfeccionistas, trabajadoras y sobre todo buenas personas. Gracias chicas porque he aprendido mucho de vosotras y me habéis hecho sentir genial. Ahora nos separamos pero me llevo a dos grandes amigas.

A Laura, Ana, Inés y Juana, porque habéis hecho que nuestro grupo perdure. Me encantan vuestras bromas científicas, entusiasmo y alegría. Mil gracias por tener siempre una palabra de apoyo. Mucho ánimo en esta última etapa para las cuatro!

A Esti, Raquel, Amy y Jorge, mis alumnos internos. Ha sido un placer aprender tantas cosas juntos, gracias por vuestra paciencia, dedicación y trabajo. Os deseo lo mejor en las próximas etapas y espero noticias de cada uno. Gracias gente!!

A Paulo, que aunque los comienzos fueron duros, al final nos entendimos e hicimos un gran equipo Resveratrol. Espero poder ir a Brasil algún día…

A Juanchin, por tu dedicación, paciencia y preocupación por mí. Los tres meses que compartimos laboratorio aprendí muchísimo de ti. Eres una gras persona y te mereces lo mejor. Me debes una visita a Logroño, con sol!

A todos aquellos que en otros momentos habéis compartido laboratorio Patricia Ojer, Raquel Martins, Lina, Elcio, Amaurí,… Muchas gracias por tener una palabra de apoyo!

A Sara Zalba y Edurne, porque siempre os echaré de menos. Me habéis hecho sentir siempre muy especial y a veces, con una sola mirada nos hemos entendido. Muchas gracias por ser tan buenas personas.

En general, a todas las personas del departamento, Hugo, Elisa, Ander, Zinnia, Cristina Tamames, Yolanda, Simón, Nuria, Ana Margarita, Paula, Melissa y todos aquellos con los que he compartido poyata. Muchas gracias.

Una mención especial al departamento de Microbiología de la Universidad de Navarra, en especial al Dr. Carlos Gamazo por haberme admitido en su equipo y dejarme aprender un

poquito sobre el gran mundo de la alergia, inmunología e inflamación. Muchas gracias por toda la ayuda prestada, por la cercanía y gran paciencia. Ha sido un auténtico placer.

Por supuesto, no puedo me puedo olvidar de Ana Camacho, un crack de la microbiología y la política, pero sobre todo una gran persona y amiga. Las largas horas en el animalario, tu paciencia conmigo con los ELISAS y la citoquinas. Gracias Ana!!!.

Marijo!! Aunque nos abandonaste por el departamento molón de Micro, en el fondo sigues teniendo una parte galena. Muchas gracias por todos tus consejos, por tu ayuda desinteresada, por ser incansable y por todo el apoyo que me has dado siempre dentro y fuera de la Universidad. Sé que me llevo a una gran persona y amiga. Gracias guapa!!

No me puedo olvidar de mis compañer@s de coche. Han sido tantos a lo largo de estos años…! Especialmente a Javi, que es con quien empecé pero no me olvido del resto: Laura, Álvaro, Miriam, Ana, María L., Esther, Tamara, María M.… ¡Siempre han sido viajes divertidos y ahorradores! Gracias a todos!!!

A todas mis amigas. Muy especialmente a Maite, Sara y Ceci, por la cercanía y por interesarse siempre por mí y por lo que hago. A mis amigas de Baños, que aunque no entiendan lo que hago, siempre se han interesado y alegrado por todo. Muchas gracias chicas!

Y esta tesis no hubiese sido igual si el apoyo incondicional de mi familia. Porque habéis creído en mí, porque me habéis aguantado en esos días difíciles, por hacerme sentir especial siempre y por estar siempre ahí!. A mis padres Pedro y Petry os lo debo todo, me habéis enseñado que el esfuerzo merece la pena y que hay que luchar por lo que cada uno quiere, al final se consigue. A mi hermano Pedro, porque aunque ahora estés lejos, desde la distancia siempre me apoyas y me enseñas a relativizar las cosas. Muchas gracias guapo y ya tengo ganas de ir a visitarte!.

Y a ti Pedro, creo que no hay palabras para agradecerte todo lo que haces por mí. Gracias por todos estos años junto a mí, por enseñarme a ser positiva, a luchar por las cosas que quiero, por apoyarme en todas mis decisiones, por enseñarme a vivir el día a día y hacerme disfrutar de cada momento.

¡¡¡¡ MUCHAS GRACIAS A TODOS !!!!

Table of contents

Abreviations

AUC	Area under the curve
CD	Cyclodextrin
Cl	Clearance
Cmax	Peak concentration
CYP450	Cytocrome P450
CYP3A4	Cytocrome P450 isoform 3A4
Fr	Relative bioavailability
FDA	Food and Drug Administration
FA	Folic acid
FA-NP-C	Folic acid loaded casein nanoparticles
FA-NP-C-P_3	Folic acid loaded casein nanoparticles treated by high hydrodynamic pressure.
FA-NP-Z	Folic acid loaded zein nanoparticles
GI	Gastrointestinal tract
HPLC	High performance liquid chromatography
HP-β-CD	2-hydroxyypropyl-β-cyclodextrin
i.v.	Intravenous administration
LPS	Lipopolysaccharide from*Salmonella enterica*serovar
Lys	Lysine
MRT	Mean residence time
NP	Nanoparticle
NP-C	Casein nanoparticles
NP-Z	Zein nanoparticles
PBS	Phosphate buffered saline
PDI	Polydispersity index
PEG-400	Poly(ethylene glycol) 400
Que	Quercetin

Que-HPCD-NP-C	Quercetin loaded casein nanoparticles containing 2-hydroxypropyl-β-cyclodextrin
Que-NP-C	Quercetin loaded casein nanoparticles
Que-HPCD-NP-Z	Quercetin loaded zein nanoparticles containing 2-hydroxypropyl-β-cyclodextrin
Que-NP-Z	Quercetin loaded zein nanoparticles
Rsv	Resveratrol
Rsv-NP-C	Resveratrol loaded casein nanoparticles
Rsv-NP-M	Resveratrol loaded zein-casein nanoparticles
Rsv-NP-Z	Resveratrol loaded zein nanoparticles
T ½	Half-life in the terminal phase
T max	Time to reach the peak concentration
TNF-α	Tumor necrosis factor
V	Volume of distribution

Chapter 1

Introduction

1. Nanotechnology

The term "nanotechnology" refers to a science that encompasses the study, design, creation, synthesis, manipulation and application of materials, devices and systems at the nanometer scale (between 1 and 1000 nm) [1].

The conceptual origins of nanotechnology dating from 1959 at the American Physical Society, when physicist Richard Feynman (Nobel Prize winner in Physics) described molecular machines built with atomic precision in his lecture "There's plenty of room at the bottom" [2]. However, it was Professor Noro Taniguchi who first used the term nanotechnology in 1974 [3,4].

In parallel, the 1950s and 60s were characterized by significant progress in pharmaceutics mainly in the field of controlled release. One of the pioneers in this area was Professor Paul Speiser (at the ETH (Swiss Federal Institute of Technology) in Zürich), whose strategy for the retarded and controlled release was the development of miniaturized delivery systems [3].

The first review article about nanoparticles was published in 1978 [5]. Soon after, Oppenheim [6] and, more comprehensively, Kreuter presented a definition of nanoparticles for pharmaceutical purposes that later was adopted by the Encyclopaedia of Pharmaceutical Technology and the Encyclopaedia of Nanotechnology [7].

Thus, nanoparticles for pharmaceutical purposes are defined by the Encyclopedia of Pharmaceutical Technology as solid colloidal particles ranging in size from 1 to 1000 nm (1 µm). They consist of macromolecular materials and can be used therapeutically as drug carriers, in which the active principle (drug or biologically active material) is dissolved, entrapped, or encapsulated, or to which the active principle is adsorbed or attached [3]

The spectacular growth of the nanotechnologies in recent years, together with the development of techniques such as TEM (transmission electron microscope), AFM (atomic force microscope), SEM (scanning electron microscopy), DLS (dynamic light scattering), etc., has led to a growing optimism about its application in medicine, pharmacy, cosmetics, nutraceuticals and food since these nano-devices have unique qualities not found in their counterparts on a macroscopic scale [8] and offer new opportunities for more effective diagnosis and treatment.

Till now different types of nanodevices and strategies based on nanotechnologies suitable for drug delivery have been proposed. In general, these devices may offer the following advantages:

- **Increase of the stability**: Encapsulation involves isolating active molecules, avoiding their interaction with the rest of the components of the matrix in order to diminish their degradation, deactivation or even lower absorption. Moreover, nanoencapsulation enables the protection of the active from its interaction with external agents such as light, oxygen, pH variation, heat…etc. and all that allows the increase of the product's half-life.
- **Retention of volatile molecules**: The cover material allows the retention of highly volatile molecules during long lasting periods, reducing the loss of scents.
- **Flavor masking**: The undesirable flavors and odors can be masked preventing their interaction with the oral mucosa.
- **Controlled release**: Nanosystems are supposed to release their content in the presence of certain stimuli (solvent, pH, temperature, osmotic pressure…etc.). Thus, the encapsulated active can be released in the desired location and target.

- **Modification of the physical characteristics**: Through encapsulation it is possible to transform a liquid in solid, what facilitates its manipulation. Moreover, the encapsulated additive can be uniformly dispersed in matrixes where it is not soluble or dispersible in its free form.
- **Reduce the required amount of active**: By encapsulating, and therefore, protecting the additive, it can be possible to reduce its required amount to obtain the desired benefit.
- **Increase of the bioavailability**: Thanks to its physico-chemical properties, the nanoparticles ensure the stability of the encapsulated active molecular drug until its arrival to the gastrointestinal tract where it is released achieving significant increases in the bioavailability. Additionally, the increase of the bioavailability can be due to an enhancement of drug absortion by facilitating diffusion through epithelium, modification of pharmacokinetic and drug tissue distribution profile and/or improving intracellular drug penetration and distribution [9].
- **Consecutive release of multiple functional additives**: When two or more active molecules react with each other, they can be encapsulated and released alone, together or consecutively.

Among others, the most popular nanodevices existing nowadays are drug nanocrystals, polymer therapeutics (polymer-drug conjugates, polymer-protein conjutages polymer micelles, polyplexes and dendrimers), lipid-based nanocarriers (liposomes, nanoemulsions, lipid nanocapsules and solid lipid nanoparticles) and polymer-based nanoparticulate delivery systems [2]. In the next section we review the most relevant aspects of polymeric nanoparticles, mainly those prepared from natural polymers.

Depending on their morphology and on the method of preparation used, it is possible to distinguish between two types of nanoparticles:

- Nanospheres are dense polymeric matrix systems where the active substance is uniformly dispersed. The active substance may also be absorbed in the surface of the nanoparticle.
- Nanocapsules are vesicular systems in which the active is confined in a cavity surrounded by a unique polymeric layer, this is, a nucleus surrounded by a fine layer of constitutive polymeric material.

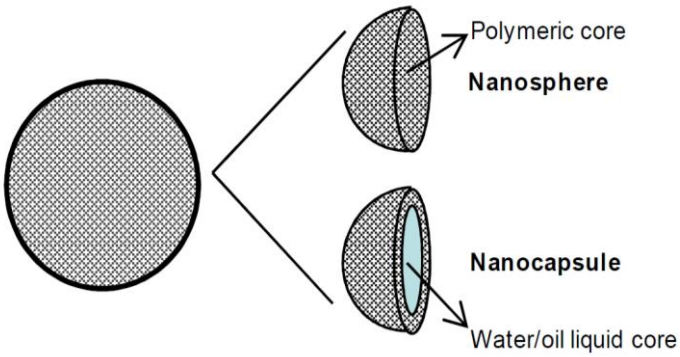

Figure 1: Schematic representation of the structure of nanospheres and nanocapsules. Adapted from reference [2].

2. Polymers for the preparation of nanoparticles

Polymeric nanoparticles can be prepared from a range of different polymers, including both synthetic and natural polymers, that must be as least biocompatible, non-toxic, free of leachable impurities and readily processable [10]. Ideally, such polymers should also be biodegradable [11].

Natural polymers offer relatively short duration of drug release and often require crosslinking agents that could denature the embebed drug [12], while synthetic polymers (i.e. poly(esters), poly(Ɛ-caprolactone), poly (alkyl cyanoacrylates), polylactides, polyglycolides, poly (lactide co-glycolides), poly(anhydrides), etc) allow obtaining sustained release of the active agent over a period of days to several weeks. However, the use of these polymers is usually limited by the need of organic solvents and harsh formulation conditions [13,14].

Consequently, synthetic polymers have received significantly more attention in this area, while natural polymers are less investigated for that purposes, being chitosan and albumin the most popular ones [2].For that reason, it is important to increase the knowledge of natural polymers in order to look for new alternatives to obtain nanoparticles that allow obtaining biodegradable nanoparticulate delivery systems by simple methods and without the use of crosslinker agents.

Since the present work has been focused on the use of natural polymers for nanoparticle design, the main types of natural polymers and its characteristics have been explained in more detail.

2.1. Carbohydrates

Most of the carbohydrates are natural and are composed by simple or modified oligomers (oligosaccharides), or polymers (polysaccharides) of sugars. They present different molecular structures, sizes and shapes and exhibit a huge variety of chemical and physical properties. Carbohydrates include more than the 90% of the dried material of the plants, and thus, they are in general available and cheap.

The most interesting polysaccharides for its use in encapsulation of therapeutic molecules can be classified according to their structural characteristics in lineal polysaccharides and ramified polysaccharides. The most relevant examples of them are described below:

2.1.1. Starch

Due to its low cost, relatively easy manipulation and versatility of applications, starch seems to be a good matrix for encapsulation and control the release of a wide variety of bioactive substances. For a chemical point it is constituted of two types of polysaccharides: amylose (20-30%) and amylopectin (70-80%). The first one presents a lineal structure consistent in residuals of D-glucopiranose linked by α-(1-4) links. These links are pancreatic α-amylase resistant, but are degraded by the colon microflora [15]. Meanwhile, amylopectin is a ramified glycan of D-glucopiranose scraps joined to the mean chain by α-(1-6) links.

Starch can be chemically modified by esterification, eterification, oxidation, hydrolysis, acidification etc. with the purpose of modifying its physico-chemical properties and applications. There are a hight number of starch derivatives including acetyl, hydroxyalkyl or carboxylates [16]. To develop insoluble starch particles and improve its applications in the field of controlled release, the trisodium trimetafosfate has been considered as a good cross-linking agent, non-toxic and applicable for oral administration [17].

2.1.2. Maltodextrins

Maltodextrins are obtained from modified maize by partial hydrolysis with acids or enzymes. These substances have the advantage of being cheap, relatively insipid and appropriate to the protection of tastes and scents from oxidation [18]. They present low hygroscopicity, good solubility, low viscosity at high concentrations and low sweetening powder.
Maltrodextrins are generally classified by their equivalent in dextrose (DE), which is inversely related with the starch polymerization grade (PG) (DE=100/GP). Thus, by reducing the DE, the stability of the polymers increases, because they have a larger chain. According to some authors [19], when this value is lower, the stability of the nanoencapsulated materials during the storage is higher.
However, their use in encapsulation has some drawbacks, due to their lack of emulsifying properties, and also because of their low retention capacity of volatile compounds [20]. For that reason, many authors have used maltodextrins with emulsifiers (for example, polysorbate 80 [21] or with other covering agents [22], such as starch, whey proteins [23]or Arabic gum [24].

2.1.3. Cyclodextrins

Cyclodextrins (CDs) are crystalline cyclic oligosaccharides containing six, seven or eight (α-1.4) linked α-D-glucopyranose units with amphiphilic properties and shape of a truncated cone or "bucket". CDs are named depending on the number of glucopyranose units. Major and industrially produced CDs are named as follows: α-CD possessing six units, β-CD possessing seven units and ϒ-CD possessing eight units. The β-CD family is the most commonly used CD. Regarding its structure, the external surface is hydrophilic, whereas the internal cavity is lipophilic. This central space is formed by the skeletal carbons, hydrogen atoms and glycosidic oxygen atoms of the glucose structure conferring the lipophilic characteristics. The external surface is hydrophilic due to the presence of secondary hydroxyl groups at the wide edge of the structure and primary hydroxyl groups at the narrow edge [25]. However, due to its low water solubility, CDs could present nephrotoxic effects. In order to avoid this phenomenon, substitution of the hydrogen bonds of the natural CDs by hydroxyl, methoxy or alkyl groups have been performed, increasing the solubility of CDs and reducing their toxic effects [25].

CDs can be considered as empty capsules of a certain molecular size that can include a great variety of molecules in their cavity. In this case, a complex called "inclusion complex" is formed, so CDs are considered as host molecules [26].

For these reasons, CDs, have been used for applications in the field of pharmacy, nutraceutics and food and as with a variety of objectives: (i) to protect lipophilic active molecules that are sensitive to oxygen, light or heat inducing degradation. ; (ii) to solubilize food colorings and vitamins; (iii) to stabilize volatile molecules or labile lipidic molecules against undesired changes; (iv) to suppress unpleasant odors or tastes.

2.1.4. Celluloses

Cellulose is a linear homopolymer formed by repeated units of *D*-glucopiranose molecules linked by β-1,4-glucoside bonds. It is the most abundant polymer and also the most versatile. Cellulose esters allow developing effective solutions for pH controlled release. Cellulose microparticles expose the active to a progressive release, depending on its diffusion through the polymeric matrix. However, nowadays, its use in the nanotechnology field is not developed yet.

2.1.5. Alginates

Alginates are linear polymers constituted by two monomeric units, β-*D*-manuronic acid (M) and L-glucuronic acid (G). They are produced by bacteria and some brown algae. The great variety of applications of these products is based on its hydrocolloid capacity and also in its reactivity with calcium; both consequences of their molecular geometry. In fact, alginate can easily be gelled with multivalent cations under gentle conditions allowing formation of gelled beads. Gelation is obtained by the stacking of guluronic acid (G) blocks with the formation of "egg-box" calcium linked junctions [27].

Due to its special properties, alginate is one of the most used polymers in microparticle formation. However, alginate is currently less commonly used in the formation of alginate nanoparticles [28].

These alginate nanoparticles can be prepared from an alginate solution by adding calcium chloride in first place and then poly-L-lysine as crosslinker agent. Since poly-L-lysine is toxic and immunogenic when injected into the human body, chitosan and Eudragit E100 have been used as alternative cationic polymers [29]. Additionally, alginate nanocapsules can be obtained by complex formation on the interface of emulsion droplets with subsequent solvent removal.

This polymer has been used for encapsulation of cells [30], proteins [31], DNA [32], venoms [33], and anti-cancer drugs, such as methotrexate [34] and 5-fluoracil [35], among others. Recently, alginate was developed as nanoparticle for the oral delivery of insulin [36].

2.1.6. Carragenates

Carragenates or carragenines are gelificant anionic hydrocolloids extracted from the cellular walls of marine red algae (Rhodophycae). They are formed by altered copolymers of β-D-galactose and 3,6-anhydro-α-D-galactose linked by α-(1,3) and β-(1,4) bonds respectively.

Commercially, there are three types of available carragenates: k-carragenate, i-carragenate and λ-carragenate. The difference between them is in the position of the ester sulfate groups, which determines their physico-chemical characteristics such as solubility, viscosity and gelificant properties. This last parameter is the most important when considering carragenate as an encapsulant agent. Only the k-carragenate and i-carragenate have this property which is directly dependent on changes in temperature or in the presence of certain cations such as potassium. Both mechanisms are used to develop nanoparticles, being k-carragenate the most interesting for this purpose. Moreover due to its negative charge these compounds are able to interact with some proteins such as k-casein [37].

2.1.7. Pectins

The term pectins include a family of the polysaccharides extracted from the cellular wall of plants. Their structures are lineal and they are constituted by units of *D*-galacturonic acid linked by α-(1,4) links. These units can be presented in their acid form, esterified with methanol, amidades or in salt forms. The relation between the free acid groups and the esterified residues define the esterification grade (EG). Depending on this EG factor, pectins are classified as compounds of high (EG<50%) or low (EG>50%) methoxyl grade. The first ones gel in acid systems while the second ones develop gels in the presence of divalent cations such as calcium through the formation of structures called “egg box” [38].
As in the case of alginates, the application of this polysaccharide without modifications is limited due to its high solubility in water [16]. Thus, in the majority of the cases it has to be combined with a cation or with another polymer such as chitosan in order to form complexes destined to the release of bioactive substances [39].

2.1.8. Chitosan

Chitosan is formed by β-(1,4)D-glucosamine chains (deacetylated units) and *N*-acetyl-D-glucosamine chains (acetylated units). It is a polysaccharide naturally found in cellular walls of some fungi; however, its main source of production is by the chitin hydrolysis in alkaline media. It is not present in mammals, although the organism can degrade it. It is biocompatible, and does not generate any kind of irritation or sensitization [40].
During the last ten years, numerous trials have been published based on the use of chitosan as a delivery and controlled release system for drugs/actives, because its behavior as a cationic polymer and also its ability to form films and gels. These characteristics permit to control the release of the drug/active and enlarge the therapeutic effect. Also, thanks to its mucoadhesive properties, chitosan has been proposed as an improver of the drug/active bioavailability (because of the increased time in the place of action or absorption) [41,42].

2.1.9. Inulin

This polysaccharide is present in the majority of the vegetables, and it is formed by D-fructose molecules linked by β-(1,2) bonds. Inulin has been proposed for the encapsulation and specific release of bioactive substances in the colon because it can bear the harsh conditions of the high gastrointestinal tract, whereas it is hydrolyzed by the intestinal bifidobacteria [43]. Moreover, it is cheap, has many health benefits and can be used with the majority of the encapsulation techniques [16].

2.1.10. Arabic or acacia gum

Arabic gum is a proteic-arabinogalactane complex with amphyphilic and emulsifying properties. Thus, it is considered the best gum to stabilize O/W emulsions because it can be absorbed in the oil-water interphase resulting in stable microemulsions. Due to these properties, arabic gum is considered one of the most interesting materials to encapsulate oily molecules. Moreover, when it is used as a covering agent of these substances through drying by aspersion, it forms a film that covers the actives protecting them against oxidation and evaporation. Additionally, it is considered a suitable polymer for particle preparation by complex coacervation. However, the particulate systems obtained with this polymer are in the range of microparticles and its high price limits its use at industrial scale [44].

2.1.11. Pullulan and Dextran

Pullulan and dextran are homopolymers produced by bacteria. Pululan is a linear macromolecule formed by glucosidic α-(1-6)D-glucopiranose and α-(1,4)D-glucopiranose links [45]. It is biodegradable, has an excellent oxygen permeability and it is non-toxic. The resulting nanoparticles are very useful to achieve controlled release systems for some actives [46].
Dextran is one of the most investigated polysaccharides for hydrogels manufacturing intended for the controlled release of proteins and peptides [46].

2.1.12. Hyaluronic acid

Hyaluronic acid is a glucosemoniglicane with a high molecular weight present in all the mammals. It is a component of the extracellular matrix, and it is constituted by iterations of the disaccharide N-acetyl glucosamine and glucuronic acid [47]. The use of hyaluronic acid for clinic applications is limited because its high water solubility and quick degradation in the body. For those reasons, some derivatives with improved stability have been developed, such as esther [48], carbodiimide [49] and sulfate derivatives, which are chemically and structurally similar to heparin [50].

2.1.13. Others

Other compounds that can be used to prepare nanoparticles are guar gum, gelano gum, xantana gum…etc.

2.2. Lipids

Lipids can be considered as biomolecules soluble in apolar organic solvents. The term lipids include a huge range of structural substances that can be used for the encapsulation of different bioactive compounds, such as lipids, oils, waxes, phospholipids…etc.

2.2.1. Fats and oils

These compounds are esters of fatty acids with glycerol, (mono, di or triacilglycerides) which are present naturally in plants and animals. Mono and diacilglycerols have an appreciable polarity due to their free hydroxyl groups, and for that reason they have emulsifying properties. Some examples are cocoa butter, coconut oil, maize oil, soya oil...etc.

2.2.2. Waxes

Waxes are esters with a large fatty acid chain and a linear mono-alcohol chain. They are solid at room temperature, and, due to their insolubility in water, they offer waterproofing characteristics. The most interesting ones are bee wax, which melts at 62-64°C, carnauba wax whose melting point is between 78-85°C, and the candelilla wax that can melt between 67-79°C.

2.2.3. Phospholipids

Phospholipids are amphipathic molecules with a hydrophilic region (polar head), composed by phosphoric acid and a molecule of choline (in the case of phosphatidilcholines) or ethanolamine and a hydrophobic region by a glycerol molecule (an apolar tail that it is formed by two long chains of fatty acids).
In water this particular structure adopts a vesicle form with an aqueous core surrounded by a bilayer of phospholipids, (Figure 2). Thus, the inland of these dispositives is aqueous, and on the contrary, the content of the micelles is a hydrophobic environment. This particular structure, also called liposomes [51], made them versatile for the encapsulation and simultaneous release of substances not only hydrosoluble but also liposoluble and amphiphilic [52].
The most abundant phospholipids are phosphatidilcholines, also known as lecithins that can be obtained from different natural sources such as eggs, milk or soya [53].

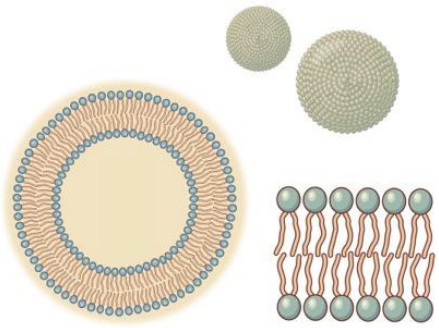

Figure 2: Lipid structure

2.3. Proteins

Proteins are biological polymers comprised of amino-acids that come in a variety of different general structures e.g. fibrous, globular or random coil. The molecular structure adopted by a particular protein depends on its aminoacid sequence, prevailing environmental conditions and environmental history.

Their application in controlled release is a good option since their own nutritional characteristics add value to the final formulation. Moreover, they are very accessible materials, cheap and found naturally in animal and vegetal matrixes, and are degraded by the digestive enzymes [54].

In addition, proteins have excellent functional properties as emulsifier and gelling agent and posses foaming and water binding capacity. Moreover, protein nanoparticles can be easily prepared and scaled up during manufacture [11].

This kind of nanoparticles has been successfully synthesized from various proteins including water-soluble proteins (e.g., bovine and human serum albumin) and insoluble proteins (e.g., zein and gliadin) [55].

It is important to consider three factors when selecting a suitable protein to design biopolymer-based delivery-systems. Firstly, establishing the conditions where the protein molecules are able to associate with other protein or no-protein structure. This requires knowledge about denaturation temperatures or isoelectric points. Secondly, establishing the electrical characteristics of the protein. The electrical charge of proteins goes from positive, below their isoelectric point (pI), zero at the pI, to negative above the pI. This would result in attractive and/or repulsive electrostatic interactions. And finally, the nature of the biopolymer particles that can be formed after protein association, such as their morphology, size, charge and stability should be taken into account. [56,57]. Proteins can be classified according to their origin as animal proteins and vegetal proteins.

2.3.1. Animal proteins

Animal proteins represent good materials since they have the advantages of absorbability and low toxicity of the degradation end products.

2.3.1.1. Gelatin

Gelatin is a denatured protein obtained from animal collagen (skin, tendons, ligaments, bones…) by acid or alkaline hydrolysis. Gelatin is widely used in pharmaceutical, cosmetic and food products and vaccines. It is considered as GRAS (Generally recognised and safe) material by the FDA. In addition, it is cheap and readily available. It has attracted great interest for its biocompatibility and biodegradability. Moreover, gelatin has relatively low antigenicity [58]. However, due to its water solubility its use in controlled release is limited. In order to solve this problem, it is necessary to use a non-toxic crosslinking agent for gelatin nanoparticles like genipin, carbodiimide or N-hydroxysuccinimide and avoiding the use of glutaraldehyde or formaldehyde whose high toxicity may limit the application of the final product. The chemical structure of gelatin is a polyampholyte having both cationic and anionic groups along with hydrophobic groups. Gelatin molecule possesses glycine, proline and alanine aminoacids triplets that are responsible for its triple helical structure [59]. Their intrinsic protein structure with a high number of different accessible functional groups bears multiple modification opportunities for coupling with gelling anionic polysaccharides such as alginate, pectin or arabic gum [58].

Gelatin nanoparticles have been reported to be successful at delivering various drugs including anti-cancer [60], anti-microbial [61], anti-inflammatory [62] and anti-diabetic [63]. In addition, natural polyphenols like epigallocatechin gallate (EGCG), tannic acid, curcumin, and theaflavin have been successfully loaded in gelatin nanoparticles [64]. Various methods including desolvation [65] coacervation [60] and nanoprecipitation [66] have been used to prepare gelatin nanoparticles.

2.3.1.2. Albumin

Albumin is a globular protein that can be obtained from a variety of sources, including white egg (ovalbumin) [67], bovine serum albumin (BSA) and human serum albumin (HSA). Albumin is a major soluble protein of the circulating system and is involved in the maintenance of osmotic pressure, binding and transport of nutrients to the cells. Many drugs and endogenous molecules are known to bind to albumin. Albumin serves as a depot and transporter protein. This protein is freely soluble in water and salt solution. The high solubility of albumin (up to 40% w/v) at pH 7.4 makes it an attractive macromolecular carrier capable of accommodating a wide variety of drugs. It is stable in the pH range of 4 to 9 and can be heated at 60°C up to 10 hours without any deleterious effects. Albumin is widely used in the preparation of nanospheres and nanocapsules. These albumin nanocarriers are biodegradable, easy to prepare, and have well-defined sizes and reactive functional groups (thiol, amino, and carboxyl) on their surface that can be used for ligand binding and other surface modifications [68]. Albumin nanoparticles have gained considerable attention as drug delivery systems because they offer several advantages: i) albumin nanoparticles exhibit high binding capacity of various drugs. Due to the high content of charged aminoacids, albumin based nanoparticles could allow the electrostatic adsorption of positively or negatively molecules. ii) HSA nanoparticles are a strategy for targeted delivery of anti-cancer drugs to tumor cells. In this context Abraxane® (paclitaxel loaded albumin nanoparticles) has been successfully designed and commercialized [69]. iii) HSA nanoparticles can cross the BBB, thus enable the delivery of a various drugs into the brain. vi) They are suitable systems for gene therapy, because HSA might avoid interactions with serum and protect the oligonucleotides from nuclease digestion.

However, because of its easy degradation, the use of a crosslinking agent is usually necessary, being glutaraldehide or methyl-polyethyleneglycol modified oxidized dextrane (Dextran-MPEG) the most frequently used. Drug release from albumin nanoparticles can be achieved naturally by protease digestion [68].

2.3.1.3. Elastin

Elastin protein is one of the major constituents of the extracellular matrix. It is an essential component in connective tissues since it is elastic and allows them to resume their shape after stretching or contracting. Elastin is formed through lysine-mediated crosslinking of its soluble precursor tropoelastin [70]. In addition to provide elasticity to tissues, it plays an active role in modulating cell behaviour and promoting tissue repair. The specific aminoacid sequence of the elastin provides a structure that allows the protein to undergo large deformations without breaking. Once the stress is removed, the protein returns to its original conformation. The most interesting feature of the elastin proteins is their Inverse Temperature Transition (ITT) behaviour. Below a certain critical temperature, the polymer remains soluble in water with the

chains relatively extended in a disordered state. At temperatures above the transition temperature (Tt), recombinant thermo-sensitive elastin proteins undergo a reversible phase transition where they hydrophobically self-assemble into an insoluble aggregate, forming nano and microparticles which could be applied in controlled release devices [71]. In this order, Herrero-Vanrell *et al.* prepared a self assembled nanoparticles of poly-elastine which showed a sustained release of dexamethasone phosphate for about 30 days. Once these particles are formed, they were stable either at room or body temperature [72].

In another study, Bessa and collaborators prepared elastin nanoparticles for the delivery of two growth factors (BMP-2 and BMP-14). In addition, they showed activity after their encapsulation [73].

2.3.1.4. Milk proteins

Milk proteins are natural vehicles for actives and due to their structural and physico-chemical properties they can be used as delivery systems. They show excellent gelling properties, phenomenon that has been recently explored with the aim of encapsulation, being the results of these studies very promising. Besides, milk proteins are very attractive as carriers because of their biocompatibility. Two milk proteins that have been investigated for drug delivery applications are casein and β-lactoglobulin (BLG).

2.3.1.5. Casein

Casein is a phosphoprotein that constitutes approximately 80% of total milk protein; is inexpensive, readily available, water soluble, non-toxic and highly thermostable [74]. It is constituted of four different basic fractions: αs1-, αs2-, β- and κ-casein. Their molecular weights are between 18 and 25 kDa and their average isoelectric point is between 4.6 and 4.8. Caseins are proline rich, open structure rheomorphic proteins as they assume any of several energetically favorable conformations in solution. These amphiphilic proteins can self-assemble into stable micellar structures in aqueous solution. Casein micelles are composed of the four previously mentioned phosphoproteins held together by hydrophobic interactions and by the binding of calcium phosphate nanoclusters that are bound to phosphorylated serine residues of the casein side chains. In the micelle structure, αs1-, αs2- and β- are binding to the calcium phosphate and form the core of the micelle. The surface is covered with κ-casein providing a hydrophilic, charged surface layer, which stabilizes the micelles through intermicellar electrostatic and steric repulsion [75,76].

In milk, casein micelles are large colloidal particles forming 50 to 600 nm in diameter (on average 150 nm). These particles can be regarded as a natural nanovehicle that delivers calcium and aminoacids from mothers to offspring [77]. These micelles form a very stable colloidal system in the milk, being a major cause of the color, heat stability and coagulation [78].

Many of the structural and physic-chemical properties of casein facilitate their functionality in drug delivery systems. These properties include binding of ions and small molecules, surface-active and stabilizing properties, emulsification and self-assembly properties with super gelation and water binding capacities and interaction with other molecules to form complexes and conjugates. In addition, casein has various shielding capabilities, essential to protect sensitive payload, enabling to control the bioaccessibility of the bioactive and promote its bioavailability.

For example, due to its UV absorbance properties, casein could serve as a shield against radiation and UV light. Given its unique physic-chemical properties, this natural polymeric surfactant is a good candidate for the preparation of conventional and novel drug and nutraceutical delivery systems. However, the limitations of casein may include its possible immunogenicity and allergenicity [75].

In bibliography, numerous authors have described forms in which casein can compact and form different structures such as: (i) casein films, in which flavors can be film-coating for tablets [79] (ii) casein-based hydrogels for the controlled release of bioactives like vitamin B12. In this case, for the gel formation crosslinkers like genipin or transglutaminase were necessary [76,80]. (iii) Casein floating beads were developed to increase the residence time of drugs in the stomach based on its emulsifying and bubble-forming properties. These systems were designed to load drugs to release and absorbed in the stomach. (iv) Casein nanoparticles, were prepared via enzymatic crosslinking, heat gelation, coacervation and polyelectrolyte ionic complexation [75,76]. Numerous drugs have been encapsulated and delivered in casein nanoparticles. In this context, flutamin, a lipophilic drug was loaded in casein nanoparticles, they were fabricated via oil-in-water emulsification and then stabilized by ionic crosslinking with polianionic sodium tripolyphosphate. The resulting nanoparticles displayed sizes around 100 nm with positive zeta potential and a sustained release of the drug during the time. Moreover, after its intravenous administration, they exhibited longer circulation time [81].

Semo et al., have demonstrated the possibility to encapsulate Vitamin D2 (fat soluble vitamin) in casein nanoparticles using the natural self-assembly tendency of bovine caseins. This re-assembled technique could provide a partial protection against UV-light induced degradation to vitamin D2 cotained in them [75].

Moreover, this protein, caseinate in form, has also been used for the nano-encapsulation of functional ingredients such as folic acid [82], fat-soluble omega-3 [83], and curcumin [84].

Casein nanoparticles have also been prepared in combination with other carbohydrates such as carragenats, pectins, gum arabic or chitosan for drug delivery purposes [77].

2.3.1.6. Whey proteins

They are mainly composed of α-lactalbumin and β-lactoglobulin. β-lactoglobulin is an 18.3 kDa protein containing two disulphide bonds and one free thiol group. The ability to preserve its native stable conformation at acidic pH makes it resistant to peptic and chymotryptic digestion. Unlike casein, it is denatured at temperatures above 70°C, becoming insoluble and resulting in the formation of thermally irreversible gels [85]. So they can be used for thermolabile molecules [54]. In addition, β-lactoglobulin has good gelling properties, which are useful in some drug delivery applications. Due to its abundance and low cost, BLG is a promising natural polymer for drug delivery applications.

There are several methods to obtain nanoparticles from these proteins, but most of them require the use of organic solvents and/or chemical crosslinking agents such as glutaraldehyde [86]. However, new nanoparticles fabrication methods without these compounds have been studied.

In this context, Helene Giroux and coworkers produced stable nanoparticles from whey proteins by pH cycling-treatment and addition of calcium. Nanoparticles size ranged from 100 to 300 nm depending on the aggregation pH. These promising approaches can be used for the encapsulation of sensitive molecules [87].

For example, Sneharani *et al*. encapsulated curcumin in β-lactoglobulin. The nanoparticles were able to encapsulate curcumin with an efficiency of 96%. They described that curcumin binds to the protein and forms a complex through hydrophobic interaction, protecting the drug from degradation [88].

In addition, İbrahim Gülseren and collaborators designed a method for the encapsulation of zinc in whey nanoparticles by desolvation method. The nanoparticles showed high encapsulation efficiencies, remaining stable after 30 days of storage at 22 °C [89].
However, new suitable encapsulation methods have been proposed using the single proteins [90] or combinations with other matrixes such as alginate [91], arabic gum [92] or pectin [93].

2.3.2. Vegetal proteins

Vegetal proteins can be classified according to their aqueous solubility by the old and simple classification proposed by Osborne in 1924 [94].

- Albumins: water soluble
- Globulins: soluble in saline aqueous solutions
    - Viciline
    - Legumin
- Prolamins: water insoluble but soluble in hydroalcoholic mixture (about 70% of ethanol)
    - Zein from maize
    - Barley hordein
    - Wheat gliadin
- Glutelins: water and alcohol insoluble, but soluble in highly alkaline or acid solutions.
    - Wheat gluten.

2.3.2.1. Globulins

Globulins are a family of globular proteins. They can be classified depending on their structure as: (i) legumin group, composed of proteins of 40 kDa. They aggregate in 11S structures without glycosylated forms. And (ii) the vicilin group derived from preproteins ranging from 50-75 kDa and with glycosylated forms. They aggregate in 7S structures. Both, legumins and vicilines are soluble in saline aqueous solutions.

2.3.2.2. Soy proteins

Soybean (Glycine max L.) is currently one of the most abundant sources of plant proteins [95]. Soybean contains approximately 40% protein and 20% oil on an average dry matter base. By removing oil at lower temperatures, soy protein isolate (SPI) is obtained, and is widely used in the food industry. SPI possesses a balanced composition of non-polar, polar and charged aminoacids, thus being able to incorporate drugs with various functional groups. Soybean seeds contain an important fraction (35-40%) of proteins mainly glycin and conglycin (50-90% of total proteins). The glycinin fraction (11S globulin) has a molecular weight of about 350 kDa, and the

conglycin fraction (7S globulin fraction) of about 70kDa [96]. Its solubility depends on the pH, heat and concentration of salts or other ingredients (surfactants, oil or carbohydrates). Thus, soy globulins show the lowest solubility between pH 4-5, and lower and higher pH significantly increases their solubility. In the same way, a solution of $CaCl_2$ (4mM) increases the solubility of soy proteins [97]. In an aqueous environment, SPI components exist as globular molecules consisting of a hydrophilic shell and a hydrophobic kernel. Upon the addition of a desolvation or crosslinking agents, SPI molecules continue to aggregate and form various structures such as microspheres, hydrogels and polymer beds, which show interesting physico-chemical and functional attributes in gel-forming, emulsifying and surfactant properties [96]. The use of SPI in nanoencapsulation has already been studied by various authors. It is generally used as an individual coating material, but it can also be mixed with polysaccharides. The combination of proteins with carbohydrates as carrier material favours better protection, oxidative stability and drying properties. Recently, soy proteins have been used for the encapsulation of curcumin [95] and α-tocopherol [98]. However it is necessary to add a crosslinker agent to stabilize the nanoparticles. For this purpose, glutaraldehide, [95] which is quite toxic and microbial transglutaminase [98] have been used.

2.3.2.3. Pea proteins

Pea bean proteins are composed of two families of proteins, globulins (80-90% w/w) and albumins (10-20% w/w). Globulins are made of three proteins, two major proteins, legumin (represents the 11S globulin fraction with a molar mass between 350-400 kDa) and vicilin (represents the 7S globulin fraction with a molar mass of about 150 kDa), with an average ratio of approximately 1:1, and a third convicilin (7S globulin fraction) in a small quantities [99].

Pea protein is a natural vegetable extract with several nutritional qualities, which include the absence of lipids, as well as appropriate physical and functional properties such as good solubility in water, high oil in water emulsifying power stability at high temperatures and good foaming capacity. However, for nanoencapsulation uses, these proteins are generally associated with polysaccharides. Thus, this association gives new functions to pea proteins without chemical or enzymatic modification, like solubility, foaming and surfactant properties [96]. These interactions can also create stable emulsions giving better particle size distribution and increasing the efficiency of the encapsulation process. In this order, several molecules have been loaded into pea microparticles like α-tocopherol, and ascorbic acid using the spray drying for the encapsulation process [100,101]. Moreover, complex coacervation has been studied to design drug delivery systems by the complexation of pea protein [102].

Ongoing studies are focused on the application of the pea protein delivery systems for the encapsulation of vitamin E and characterizing the physical and chemical stability of the active compound as well as its cell absorption in ex vivo studies [99].

2.3.2.4. Prolamins

Prolamins are a group of plant storage proteins having a high proline content and found in the seeds of cereal grains: wheat (gliadin), barley (hordein), corn (zein), sorghum (kafirin) and as minor protein, avenin in oats. They are characterized by a high glutamine and proline content and are generally soluble in strong alcoholic solutions.

2.3.2.5. Zein

Zein is the main storage of maize seeds (Zea mays L.) It has long been a subject of research for scientific interest as well as industrial applications (as material used in production of coating, fibers and printing ink) [103].

Zein belongs to the class of prolamins with a molecular weight of about 40 kDa. It has been classified into four classes: α-zein, that consists of 35% of proteins with two bands of 22 and 24 kDa, β-zein, a polymer of 17 kDa with high methionine, ϒ-zein that consists of two parts of 27 kDa and 18 kDa, and δ-zein, with a minor fraction of 10 kDa [104]. Zein is a hydrophobic protein, insoluble in water but soluble in the presence of hydroalcoholic solutions (ethanol content higher than 70%), high concentrations of urea, high concentrations of alkali (pH 11) or anionic detergents. Concerning its aminoacid composition, zein is rich in glutamic acid (21-26%), leucine (20%), proline (10%) and alanine (10%), but deficient in basic and acid amino acids [105]. Matsuhima *et all*. [106], described the molecular structure of zein as an amphiphilic structure, with an hydrophylic top and botton with hydrophobic outer surface. Due to its major hydrophobic internal core it serves as an excellent water barrier and is therefore used as coating material. Commercially, zein is available in two forms, yellow zein and white zein, being the white zein more pure and obtained from decolorization of the yellow one. Zein is widely utilized in the food and pharmaceutical industry. It can be transformed into films, fibers, gels, microspheres and nanoparticles. In addition, zein has mucoadhesive characteristics and can sustain the gastric environment and hence can be used for mucosal delivey of drugs and vaccines [103]. The isoelectrical point of zein is 6.2, so, zein colloidal systems prepared at this pH could undergo aggregation. Therefore stabilizers such as casein, lecithin, tween 20 or polyvinilpyrrolidone have been used to alter the pH of the preparation medium and develop more stable zein micro/nanoparticle dispersions.

Zein nanoparticles offer advantages over other materials in terms of biodegradability and safety. In addition, they provide a number of beneficial opportunities due to the enhanced permeability and retention effect in the tumour tissue and bypassing multidrug resistance [107]. Several methods have been used to prepare solid core zein based nanoparticles systems with different bioactives and purposes. Liquid-liquid dispersion, antisolvent approach, and phase separation coacervation are few of them [108].

There are a high number of studies carried out with zein nanocarriers in drug delivery (table 1 summarizes some of them).

Table 1: Summary of studies conducted with zein nanoparticles in drug delivery.

Approach	Bioactive	Purpose	Comments	Ref
Phase separation method	5-fluorouracil	Liver targeting	Size: 115 nm	[109]
Electrodinamic atomization	Curcumin	Better encapsulation	Size: 175-250 nm	[110]
Phase separation method	Metformin	Higher encapsulation	Size: 120 nm	[111]
pH controlled nanoprecipitation	6,7-dihydroxy coumarin	Optimization of the formulation	Size: 250 nm	[112]
Antisolvent precipitation method	Thymol	Antimicrobial activity	Size: 175 nm	[113]
Antisolvent-precipitation method	Daidzin	Oral bioavailability	Size 160-230 nm	[114]

Additionally, zein has already been utilized extensively for encapsulation of functional actives ranging from essential oils to natural antioxidants all of which are frequently used ingredients in food products. [104]. Curcumin [112], vitamin D3 [115], lutein [116], β-carotene [117] folic acid or resveratrol are examples of some components loaded in zein nanoparticles.

2.3.2.6. Gliadin

The term gliadin encompasses a group of proteins extracted from wheat gluten with ethanol at 70%. The extracted protein fraction is heterogeneous and it is formed by single polypeptide chains [118].

Despite being soluble in hydroalcoholic mixtures, these proteins are characterized for being water insoluble, except in extreme pH conditions. This low water solubility is due to the presence of intramolecular disulfide bridges, and also due to the wide number of existing hydrophobic interactions. Also, gliadin in solution is very pH and ionic sensitive. Thus, at pH 7 gliadin aggregates thanks to the intramolecular hydrogen bridges [119].

Due to its hydrophobic characteristics gliadin can be used to obtain nanoparticles able to encapsulate and controlled release of actives such as all-trans-retinoic acid [120], α-tocopherol [121], carbazole [122], linalool-linalyl acetate, benzalconium chloride [123] kaempherol [45] and quercetin [124], among others.

Nevertheless, gliadin is a component of the gluten and the main problem associated is that gluten is responsible for celiac disease in genetically susceptible people [125].

2.3.2.7. Glutelins

Gluteins are water and alcohol insoluble, but soluble in highly alkaline or acid solutions.

2.3.2.8. Wheat gluten

Wheat contains a specific protein: gluten, obtained as a by-product during starch isolation from wheat flour. Gluten represents 80% of wheat seeds proteins, plays an important role in wheat flour quality and is used essentially as a human and animal food source. Gluten is water insoluble that limits its use in cosmetics and drugs. However, it plays an important role for traditional applications in bread and bakery products [86].

Wheat gluten is the most studied cereal protein in microencapsulation field. Because of its water insolubility and viscoelasticity, this plant polymer provides various interesting physico-chemical characteristics such as gel- and film-forming properties. Wheat proteins alone, or in combination with polysaccharides are good for encapsulating active core materials [96]. In addition, it has been reported that wheat proteins may specifically recognize and bind to glycositaled membrane components on the intestinal surface, resulting in oral specific bioadhesion. The potential of whey protein for oral drug delivery has been provened by in vitro experiments with Caco-2 cells [126]. In addition, whey proteins show low toxicity and are resistant to proteolytic degradation. An association between lipid nanoparticles and wheat protein was used for encapsulation of bufalin resulting in an increase of the oral bioavailability of the drug lipid nanoparticles [127].

2.3.2.9. Rice proteins

Rice is one of the most important cereal crops in the world. It contains from 12 to 20% proteins. Rice properties were studied by Chandi and Sogi (2007) and they noticed the excellent foaming stability lasting several days, the high emulsifying capacity in sugar solutions and the good stability of emulsions depending on the pH and salt/sugar presence [128]. These physico-chemical properties are similar to those of casein. Focusing on technology, rice protein has been associated with alginate and carragenate to form complex precipitates with possible new wall material obtaining microcapsules. However overall, the application of this protein for nanoparticle preparation it has not been described, and its use in industry is not very extended [96].

2.3.2.10. Sunflower proteins

Sunflowers are mainly cultivated for the production of oil; however the proteins extracted from sunflower have several properties. The proteins present in the sunflowers are globulins, albumins and prolamins. The aminoacid composition of sunflower proteins is similar to soy proteins, for that reason the physico-chemical properties of the sunflower proteins have been studied. They possess higher emulsifying properties than soy proteins at pH 7-8 and they are less efficient at forming foam than soy proteins. Nevertheless, sunflower protein foams are stable over the time. Thus, it could be an interesting approach for pharmaceutical industries. In this order, Huaiqiong Chen and collaborators, prepared a thermal and UV stability microemulsion of β-carotene with sunflower protein, lecithin and tween 20 [129]

3. Encapsulation techniques

Several methods have been developed to prepare polymeric nanoparticles. The selection of a particular one depends on the nature of the polymer and on the properties of the drug molecule to be encapsulated.

Two main procedures can be followed to form polymeric nanoparticles, namely bottom-up and top-down techniques (Figure 3). The top-down methods use size reduction to obtain controlled size nanoparticles, and involve the use of preformed polymers or purified natural macromolecules. The size reduction is based on the application of strong shear stress by wave sound emission (sonication), high pressure (microfluidization) and high speed agitation (homogenization). The bottom-up approaches; in contrast, start from individual molecules to form nanoparticles, by polymerization. The polymerization methods commonly used are emulsion polymerization (W/O, O/W, polimerization in bicontinuous structures), dispersion polymerization and interfacial polymerization [130]. The main drawbacks of the bottom-up methods are: i) the presence of residual sub-products in the final nanoparticles that can impart toxicity to the nanoparticles; ii) the difficulty in the prediction of polymer molecular weight, affecting the biodistribution and release behaviour of the drug from the nanoparticles; iii) the possibility of cross reaction of the drug with activated monomers present during polymerization [131]. To overcome these limitations, top-down methods were developed using naturals and synthetic polymers. These techniques are more commonly used to prepare biodegradable nanoparticles since they avoid the problems associated with bottom-up techniques. Among the different top-down techniques developed, two approaches are conventionally used. The first one is related with emulsification-based methods, and the second one is based on spontaneous formation of nanoparticles without involving emulsification steps (Figures 3 and 4).

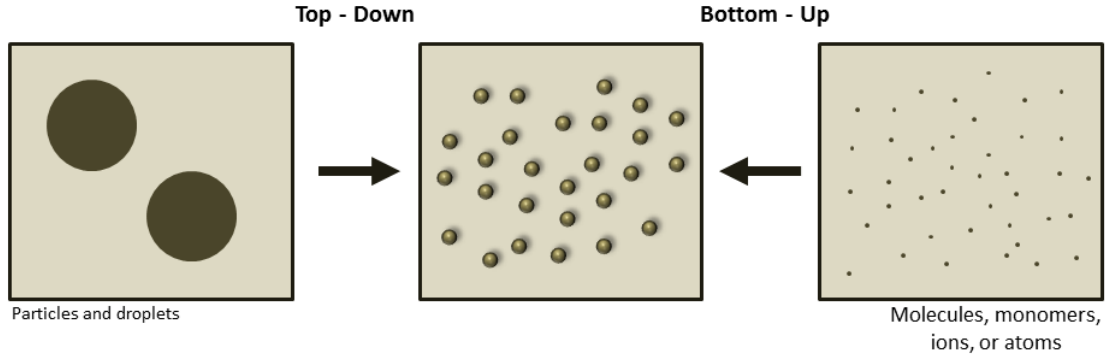

Figure 3: General approaches of fabricating colloidal delivery systems

3.1. Emulsification based methods

Methods based on nano-emulsion templates derive from microparticle preparation techniques. The principle of nano-emulsion formation is based on the spontaneous emulsification that occurs by mixing an organic phase and an aqueous phase. The organic phase is a homogeneous solution of oil, lipophilic surfactant and water miscible solvent, whereas the aqueous phase consists of hydrophilic surfactant and water.

For the W/O emulsions, an aqueous polymer solution is homogenized with an oil phase containing an oil-soluble emulsifier to form a water-in-oil-emulsion (W/O). The water droplet

size can be controlled by varying either the homogenization conditions (pressure and number of passes) or the solution composition (oil-to-water-ratio emulsifier-water ratio). The inner water phase is then gelled using a mechanism appropriate for the particular biopolymer used, like temperature change, addition of cross-linking agents or pH/ionic strength change. Finally, the biopolymer particles can be obtained by centrifugation/filtration. The resulting biopolymer particles can be dispersed in aqueous solution or dried. This method has been used to form biopolymer particles based on alginate [57].

A similar approach was used to form O/W emulsions. In this case initially a polymer solution is prepared in an organic solvent containing the drug dispersed. This solution is mixed with an external aqueous phase where the organic solvent is immiscible and, if necessary, may include surfactants. Once formed the O/W emulsion, the organic solvent is evaporated. The evaporation process causes the polymer precipitation leaving the additive trapped inside. By changing the speed and stirring conditions the particle size can be controlled. Finally, the particles are collected by filtration, centrifugation and drying.

This method requires the use of organic solvents such as dichloromethane, which although it is removed by evaporation, it can leave traces in the final product that can cause toxicity.

Other techniques that involve emulsification methods traditionally used for nanoparticle preparation are spontaneous emulsification/diffusion [132] and salting-out [133].

Another way to encapsulate lipophilic actives by emulsification-evaporation is to emulsify the lipid encapsulated in an aqueous solution containing the coating material, and subsequently removing the aqueous solvent by spray drying.

Table 2 summarizes the advantages and disadvantages and examples of emulsification/solvent evaporation nanoparticles production method.

Table 2. Emulsification-solvent evaporation method. Advantages, disadvantages, examples .

Advantages	Disadvantages	Examples		
		Polymer	**Drug loaded**	**Comments**
Encapsulation of hydrophobic and lipophilic drugs.	Use of organic solvents, Possible coalescence of nanodroplets during evaporation, Residues of organic solvents can cause toxicity.	Gelatin	Insulin [134]	Glutaraldehide (CL)
		Gelatin	Cloroquine [135]	Glutaraldehide saturated toluene (CL)
		Albumin	Cefamandole nafate [136]	Glutaraldehide (CL)
		Albumin (BSA nanoparticles)	10-Hydroxycamptothecin [137]	Thermal stabilization (CL)
		Albumin (Ovoalbumin nanoparticles)	Mucosal vaccine [138]	
		Wax cethyl palmitate/ poloxamer 407	Insulin [139]	W/O/W
		Glyceryl monostearate/Soya lecitin	Quercetin [140]	Low temperature solidification method (CL)
		Chitosan coated lipid nanoparticles	Calcitonin [141]	
		Sodium caseinate	B-carotene [142]	High pressure homogenizator . Microfluidizer
		Starch	Vitamin E [143]	Spray drier
		Chitosan/ maltodextrins/ whey proteins	Omega 3 [144]	
		Chitosan	Resveratrol [145]	Vainillin (CL)

CL: crosslinker

3.2. Spontaneous nanoparticle formation methods

Depending on the solubility or gelling properties of a dissolved polymer, nanoparticles can be formed spontaneously. The general principle of this method consists of the preparation of a solution of the polymer and then induce a phase separation by modifying the surrounded environment (solvent, pH, electrolyte, temperature, etc). Among others, the most commonly used preparation methods are detailed below.

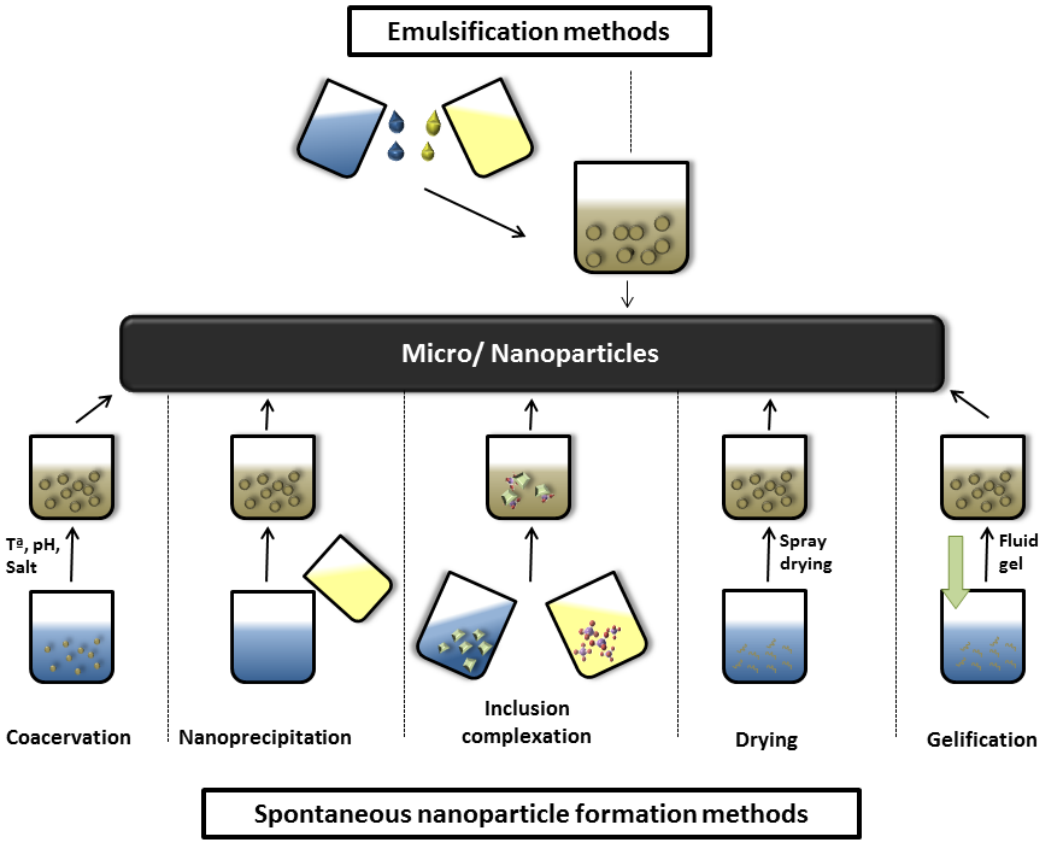

Figure 4: Resume of the different methods to fabricate colloidal delivery systems .

3.2.1. Coacervation

Coacervation is a process during which a homogeneous solution of macromolecules undergoes liquid-liquid phase separation, giving rise to a polymer rich dense phase and a transparent solution. These two liquid phases are incompatible, immiscible and are in equilibrium [146].
There exist two different types of coacervation: simple and complex:
Simple coacervation or desolvation is based on the differential solubility of polymers in solvents as a function of solvent polarity, pH, ionic strength and presence of electrolytes. The coacervation process reduces the solubility of the polymer in a medium, leading to phase separation. The addition of desolvating agents leads to changes in the polymer structure resulting in its coacervation or precipitation. By controlling processing variables, the size of nanoparticles in the coacervate can be controlled [147]. Finally, after nanoparticles are formed, they are stabilized by desolvation, thermal treatment or by the addition of cross-linking agents such as glutaraldehyde and glyoxal [148]. Thus, simple coacervation is a phenomenon in which

the addition of a substance reducing hydration (poor solvent) to a hydrophilic colloidal solution results in the formation of two phases, one of which is rich in colloid molecules (coacervate), and the other is poor in them.

In this case, to obtain an effective encapsulation is important to have a correct polymer /solvent /coacervation agent relationship. For example, for albumin nanoparticles, an increase in antisolvent/solvent ratio decreases the particle size due to rapid extraction or diffusion of the solvent into the antisolvent phase, which limits the growth of particles [149]. Preferably, the molecule to be encapsulated should be dispersed in the initial dissolved polymer solution and the coacervation agent miscible with the polymer solvent [150].

Coacervation/desolvation is the most commonly used method of preparation for protein nanoparticles, usually with organic solvents such as acetone and ethanol as antisolvents [147].

Additionally, this type of method is usually carried out with polymers such as gelatin, methylcellulose, carragenat, chitosan or gliadins, which are dissolved in aqueous media, and its "insolubilization" is induced by the addition of water-miscible solvents or electrolytes like calciumn the cases where it is desired to encapsulate hydrosoluble drugs, it is recommended to perform the coacervation in non aqueous media, using hydrophobic polymers as ethyl cellulose.

In the case of complex coacervation, this method is defined as the separation of a macromolecular solution composed of two opposite charged polymers into two immicible liquid phases [151]. When a solution of biopolymers of opposite charge is mixed, a complex is formed. Many factors like biopolymer type, pH, ionic strength, concentration and the ratio of the biopolymers affect the strength of the interaction between the biopolymers and the nature of the complex formed [152]. Besides the electrostatic interactions, hydrophobic interaction and hydrogen bonding can also contribute to the complex formation.

Coacervates may be formed when a protein at a pH below its isoelectric point (positive charge) is mixed with a polyanion.

As an example, a mixture of whey protein or gelatin with Arabic gum at a pH below the isoelectric point of the proteins. Similarly, solutions containing cationic polysaccharides like chitosan and an anionic polysaccharide like alginate have the ability to form coacervates [153,154].

One of the factors that limit the use of coacervation in encapsulation is their sensibility to pH and ionic strength. To increase the robustness of coacervates, they may be cross-linked. Glutaraldehyde is an effective cross-linker, but because of its toxicity, enzymatic cross-linkers such as trasglutaminase, genipin and plant proteins have been used to cross-link gelatin based coacervates. In general, the methods of coacervation (simple or complex) are very versatile can isolate a large number of substances and are potentially suitable techniques to prepare monodisperse nanoparticles for drug delivery purposes [155]. Tables 3 and 4 summarizes the advantages and disadvantages and examples of simple and complex coacervation nanoparticles production method.

Table 3. Simple coacervation preparation method. Advantages, disadvantages, examples.

Advantages	Disadvantages	Examples		
		Polymer	**Drug loaded**	**Comments**
Easy to scale up **Simply method**	Coacervate phase needs consolidation (i.e. cross-likage)	Gelatin	Paclitaxel [156]	
		Gelatin	Phenacetin [157]	By adding water-ethanol-propanolol
		Albumin (BSA) reduced with disulphide bond	Tamoxifeno [158]	Disulphide-bonds
		Alginate (thyolated)	Tamoxifeno [158]	L-Cysteine (CL)
		Sodium caseinate	Folic acid [82]	
		Zein	5-fluoracile [159]	Freeze drying
		Soy glicinin	Hexadecane [160]	Glutaraldehide (CL)
		Chitosan + dextran sulfate	Peptide for anti-angiogenesis [161]	

CL: crosslinker

Table 4. Complex coacervation preparation method. Advantages, disadvantages, examples.

Advantages	Disadvantages	Examples		
		Polymer	**Drug loaded**	**Comments**
Simply method	Low reproducibility Expensive	Gelatin	Metronidazhol, Diclophenac, Indometacine[162]	Alginate/pectin
		Chitosan	Nucleic acids [163]	
		Whey proteins	Thiamine [164]	Pectin
		Zein proteins	Vitamin D3 [115]	Carboxymethyl-Chitosan
		Gelatin, at pH5 (positively charged)	DNA (negative charged) [165]	
		Albumin (HSA)-polyethyleneimine.	DNA (solubilized in sodium sulphate solution)[166].	Carbodiimide
		Collagen-Chitosan	Lavender oil [167]	Sodium sulphate

CL: Crosslinker

3.2.2. Nanoprecipitation

This method is suitable for producing nanoparticles from polysaccharides and/or proteins. It is a straightforward technique, rapid and easy to perform. The nanoparticle formation is instantaneous and the entire procedure is carried out in only one step. Polymer and drug are dissolved together and precipitated in a non solvent, miscible with the former one. Nanoprecipitation occurs by a rapid desolvation of the polymer and enables the production of small nanoparticles with narrow size distribution [168]. Therefore, and on the contrary than coacervation methods, nanoprecipitation technique does not require the consolidation of the particles (ie, by cross-linkage). Therefore, after the particles are formed, it is important that there is a sufficiently strong repulsion between them to prevent them from aggregating. Nanoprecipitation is an attractive technology as there is no need for specialized equipment and complex operating conditions, the associated costs are quite low and the technique can reasonably easily be scaled up [155]. This technique is mostly suitable for compounds with hydrophobic nature, but formation and process modifications were recently investigated to encapsulate hydrophilic drugs [169]. A variety of materials can be used with this technique, thus, albumin, gelatin, fribroin, zein and gliadin are good examples in which this technique is useful for encapsulation of antimicrobials or antioxidants [170].

Several authors have used the anti-solvent precipitation method for the encapsulation of different compounds. For this purpose, Ezpeleta and collaborators used a binary alcohol-water system/water as Solvent/anti-solvent solution to encapsulate trans-retinoic acid in gliadin nanoparticles. They obtained spherical nanoparticles of about 500 nm [171]. With the same solvent/anti-solvent solution, Duclairoir and collaborators loaded vitamin E in gliadin nanoparticles. Although the shape of the nanoparticles was similar, the size was higher (900 nm) [172]. Other authors encapsulated curcumin [173] and thymol [174] in zein nanoparticles after the addition of water into a zein-water solution mixture. The resulting nanoparticles displayed sizes between 150 nm (curcumin) and 200 nm (Tymol). More recently, Subia & Kundu, used Silk Fibroin-albumin to encapsulate methotrexate. In this case, after the dissolution of the biopolymer in water, the nanoparticles were formed by the addition of acetone. The resulting nanoparticles displayed sizes of 200 nm with spherical shape [175].

Table 5 summarizes the advantages and disadvantages and examples of nanoprecipitation preparation method for nanoparticles formation.

Table 5. Nanoprecipitation preparation method. Advantages, disadvantages, examples.

Advantages	Disadvantages	Examples		
		Polymer	**Drug loaded**	**Comments**
Simple, fast, reproducible and easy to scale up. Nanoparticles with narrow unimodal distribution.	Presence of surfactants Use of organic solvents	Zein	5-fluorouracil [109]	
		Soy matrix	Theophyline [176]	Need CL
		Gliadin	All-trans-retinoic acid [120]	Ethanol-water/water)
		Gliadin	Carbazole [122]	
		Gliadin	Hydrophobic drugs [123]	Ethanol-water system/ water
		Gliadin	α-Tocopherol [121]	Ethanol-water system/ water
		Zein	Curcumin [177]	Ethanol-water system/ water
		Fibroin-albumin	Methotrexate [175]	Water / acetone

CL: crosslinker

3.2.3. Inclusion complexation

Molecular inclusion is generally achieved by using cyclodextrins (CDs) as the encapsulating materials. Cyclodextrins, can develop interactions with lipophilic molecules or lipophilic groups from the guest molecule originating complexes, that can be more water soluble than the molecule on its own. The external hydrophilic surface of cyclodextrins can result in poor affinity for biological barriers that is why encapsulating these complexes could increase the bioavailability [178]. Inclusion complexes have been used for the encapsulation of lipophilic drugs and, in the food industry, to mask odors or flavors or preserve aromas [155].
A large number of weakly water soluble molecules were trapped in cyclodextrins. The inclusion in these cage-like structures led to an increase in their water solubility as well as in their antioxidant capacity [152].

Furthermore, CDs appeared to be good thermal protectors and very strong photo-protectors of polyphenolic compounds subject to ultraviolet radiation [179,180].

In addition to cyclodextrins, self-assembly and co-assembly can occur between actives and some milk proteins like β-Lactoglobulin (β-Lg). β-Lg has the ability to encapsulate by ligand-binding different bioactive compounds like vitamin D, retinoid, fatty acids or resveratrol. In addition, this protein, due to its structural characteristics, provides protection against oxidative degradation. This natural self-assembly, can be improved by forming conjugates with polysaccharides, pectin, chitosan or dextran sulphate. Apart from ligand-binding, self and co-assembly properties, β-Lg acts as a stabilizing agent in nanoemulsions [181].

Table 6 summarizes the advantages and disadvantages and examples of inclusion complexation nanoparticles production method.

Table 6. Inclusion complexation nanoparticles preparation method. Advantages, disadvantages, examples.

Advantages	Disadvantages	Examples	
		Polymer	**Drug loaded/ examples**
Very simple **Easy to achieve**	Optimization process to adjust the ratios between oligossacharide and drug. Expensive	B-cyclodextrins Maltosyl- B-cyclodextrins 2-hydroxypropyl- B-cyclodextrins α-cyclodextrin	Resveratrol, Rutin, Kaempherol, Quercetin, Myrcetin, 3-hydroxyflavone [152,179,180]
		2-hydroxypropyl- B-cyclodextrins	Cisapride (Propulsid ®), Hydrocortisone (Dexocort ®) Indometacin (Indocid ®) Itraconazol (Sporanox ®) Mitomycin (Mitozytrex ™) [25]
		β-Lactoglobulin	Vitamin D, Retinoid, Fatty acids, Resveratrol, B-carotene [182]

3.2.4. Ionic Gelation

The gelation process consists of extruding an aqueous solution of polymer through a syringe needle or a nozzle, in which the active material is dissolved or dispersed, through a gelling medium. After reaction, droplets are transformed into gels with different structural and release properties depending on the polymer used [152]. Proteins are preferred over synthetic polymers and carbohydrates for the gel formation because proteins contain considerable amounts of acid and basic groups that can either accept or release protons and change the gel structure and release profile depending on the pH of the medium.Therefore, they are suitable for pH-sensitive drug delivery systems [183].

This method has often been used to form alginate beads as alginate will form a physical gel in presence of calcium ions. To create these beads, individual droplets of an alginate solution are injected into a calcium solution bath where gelation occurs and the beads harden. The micro/nanobeads formed have shown great promise as micro/nanoencapsulation devices for pharmaceutical drugs. Since this method is economic and relatively easy to control, it is quite feasible to produce alginate micro/nanobeads on an industrial scale. Besides, alginate microbeads, could be formed from other polymers such as injecting a pectin solution into a calcium solution (ionic gelation), injecting a whey protein into a hot liquid (heat-set gelation) or injecting a gelation solution into a cold liquid (cold-set gelation) [184].

In addition to alginate, the preparation of chitosan nanoparticles by ionic gelation method has been described [185]. Particles showed to be good nanosystems for slow drug release by diffusion. Moreover, Catechin and epigallocatechin were inmovilized in chitosan nanoparticles by the same ionic gelation method and showed better antioxidant protection than when they were loaded in chitosan tripolyphosphate nanoparticles [152].

Table 7 summarizes the advantages and disadvantages and examples of ionic gelation nanoparticles production method.

Table 7. Ionic gelation preparation method. Advantages, disadvantages, examples.

Advantages	Disadvantages	Examples		
		Polymer	**Drug loaded**	**Comments**
Organic solvent free method	Low stability due to the weakness of the ionic interaction	Alginate	Doxorrubicin [186].	Calcium chloride/ poly-lisine (CL)
		Alginate	Insulin [187]	Calcium chloride / chitosan (CL)
		Alginate	Cisplatin [188]	Chitosan (CL)
		Alginate	Gliclazide [189]	Eudragit E 100 (CL)
		Alginate	5-fluorouracil [190]	$Ca(OH)_2$ (CL)
		Alginate	Folic acid [20]	Pectin (CL)
		Chitosan	Catechin and epigallocatechin [152]	Tripolyphosphate (CL)

CL: Cross-linker

Once nanoparticles are obtained, supplementary steps in the preparative process may be necessary. These steps may involve purification process such as tangential flow filtration [191], centrifugal filtration [192] or ultracentrifugation [193,194]. Finally, nanoparticles are usually presented as a dry powder in order to improve their stability as well as facilitate their manipulation, shipping and storage. Usually, the drying process of nanoparticles suspensions is achieved by lyophilization [194], or, more recently by spray drying [195], that is an economic and easy to scale up technique. These special advantages of the spray drying and other drying techniques are detailed below.

3.2.5. Spray drying

Spray drying is an established method that is initiated by atomizing/spraying a suspension of droplets followed by a drying process, resulting in the production of solid particles.
Spray drying in the food industry for encapsulation technology has been used since 1950. It is economic, flexible, it operates continuously and produces particles of good quality. Hence, this technique is widely used in the industry for the encapsulation of different compounds [196]. However, the particles obtained by this methodology are in the range of micrometers. For that reason, in the field of nanotechnology, spray drying is used to dry nanoparticles suspensions obtaining a dry powder easy to reconstitute [57].

To dry a suspension of nanoparticles (Figure 5), such suspension is passed through a small nozzle, which leads to the formation of a mist of fine drops. The outlet of the nozzle is located in a controlled high temperature environment, so the volatile liquid phase within the drops quickly evaporates. The temperatures at which the spray dryer tipically works are between 100-300°C, depending on the material being prepared [152]. Usually, the temperature experienced by the material and the active loaded is lower than that applied because of the latent heat associated with liquid evaporation and the high surface-to-volume ratio of the drops that allows rapid drying, and minimizes the thermal damage. Like this, water is evaporated by the hot air contacting the atomized material and the capsules are then collected after they fall to the bottom of the drier. One limitation of the spray drying is the atomization temperature, the outlet temperature of the air and the inflow of sample also affect the final characteristics of the obtained product (particle size, encapsulation efficiency, formation aggregates, etc.). In fact, the air inlet temperature is directly proportional to the rate of drying. When it is low, the solvent evaporation rate is slow, resulting in the formation of dense membranes and particles of high water content. However, if the temperature is high, the solvent evaporates too quickly and the membranes of the resulting particles can be altered or cracked, which affects to the degradation and premature release of the encapsulated drug [197]. In view of this, it is necessary to control the atomization temperature (usually between 100-300 °C) and the sample flow to obtain an effective drying and encapsulation without compromising the stability of the particles and the material to be encapsulated.
Although spray drier is a promoting microencapsulation technique, its use in the nanotech field is not developed. The atomizator of the spray drier has been designed for the microencapsulation technique. However, spray drier can be used to dry nanoparticles formulations previously prepared.

In the laboratory market there are new equipment to produce nanoparticles with a similar technology than spray drier based on the atomization of the sample. Thus, Buchi has commercialized Nano Spray Drier B-90, which is enables the production of small particles. Its use in pilot plant is not developed yet.

3.2.6. Spray-cooling and spray-chilling

There are two commercially practiced encapsulation processes similar to spray drying. Both involve dispersing the core ingredient into a liquid coating material and spraying it through nozzles to a controlled environment. However, two differences can be seen, i) there is no water to be evaporated since the coating material is a fat, ii) the temperature of the air and the type of coating dispersion are different. Spray drying employs hot air to volatize the solvent from a coating dispersion. In contrast, spray cooling and spray chilling use air cooled to ambient temperature or refrigerate temperatures. In the case of spray cooling, the process uses carriers with a melting point between 45 and 122°C and spray chilling uses carriers with a melting point between 32 and 42°C, air cooling or refrigerated temperatures [198,199]. The core and wall mixture are atomized in the ambient or chilling air that causes the matrix solidify around the core, thereby forming an encapsulated product. Thanks to the low temperatures applied in the process, these techniques are adequate to protect labile and volatile materials.

The microcapsules obtained by these methods are insoluble in water due to its lipid coating. Therefore, they are often used to encapsulate water soluble substances as ferrous sulfate, some vitamins, minerals, acidulants and flavors [198,199].

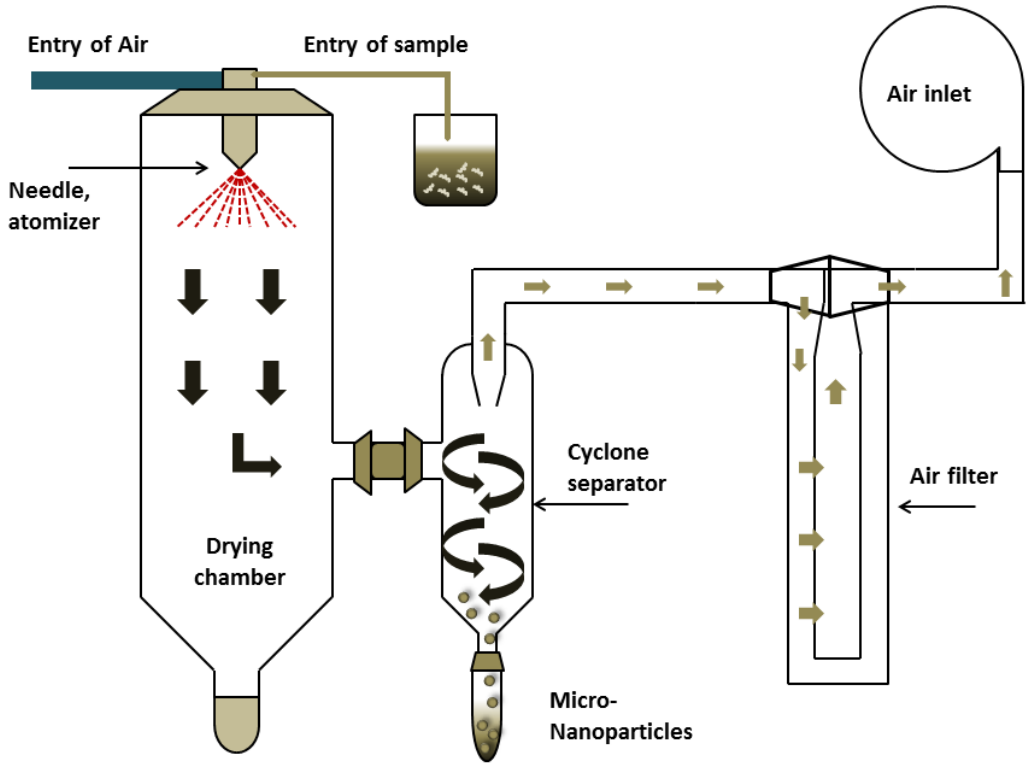

Figure 5: Spray drying.

4. Biopolymer particle properties

The functional performance of a biopolymer particulate system depends on its structure, electric charge and physic-chemical properties. It is important to highlight the most relevant characteristics of the biopolymer particles and how they influence their behaviour in the body.

Regarding the particle size and the external structure, the dimensions and morphology of biopolymer particles can be manipulated by controlling the preparation methdos. Depending on the material used and how these particles are fabricated their size can vary from a few nanometers to several micrometers. In this context, it is interesting that those particles whose size is below 200 nm present better interaction with the gut and could be capable of penetrating the mucus layer. However, particle sizes higher than 500 nm demonstrated lower effective diffusion coefficient [200]. In the case of the shape, it can be controlled by the excipients and the conditions of the preparation process. The most common shape is spherical; however non-spherical biopolymer particles can be produced and its appearance, rheology, mouth feel and release are often quite different than spherical ones. The shape of the particles is therefore important [184,201].

The internal structure of the biopolymer has large impact on functionality and can affect to factors like encapsulation efficiency, loading capacity, permeability, integrity and digestibility. In this order, the porosity of the particles should allow for an easily access of the active encapsulated [184].

On the other hand, biopolymer particle charge is a good parameter for predicting the stability of colloidal delivery systems. The electric charge of the individual particles influence whether or not they aggregate. If the charge is large, then there will be an electrostatic repulsion between them that may prevent aggregation. In addition, the particle charge also determines how biopolymer particles interact with different surfaces in the digestive system, thus cationic polymer can bind to the anionic surface of the mucosa [16].

The physic-chemical properties of biopolymer particles include parameters such as density, refractive index, rheology, polarity and porosity. These properties determine how other molecular species interact affecting their properties [184].

One of the most important approaches in the design of a biopolymer particle is to know its release mechanisms. Thus, in addition to protect the active, the particles may be designed to release the active component at a particular site in the body [202]. Developing a model for such processes requires an understanding of the physic-chemical mechanisms leading to release. In this context, different types of release mechanisms [203,204] have been described:

- **Diffusion**: the drug is released through the matrix or tridimensional net of the covering membrane. The permeability through the matrix and the solubility of the component of the shell of the particle influence the release rate.
- **Barrier:** the release of the active molecule depends on the difference of concentration between the inside and the outside of the cover, its thickness, permeability and diffusion coefficient.

- **Pressure:** the drug is released when the particle is under pressure, for example, when opening a vacuum-sealed container.
- **Breakage:** the particle can be broken by pressure or shear forces. This control release system is the most common in the gums.
- **Solvent activation:** the encapsulated substance is released when the formulation contacts with a solvent that hydrates or dissolve the particle.
- **Enzymatic effect:** certain enzymes present in the mouth or in the gastrointestinal tract can degrade the nanoparticles facilitating the release of the loaded compound.
- **Osmotic effect:** the loaded active is released due to the huge osmotic pressures created inside the particle.
- **pH effect:** the active ingredient **i**s released under specific pH conditions.
- **Thermic effect:** the active ingredient is released because of a change in the temperature.
- **Activation by fusion:** the oils or waxes used as covering material melt when heating the formulation and the active ingredient is released. This mechanism is characteristic for particles that have been obtained by cool drying.
- **Combined systems:** the active ingredient is released as the result of a combination of different mechanisms.

According to the polymer used, the size of the particle, the encapsulation technique and the mechanism of activation, the release rate can be constant over time (zero-order kinetics) or vary proportionally to the quantity of substance contained in the nanoparticle, exponentially decreasing over time (one-order kinetics).

In this second case, it is very frequent to have an immediate first release phase, which is known as burst effect. Moreover, the release profile also depends on the route of administration.

Thus, it is possible to meet a wide variety of release profiles, some examples are shown below:

- **Lineal profile** (Figure 6): the % of substance that is released is constant during a prolonged period of time. In many cases, it is the most desirable release profile because it allows foreseeing reliably the behavior of the system.
- **Burst initial effect** (Figure 7): when the particles contact with the media that triggers the process, initially it can be seen a sharp release of the % released and later, a constant rate release takes place.
- **Burst delayed effect** (Figure 8): at the beginning of the process the encapsulated substance is released inside the particles. After a certain time it can be observed a burst effect. This profile can be obtained, for example, by an osmotic effect.

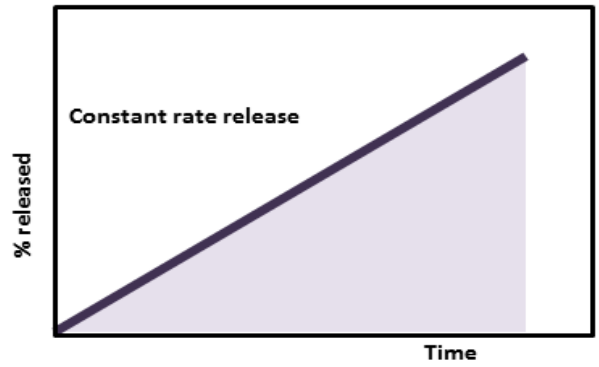

Figure 6: Constant rate release profile. The percentage of the released compound is directly proportional to the time. This system fits with a zero-order kinetic.

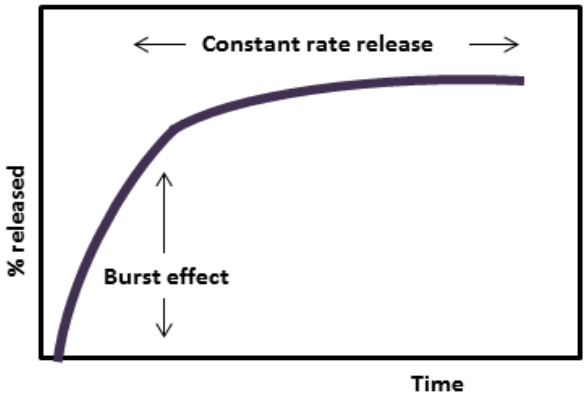

Figure 7: Release profile with an initial burst effect.

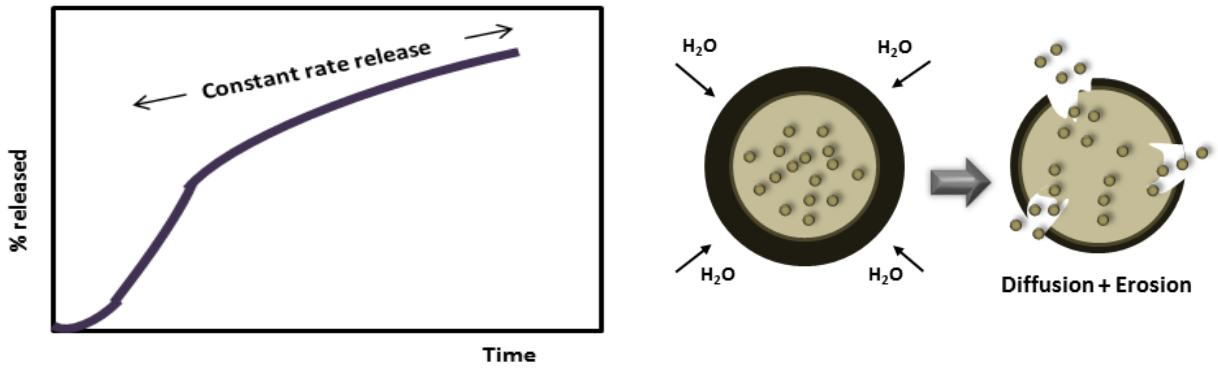

Figure 8: Release profile of a burst delayed effect (A) and a schematic example of the release process by an osmotic mechanism (B).

5. Nanoparticles in the GIT

The oral absorption of drugs and nutraceuticals occurs along different parts of the gastro-intestinal tract. In general, small molecular species (water, ions and alcohol) are taken up in the stomach while higher drugs and molecules re-absorption of GI secretions occur through various active and passive mechanisms along the small intestine. The colonic role in the absorption is considered to be limited but not restricted to the absorption of water, electrolytes, vitamin K, biotin and microbial fermentation metabolites, e.g. short chain fatty acids (Revital cohen Benshitrit, 2011).
The digestion process has various steps, such as, mastication, in the mouth, which involves shearing, mixing and dilution with saliva. During this process, the food is exposed to α-amilases and lingual lipase. During the second process, the digestion, occurring in the stomach, highly acid conditions and enzymatic secretion display. At the end of the acid phase, the chime is formed. Then, in the intestine, the chime is mixed with secretions of the gall bladder and pancreas, which elevates the pH. The small intestine comprises of three structurally distinct loci: duodenum, jejunum and ileum; all with unique structures that provide a large surface area for efficient absorption of substances. Finally, the not absorbed substances arrive to the colon, where the re-uptake water and minerals takes place [205].

The human intestinal epithelium is highly absorptive, composed of villi that enlarge the absorptive surface up to approximately 400 m^2 [206]. Absorptive enterocyte cells and mucus secreting globet cells cover the villi, and scattered between the villi there is follicle-associated epithelium (FAE). These lymphoid nodules (Peyer's patches) are covered with microfold cells (M cells), responsible of antigen sampling. M cells need to be taken into account regarding drug delivery since they are less protected by mucus and develop a significant transcytotic activity [207]. Despite this fact, these cells represent less than 1% of the intestinal epithelial cells and therefore do not constitute the major route of absorption.

In this environment, nanocarriers can improve the stability of the loaded substances against enzyme degradation, achieve desired therapeutic levels in target tissues for the required duration with a lower number of doses, and might ensure an optimal pharmacokinetic profile to meet specific needs [205].

However, the viscous, elastic, and sticky mucus layer that lines all mucosa tissues (even with different characteristics) has evolved to protect the intestinal epithelium by rapidly trapping and removing foreign particles and hydrophobic molecules. In view of this, mucoadhesion defined as the ability of nanoparticle to adhere to the mucus enhancing drug absorption and mucopenetration inside the mucus layer, could be a strategy to enhance the residence time of the nanosystem and enhance absorption and bioavailability of the active. Because of this, transport across the epithelium can be facilitated. These interactions are generally achieved with natural or synthetic polymers which can form hydrogen bonds and hydrophobic (mucoadhesion) and hydrophilic (mucopenetration) or electrostatic interactions with mucin [208].
Particle size, shape, and surface properties of the nanoparticles play a crucial role in the uptake of nanosized delivery systems across the mucosal membrane.

Different mechanism have been described (figure 9), the most predominant are:

- Paracellular
- Trancelular
- Transcytosing, which develops one of this mechanism (pinocytosis, macropinocitosis or clathrin-mediated endocytosis).

Concerning the paracellular [209] and transcellular [210] mechanisms, a particle can theoretically cross the intestinal epithelium by paracellular route (between adjacent cells) or by the transcellular route. In physiological conditions, the paracellular route is very limited due to the small surface area of the intracellular spaces and the tightness of the junctions between them (ranging from 3 to 10 Å) [209]. Different strategies to enhance this transport such as surfactants or compounds like chitosan [211], poly (acrylic acids) or thiolated polymers have demonstrated their ability [212]. The transcellular transport occurs by transcytosis, a process by which particles are taken up by cells. An endocytic process takes place at the apical membrane that ends up with the particles being transported through the cells and released at the basolateral pole [211]. In this case, nanoparticles play a role in the uptake of nanosized delivery systems across the mucosal membrane. Nanoparticles with particle size between 50-300 nm, electrostatic repulsion and hydrophobic surface were found to have better uptake as their counterparts [213].

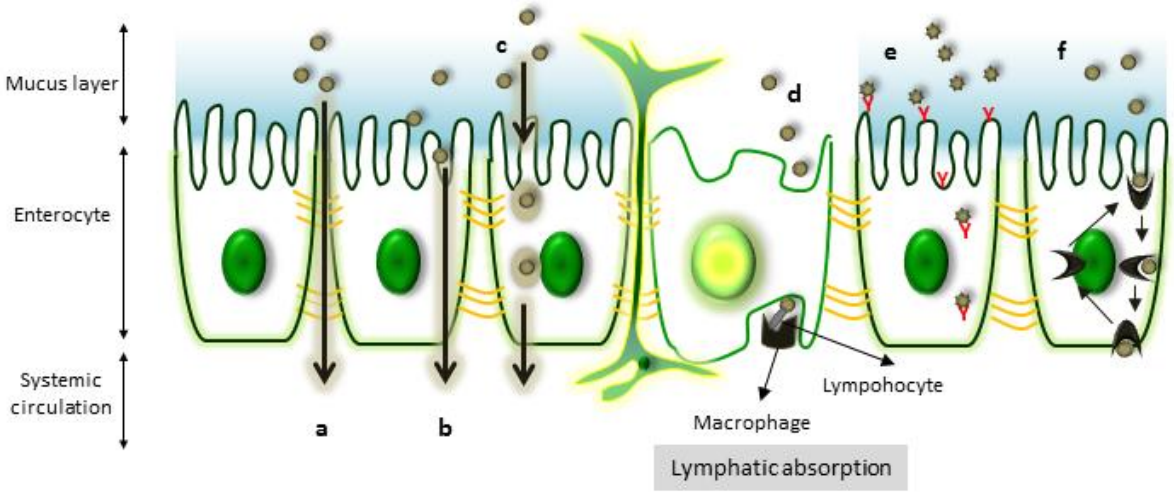

Figure 9: Different ways of intestinal absortion or translocation: (a) paracellular transport; (b) passive diffusion; (c) transcellulat transport; (d) M cell mediated transport; (e) receptor mediated transport; (f) carrier mediated transport.

The third mechanism is due to the epithelium capacity of transcytosing particles. The process develops by one of these mechanisms: pinocytosis, macropinocitosis or clathrin-mediated endocytosis. Pinocytosis and clathrin-mediated endocytosis are receptor mediated, the first one being able to internalize particles smaller than 150 nm and the second up to several µm. Macropinocytosis is not receptor-mediated and can internalize larger volumes of fluid containing particles smaller than 5 µm [214].

As a less relevant method, the transportat mediated by M cells is also energy dependent, via fluid phase endocytosis. However, other mucose associated lymphoid tissues and lymphatic adsorption via chylomicron is presented (mediated by lipase for various lipid-based drug delivery systems) [205].

6. Nanotechnologies in the market

Nowadays, in the market there are different products which contain nanoparticles. In clinics, Abraxane®, is the first developed formulation based on paclitaxel albumin nanoparticles.

Abraxane™: Paclitaxel protein-bound particles (nab paclitaxel; ABI-007) is a novel formulation of paclitaxel that does not employ the Cremophor EL® (CrEL) as solvent. This formulation was approved by the FDA in 2005 and commercialized as intravenous alternative to Taxol®. Abraxane was approved in Europe in 2008 to treat metastatic breast cancer in adults who have not responded to the first line treatment or for patients to whom the anthracycline alternative is not suitable. It is prepared by high-pressure homogenisation of paclitaxel in the presence of human serum albumin at a concentration of 3-4%, similar to the blood concentration of albumin, resulting in a nanoparticle colloidal suspension [138]. The nanoparticle suspension displays a mean particle diameter of 130-150 nm, thus eliminating the need of any solvent. Furthermore, the absence of CrEL eliminates the need for steroid premedication and alleviates the danger of leaching plasticizers from infusion bags and tubing.

The application of food nanotechnology to the field of nutrition has been focused on the development of nanosized food ingredients and additives and the delivery systems for nutrients and supplements in the form of nutraceuticals. Nanotechnology offers opportunities to modify and manipulate food and beverage products to achieve a more effective nutrients, such as, vitamins, proteins, minerals or antioxidants and additives to improve health benefits to consumers [215].

Table 8: Products containing NPs that are currently available for application in food products

Name	Producer	Type of product
LycoVit ®	BASF (Germany)	Starch-based and gelatine-based NPs containing lycopene
NANO B12 ®(vitamin spray)	Nutrition By Nanotech (USA)	Nano delivery system
NanoCurcuminoids ®	Life Enhancement (USA)	Solid-lipid nanospheres (SLNs)
NanoResveratrol ®	Life Enhancement (USA)	Phospholipid nanospheres

References

[1] D. Bhowmik, C.R. Chiranjib, B. Jayakar, Role of nanotechnology in novel drug delivery system, Journal of Pharmaceutical Science and Technology 1 (2009) 20-35.

[2] J.M. Irache, I. Esparza, C. Gamazo, M. Agüeros, S. Espuelas, Nanomedicine: novel approaches in human and veterinary therapeutics, Vet. Parasitol. 180 (2011) 47-71.

[3] J. Kreuter, Nanoparticles—a historical perspective, Int. J. Pharm. 331 (2007) 1-10.

[4] J. Corbett, P. McKeown, G. Peggs, R. Whatmore, Nanotechnology: international developments and emerging products, CIRP Annals-Manufacturing Technology 49 (2000) 523-545.

[5] J. Kreuter, Nanoparticles and nanocapsules--new dosage forms in the nanometer size range, Pharm. Acta Helv. 53 (1978) 33-39.

[6] R.C. Oppenheim, Solid colloidal drug delivery systems: nanoparticles, Int. J. Pharm. 8 (1981) 217-234.

[7] J. Kreuter, Evaluation of nanoparticles as drug-delivery systems. 1. Preparation methods, Pharm. Acta Helv. 58 (1983) 196-209.

[8] M. Singh, S. Manikandan, A. Kumaraguru, Nanoparticles: A new technology with wide applications, Res.J.Nanosci.Nanotechnol 1 (2011) 1-11.

[9] P. Couvreur, C. Vauthier, Nanotechnology: intelligent design to treat complex disease, Pharm. Res. 23 (2006) 1417-1450.

[10] F. Chiellini, Perspectives on: in vitro evaluation of biomedical polymers, J. Bioact. Compatible Polym. 21 (2006) 257-271.

[11] A.O. Elzoghby, W.M. Samy, N.A. Elgindy, Protein-based nanocarriers as promising drug and gene delivery systems, J. Controlled Release 161 (2012) 38-49.

[12] W.A. Goddard III, D. Brenner, S.E. Lyshevski, G.J. Iafrate, Handbook of Nanoscience, Engineering, and Technology, CRC press, 2007.

[13] A. Kumari, S.K. Yadav, S.C. Yadav, Biodegradable polymeric nanoparticles based drug delivery systems, Colloids and Surfaces B: Biointerfaces 75 (2010) 1-18.

[14] J. Park, M. Ye, K. Park, Biodegradable polymers for microencapsulation of drugs, Molecules 10 (2005) 146-161.

[15] A.O. Elzoghby, W.S. Abo El-Fotoh, N.A. Elgindy, Casein-based formulations as promising controlled release drug delivery systems, J. Controlled Release 153 (2011) 206-216.

[16] S.H. Bakhru, S. Furtado, A.P. Morello, E. Mathiowitz, Oral delivery of proteins by biodegradable nanoparticles, Adv. Drug Deliv. Rev. 65 (2013) 811-821.

[17] M. Agüeros, I. Esparza, C. Gonzales, C.J. Gonzalez, J.M. Irache, A. Romo, Nanopartículas para encapsulación de compuestos, su preparación y usos WO 2011104410 A1 (2011).

[18] European Commission, Regulation (EC) No 1924/2006 of the European Parliament and of the Council of 20 December 2006 on nutrition and health claims made on foods, Official Journal of the European Union (2007).

[19] N. Garti, Delivery and Controlled Release of Bioactives in Foods and Nutraceuticals., Woodhead Publishing Ltd, 2008.

[20] H. Madziva, K. Kailasapathy, M. Phillips, Alginate-pectin microcapsules as a potential for folic acid delivery in foods, J. Microencapsul. 22 (2005) 343-351.

[21] M.A. Augustin, Y. Hemar, Nano-and micro-structured assemblies for encapsulation of food ingredients, Chem. Soc. Rev. 38 (2009) 902-912.

[22] M. Stevanovic, A. Radulovic, B. Jordovic, D. Uskokovic, Poly (DL-lactide-co-glycolide) nanospheres for the sustained release of folic acid, Journal of Biomedical Nanotechnology 4 (2008) 349-358.

[23] C. Gallardo, C. Castaño, C. Guzmán, S.M. Lopera, Desarrollo y carazterización de nanopartículas de ácido fólico formadas por secado por aspersión, utilizando goma arábiga y maltodextrina como materiales de pared., Vitae 16 (2009) 55-65.

[24] M. Lopera, C. Guzman, C. Castaño, C. Gallardo, Development and characterization of folic acid microparticles formed by spray-drying with gum arabic and maltodextrin, Vitae 16 (2009) 55-65.

[25] P. Calleja, J. Huarte, M. Agüeros, L. Ruiz-Gatón, S. Espuelas, J.M. Irache, Molecular buckets: cyclodextrins for oral cancer therapy, Therapeutic Delivery 3 (2012) 43-57.

[26] G. Astray, C. Gonzalez-Barreiro, J.C. Mejuto, R. Rial-Otero, J. Simal-Gándara, A review on the use of cyclodextrins in foods, Food Hydrocoll. 23 (2009) 1631-1640.

[27] W. Plazinski, Molecular basis of calcium binding by polyguluronate chains. Revising the egg-box model, Journal of Computational Chemistry 32 (2011) 2988-2995.

[28] M. Hans, A. Lowman, Biodegradable nanoparticles for drug delivery and targeting, Current Opinion in Solid State and Materials Science 6 (2002) 319-327.

[29] S. De, D. Robinson, Polymer relationships during preparation of chitosan–alginate and poly-L-lysine–alginate nanospheres, J. Controlled Release 89 (2003) 101-112.

[30] N.E. Simpson, S.C. Grant, L. Gustavsson, V. Peltonen, S.J. Blackband, I. Constantinidis, Biochemical consequences of alginate encapsulation: a NMR study of insulin-secreting cells, Biomaterials 27 (2006) 2577-2586.

[31] W.R. Gombotz, S.F. Wee, Protein release from alginate matrices, Adv. Drug Deliv. Rev. 64 (2012) 194-205.

[32] D. Quoagi, D. Poncekr, 9. Extemal versus internal source of calcium during the gelation of alginate beads for DNA encapsulation, DNA Encapsulation within Membrane Coated Alginate Beads (1998).

[33] L. Xing, C. Dawei, X. Liping, Z. Rongqing, Oral colon-specific drug delivery for bee venom peptide: development of a coated calcium alginate gel beads-entrapped liposome, J. Controlled Release 93 (2003) 293-300.

[34] K. Santhi, S. Dhanraj, D. Nagasamyvenkatesh, S. Sangeetha, B. Suresh, Preparation and optimization of sodium alginate nanospheres of methotrexate, Indian Journal of Pharmaceutical Sciences 67 (2005) 691-696.

[35] C. Yu, L. Jia, B. Yin, X. Zhang, S. Cheng, R. Zhuo, Fabrication of nanospheres and vesicles as drug carriers by self-assembly of alginate, The Journal of Physical Chemistry C 112 (2008) 16774-16778.

[36] N.K. Raj, C.P. Sharma, Oral insulin--a perspective, J. Biomater. Appl. 17 (2003) 183-196.

[37] M.V. Chandra-Hioe, R. Addepalli, S.A. Osborne, I. Slapetova, R. Whan, M.P. Bucknall, J. Arcot, Transport of folic acid across Caco-2 cells is more effective than 5-methyltetrahydrofolate following the in vitro digestion of fortified bread, Food Res. Int. 53 (2013) 104-109.

[38] J. Barat, É Pérez-Esteve, A. Bernardos, R. Martínez-Mañez, Nutritional effects of folic acid controlled release from mesoporous materials, Procedia Food Science 1 (2011) 1828-1832.

[39] I.R. Younis, M.K. Stamatakis, P.S. Callery, P.J. Meyer-Stout, Influence of pH on the dissolution of folic acid supplements, Int. J. Pharm. 367 (2009) 97-102.

[40] S.K. Shukla, A.K. Mishra, O.A. Arotiba, B.B. Mamba, Chitosan-based nanomaterials: A state-of-the-art review, Int. J. Biol. Macromol. 59 (2013) 46-58.

[41] M.Z. Elsabee, E.S. Abdou, Chitosan based edible films and coatings: A review, Materials Science and Engineering: C 33 (2013) 1819-1841.

[42] N. Mati-Baouche, P. Elchinger, H. de Baynast, G. Pierre, C. Delattre, P. Michaud, Chitosan as an adhesive, European Polymer Journal 60 (2014) 198-212.

[43] M. Esmaili, S.M. Ghaffari, Z. Moosavi-Movahedi, M.S. Atri, A. Sharifizadeh, M. Farhadi, R. Yousefi, J. Chobert, T. Haertlé, A.A. Moosavi-Movahedi, Beta casein-micelle as a nano vehicle for solubility enhancement of curcumin; food industry application, LWT-Food Science and Technology 44 (2011) 2166-2172.

[44] H.D. Silva, M.Â Cerqueira, A.A. Vicente, Nanoemulsions for food applications: development and characterization, Food and Bioprocess Technology 5 (2012) 854-867.

[45] V. García-Mediavilla, I. Crespo, P.S. Collado, A. Esteller, S. Sánchez-Campos, M.J. Tuñón, J. González-Gallego, The anti-inflammatory flavones quercetin and kaempferol cause inhibition of inducible nitric oxide synthase, cyclooxygenase-2 and reactive C-protein, and down-regulation of the nuclear factor kappaB pathway in Chang Liver cells, Eur. J. Pharmacol. 557 (2007) 221-229.

[46] Kalmbach, Renee Choumenkovitch, Silvina Troen, Aron D'Agostino, Ralph Jacques,Paul Selhub, Jacob, Circulating folic acid in plasma: relation to folic acid fortification., Am. J. Clin. Nutr. 88 (2008) 763-768.

[47] S.J. Hur, S.H. Kang, H.S. Jung, S.C. Kim, H.S. Jeon, I.H. Kim, J.D. Lee, Review of natural products actions on cytokines in inflammatory bowel disease, Nutr. Res. 32 (2012) 801-816.

[48] M. Russo, C. Spagnuolo, I. Tedesco, S. Bilotto, G.L. Russo, The flavonoid quercetin in disease prevention and therapy: Facts and fancies, Biochem. Pharmacol. 83 (2012) 6-15.

[49] A. Zlotogorski, A. Dayan, D. Dayan, G. Chaushu, T. Salo, M. Vered, Nutraceuticals as new treatment approaches for oral cancer: II. Green tea extracts and resveratrol, Oral Oncol. 49 (2013) 502-506.

[50] A.P. Rogerio, C.L. Dora, E.L. Andrade, J.S. Chaves, L.F.C. Silva, E. Lemos-Senna, J.B. Calixto, Anti-inflammatory effect of quercetin-loaded microemulsion in the airways allergic inflammatory model in mice, Pharmacological Research 61 (2010) 288-297.

[51] L. Nygren-Babol, K.L. Karonen, The effect of different folate forms on denaturation of bovine folate binding protein, Int. Dairy J. 19 (2009) 437-442.

[52] J. Weiss, E.A. Decker, D.J. McClements, K. Kristbergsson, T. Helgason, T. Awad, Solid lipid nanoparticles as delivery systems for bioactive food components, Food Biophysics 3 (2008) 146-154.

[53] P. Ezhilarasi, P. Karthik, N. Chhanwal, C. Anandharamakrishnan, Nanoencapsulation techniques for food bioactive components: a review, Food and Bioprocess Technology 6 (2013) 628-647.

[54] J.M. Irache, L. Bergougnoux, I. Ezpeleta, J. Gueguen, A. Orecchioni, Optimization and in vitro stability of legumin nanoparticles obtained by a coacervation method, Int. J. Pharm. 126 (1995) 103-109.

[55] W. Lohcharoenkal, L. Wang, Y.C. Chen, Y. Rojanasakul, Protein Nanoparticles as Drug Delivery Carriers for Cancer Therapy, BioMed Research International 2014 (2014).

[56] I. Ezpeleta, J.M. Irache, S. Stainmesse, J. Gueguen, A. Orecchioni, Preparation of small-sized particles from vicilin (vegetal protein from *Pisum sativum L.*) by coacervation, European Journal of Pharmaceutics and Biopharmaceutics 42 (1996) 36-41.

[57] A. Matalanis, O.G. Jones, D.J. McClements, Structured biopolymer-based delivery systems for encapsulation, protection, and release of lipophilic compounds, Food Hydrocoll. 25 (2011) 1865-1880.

[58] A.O. Elzoghby, Gelatin-based nanoparticles as drug and gene delivery systems: Reviewing three decades of research, J. Controlled Release 172 (2013) 1075-1091.

[59] M.C. Menet, C.H. Cottart, M. Taghi, V. Nivet-Antoine, D. Dargère, F. Vibert, O. Laprévote, J.-. Beaudeux, Ultra high performance liquid chromatography-quadrupole-time of flight analysis for the identification and the determination of resveratrol and its metabolites in mouse plasma, Anal. Chim. Acta 761 (2013) 128-136.

[60] E. Leo, M. Angela Vandelli, R. Cameroni, F. Forni, Doxorubicin-loaded gelatin nanoparticles stabilized by glutaraldehyde: Involvement of the drug in the cross-linking process, Int. J. Pharm. 155 (1997) 75-82.

[61] M. Nahar, D. Mishra, V. Dubey, N.K. Jain, Development, characterization, and toxicity evaluation of amphotericin B–loaded gelatin nanoparticles, Nanomedicine: Nanotechnology, Biology and Medicine 4 (2008) 252-261.

[62] R. Kumar, R.C. Nagarwal, M. Dhanawat, J.K. Pandit, In-vitro and in-vivo study of indomethacin loaded gelatin nanoparticles, Journal of Biomedical Nanotechnology 7 (2011) 325-333.

[63] Y. Zhao, X. Li, C. Lu, Y. Xu, H. Lv, D. Dai, L. Zhang, C. Sun, W. Yang, X. Li, Experiment on the feasibility of using modified gelatin nanoparticles as insulin pulmonary administration system for diabetes therapy, Acta Diabetol. 49 (2012) 315-325.

[64] T.G. Shutava, S.S. Balkundi, P. Vangala, J.J. Steffan, R.L. Bigelow, J.A. Cardelli, D.P. O'Neal, Y.M. Lvov, Layer-by-layer-coated gelatin nanoparticles as a vehicle for delivery of natural polyphenols, ACS Nano 3 (2009) 1877-1885.

[65] C. Coester, K. Langer, H. Von Briesen, J. Kreuter, Gelatin nanoparticles by two step desolvation a new preparation method, surface modifications and cell uptake, J. Microencapsul. 17 (2000) 187-193.

[66] E.J. Lee, S.A. Khan, J.K. Park, K. Lim, Studies on the characteristics of drug-loaded gelatin nanoparticles prepared by nanoprecipitation, Bioprocess and Biosystems Engineering 35 (2012) 297-307.

[67] Y. An, B. Cui, Y. Wang, W. Jin, X. Geng, X. Yan, B. Li, Functional properties of ovalbumin glycosylated with carboxymethyl cellulose of different substitution degree, Food Hydrocoll. 40 (2014) 1-8.

[68] A.O. Elzoghby, W.M. Samy, N.A. Elgindy, Albumin-based nanoparticles as potential controlled release drug delivery systems, J. Controlled Release 157 (2012) 168-182.

[69] E. Miele, G.P. Spinelli, E. Miele, F. Tomao, S. Tomao, Albumin-bound formulation of paclitaxel (Abraxane ABI-007) in the treatment of breast cancer, Int. J. Nanomedicine 4 (2009) 99-105.

[70] L. Debelle, A.M. Tamburro, Elastin: molecular description and function, Int. J. Biochem. Cell Biol. 31 (1999) 261-272.

[71] A.O. Elzoghby, W.M. Samy, N.A. Elgindy, Protein-based nanocarriers as promising drug and gene delivery systems, J. Controlled Release 161 (2012) 38-49.

[72] R. Herrero-Vanrell, A. Rincon, M. Alonso, V. Reboto, I. Molina-Martinez, J. Rodriguez-Cabello, Self-assembled particles of an elastin-like polymer as vehicles for controlled drug release, J. Controlled Release 102 (2005) 113-122.

[73] P.C. Bessa, R. Machado, S. Nürnberger, D. Dopler, A. Banerjee, A.M. Cunha, J.C. Rodríguez-Cabello, H. Redl, M. van Griensven, R.L. Reis, Thermoresponsive self-assembled elastin-based nanoparticles for delivery of BMPs, J. Controlled Release 142 (2010) 312-318.

[74] D.G. Dalgleish, Chapter 3 - The Basis of Structure in Dairy-Based Foods: Casein Micelles and their Properties, in: M. Boland, M. Golding, H. Singh (Eds.), Food Structures, Digestion and Health, Academic Press, San Diego, 2014, pp. 83-105.

[75] E. Semo, E. Kesselman, D. Danino, Y.D. Livney, Casein micelle as a natural nano-capsular vehicle for nutraceuticals, Food Hydrocoll. 21 (2007) 936-942.

[76] A.O. Elzoghby, W.S. Abo El-Fotoh, N.A. Elgindy, Casein-based formulations as promising controlled release drug delivery systems, J. Controlled Release 153 (2011) 206-216.

[77] A.O. Elzoghby, W.S. Abo El-Fotoh, N.A. Elgindy, Casein-based formulations as promising controlled release drug delivery systems, J. Controlled Release 153 (2011) 206-216.

[78] D.S. Horne, Chapter 6 - Casein Micelle Structure and Stability, in: H. Singh, M. Boland, A. Thompson (Eds.), Milk Proteins (Second Edition), Academic Press, San Diego, 2014, pp. 169-200.

[79] O. Abu Diak, A. Bani-Jaber, B. Amro, D. Jones, G. Andrews, The manufacture and characterization of casein films as novel tablet coatings, Food Bioprod. Process. 85 (2007) 284-290.

[80] D.S. Horne, Casein structure, self-assembly and gelation, Current Opinion in Colloid & Interface Science 7 (2002) 456-461.

[81] A.O. Elzoghby, M.W. Helmy, W.M. Samy, N.A. Elgindy, Novel ionically crosslinked casein nanoparticles for flutamide delivery: formulation, characterization, and in vivo pharmacokinetics, International Journal of Nanomedicine 8 (2013) 1721.

[82] R. Penalva, I. Esparza, M. Agüeros, C.J. Gonzalez-Navarro, C. Gonzalez-Ferrero, J.M. Irache, Casein nanoparticles as carriers for the oral delivery of folic acid, Food Hydrocolloids 44 (2015) 399–406.

[83] P. Zimet, D. Rosenberg, Y.D. Livney, Re-assembled casein micelles and casein nanoparticles as nano-vehicles for ω-3 polyunsaturated fatty acids, Food Hydrocoll. 25 (2011) 1270-1276.

[84] A. Sahu, N. Kasoju, U. Bora, Fluorescence study of the curcumin− casein micelle complexation and its application as a drug nanocarrier to cancer cells, Biomacromolecules 9 (2008) 2905-2912.

[85] A.O. Elzoghby, W.M. Samy, N.A. Elgindy, Protein-based nanocarriers as promising drug and gene delivery systems, J. Controlled Release 161 (2012) 38-49.

[86] I. Ezpeleta, J.M. Irache, S. Stainmesse, C. Chabenat, J. Gueguen, Y. Popineau, A. Orecchioni, Gliadin nanoparticles for the controlled release of all-< i> trans-retinoic acid, Int. J. Pharm. 131 (1996) 191-200.

[87] H.J. Giroux, J. Houde, M. Britten, Preparation of nanoparticles from denatured whey protein by pH-cycling treatment, Food Hydrocoll. 24 (2010) 341-346.

[88] A.H. Sneharani, J.V. Karakkat, S.A. Singh, A.A. Rao, Interaction of Curcumin with β-Lactoglobulin Stability, Spectroscopic Analysis, and Molecular Modeling of the Complex, J. Agric. Food Chem. 58 (2010) 11130-11139.

[89] İ Gülseren, Y. Fang, M. Corredig, Zinc incorporation capacity of whey protein nanoparticles prepared with desolvation with ethanol, Food Chem. 135 (2012) 770-774.

[90] O.L. Ramos, R.N. Pereira, R. Rodrigues, J.A. Teixeira, A.A. Vicente, F. Xavier Malcata, Physical effects upon whey protein aggregation for nano-coating production, Food Res. Int. 66 (2014) 344-355.

[91] S. Wichchukit, M.H. Oztop, M.J. McCarthy, K.L. McCarthy, Whey protein/alginate beads as carriers of a bioactive component, Food Hydrocoll. 33 (2013) 66-73.

[92] T. Moschakis, B.S. Murray, C.G. Biliaderis, Modifications in stability and structure of whey protein-coated o/w emulsions by interacting chitosan and gum arabic mixed dispersions, Food Hydrocoll. 24 (2010) 8-17.

[93] F.N. Souza, C. Gebara, M.C.E. Ribeiro, K.S. Chaves, M.L. Gigante, C.R.F. Grosso, Production and characterization of microparticles containing pectin and whey proteins, Food Res. Int. 49 (2012) 560-566.

[94] T. Osborne, Classification of vegetable proteins, in: Classification of vegetable proteins, Green and Co. ed., Longmans, New York, 1924, pp. 25-35.

[95] Z. Teng, Y. Luo, Q. Wang, Nanoparticles synthesized from soy protein: preparation, characterization, and application for nutraceutical encapsulation, J. Agric. Food Chem. 60 (2012) 2712-2720.

[96] A. Nesterenko, I. Alric, F. Silvestre, V. Durrieu, Vegetable proteins in microencapsulation: A review of recent interventions and their effectiveness, Industrial Crops and Products 42 (2013) 469-479.

[97] K. Nishinari, Y. Fang, S. Guo, G. Phillips, Soy proteins: A review on composition, aggregation and emulsification, Food Hydrocoll. 39 (2014) 301-318.

[98] A. Nesterenko, I. Alric, F. Violleau, F. Silvestre, V. Durrieu, The effect of vegetable protein modifications on the microencapsulation process, Food Hydrocoll. 41 (2014) 95-102.

[99] F. Donsì, B. Senatore, Q. Huang, G. Ferrari, Development of novel pea protein-based nanoemulsions for delivery of nutraceuticals, J. Agric. Food Chem. 58 (2010) 10653-10660.

[100] A.P.T. Pierucci, L.R. Andrade, E.B. Baptista, N.M. Volpato, M.H.M. Rocha-Leão, New microencapsulation system for ascorbic acid using pea protein concentrate as coat protector, J. Microencapsul. 23 (2006) 654-662.

[101] A.P.T. Pierucci, L.R. Andrade, M. Farina, C. Pedrosa, M.H.M. Rocha-Leão, Comparison of α-tocopherol microparticles produced with different wall materials: pea protein a new interesting alternative, J. Microencapsul. 24 (2007) 201-213.

[102] K.J. Klemmer, L. Waldner, A. Stone, N.H. Low, M.T. Nickerson, Complex coacervation of pea protein isolate and alginate polysaccharides, Food Chem. 130 (2012) 710-715.

[103] A.R. Patel, K.P. Velikov, Zein as a source of functional colloidal nano- and microstructures, Current Opinion in Colloid & Interface Science (2014) in press.

[104] R. Paliwal, S. Palakurthi, Zein in controlled drug delivery and tissue engineering, J. Controlled Release 189 (2014) 108-122.

[105] R. Shukla, M. Cheryan, Zein: the industrial protein from corn, Industrial Crops and Products 13 (2001) 171-192.

[106] N. Matsushima, G. Danno, H. Takezawa, Y. Izumi, Three-dimensional structure of maize α-zein proteins studied by small-angle X-ray scattering, Biochimica Et Biophysica Acta (BBA) - Protein Structure and Molecular Enzymology 1339 (1997) 14-22.

[107] C. Yewale, D. Baradia, I. Vhora, A. Misra, Proteins: emerging carrier for delivery of cancer therapeutics, Expert Opinion on Drug Delivery 10 (2013) 1429-1448.

[108] R. Paliwal, S. Palakurthi, Zein in controlled drug delivery and tissue engineering, J. Controlled Release 189 (2014) 108-122.

[109] L. Lai, H. Guo, Preparation of new 5-fluorouracil-loaded zein nanoparticles for liver targeting, Int. J. Pharm. 404 (2011) 317-323.

[110] J. Gomez-Estaca, M. Balaguer, R. Gavara, P. Hernandez-Munoz, Formation of zein nanoparticles by electrohydrodynamic atomization: Effect of the main processing variables and suitability for encapsulating the food coloring and active ingredient curcumin, Food Hydrocoll. 28 (2012) 82-91.

[111] C. Liu, W. Yao, L. Zhang, H. Qian, W. Wu, X. Jiang, Cell-penetrating hollow spheres based on milk protein, Chem.Commun. 46 (2010) 7566-7568.

[112] S. Podaralla, O. Perumal, Influence of Formulation Factors on the Preparation of Zein Nanoparticles, Aaps Pharmscitech 13 (2012) 919-927.

[113] K. Li, S. Yin, Y. Yin, C. Tang, X. Yang, S. Wen, Preparation of water-soluble antimicrobial zein nanoparticles by a modified antisolvent approach and their characterization, J. Food Eng. 119 (2013) 343-352.

[114] T. Zou, L. Gu, TPGS emulsified zein nanoparticles enhanced oral bioavailability of daidzin: in vitro characteristics and in vivo performance, Molecular Pharmaceutics 10 (2013) 2062-2070.

[115] Y. Luo, Z. Teng, Q. Wang, Development of zein nanoparticles coated with carboxymethyl chitosan for encapsulation and controlled release of vitamin D3, J. Agric. Food Chem. 60 (2012) 836-843.

[116] D. Hu, C. Lin, L. Liu, S. Li, Y. Zhao, Preparation, characterization, and in vitro release investigation of lutein/zein nanoparticles via solution enhanced dispersion by supercritical fluids, J. Food Eng. 109 (2012) 545-552.

[117] S. Quispe-Condori, M.D. Saldaña, F. Temelli, Microencapsulation of flax oil with zein using spray and freeze drying, LWT-Food Science and Technology 44 (2011) 1880-1887.

[118] M.E. Juan, M. Maijó, J.M. Planas, Quantification of trans-resveratrol and its metabolites in rat plasma and tissues by HPLC, J. Pharm. Biomed. Anal. 51 (2010) 391-398.

[119] H. Park, C. Lee, I.D. Jung, J.S. Lee, Y. Jeong, J.H. Chang, S. Chun, M. Kim, I. Choi, S. Ahn, Y.K. Shin, S. Yeom, Y. Park, Quercetin regulates Th1/Th2 balance in a murine model of asthma, Int. Immunopharmacol. 9 (2009) 261-267.

[120] I. Ezpeleta, J.M. Irache, S. Stainmesse, C. Chabenat, J. Gueguen, Y. Popineau, A. Orecchioni, Gliadin nanoparticles for the controlled release of all-< i> trans-retinoic acid, Int. J. Pharm. 131 (1996) 191-200.

[121] C. Duclairoir, A. Orecchioni, P. Depraetere, E. Nakache, α-Tocopherol encapsulation and in vitro release from wheat gliadin nanoparticles, J. Microencapsul. 19 (2002) 53-60.

[122] M.A. Arangoa, M.A. Campanero, M.J. Renedo, G. Ponchel, J.M. Irache, Gliadin nanoparticles as carriers for the oral administration of lipophilic drugs. Relationships between bioadhesion and pharmacokinetics, Pharm. Res. 18 (2001) 1521-1527.

[123] C. Duclairoir, A. Orecchioni, P. Depraetere, F. Osterstock, E. Nakache, Evaluation of gliadins nanoparticles as drug delivery systems: a study of three different drugs, Int. J. Pharm. 253 (2003) 133-144.

[124] A.P. Rogerio, C.L. Dora, E.L. Andrade, J.S. Chaves, L.F.C. Silva, E. Lemos-Senna, J.B. Calixto, Anti-inflammatory effect of quercetin-loaded microemulsion in the airways allergic inflammatory model in mice, Pharmacological Research 61 (2010) 288-297.

[125] O.V. Kharissova, H.V.R. Dias, B.I. Kharisov, B.O. Pérez, V.M.J. Pérez, The greener synthesis of nanoparticles, Trends Biotechnol. 31 (2013) 240-248.

[126] M. Wirth, C. Kneuer, C. Lehr, F. Gabor, Lectin-mediated drug delivery: discrimination between cytoadhesion and cytoinvasion and evidence for lysosomal accumulation of wheat germ agglutinin in the Caco-2 model, J. Drug Target. 10 (2002) 439-448.

[127] Y. Liu, P. Wang, C. Sun, J. Zhao, Y. Du, F. Shi, N. Feng, Bioadhesion and enhanced bioavailability by wheat germ agglutinin-grafted lipid nanoparticles for oral delivery of poorly water-soluble drug bufalin, Int. J. Pharm. 419 (2011) 260-265.

[128] G.K. Chandi, D. Sogi, Functional properties of rice bran protein concentrates, J. Food Eng. 79 (2007) 592-597.

[129] H. Chen, Q. Zhong, Thermal and UV stability of β-carotene dissolved in peppermint oil microemulsified by sunflower lecithin and Tween 20 blend, Food Chem. 174 (2015) 630-636.

[130] E.N. Nathalie Poulain, F. Candau, A. Orecchion, J.M. Irache, Biopolymer and polymer nanoparticles and their biomedical applications. , in: H.S. Nalwa (Ed.), Handbook of Nanostructured Materials and Nanotechnology, 2000, pp. 577-635.

[131] News-Medical.Net, Launch date announced for Abraxane to treat metastatic breastcancer, Http://Www.News-Medical.Net/?id=7489. (2005).

[132] T. Niwa, H. Takeuchi, T. Hino, N. Kunou, Y. Kawashima, Preparations of biodegradable nanospheres of water-soluble and insoluble drugs with D,L-lactide/glycolide copolymer by a novel spontaneous emulsification solvent diffusion method, and the drug release behavior, J. Controlled Release 25 (1993) 89-98.

[133] E. Allemann, R. Gurny, E. Doelker, Preparation of aqueous polymeric nanodispersions by a reversible salting-out process: influence of process parameters on particle size, Int. J. Pharm. 87 (1992) 247-253.

[134] Y. Zhao, X. Li, C. Lu, Y. Xu, H. Lv, D. Dai, L. Zhang, C. Sun, W. Yang, X. Li, Experiment on the feasibility of using modified gelatin nanoparticles as insulin pulmonary administration system for diabetes therapy, Acta Diabetol. 49 (2012) 315-325.

[135] A. Bajpai, J. Choubey, Design of gelatin nanoparticles as swelling controlled delivery system for chloroquine phosphate, J. Mater. Sci. Mater. Med. 17 (2006) 345-358.

[136] F. Crisante, I. Francolini, M. Bellusci, A. Martinelli, L. D'Ilario, A. Piozzi, Antibiotic delivery polyurethanes containing albumin and polyallylamine nanoparticles, European Journal of Pharmaceutical Sciences 36 (2009) 555-564.

[137] L. Yang, F. Cui, D. Cun, A. Tao, K. Shi, W. Lin, Preparation, characterization and biodistribution of the lactone form of 10-hydroxycamptothecin (HCPT)-loaded bovine serum albumin (BSA) nanoparticles, Int. J. Pharm. 340 (2007) 163-172.

[138] A.O. Elzoghby, W.M. Samy, N.A. Elgindy, Albumin-based nanoparticles as potential controlled release drug delivery systems, J. Controlled Release 157 (2012) 168-182.

[139] B. Sarmento, S. Martins, D. Ferreira, E.B. Souto, Oral insulin delivery by means of solid lipid nanoparticles, Int. J. Nanomedicine 2 (2007) 743-749.

[140] H. Li, X. Zhao, Y. Ma, G. Zhai, L. Li, H. Lou, Enhancement of gastrointestinal absorption of quercetin by solid lipid nanoparticles, J. Controlled Release 133 (2009) 238-244.

[141] M. Garcia-Fuentes, C. Prego, D. Torres, M. Alonso, A comparative study of the potential of solid triglyceride nanostructures coated with chitosan or poly (ethylene glycol) as carriers for oral calcitonin delivery, European Journal of Pharmaceutical Sciences 25 (2005) 133-143.

[142] B. Chu, S. Ichikawa, S. Kanafusa, M. Nakajima, Preparation of protein-stabilized β-carotene nanodispersions by emulsification–evaporation method, J. Am. Oil Chem. Soc. 84 (2007) 1053-1062.

[143] C. Chen, G. Wagner, Vitamin E nanoparticle for beverage applications, Chem. Eng. Res. Design 82 (2004) 1432-1437.

[144] W. Klaypradit, Y. Huang, Fish oil encapsulation with chitosan using ultrasonic atomizer, LWT-Food Science and Technology 41 (2008) 1133-1139.

[145] H. Peng, H. Xiong, J. Li, M. Xie, Y. Liu, C. Bai, L. Chen, Vanillin cross-linked chitosan microspheres for controlled release of resveratrol, Food Chem. 121 (2010) 23-28.

[146] B. Mohanty, V. Aswal, J. Kohlbrecher, H. Bohidar, Synthesis of gelatin nanoparticles via simple coacervation, Journal of Surface Science and Technology 21 (2005) 149.

[147] W. Lohcharoenkal, L. Wang, Y.C. Chen, Y. Rojanasakul, Protein Nanoparticles as Drug Delivery Carriers for Cancer Therapy, BioMed Research International 2014 (2014).

[148] K. Langer, S. Balthasar, V. Vogel, N. Dinauer, H. Von Briesen, D. Schubert, Optimization of the preparation process for human serum albumin (HSA) nanoparticles, Int. J. Pharm. 257 (2003) 169-180.

[149] G. Wang, K. Siggers, S. Zhang, H. Jiang, Z. Xu, R.F. Zernicke, J. Matyas, H. Uludağ, Preparation of BMP-2 containing bovine serum albumin (BSA) nanoparticles stabilized by polymer coating, Pharm. Res. 25 (2008) 2896-2909.

[150] D. Ramos Picos, M. Gómez Carril, D. Fernández Mena, Métodos de obtención de microesferas biodegradables, Revista Cubana De Farmacia 35 (2001) 126-135.

[151] E. Kizilay, A.B. Kayitmazer, P.L. Dubin, Complexation and coacervation of polyelectrolytes with oppositely charged colloids, Adv. Colloid Interface Sci. 167 (2011) 24-37.

[152] A. Munin, F. Edwards-Lévy, Encapsulation of natural polyphenolic compounds; a review, Pharmaceutics 3 (2011) 793-829.

[153] M.A. Augustin, Y. Hemar, Nano-and micro-structured assemblies for encapsulation of food ingredients, Chem. Soc. Rev. 38 (2009) 902-912.

[154] C. Sanchez, G. Mekhloufi, D. Renard, Complex coacervation between< i> β-lactoglobulin and Acacia gum: A nucleation and growth mechanism, J. Colloid Interface Sci. 299 (2006) 867-873.

[155] I.J. Joye, D.J. McClements, Biopolymer-based nanoparticles and microparticles: Fabrication, characterization, and application, Current Opinion in Colloid & Interface Science (2014).

[156] T.K. Yeh, Z. Lu, M.G. Wientjes, J.L. Au, Formulating paclitaxel in nanoparticles alters its disposition, Pharm. Res. 22 (2005) 867-874.

[157] K. Shimokawa, K. Saegusa, Y. Wada, F. Ishii, Physicochemical properties and controlled drug release of microcapsules prepared by simple coacervation, Colloids and Surfaces B: Biointerfaces 104 (2013) 1-4.

[158] A. Martínez, I. Iglesias, R. Lozano, J. Teijón, M. Blanco, Synthesis and characterization of thiolated alginate-albumin nanoparticles stabilized by disulfide bonds. Evaluation as drug delivery systems, Carbohydr. Polym. 83 (2011) 1311-1321.

[159] L. Lai, H. Guo, Preparation of new 5-fluorouracil-loaded zein nanoparticles for liver targeting, Int. J. Pharm. 404 (2011) 317-323.

[160] J. Lazko, Y. Popineau, J. Legrand, Soy glycinin microcapsules by simple coacervation method, Colloids and Surfaces B: Biointerfaces 37 (2004) 1-8.

[161] Y. Chen, V.J. Mohanraj, J.E. Parkin, Chitosan-dextran sulfate nanoparticles for delivery of an anti-angiogenesis peptide, Lett. Peptide Sci. 10 (2003) 621-629.

[162] M. Saravanan, K.P. Rao, Pectin–gelatin and alginate–gelatin complex coacervation for controlled drug delivery: Influence of anionic polysaccharides and drugs being encapsulated on physicochemical properties of microcapsules, Carbohydr. Polym. 80 (2010) 808-816.

[163] H. Mao, K. Roy, V.L. Troung-Le, K.A. Janes, K.Y. Lin, Y. Wang, J.T. August, K.W. Leong, Chitosan-DNA nanoparticles as gene carriers: synthesis, characterization and transfection efficiency, J. Controlled Release 70 (2001) 399-421.

[164] G.K. Bédié, S.L. Turgeon, J. Makhlouf, Formation of native whey protein isolate–low methoxyl pectin complexes as a matrix for hydro-soluble food ingredient entrapment in acidic foods, Food Hydrocoll. 22 (2008) 836-844.

[165] V.L. Truong-Le, J.T. August, K.W. Leong, Controlled gene delivery by DNA-gelatin nanospheres, Hum. Gene Ther. 9 (1998) 1709-1717.

[166] S. Rhaese, H. von Briesen, H. Rübsamen-Waigmann, J. Kreuter, K. Langer, Human serum albumin–polyethylenimine nanoparticles for gene delivery, J. Controlled Release 92 (2003) 199-208.

[167] B. Ocak, Complex coacervation of collagen hydrolysate extracted from leather solid wastes and chitosan for controlled release of lavender oil, J. Environ. Manage. 100 (2012) 22-28.

[168] F. Chiellini, A.M. Piras, C. Errico, E. Chiellini, Micro/nanostructured polymeric systems for biomedical and pharmaceutical applications (2008).

[169] U. Bilati, E. Allémann, E. Doelker, Development of a nanoprecipitation method intended for the entrapment of hydrophilic drugs into nanoparticles, European Journal of Pharmaceutical Sciences 24 (2005) 67-75.

[170] I.J. Joye, D.J. McClements, Production of nanoparticles by anti-solvent precipitation for use in food systems, Trends Food Sci. Technol. 34 (2013) 109-123.

[171] I. Ezpeleta, J.M. Irache, S. Stainmesse, C. Chabenat, J. Gueguen, Y. Popineau, A. Orecchioni, Gliadin nanoparticles for the controlled release of all-< i> trans-retinoic acid, Int. J. Pharm. 131 (1996) 191-200.

[172] C. Duclairoir, A. Orecchioni, P. Depraetere, F. Osterstock, E. Nakache, Evaluation of gliadins nanoparticles as drug delivery systems: a study of three different drugs, Int. J. Pharm. 253 (2003) 133-144.

[173] A. Patel, Y. Hu, J.K. Tiwari, K.P. Velikov, Synthesis and characterisation of zein–curcumin colloidal particles, Soft Matter 6 (2010) 6192-6199.

[174] K. Li, S. Yin, X. Yang, C. Tang, Z. Wei, Fabrication and characterization of novel antimicrobial films derived from thymol-loaded zein–sodium caseinate (SC) nanoparticles, J. Agric. Food Chem. 60 (2012) 11592-11600.

[175] B. Subia, S. Kundu, Drug loading and release on tumor cells using silk fibroin–albumin nanoparticles as carriers, Nanotechnology 24 (2013) 035103.

[176] C.M. Vaz, P.F. van Doeveren, R.L. Reis, A.M. Cunha, Soy matrix drug delivery systems obtained by melt-processing techniques, Biomacromolecules 4 (2003) 1520-1529.

[177] A. Patel, Y. Hu, J.K. Tiwari, K.P. Velikov, Synthesis and characterisation of zein–curcumin colloidal particles, Soft Matter 6 (2010) 6192-6199.

[178] Z. Fang, B. Bhandari, Encapsulation of polyphenols – a review, Trends Food Sci. Technol. 21 (2010) 510-523.

[179] C. Anselmi, M. Centini, M. Maggiore, N. Gaggelli, M. Andreassi, A. Buonocore, G. Beretta, R.M. Facino, Non-covalent inclusion of ferulic acid with α-cyclodextrin improves photo-stability and delivery: NMR and modeling studies, J. Pharm. Biomed. Anal. 46 (2008) 645-652.

[180] M.Á López-García, Ó López, I. Maya, J.G. Fernández-Bolaños, Complexation of hydroxytyrosol with β-cyclodextrins. An efficient photoprotection, Tetrahedron 66 (2010) 8006-8011.

[181] F.J. Gutiérrez, S.M. Albillos, E. Casas-Sanz, Z. Cruz, C. García-Estrada, A. García-Guerra, J. García-Reverter, M. García-Suárez, P. Gatón, C. González-Ferrero, I. Olabarrieta, M. Olasagasti, S. Rainieri, D. Rivera-Patiño, R. Rojo, A. Romo-Hualde, M. Sáiz-Abajo, M. Mussons, Methods for the nanoencapsulation of β-carotene in the food sector, Trends Food Sci. Technol. 32 (2013) 73-83.

[182] F.J. Gutiérrez, S.M. Albillos, E. Casas-Sanz, Z. Cruz, C. García-Estrada, A. García-Guerra, J. García-Reverter, M. García-Suárez, P. Gatón, C. González-Ferrero, I. Olabarrieta, M. Olasagasti, S. Rainieri, D. Rivera-Patiño, R. Rojo, A. Romo-Hualde, M. Sáiz-Abajo, M. Mussons, Methods for the nanoencapsulation of β-carotene in the food sector, Trends Food Sci. Technol. 32 (2013) 73-83.

[183] N. Reddy, Y. Yang, Potential of plant proteins for medical applications, Trends Biotechnol. 29 (2011) 490-498.

[184] A. Matalanis, O.G. Jones, D.J. McClements, Structured biopolymer-based delivery systems for encapsulation, protection, and release of lipophilic compounds, Food Hydrocoll. 25 (2011) 1865-1880.

[185] L. Qi, Z. Xu, X. Jiang, C. Hu, X. Zou, Preparation and antibacterial activity of chitosan nanoparticles, Carbohydr. Res. 339 (2004) 2693-2700.

[186] P. Lertsutthiwong, P. Rojsitthisak, U. Nimmannit, Preparation of turmeric oil-loaded chitosan-alginate biopolymeric nanocapsules, Materials Science and Engineering: C 29 (2009) 856-860.

[187] B. Sarmento, D. Ferreira, L. Jorgensen, M. Van De Weert, Probing insulin's secondary structure after entrapment into alginate/chitosan nanoparticles, European Journal of Pharmaceutics and Biopharmaceutics 65 (2007) 10-17.

[188] S.K. Motwani, S. Chopra, S. Talegaonkar, K. Kohli, F.J. Ahmad, R.K. Khar, Chitosan–sodium alginate nanoparticles as submicroscopic reservoirs for ocular delivery: Formulation, optimisation and< i> in vitro characterisation, European Journal of Pharmaceutics and Biopharmaceutics 68 (2008) 513-525.

[189] D. Chang, J. Lei, H. Cui, N. Lu, Y. Sun, X. Zhang, C. Gao, H. Zheng, Y. Yin, Disulfide cross-linked nanospheres from sodium alginate derivative for inflammatory bowel disease: Preparation, characterization, and in vitro drug release behavior, Carbohydr. Polym. 88 (2012) 663-669.

[190] K. Santhi, S. Dhanraj, D. Nagasamyvenkatesh, S. Sangeetha, B. Suresh, Preparation and optimization of sodium alginate nanospheres of methotrexate, Indian Journal of Pharmaceutical Sciences 67 (2005) 691-696.

[191] G. Dalwadi, V.B. Sunderland, Purification of PEGylated nanoparticles using tangential flow filtration (TFF), Drug Dev. Ind. Pharm. 33 (2007) 1030-1039.

[192] R. Da Costa Martins, C. Gamazo, J.M. Irache, Design and influence of γ-irradiation on the biopharmaceutical properties of nanoparticles containing an antigenic complex from< i> Brucella ovis, European Journal of Pharmaceutical Sciences 37 (2009) 563-572.

[193] H. Fessi, F. Puisieux, J.P. Devissaguet, N. Ammoury, S. Benita, Nanocapsule formation by interfacial polymer deposition following solvent displacement, Int. J. Pharm. 55 (1989) R1-R4.

[194] M. Agüeros, L. Ruiz-Gatón, C. Vauthier, K. Bouchemal, S. Espuelas, G. Ponchel, J.M. Irache, Combined hydroxypropyl-β-cyclodextrin and poly(anhydride) nanoparticles improve the oral permeability of paclitaxel, European Journal of Pharmaceutical Sciences 38 (2009) 405-413.

[195] P. Ojer, H. Salman, R. Da Costa Martins, J. Calvo, A. López de Cerain, C. Gamazo, J. Lavandera, J. Irache, Spray-drying of poly (anhydride) nanoparticles for drug/antigen delivery, Journal of Drug Delivery Science and Technology 20 (2010) 353-359.

[196] K.G.H. Desai, H. Jin Park, Recent developments in microencapsulation of food ingredients, Drying Technol 23 (2005) 1361-1394.

[197] A. Gharsallaoui, G. Roudaut, O. Chambin, A. Voilley, R. Saurel, Applications of spray-drying in microencapsulation of food ingredients: An overview, Food Res. Int. 40 (2007) 1107-1121.

[198] P.K. Okuro, de Matos Junior, Fernando Eustáquio, C.S. Favaro-Trindade, Technological Challenges for Spray Chilling Encapsulation of Functional Food Ingredients, Food Technology and Biotechnology 51 (2013) 171-182.

[199] E. Ortega-Rivas, P. Juliano, H. Yan, Encapsulation processes, in: Encapsulation processesFood Powders: Physical Properties, Processing, and Functionality, Springer, 2006, pp. 199-219.

[200] E. Fröhlich, T. Kueznik, C. Samberger, E. Roblegg, C. Wrighton, T.R. Pieber, Size-dependent effects of nanoparticles on the activity of cytochrome P450 isoenzymes, Toxicol. Appl. Pharmacol. 242 (2010) 326-332.

[201] A. Matalanis, U. Lesmes, E.A. Decker, D.J. McClements, Fabrication and characterization of filled hydrogel particles based on sequential segregative and aggregative biopolymer phase separation, Food Hydrocoll. 24 (2010) 689-701.

[202] Q. Zhong, H. Tian, S. Zivanovic, Encapsulation of fish oil in solid zein particles by liquid-liquid dispersion, J. Food Process. Preserv. 33 (2009) 255-270.

[203] E. Semo, E. Kesselman, D. Danino, Y.D. Livney, Casein micelle as a natural nano-capsular vehicle for nutraceuticals, Food Hydrocoll. 21 (2007) 936-942.

[204] Z. Teng, Y. Luo, Q. Wang, Nanoparticles synthesized from soy protein: preparation, characterization, and application for nutraceutical encapsulation, J. Agric. Food Chem. 60 (2012) 2712-2720.

[205] A.R. Bilia, C. Guccione, B. Isacchi, C. Righeschi, F. Firenzuoli, M.C. Bergonzi, Essential Oils Loaded in Nanosystems: A Developing Strategy for a Successful Therapeutic Approach, Evidence-Based Complementary and Alternative Medicine 2014 (2014).

[206] M. Schenk, C. Mueller, The mucosal immune system at the gastrointestinal barrier, Best Practice & Research Clinical Gastroenterology 22 (2008) 391-409.

[207] L. Plapied, N. Duhem, A. des Rieux, V. Préat, Fate of polymeric nanocarriers for oral drug delivery, Current Opinion in Colloid & Interface Science 16 (2011) 228-237.

[208] L.M. Ensign, R. Cone, J. Hanes, Oral drug delivery with polymeric nanoparticles: The gastrointestinal mucus barriers, Adv. Drug Deliv. Rev. 64 (2012) 557-570.

[209] H.N. Nellans, (B) Mechanisms of peptide and protein absorption:(1) Paracellular intestinal transport: modulation of absorption, Adv. Drug Deliv. Rev. 7 (1991) 339-364.

[210] P.S. Burton, R.A. Conradi, A.R. Hilgers, (B) Mechanisms of peptide and protein absorption:(2) Transcellular mechanism of peptide and protein absorption: passive aspects, Adv. Drug Deliv. Rev. 7 (1991) 365-385.

[211] C. Prego, D. Torres, M.J. Alonso, The potential of chitosan for the oral administration of peptides (2005).

[212] A. Bernkop-Schnürch, C. Kast, D. Guggi, Permeation enhancing polymers in oral delivery of hydrophilic macromolecules: thiomer/GSH systems, J. Controlled Release 93 (2003) 95-103.

[213] E. Roger, F. Lagarce, E. Garcion, J. Benoit, Biopharmaceutical parameters to consider in order to alter the fate of nanocarriers after oral delivery, Nanomedicine 5 (2010) 287-306.

[214] S.D. Conner, S.L. Schmid, Regulated portals of entry into the cell, Nature 422 (2003) 37-44.

[215] R. Peters, G.t. Dam, H. Bouwmeester, H. Helsper, G. Allmaier, F.v. Kammer, R. Ramsch, C. Solans, M. Tomaniová, J. Hajslova, S. Weigel, Identification and characterization of organic nanoparticles in food, TrAC Trends in Analytical Chemistry 30 (2011) 100-112.

Chapter 2

Objectives

Objetivos

El **objetivo general** del presente trabajo consiste en diseñar, optimizar y evaluar distintos tipos de nanopartículas a partir de proteínas de origen natural para incrementar la biodisponibilidad oral y eficacia de moléculas activas con potencial interés en los sectores farmacéutico, nutracéutico y alimentario.

Para llegar a la consecución de esta meta final, en el presente estudio se propusieron los siguiente **objeticos parciales**:

1. Diseño, optimización y caracterización de **nanopartículas de caseína** para la administración oral de moléculas activas.
    a. Preparación, optimización y evaluación de nanopartículas de caseína para la encapsulación de **ácido fólico** como modelo de molécula hidrosoluble. Evaluación del perfil de liberación *in vitro* y biodisponibilidad oral.
    b. Preparación, optimización y evaluación de nanopartículas de caseína para la encapsulación de **resveratrol** como molécula liposoluble de clase II. Evaluación de la cinética de liberación *in vitro,* biodistribución e interacción *ex vivo* con mucosa intestinal y biodisponibilidad oral.
    c. Preparación, optimización y evaluación de nanopartículas de caseína y nanopartículas de caseína con 2-hydroxi-propil-β-ciclodextrina para la encapsulación de **quercetina** como molécula liposoluble de clase IV. Evaluación de la cinética de liberación *in vitro* y biodisponibilidad oral.

2. Diseño, optimización y caracterización de **nanopartículas de zeína** para la administración oral de moléculas activas.
    a. Preparación, optimización y evaluación de nanopartículas de zeina para la encapsulación de **ácido fólico** como modelo de molécula hidrosoluble. Evaluación del perfil de liberación *in vitro*, biodistribución e interación *ex vivo* con mucosa intestinal y biodisponibilidad oral.
    b. Preparación, optimización y evaluación de nanopartículas de zeína y nanopartículas de zeína-caseína para la encapsulación de **resveratrol** como molécula liposoluble de clase II. Evaluación de la cinética de liberación *in vitro,* biodisponibilidad oral y eficacia en un modelo animal como antiinflamatorio.
    c. Preparación, optimización y evaluación de nanopartículas de zeína y nanopartículas de zeína con 2-hydroxi-propil-β-ciclodextrina para la encapsulación de **quercetina** como molécula liposoluble de clase IV. Evaluación de la cinética de liberación *in vitro,* biodisponibilidad oral y eficacia en un modelo animal como antiinflamatorio.

Chapter 3

Casein nanoparticles as carriers for the oral delivery of folic acid

Food hydrocolloids, 2015.(44):399-406

Abstract

Food grade proteins can be viewed as an adequate material for the preparation of nanoparticles and microparticles. They offer several advantages such as their digestibility, low price and a good capability to interact with a wide variety of compounds and nutrients. The aim of this work was to prepare and characterize casein nanoparticles for the oral delivery of folic acid. These nanoparticles were prepared by a coacervation process, stabilized with either lysine or arginine and, finally, dried by spray-drying. For some batches, the effect of a supplementary treatment of nanoparticles (before drying) with high hydrostatic pressure on the properties of the resulting carriers was also evaluated. The resulting nanoparticles displayed a mean size close to 150 nm and a folic acid content of around 25 µg per mg nanoparticle. From the *in vitro* release studies, it was observed that casein nanoparticles acted as gastro-resistant devices and, thus, folic acid was only released under simulated intestinal conditions. For the pharmacokinetic study, folic acid was orally administered to laboratory animals as a single dose of 1 mg/kg. Animals treated with folic acid-loaded casein nanoparticles displayed significantly higher serum levels than those observed in animals receiving an aqueous solution of the vitamin. As a consequence, the oral bioavailability of folic acid when administered as casein nanoparticles was calculated to be around 52%, a 50% higher than the traditional aqueous solution. Unfortunately, the treatment of casein nanoparticles by high hydrostatic pressure modified neither the release profile of the vitamin nor its oral bioavailability.

1 Introduction

In recent years, nano- and microencapsulation has been of a growing interest for pharmaceutical, nutraceutical and food applications. For food applications, these nano- and microencapsulation approaches may be of interest for any of the following reasons: i) protect the compound of interest from its premature degradation (during processing or storage) or undesirable interactions with the environment; ii) mask astringency tastes; iii) facilitate its processability (improving solubility and dispersability); iv) control and/or prolong its release; and/or v) improve its oral bioavailability [1,2].

Alimentary proteins, naturally present in food, offer a great potential as a material for the preparation of nanoparticles and microparticles. Overall they are biodegradable, digestible, cheap, offer a nutritional value, and, due to the presence of a number of functional groups, they can interact with a wide variety of compounds in a relatively non-specific way. Another important point is that they are usually considered as GRAS (generally recognized as safe) compounds. In addition, the procedures to transform these proteins into nanoparticles or microparticles are simple and can be performed in an aqueous medium or in environmentally and food grade accepted solvents. Examples of these proteins include legumin and vicilin from peas (*Pisumsativum* L.) [3,4], gliadin from wheat [3,5], zein from corn [6] or proteins from soy (*Glycine max* L.) [7].

Another interesting protein for micro- and nanoparticle design is casein. Casein is the major milk protein and possesses many structural and physicochemical properties that facilitate its functionality in drug delivery systems [8]. Thus, casein-based devices have been proposed for delivering hydrophobic bioactives and drugs including vitamin D2 [8], thymol[9], curcumin[10], and paclitaxel [11].

Folic acid (pteroyl-L-glutamic acid, vitamin B9) is a water-soluble vitamin that is essential in the human diet. The naturally occurring form of folic acid, folate, is typically obtained through consumption of green vegetables or dietary supplements [12]. This vitamin is especially important during the periods of rapid cell division and growth such as pregnancy and infancy when it is often necessary to take specific dosages of folic acid on daily basis [13]. The insufficiency of folic acid has long been known to be related to certain diseases such as neural tube defects in fetus and megaloblasticanaemia[14]. Other ailments associated with low levels of folic acid range from nervous system disturbances to cardiovascular disorders and cancer [15,16]. It is assumed that on a population level, nutritional requirements for folate cannot be completely covered by a varied diet, as recommended by national health authorities [15]. Thus, fortification with folic acid in one or more of the commonly consumed dietary items (i.e maize flour, milk, bread, etc) has been proposed as the best method to ensure that increased folate intake reduces the risks associated with folate deficiency. However, folic acid and folates are rather unstable molecules. In fact, folic acid is photosensitive and suffers from oxidative degradation, which is enhanced by oxygen, heat and acid pH conditions [17,18]. This results in a splitting of the molecule into biologically inactive forms [19] and, as suggested from different studies, in a significant decrease in the oral bioavailability of the vitamin [20,21].

The aim of this work was to design casein nanoparticles for the oral delivery of folic acid. The encapsulation of this vitamin in these carriers may be of interest to minimize the adverse effects and deteriorative reactions induced during food processing and cooking as well as to improve the oral bioavailability. In order to evaluate the capability of casein nanoparticles to promote the oral bioavailability of folic acid, a pharmacokinetic study in laboratory animals was carried out.

2 Materials and methods

2.1 Materials

Sodium caseinate was obtained from ANVISA (Madrid, Spain). Folic acid, lysine, arginine, pepsin, pancreatin, mannitol and sodium chloride were from Sigma-Aldrich (Germany) whereas ethanol and acetonitrile (HPLC grade) were from Merck (Darmstadt, Germany). AccuDiag™ Folate-Folic acid ELISA Kit was purchased from Diagnostic Automation/ Cortez Diagnostics Inc. (USA). All reagents and chemicals used were of analytical grade.

2.2 Preparation of casein nanoparticles

Casein nanoparticles were prepared by simple coacervation procedure followed by a purification step by ultrafiltration and subsequent drying by spray-drying [22].

2.3 Empty casein nanoparticles (NP)

Briefly, 1 g sodium caseinate and a determined amount of a basic aminoacid (either lysine or arginine) were firstly dissolved in 75 mL purified water by magnetic agitation at room temperature. Then, nanoparticles were formed by the addition of 40 mL of a calcium chloride solution in deionized water (0.8% w/v). The suspension was purified by ultrafiltration through a polysulfone membrane cartridge of 50 kDa pore size (Medica SPA, Italy). Finally, 20 mL of an aqueous solution of mannitol (100 mg/mL), was added to the suspension of casein nanoparticles in order to prevent irreversible aggregation of nanoparticles during the drying step, and the suspension was dried in a Büchi Mini Spray Drier B-290 apparatus (BüchiLabortechnik AG, Switzerland) under the following experimental conditions: (i) inlet temperature of 90°C, (ii) outlet temperature 45-50°C, (iii) air pressure: 2-5 bar, (iv) pumping rate of 2-6 mL/min, (v) aspirator of 100% and (vi) air flow at 900 L/h.

2.4 Folic acid-loaded casein nanoparticles (FA-NP)

The preparation of casein nanoparticles loaded with folic acid was similar to that of the empty particles, however some minor adjustments. Thus, 1 g sodium caseinate and 50 mg lysine were dissolved in 75 mL purified water. In parallel, 300 mg folic acid was dissolved in an aqueous solution of lysine (8 mg/mL). Then, 9 mL of the aqueous folic acid solution was added to the caseinate solution and the resulting mixture was incubated at room temperature for 10 min under magnetic stirring. Casein nanoparticles were obtained by the addition of 40 mL of a calcium chloride solution in purified water (0.8% w/v). The suspension was purified and dried as described above.

In order to evaluate the effect of a high pressure treatment on the main properties of these nanoparticles, some batches were subjected to different cycles of high hydrostatic pressure in an ISO-LAB FPG11500 apparatus (Stansted Fluid Power Ltd, UK) prior to the drying step.

For the identification of the different formulations, the following abbreviations were used: FA-NP-C (casein nanoparticles containing folic acid), FA-NP-C-P_X (folic acid-loaded casein nanoparticles stabilized by high pressure) and NP-C (control empty casein nanoparticles).

2.5 Characterization of nanoparticles

2.5.1 Size, zeta potential and morphology

The particle size distribution and zeta potential of the above formulations were measured by photon correlation spectroscopy (PCS) and electrophoretic laser Doppler anemometry, respectively, using a Zetaplus apparatus (Brookhaven Instrument Corporation, USA). The diameter of the nanoparticles was determined after dispersion in distilled water (1:10) and measured at 25°C with a scattering angle of 90°. The zeta potential was measured after dispersion of the dried nanoparticles in 1 mM pH 6 KClsolution.

The morphology and shape of nanoparticles was examined using a field emission scanning electron microscope FE-SEM (ULTRA Plus, Zeiss, The Netherlands). Prior to analysis, particles were washed to remove mannitol. For this purpose, spray-dried nanoparticles were resuspended in distilled water and centrifuged at 27,000xg for 10 min. Then, the supernatants were discarded and the obtained pellets were mounted on copper grids. Finally, the pellet was shaded with an amalgam of gold/palladium during fifteen seconds using a sputter coater (K550X Emitech, Ashford, UK).

2.5.2 Yield of the preparative process

In order to quantify the amount of protein transformed into nanoparticles, 10 mg of the nanoparticle formulation was dispersed in water and centrifuged at 17,000 x g for 20 min. Supernatants were discarded and the pellets were digested with NaOH 0.05M (casein nanoparticles). Then, the amount of protein was quantified by UV spectrophotometry at 282 nm in an Agilent 8453 system (Agilent Technologies, USA). For analysis, calibration curves were constructed between 150 and 1500 µg/mL (R^2> 0.9992; quantitation limit = 119 µg/mL).

The amount of protein forming nanoparticles in the formulation was estimated as the ratio between the amount of the protein quantified in the pellet of the centrifuged samples and the total amount of protein used for the preparation of nanoparticles and expressed as follows:

$$Yield\ (\%) = \frac{(Protein\ in\ pellet)}{(Total\ protein\ in\ the\ formulation)} \times 100 \text{ (Eq. 1)}$$

2.5.3 Folic acid analysis

The amount of folic acid loaded into the nanoparticles was quantified by HPLC-UV following an analytical method previously published [23] with minor modifications. Analysis was carried out in a 1100 series LC (Agilent, Germany) and a diode-array detector set at 290 nm. The chromatographic system was equipped with a reversed-phase 150 mm x 2.1 mm C18 Alltima column (5 µm particle size; Altech, USA) and a Gemini C18 precolumn (5 µm particle size;

Phenomenex, CA, USA). The mobile phase, pumped at 0.25 mL/min, was a gradient mixture (Table 1) of phosphoric acid (33 mM, pH 2.3) and acetonitrile. Under these conditions, folic acid eluted at 21.2 ± 0.5 min. For calculations, calibration curves were designed over the range of 2 and 200 μg/mL (R^2> 0.999). The limit of quantification was calculated to be 4.3 μg/mL.

Table 1. Folic Acid HPLC gradient (A: phosphoric acid 33mM, B: acetonitrile).

Time (min)	A (%)	B (%)
0	95	5
8	95	5
33	82.5	17.5
45	95	5

For analysis, 10 mg of nanoparticles were dispersed in 1 mL of water and centrifuged. In order to determine the amount of folic acid loaded inside the nanoparticles, the pellets were digested with NaOH 0.05 M. Each sample was assayed in triplicate and results were expressed as follows:

$$Folic\ acid\ loading\ (\mu g/\ mg\ NP) = \frac{FA\,p}{W\,p} \times 100 \text{ (Eq. 2)}$$

$$Encapsulation\ efficency\ (\%) = \frac{FA\,p}{FA\,t} \times 100 \text{ (Eq. 3)}$$

in which FAp corresponds to the amount of folic acid quantified in the pellets; FAt is the total amount of folic acid added and Wp being the amount of protein quantified as described in section 2.3.2).

2.6 In vitro release study

Release experiments were conducted under sink conditions at 37°C using simulated fluids for gastric (SGF; pH 1.2; pepsin 0.32% w/v) and intestinal (SIF; pH 6.8; pancreatin 1% w/v) conditions. The studies were performed under agitation in a Vortemp 56TM Shaking Incubator (Labnet International Inc., NJ USA) after the dispersion of the nanoparticles in the appropriate medium.

For each specific each time interval, the equivalent amount of nanoparticles encapsulating 20 μg of folic acid was resuspended in 1 mL of the corresponding simulated fluid. The different formulations were kept in the SGF for 2 hours before being transferred to SIF for a subsequent 20 hours. At different intervals, samples were collected and centrifuged at 17,000 rpm for 20 minutes. The amount of folic acid released was quantified by HPLC from the supernatants as described above.

2.7 In vivo pharmacokinetic studies in male Wistar rats

2.7.1 Pharmacokinetic studies

Pharmacokinetic studies were performed in male Wistar rats (200-250 g) obtained from Harlan (Barcelona, Spain). Studies were approved by the Ethical Committee for Animal Experimentation of the University of Navarra (protocol number 014-10) in accordance with the European legislation on animal experiments. Prior to the experiment, animals were adaptively fed for 1 week with free access to a Folic Acid deficient diet (TD 95247, Harlan, USA) and drinking water

(22±2°C; 12-h light and 12-h dark cycles; 50-60% relative humidity). Previous to the oral administration of the formulations, animals were fasted overnight to avoid interference with the absorption, allowing free access to water.

For the pharmacokinetic study, rats were randomly divided into 5 groups of 6 animals each. The experimental groups were: (i) aqueous solution of folic acid [Folic acid dissolved in PBS], (ii) folic acid-loaded casein nanoparticles (FA-NP-C) and (iii) folic acid-loaded casein nanoparticles treated by high pressure (400 MPa, 5 min) (FA-NP-C-P_3). For controls, a group of animals were intravenously (iv) administered with a solution of folic acid in PBS and the last group of rats group received PBS orally. Each treated animal received a folic acid dose of 1 mg/kg body weight. Folic acid or PBS solutions were administered either orally with a blunt needle via the oesophagus into the stomach or intravenously via tail vein.

Blood samples were collected at different times post-administration in specific serum tubes (SARSTEDT Microtube 1.1 mL Z-Gel). The volemia was recovered intraperitoneally with an equal volume of sterile saline solution pre-heated to body temperature. Samples were immediately centrifuged at 10,000 rpm for 10 min. Serum was separated into clean tubes and kept frozen at -80 °C until analysis.

2.7.2 Determination of Folic Acid in serum

The amount of folic acid in serum was determined by an Enzyme Immunoassay. Calibrator and quality control samples were prepared by adding appropriate volumes of standard folic acid solution in PBS to serum. Calibration curves were designed over the range 4-450 ng/mL (r^2> 0.996). For analysis, 100 µL of the serum samples were added to each well of the microtiter plate, followed by the addition of 50 µL of folic acid antibody. After incubation for 60 min at room temperature, the plate was washed three times with the washing solution (PBS-Tween 20 0.5%). Then, 100 µL of conjugate (anti-mouse-IgG-HRP) was added into each well and after 60 min at room temperature, the plate was washed again for three times with the washing solution. For the reaction, 100 µL of substrate was added into each well and incubated in the dark for 20 min at room temperature. The reaction was stopped by the addition of 100 µL sulphuric acid 0.5 M into each well. Finally, the absorbance was measured at 450 nm in an ELISA reader (LabsystemsiEMS Reader MF).

Under these experimental conditions, the limit of quantification of this method was calculated to be 4 ng/mL. The recovery of folic acid from serum samples was 90.1 ± 0.3 %. Accuracy values during the same day (intraday assay) at low, medium and high concentrations of FA were always within the acceptable limits (less than 15%).

2.7.3 Pharmacokinetic data analysis

The pharmacokinetic analysis of serum concentration plotted against time data, obtained after administration of the different folic acid formulations, was performed using a non-compartmental model with the WinNonlin 5.2 software (Pharsight Corporation, Mountain View, USA). The following parameters were estimated: maximal serum concentration (C_{max}), time taken to reach C_{max} (T_{max}), area under the concentration-time curve from time 0 to ∞ (AUC), mean residence time (MRT), clearance (Cl), volume of distribution (V) and half-life in the

terminal phase ($t_{1/2}$). Furthermore, the relative oral bioavailability (Fr %) of folic acid was estimated using the following equation:

$$Fr\ (\%) = \frac{AUC\ oral}{AUC\ iv} \times 100 \quad \text{[Eq. 4]}$$

where AUC iv and AUC oral are the areas under the curve for the iv and oral administrations, respectively.

2.8 Statistical analysis

Data are expressed as the mean ± standard deviation (S.D.) of at least three experiments. The non-parametric Kruskall-Wallis followed by Mann-Whitney U-test was used to investigate statistical differences. In all cases, $p< 0.05$ was considered to be statistically significant. All data processing was performed using SPSS® statistical software (SPSS® 15, Microsoft, USA).

3 Results

3.1 Optimization of the preparative process of casein nanoparticles

Casein nanoparticles were prepared by simple coacervation in the presence of calcium. However, the resulting nanoparticles displayed a low stability in an aqueous environment. Thus, the first step of this work was to optimize the preparative process of casein nanoparticles in order to stabilize them by preventing their aggregation that occurs with time in an aqueous environment. For this purpose, the influence of the presence of either lysine or arginine on the physico-chemical properties and stability of the resulting nanoparticles was carried out. Table 2 summarizes the physico-chemical properties of casein nanoparticles when prepared at an aminoacid/protein ratio (by weight; g/g) of 0.12. Interestingly, when nanoparticles were prepared in the presence of a basic aminoacid, the mean diameter of the resulting nanoparticles decreased significantly. Similarly, the polydispersity index was also slightly lower than for nanoparticles prepared in the absence of the aminoacid. In all cases, the yield of the preparative process was high, with more than 95% of the initial protein transformed into nanoparticles.

On the other hand, the stabilizing effect of both lysine and arginine was found to be adequate with an amino acid/protein ratio ranged from 0.02 to 0.25 (data not shown).

Regarding the stability of these nanoparticles in an aqueous medium, it was observed that for non-stabilised nanoparticles (NP-1 in Table 2) the mean size and the polydispersity index increased rapidly with time. In fact, two hours of incubation in water produced nanoparticles with a mean size close to 330 nm and a PDI of about 0.5. On the contrary, the size of nanoparticles stabilised with lysine were not affected for at least 48 h, whereas nanoparticles stabilised with arginine displayed a similar size and PDI for 16 h.

Table 2.Physico-chemical characteristics of casein nanoparticles prepared in the presence of either lysine or arginine as stabilizing agents at an amino acid/protein ratio of 0.12 before the drying step. Data expressed as mean ± SD, n=6. PDI: polydispersity index.

	Stabilising agent	Size (nm)[a]	PDI	Zeta potential (mV)[b]	Yield (%)[c]
NP-1	None	154 ± 30	0.24±0.04	-17.6 ± 0.3	97 ± 5
NP-2	Lysine	128 ± 4	0.18 ±0.01	- 14.0 ± 0.5	95 ± 3
NP-3	Arginine	135 ± 2	0.17 ±0.01	- 14.5 ± 0.6	97 ± 1

NP-1:Casein nanoparticles prepared without lysine, NP-2: Casein nanoparticles prepared with a lysine/casein ratio of 0.12 (by weight; g/g) and NP-3: Casein nanoparticles prepared with an arginine/casein ratio of 0.12 (by weight; g/g).

[a] Determination of the nanoparticle size (nm) by photon correlation spectroscopy.

[b] Determination of the zeta potential (mV) by electrophoretic laser Doppler anemometry.

[c] Determination of yield process (%).

After purification of nanoparticles, the last step was to dry the suspensions in a Spray-drier apparatus. Once more, the presence of the basic aminoacid was a key factor to minimize the aggregation phenomenon between casein nanoparticles and the stability of the resulting nanoparticles (Table 3). In fact, for stabilised nanoparticles the mean size slightly increased (in comparison to fresh suspensions before the drying step, see Table 2); although, in all cases, the mean size of the resulting nanoparticles remained below 200 nm. On the contrary, for unstabilised nanoparticles (NP-1), the mean size after drying increased significantly up until a size reaching around 300 nm.

Table 3.Effect of the drying step with a Spray-drying apparatus on the physico-chemical properties of casein nanoparticles. Data expressed as mean ± SD, n=3. PDI: polydispersity index.

	Stabilizing agent	Size (nm)[a]	PDI	Zeta potential (mV)[b]
NP-1	None	305 ± 56	0.45 ± 0.02	-9.8 ± 0.2
NP-2	Lysine	170 ± 4	0.25 ± 0.02	-11.9 ± 0.9
NP-3	Arginine	184 ± 2	0.25 ± 0.01	-9.4 ± 0.2

NP-1:Casein nanoparticles prepared without lysine, NP-2: Casein nanoparticles prepared with a lysine/casein ratio of 0.12 (by weight; g/g) and NP-3: Casein nanoparticles prepared with an arginine/casein ratio of 0.12 (by weight; g/g).

[a]Determination of the nanoparticle size (nm) by photon correlation spectroscopy.

[b]Determination of the zeta potential (mV) by electrophoretic laser Doppler anemometry.

3.2 Folic-acid loaded casein nanoparticles

Table 4 summarizes the main physico-chemical properties of folic acid loaded nanoparticles. When the vitamin was encapsulated into casein nanoparticles, a moderate decrease in the mean size of the resulting carriers was observed (about 170 nm for empty nanoparticles vs 157 nm for FA-NP-C). Similarly, the negative zeta potential of nanoparticles slightly increased to -17 mV. The folic acid loading into the casein nanoparticles (FA-NP-C) was calculated to be around 25 µg/mg nanoparticle with encapsulation efficiencies of about 40%.

In order to study the effect of a high hydrostatic pressure treatment on the physico-chemical characteristics of nanoparticles, different batches were subjected to increasing pressure conditions (from 100 to 600 MPa) for a period of 5 min. Table 4 summarizes these results. High pressure processing slightly decreased the mean size and the negative zeta potential of the resulting nanoparticles. On the contrary, the folic acid loading was not affected by a pressure treatment below 400 MPa. Under more drastic conditions (600 MPa for 5 min) the folic acid loading appeared to increase; although this result can be related to a decrease in the recovery of small nanoparticles by centrifugation (see Methods).

Table 4.Physico-chemical characteristics of folic acid-loaded casein nanoparticles. Data expressed as mean ± SD (n = 4).

	High pressure treatment	Size (nm)[a]	PDI	Zeta potential (mV)[b]	FA loading (µg/mg NP)[c]
NP-C	NA	170±4	0.25±0.02	- 11.9±0.9	
FA-NP-C	NA	157±5	0.17±0.01	-17.2±1.2	24±1
FA-NP-C-P_1	100 MPa / 5 min	144± 3	0.13±0.01	-13.6±0.2	25±5
FA-NP-C-P_2	200 MPa / 5 min	139± 1	0.22±0.02	-13.2±0.5	23±1
FA-NP-C-P_3	400 MPa / 5 min	134±3	0.14±0.01	-14.1±2.3	25±2
FA-NP-C-P_4	600 MPa / 5 min	111±2	0.15±0.01	-12.8±0.4	31±3

Figure 1 shows the SEM microphotographs of folic acid-loaded casein nanoparticles. Nanoparticles prepared without using the high pressure treatment appear to be spherical. However, the same nanoparticles displayed an irregular shape with a rough surface following treatment with high hydrostatic pressure. In any case, the apparent sizes observed by SEM were similar to those values obtained by photon correlation spectroscopy.

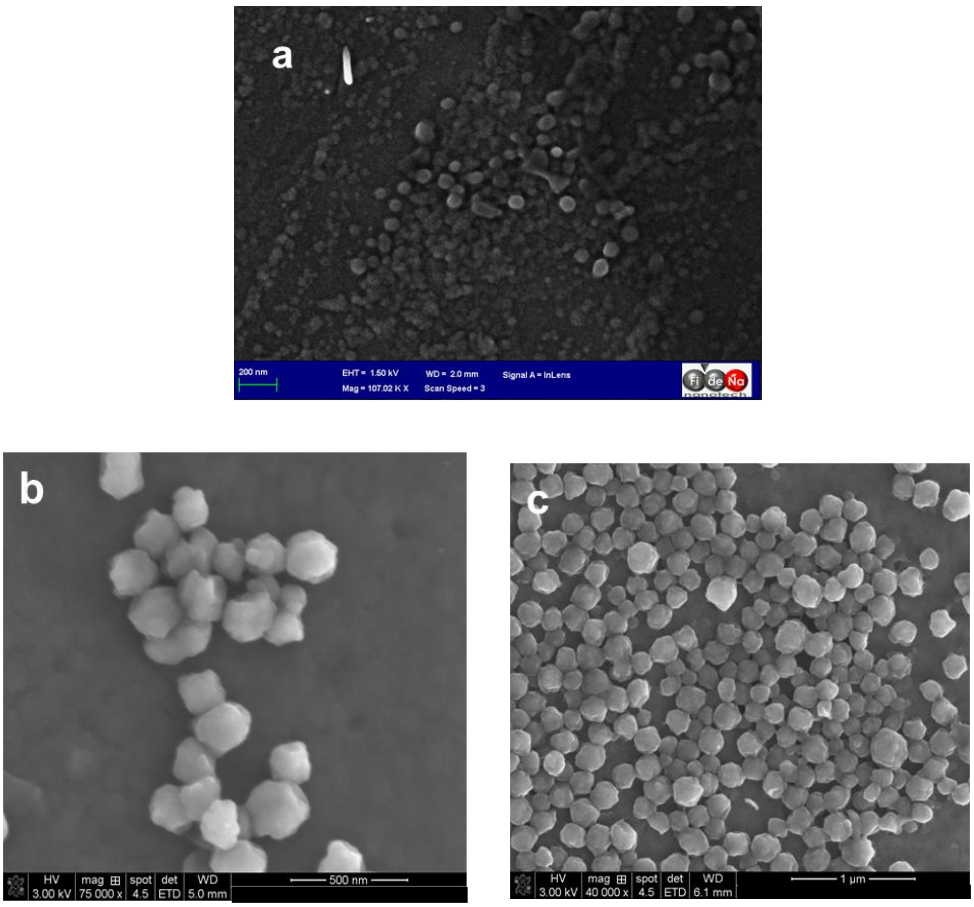

Figure 1 .Scanning electron microscopy (SEM) of folic acid-loaded casein nanoparticles. a) Nanoparticles prepared in normal conditions without using a high pressure procedure (FA-NP-C); b) Nanoparticles prepared with a hydrodynamic pressure treatment of 100 MPa/ 5 min (FA-NP-C-P_1); c) Nanoparticles prepared with a hydrodynamic pressure treatment of 400 MPa/ 5 min (FA-NP-C-P_3).

3.3 In vitro release study

Folic acid release kinetics from casein nanoparticles were evaluated in two different media: simulated gastric fluid (SGF) and simulated intestinal fluid (SIF). Figure 2 represents the release profiles of folic acid from the different assayed formulations as cumulative percentage of drug released as a function of time.

For all the formulations evaluated, there was no release of folic acid when nanoparticles were dispersed in SGF. In contrast, when nanoparticles were dispersed in the SIF, the release behavior of folic acid from the nanoparticles exhibited a biphasic pattern. For conventional casein nanoparticles (FA-NP-C), an extremely rapid discharge of folic acid (close to 60-70% of the loaded vitamin) was exhibited followed by a more sustained and slow release of the vitamin. Finally, around 90% of the loaded vitamin was released. For the formulations of casein nanoparticles stabilized by high pressure (FA-NP-C_3), again, the first pulse of folic acid release was also around 60-70%; although after this stage, no further release was displayed for at least 7 hours.

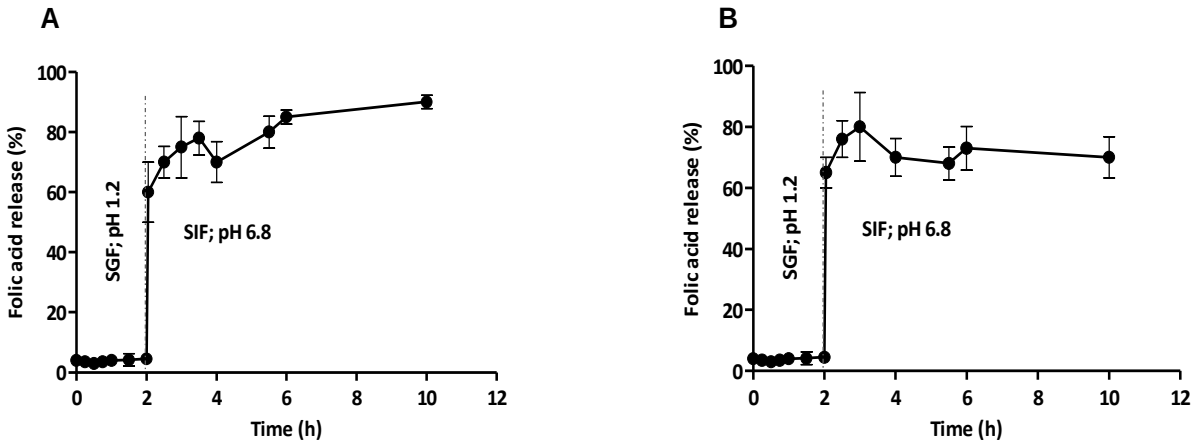

Figure 2. In vitro release studies of folic acid from casein nanoparticles after its incubation in simulated gastric fluid (SGF) during the first 2 hours and simulated intestinal fluid (SIF) (2-24h). A) Nanoparticles without high pressure treatment (FA-NP-C), B) Nanoparticles treated with high pressure (FA-NP-C-P_3). Data expressed as mean ± SD (n=4).

3.4 Pharmacokinetic studies in Wistar rats

The serum concentration profiles for the folic acid solution in PBS after a single intravenous injection (dose 1 mg/kg) are presented in **Figure 3**. Data were adjusted to a non-compartmental model. The folic acid serum concentration decreased rapidly displaying a biphasic pattern. The peak plasma concentration (C_{max}) of folic acid was about 6 µg/mL. The values obtained for AUC and half-life ($t_{1/2}$) were 3.7 µg h/mL and 1.1 hours, respectively. The mean residence time (MRT) was 0.9 hours; whereas the folic acid clearance and its volume of distribution were calculated to be 0.06 L/h and 0.1 L, respectively (Table 5).

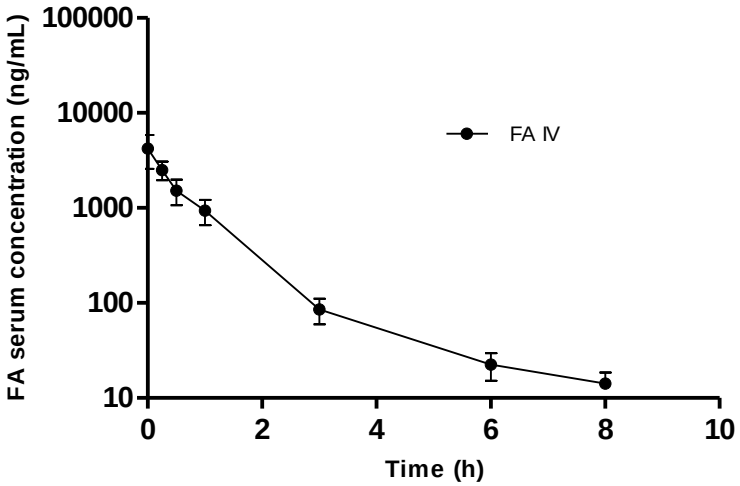

Figure 3. Folic acid concentration vs time after a single intravenous administration of folic acid solution (dose 1 mg/kg). Data expressed as mean± SD, (n= 6).

Figure 4 shows the serum concentration versus time profile after oral administration of folic acid (single dose of 1 mg/kg) formulated as aqueous solution or loaded in casein nanoparticles. From the oral administration of the aqueous solution, the folic acid levels in the serum of animals increased rapidly during the first 1 hour post-administration (in which the $C_{max}$was reached). Then, the amount of vitamin in serum decreased slowly until the end of the experiment (24 h post-administration). For nanoparticle formulations, the folic acid serum levels vs. time displayed similar profiles to the one obtained for the free folic acid (FA solution). However, in all cases, the serum levels of the vitamin from nanoparticles were significantly higher than these observed for the aqueous solution of folic acid. Surprisingly, the treatment of casein nanoparticles by high hydrostatic pressure did not significantly modify the serum vitamin levels observed with untreated nanoparticles.

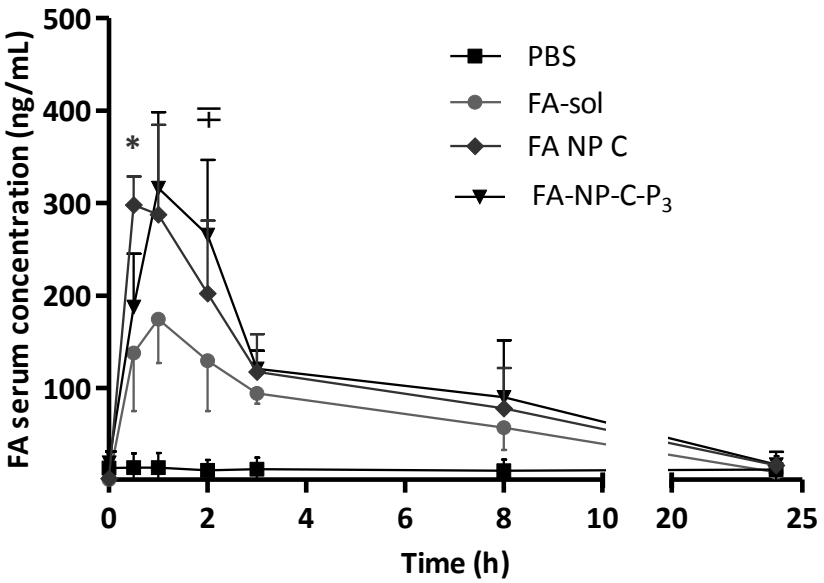

Figure 4. Folic acid concentration vs time after a single oral administration of the different formulations at dose of 1mg/kg. i) PBS (■), ii) Folic acid (FA) solution (FA sol, ●), iii) FA-loaded casein nanoparticles (FA-NP-C, ♦), iv) FA-loaded casein nanoparticles treated by high hydrodynamic pressure (FA-NP-C-P_3, ▼). Data expressed as mean± SD,(n= 6).* p<0.05 FA-NP-C *vs* FA solution. U de Mann Whitney test.
‡p< 0.05 FA-NP-C-P_3*vs* FA solution. U de Mann Whitney test.

Table 5 summarizes the pharmacokinetic parameters estimated for the analysis of the experimental data obtained after the administration of the different folic acid formulations to rats.When folic acid was administrated as aqueous solution, the AUC was around 1.4 μg h/mL. In the case of folic acid encapsulated in casein nanoparticles, the AUC was around 2.0 μg h/mL and a similar value was observed when the nanoparticles were treated with high pressure (2.2 μg h/mL). In any case, the AUC values of nanoparticles were significantly higher than those of orally administered free folic acid (p< 0.05). Similarly, the peak plasma concentration (C_{max}) of folic acid in the nanoparticles was around 1.5- times higher than for the aqueous solution of the vitamin. On the contrary, other important pharmacokinetic parameters of folic acid (eg. volume of distribution, clearance or half-life of the terminal phase) were statistically similar when the vitamin was administered as aqueous solution or loaded in casein nanoparticles (p<0.05). Finally, the relative oral bioavailability of folic acid when incorporated to casein nanoparticles was of about 52%, whereas for the folic acid aqueous solution the oral bioavailability was only of 35%.

Table 5. Pharmacokinetic parameters estimated after a single dose of 1 mg/kg body weight of folic acid formulated in nanoparticles or in a solution, either orally or intravenously administered. FA: folic acid; FA sol: folic acid aqueous solution; FA-NP-C: FA-loaded casein nanoparticles; FA-NP-C-P3: FA-loaded casein nanoparticles treated by high hydrodynamic pressure. (n=6).

	Route	C max (µg/mL)	T max (h)	AUC (µgh/mL)	t ½ (h)	Cl (L/h)	Vd (L)	MRT (h)	Fr (%)
PBS	p.o	-	-	-	-	-		-	-
FA i.v.	p.iv	5.5 ± 2.7**	0	3.7 ± 0.4**	1.2±0.6	0.06±0.01	0.10±0.05	0.9±0.2**	100**
FA sol	p.o.	0.2 ± 0.0	1.0 ± 0.6	1.3 ± 0.3	5.9±1.9	0.06±0.02	0.44±0.07	5.7±1.6	35
FA-NP-C	p.o.	0.3 ± 0.1	1.2 ± 0.4	2.1± 0.6 *	5.8±2.1	0.05±0.02	0.42±0.10	5.8±1.2	52*
FA-NP-C_3	p.o.	0.3 ± 0.0*	0.8 ± 0.3	2.2 ± 0.4 *	7.3±2.3	0.05±0.01	0.54±0.24	6.1±0.9	53*

AUC: area under the curve concentration-time from time 0 to ∞, C_{max} : peak plasma concentration; T_{max} : time to peak plasma concentration; $t_{1/2\,z}$: half-life of the terminal phase; Cl: clearance; MRT: mean residence time; Fr: relative oral bioavailability.

* $p<0.05$ vs FA solution.U de Mann Whitney Test.

** $p<0.01$ vs FA solution. U de Mann Whitney test.

4 Discussion

In this work we describe the preparation of casein nanoparticles under mild conditions in an aqueous environment using a basic amino-acid (eg. lysine or arginine) as a stabilizing agent of the resulting nanocarriers. These nanoparticles were subsequently dried using a Spray-drying apparatus. Casein nanoparticles were prepared by a coacervation method in which the addition of a calcium salt to an aqueous solution of sodium caseinate produces the formation of "insoluble" calcium caseinate that, in our experimental conditions, adopted the form of nanoparticulates. It is well known that calcium ions specifically bind to phosphoserine residues on the caseins [24], thereby modifying the molecular charge distribution, self-assembly behavior, and aggregation/flocculation properties [25,26]. In our case, the formation of homogeneous batches of nanoparticles would be related with the presence of a basic aminoacid (either lysine or arginine). In fact, the presence of a basic aminoacid prevented the aggregation of casein nanoparticles when dispersed in an aqueous medium (Tables 2 and 3). In the case of nanoparticles stabilized with lysine, there was no variation in the physico-chemical properties of these nanoparticles 48 h after their incubation in an aqueous medium (section 3.1). This effect would be directly related with the development of electrostatic interactions between amino groups (of either lysine or arginine) and carboxyl moieties (-COOH residues in glutamic and/or aspartic acids) of casein. Sodium caseinate is rich in aspartic (about 8%) and glutamic acids (around 22%) [27] and the development of these interactions have been extensively described in the literature [28,29] and they would be involved in the stabilization of peptides [30] and actin depolymerisation[31]. As a consequence of these interactions between aspartic and glutamic acids in casein nanoparticles and the basic aminoacid, the surface of the resulting nanoparticles would be more hydrophilic minimizing the possibilities of aggregation as observed for unstabilized nanoparticles.

Casein nanoparticles were evaluated as oral delivery systems for folic acid. The use of casein offers an important advantage due to its capability to bind, through hydrophobic bonds, with vitamin B9 thus protecting the folic acid against photodecomposition [32]. The resulting folic acid-loaded nanoparticles were spherical (Figure 1) and displayed a size of around 157 nm with a vitamin loading of about 25 µg per mg nanoparticle (Table 3). Some batches of casein nanoparticles were treated with high hydrostatic pressure in order to harden them, thus to modify and modulate the release rate and the bioavailability of folic acid. Following an ultra-high pressure homogenization process the average diameter of folic acid-loaded casein nanoparticles decreased. Thus, at 400 MPa for 5 min, the mean size of nanoparticles was 15% lower than with untreated nanoparticles. This finding is consistent with those of Semo and co-workers who found a decrease in the average diameter of β-casein micelles treated by ultra-high pressure homogenization [8]. In our case, the high pressure treatment also resulted in a morphology change of the resulting nanoparticles, which displayed an irregular shape as observed by SEM (Figure 1).

The release profile of folic acid from casein nanoparticles was found to be dependent on the pH conditions (Figure 2). Thus, under simulated gastric conditions (pH 1.2), no vitamin release was observed from the casein nanoparticles. This effect could be due to the fact that pepsin preferably attacks peptide bonds involving hydrophobic aromatic amino acids. These residues,

due to their hydrophobicity, would be trapped inside the protein network during the preparation of casein nanoparticles by the addition of calcium chloride [33]. On the contrary, under simulated intestinal conditions, the folic acid release profile was firstly characterized by a rapid release of the cargo followed by a more continuous and slower unloading of the remaining folic acid. This phenomenon can be related with the repulsion effect between the negative charges of both folic acid and casein at a neutral pH. In fact, casein is a phosphoprotein with an apparent isoelectric point of 4.6 [34] and therefore, at pH 6.8, both casein and folic acid should present a net negative charge that would eject the vitamin from the carrier. On the other hand, the treatment of casein nanoparticles with a high pressure procedure had little effect on the release profile of folic acid. The main difference was that, at intestinal pH, the folic acid release was around 10% lower than that observed with untreated casein nanoparticles.

For the *in vivo* pharmacokinetic studies, a single dose of 1 mg/kg of folic acid was selected. When folic acid was administered orally, either as aqueous solution or loaded in casein nanoparticles, the serum levels of the vitamin increased rapidly and the maximum plasma concentrations were achieved within a very short time period, ie. within 1.5 h post-administration. Following this, the folic acid levels declined slowly and were quantified in serum up to 24 h post-administration. Interestingly, these profiles of folic acid serum concentration *vs.* time were similar to those reported previously by other authors, in which human studies were used [35,36]. In any case, folic acid serum levels and AUC from casein nanoparticles were significantly higher than those observed with the traditional aqueous solution (Table 4). With the different formulations tested, the rank order of the mean AUC of serum folic acid concentration *vs*. time was as follows: FA-NP-C-P_3 = FA-NP-C > FA solution ($p < 0.05$). In accordance to this, the relative oral bioavailability (calculated as the ratio between the AUC of folic acid when administered orally and the AUC of the intravenous solution) was calculated to be 35% for the aqueous solution and 52% for casein nanoparticles.The treatment of casein nanoparticles by high pressure (400 MPa) had not significant effect on this pharmacokinetic parameter.

The values obtained from the pharmacokinetic bioavailability study are not easily comparable with previous results due to a scarcity of this information in the literature. In addition some factors such as the interindividual variation, the diet and the dose may produce different results [12]. In this context, in a recent study, Nguyen et al. compared the serum levels of a single dose of folic acid in non-pregnant women. At low doses of the vitamin (20 and 70 µg/kg) they stated that a proportional relationship between folic acid dosing and pharmacokinetics (AUC) exists [36]. On the contrary, another interesting work in which folic acid was evaluated in healthy volunteers at a single dose of either 0.6 or 3 mg/kg, the oral bioavailability of the vitamin appeared to be highly influenced by the dose. Thus, with the lower dose, the bioavailability was particularly high (around 60%); differently, with the higher dose tested, this parameter was only around 17% [37]. This observation could be related to the fact that, at least in part, intestinal absorption of folic acid through the small intestine is a saturable process [38,39].

Conclusions

In summary, casein nanoparticles can be prepared by coacervation with calcium and subsequently dried in a Spray-drying apparatus. The use of either lysine or arginine allows for a successful stabilization of the resulting nanoparticles, preventing their aggregation in an aqueous environment. In this way, casein nanoparticles were capable of encapsulating folic acid, preventing its release in an acid environment and thus promoting its oral bioavailability, as observed during studies using a rat model. Unfortunately, under the experimental conditions used in this work, the treatment of casein nanoparticles with a high hydrostatic pressure did not significantly modify the release profile and oral bioavailability of folic acid. In any case, the oral bioavailability of folic acid when administered in casein nanoparticles was around 50% higher than when formulated as an aqueous solution.

Acknowledgements

This work was supported by the Regional Government of Navarra (Alimentos funcionales, Euroinnova call) and the Spanish Ministry of Science and Innovation and Gobierno de Navarra (ADICAP; ref. IPT-2011-1717-900000). Rebeca Penalvaacknowledgesthe “Asociación de Amigos Universidad de Navarra” forthefinancialsupport.

References

[1] K.G.H. Desai, H. Jin Park, Recent developments in microencapsulation of food ingredients, Drying Technol 23 (2005) 1361-1394.

[2] M.X. Quintanilla-Carvajal, B.H. Camacho-Díaz, L.S. Meraz-Torres, J.J. Chanona-Pérez, L. Alamilla-Beltrán, A. Jimenéz-Aparicio, G.F. Gutiérrez-López, Nanoencapsulation: a new trend in food engineering processing, Food Engineering Reviews 2 (2010) 39-50.

[3] I. Ezpeleta, J.M. Irache, S. Stainmesse, J. Gueguen, A. Orecchioni, Preparation of small-sized particles from vicilin (vegetal protein from *Pisum sativum L.*) by coacervation, European Journal of Pharmaceutics and Biopharmaceutics 42 (1996) 36-41.

[4] J.M. Irache, L. Bergougnoux, I. Ezpeleta, J. Gueguen, A. Orecchioni, Optimization and in vitro stability of legumin nanoparticles obtained by a coacervation method, Int. J. Pharm. 126 (1995) 103-109.

[5] M.A. Arangoa, M.A. Campanero, M.J. Renedo, G. Ponchel, J.M. Irache, Gliadin nanoparticles as carriers for the oral administration of lipophilic drugs. Relationships between bioadhesion and pharmacokinetics, Pharm. Res. 18 (2001) 1521-1527.

[6] Q. Zhong, H. Tian, S. Zivanovic, Encapsulation of fish oil in solid zein particles by liquid-liquid dispersion, J. Food Process. Preserv. 33 (2009) 255-270.

[7] Z. Teng, Y. Luo, Q. Wang, Nanoparticles synthesized from soy protein: preparation, characterization, and application for nutraceutical encapsulation, J. Agric. Food Chem. 60 (2012) 2712-2720.

[8] E. Semo, E. Kesselman, D. Danino, Y.D. Livney, Casein micelle as a natural nano-capsular vehicle for nutraceuticals, Food Hydrocoll. 21 (2007) 936-942.

[9] X. Pan, M. Mu, B. Hu, P. Yao, M. Jiang, Micellization of casein-graft-dextran copolymer prepared through Maillard reaction, Biopolymers 81 (2006) 29-38.

[10] M. Esmaili, S.M. Ghaffari, Z. Moosavi-Movahedi, M.S. Atri, A. Sharifizadeh, M. Farhadi, R. Yousefi, J. Chobert, T. Haertlé, A.A. Moosavi-Movahedi, Beta casein-micelle as a nano vehicle for solubility enhancement of curcumin; food industry application, LWT-Food Science and Technology 44 (2011) 2166-2172.

[11] A. Shapira, I. Davidson, N. Avni, Y.G. Assaraf, Y.D. Livney, β-Casein nanoparticle-based oral drug delivery system for potential treatment of gastric carcinoma: Stability, target-activated release and cytotoxicity, European Journal of Pharmaceutics and Biopharmaceutics 80 (2012) 298-305.

[12] I.A. Brouwer, M. van Dusseldorp, C.E. West, R.P. Steegers-Theunissen, Bioavailability and bioefficacy of folate and folic acid in man, Nutrition Research Reviews 14 (2001) 267-294.

[13] Y. Lamers, Folate recommendations for pregnancy, lactation, and infancy, Ann. Nutr. Metab. 59 (2011) 32-37.

[14] H. Heseker, Folic acid and other potential measures in the prevention of neural tube defects, Ann. Nutr. Metab. 59 (2011) 41-45.

[15] R. Iyer, S. Tomar, Folate: a functional food constituent, J. Food Sci. 74 (2009) R114-R122.

[16] A.F. Kolb, L. Petrie, Folate deficiency enhances the inflammatory response of macrophages, Mol. Immunol. 54 (2013) 164-172.

[17] M.J. Akhtar, M.A. Khan, I. Ahmad, Photodegradation of folic acid in aqueous solution, J. Pharm. Biomed. Anal. 19 (1999) 269-275.

[18] M.K. Off, A.E. Steindal, A.C. Porojnicu, A. Juzeniene, A. Vorobey, A. Johnsson, J. Moan, Ultraviolet photodegradation of folic acid, Journal of Photochemistry and Photobiology B: Biology 80 (2005) 47-55.

[19] H. Madziva, K. Kailasapathy, M. Phillips, Evaluation of alginate–pectin capsules in Cheddar cheese as a food carrier for the delivery of folic acid, LWT-Food Science and Technology 39 (2006) 146-151.

[20] K. O'Leary, P. Sheehy, Effects of preparation and cooking of folic acid-fortified foods on the availability of folic acid in a folate depletion/repletion rat model, J. Agric. Food Chem. 49 (2001) 4508-4512.

[21] V.E. Ohrvik, C.M. Witthoft, Human folate bioavailability, Nutrients 3 (2011) 475-490.

[22] Agüeros, M., Esparza,, I., González-Ferrero, C., González-Navarro, C.J., Irache, J.M., Romo, A, Nanoparticles for encapsulating compounds, preparation thereof and use of same. (2011).

[23] I. Sierra, C. Vidal-Valverde, A simple method to determine free and glycosylated vitamin B6 in legumes, J. Liq. Chromatogr. Rel. Technol. 20 (1997) 957-969.

[24] H.E. Swaisgood, Chemistry of milk proteins, in: P.F. Fox (Ed.), Developments in Dairy Chemistry-1: Proteins, Applied Science Publishers, New York, NY, 1982, pp. 1-59.

[25] D.S. Horne, Casein interactions: casting light on the black boxes, the structure in dairy products, Int. Dairy J. 8 (1998) 171-177.

[26] A. Pitkowski, T. Nicolai, D. Durand, Stability of caseinate solutions in the presence of calcium, Food Hydrocoll. 23 (2009) 1164-1168.

[27] S. Sindayikengera, Nutritional evaluation of caseins and whey proteins and their hydrolysates from Protamex, Journal of Zhejiang University Science B 7 (2006) 90-98.

[28] B. Wiman, P. Wallén, Structural Relationship between “Glutamic Acid” and “Lysine” Forms of Human Plasminogen and Their Interaction with the NH2-Terminal Activation Peptide as Studied by Affinity Chromatography, European Journal of Biochemistry 50 (1975) 489-494.

[29] J.M. Scholtz, H. Qian, V.H. Robbins, R.L. Baldwin, The energetics of ion-pair and hydrogen-bonding interactions in a helical peptide, Biochemistry (N. Y.) 32 (1993) 9668-9676.

[30] R. Sudha, M. Kohtani, G.A. Breaux, M.F. Jarrold, π-Helix preference in unsolvated peptides, J. Am. Chem. Soc. 126 (2004) 2777-2784.

[31] C.Y. Lee, J. Lou, K.K. Wen, M. McKane, S.G. Eskin, S. Ono, S. Chien, P.A. Rubenstein, C. Zhu, L.V. McIntire, Actin depolymerization under force is governed by lysine 113:glutamic acid 195-mediated catch-slip bonds, Proc. Natl. Acad. Sci. U. S. A. 110 (2013) 5022-5027.

[32] J. Zhang, Y. Liu, X. Liu, Y. Li, X. Yin, M. Subirade, P. Zhou, L. Liang, The folic acid/β-casein complex: Characteristics and physicochemical implications, Food Res. Int. 57 (2014) 162-167.

[33] L. Beaulieu, L. Savoie, P. Paquin, M. Subirade, Elaboration and characterization of whey protein beads by an emulsification/cold gelation process: application for the protection of retinol, Biomacromolecules 3 (2002) 239-248.

[34] C. Holt, Structure and Stability of Bovine Casein Micelles, in: Structure and Stability of Bovine Casein MicellesAdvances in Protein Chemistry, Academic Press, 1992, pp. 63-151.

[35] N.C. Alemdaroglu, U. Dietz, S. Wolffram, H. Spahn-Langguth, P. Langguth, Influence of green and black tea on folic acid pharmacokinetics in healthy volunteers: potential risk of diminished folic acid bioavailability, Biopharm. Drug Dispos. 29 (2008) 335-348.

[36] P. Nguyen, R. Boskovic, P. Yazdani, B. Kapur, H. Vandenberghe, G. Koren, Comparing folic acid pharmacokinetics among women of childbearing age: single dose ingestion of 1.1 versus 5 MG folic acid, Can. J. Clin. Pharmacol. 15 (2008) 314-22.

[37] J.C. Schmitz, R.K. Stuart, D.G. Priest, Disposition of folic acid and its metabolites: a comparison with leucovorin, Clinical Pharmacology & Therapeutics 55 (1994) 501-508.

[38] R.M. Russell, B.B. Golner, S.D. Krasinski, J.A. Sadowski, P.M. Suter, C.L. Braun, Effect of antacid and H2 receptor antagonists on the intestinal absorption of folic acid, J. Lab. Clin. Med. 112 (1988) 458-463.

[39] J.B. Mason, R. Shoda, M. Haskell, J. Selhub, I.H. Rosenberg, Carrier affinity as a mechanism for the pH-dependence of folate transport in the small intestine, Biochimica Et Biophysica Acta (BBA)-Biomembranes 1024 (1990) 331-335.

Chapter 4

Casein based nanoparticles as carriers for the oral delivery of resveratrol

Abstract.

The interest in resveratrol has increased due to its pharmacological effects that include cardioprotective and anticarcinogenic effects. However, apart from its low stability, this compound has a poor oral bioavailability being rapidly and extensively metabolized and excreted. In order to minimize these problems, the use of nanoparticulate delivery systems have been proposed.

The aim of this work was to evaluate the capability of casein nanoparticles as oral carriers for resveratrol. Casein nanoparticles were prepared by a simple coacervation process and subsequent drying in a Spray-drier apparatus. The mean particle size of the resulting nanoparticles was around 200 nm with a negative zeta potential and resveratrol content close to 31 μg/mg nanoparticle. *In vitro* release studies, conducted under simulated gastric and intestinal fluids, demonstrated that the resveratrol release from casein nanoparticles was not affected by the pH conditions and followed a zero-order kinetic. When nanoparticles were administered orally to rats, resveratrol plasma levels were high and sustained for at least 8 hours. Interestingly, the oral bioavailability of resveratrol when loaded in casein nanoparticles was calculated to be 26.5%, 10-times higher than when the polyphenol was administered as oral solution of PEG400 and water. Finally, a good correlation between the amount of resveratrol released in vivo and the absorbed fraction in vivo was found.

1. Introduction.

Resveratrol (Rsv) is a stilbenoid named *trans*-3,4',5,-trihydroxystilbene and consists of two aromatic rings which are linked through a methylene bridge. It is a natural phenol produced naturally by 72 different plant species especially grapevines, pines, and legumes [1,2]. One of the more important sources for human consumption is red wine, although its contentdepens on a number of factors including the grape variety, vineyard location, cultivation system, climate and soil type and production process among others [3]. The interest of the scientific community in resveratrol was originally sparked by epidemiological studies,indicating an inverse relationship between moderate wineconsumption and risk of coronary heart disease, the socalled "French Paradox" [4,5] and by the fact that cancer preventive properties of resveratrol was observed *in vitro* and *in vivo*[6].

The mechanism by which resveratrol exerts such arange of beneficial effects across species and disease modelsis not yet elucidated. However, these effects would be related to the capability of this polyphenol to enhance the nitric oxide bioactivity and/or its inhibitory effect on platelet COX-1 and NF-kB [7,8].

In this context, resveratrol would block the platelet aggregation by its ability to specifically inhibit prostaglandins synthesized by COX-1 [9] such as thromboxane A2, which is a potent inducer of platelet aggregation and vasoconstrictor [10,11]. Apart from the vasorelaxant effect due to the inhibition of thromboxane A2 synthesis, resveratrol would also induce vasodilatation by its ability to enhance nitric oxide signaling in the endothelium [12], leading to a reduction in its inactivation rate [13].

On the other hand, it has been demonstrated that resveratrol possesses cancer chemo-preventive and chemotherapeutic activity. Resveratrol would affect the processes underlying all three stages of carcinogenesis; i) tumour initiation, ii) promotion and iii) progression [14]. This fact would be related with its inhibitory effect over cyclooxygenase [3], NF-kB [15] and protein kinase C [16], among others. Moreover, resveratrol would inhibit the tumour-induced neovascularization acting as an antiangiogenic agent [17-19].

In spite of all of these advantages, resveratrol also possesses some drawbacks that limit its use. Thus, resveratrol shows a very low aqueous solubility (0.02-0.03 mg/mL [20]. In addition, resveratrol is very sensitive to degradation by exposure to oxygen, light, temperature and oxidative enzymes [21,22]. Under these circumstances trans-resveratrol may be isomerized to the inactive cis-version, reducing its activity [23-26]. Another limiting and important factor is its poor oral bioavailability (less than 5%) and rapid metabolism and elimination [27]. Resveratrol suffers a presystemic metabolism through first-pass glucuronidation and sulphate conjugation of the phenolic groups in the enterocyte and liver. In addition, resveratrol hydrogenation of the aliphatic trans double bond by the intestinal microflora was showed. The major resveratrol metabolites encountered after oral administration of resveratrol includes resveratrol-3-O-sulphate, resveratrol-3-O-glucuronide and dihydroresveratrol conjugates which results in low oral bioavailability [22,28,29]. Very little is known about the bioactivity of resveratrol metabolites. However, it was recently investigated the strong *in vitro* anti-estrogenic activity of resveratrol-3-O-sulfate [30].

The aim of this work was to evaluate the capability of casein nanoparticles as carriers for the oral delivery of resveratrol. Casein is a food-grade protein that may be transformed into

nanoparticles under mild conditions [31] and, thus, produce devices with potential application in different areas such as food fortification, nutraceutical and pharmaceutical properties. More particularly, this work reports the capability of these devices to promote the oral bioavailability of resveratrol in rats.

2. Materials and methods.

2.1. Reagents.

Sodium caseinate was purchased from ANVISA (Madrid, Spain). Resveratrol, lysine, mannitol, polytethyleneglycol 400 (PEG 400), DAPI (4',6-diamidino-2-phenylindole), formaldehyde and tween 20, were obtained from Sigma-Aldrich (Germany). Calcium chloride was from Merk (Darmstadt, Germany). Resveratrol-3-O-D-glucuronide was from @rtMolecule (Cedex-France). Gallium-67citrate from IBA Molecular SA (Spain). NOTA from MacrocyclicsInc, (Dallas, USA). Ethanol, methanol, acetonitrile and acetic acid HLPC grade were obtained from Merk (Darmastadt, Germany). Lumogen® F red 305 was from Kremer (Aichstetten, Germany). Tissue-Tek® OCT compound was obtained from Sakura (Alphen, Netherlands). Deionized reagent water (18.2 MΩ resistivity) was prepared by a water purification system (Wasserlab, Spain). All reagents and chemicals used were of analytical grade.

2.2. Preparation of resveratrol-loaded nanoparticles

Resveratrol-loaded casein nanoparticles (Rsv-NP-C) were prepared as described previously [31] with some minor modifications. Briefly, 600 mg of sodium caseinate and 60 mg of lysine were dissolved in 40 mL of purified water. In parallel, 26 mg of resveratrol were dissolved in 2.6 mL of ethanol and added to the casein solution in darkness conditions. Under magnetic stirring, nanoparticles were formed by the addition of 24 mL of $CaCl_2$ 0.8% w/v. The resulting suspension of nanoparticles was purified by ultrafiltration through a polysulfone membrane cartridge of 50 kDa pore size (Medica SPA, Italy). Finally, 20 mL of an aqueous solution of mannitol (100 mg/ml) was added to the suspension of casein nanoparticles before drying in a Büchi Mini Spray Drier B-290 apparatus (BüchiLabortechnik AG, Switzerland) under the following experimental conditions: (i) inlet temperature of 90°C, (ii) outlet temperature 45-50°C, (iii) air pressure: 2-5 bar, (iv) pumping rate of 2-6 mL/min, (v) aspirator of 100% and (vi) air flow at 900 L/h.
Empty nanoparticles (NP-C) were prepared in the same way as described above but in the absence of resveratrol.

2.2.1. Preparation of resveratrol conventional formulations

Two different formulations of resveratrol were also prepared. The first one consisted of a solution of the polyphenol in a mixture of PEG 400 and water (Rsv-sol). For this purpose, 37.5 mg of resveratrol were dissolved in 5 mL of PEG 400 under magnetic stirring. Then 5 mL of purified water were added and the final mixture was agitated in darkness conditions for 10 min.
The second one was an extemporary suspension of resveratrol (Rsv-susp) in purified water. Briefly, 37.5 mg of resveratrol were dispersed in 10 mL of purified water under magnetic

agitation for 10 min. The suspension was used after visual inspection for absence of aggregates (Size: 21439 ± 9240; PDI: 0.510 ± 0.042).

2.3. Characterization of resveratrol-loaded nanoparticles

2.3.1. Physicochemical characterization

The mean hydrodynamic diameter and the zeta potential of nanoparticles were determined by photon correlation spectroscopy (PCS) and electrophoretic laser Doppler anemometry, respectively, using a Zetamaster analyser system (Malvern Instruments Ltd., Worcestershire, UK). The diameter of the nanoparticles was determined after dispersion in ultrapure water (1:10) and measured at 25°C with a scattering angle of 90°. The zeta potential was measured after dispersion of the dried nanoparticles in 1 mMKCl solution.

The morphology of the nanoparticles was studied using a field emission scanning electron microscopy (FE-SEM) in a Zeiss DSM940 digital scanning electron microscope (Oberkochen, Germany) coupled with a digital image system (Point Electronic GmBh, Germany). The yield of the process was calculated by gravimetry as described previously [31,32].

2.3.2. Resveratrol analysis

The amount of resveratrol loaded into the nanoparticles was quantified by HPLC-UV followed an analytical method previously published with minor modifications. Analysis were carried out in an Agilent model 1100 series LC and diode-array detector set at 306 nm. Data were analyzed in chemstation G2171 program (B.01.03). The chromatographic system was equipped with a reverse phase 150 mm x 2.1 mm C18 Alltima column (particle size 5 µm; Altech, USA) and a Gemini C18 support AJO-7596 precolumn. The mobile phase, pumped at 0.25 mL/min was a mixture of water/methanol/acetic acid in a gradient condition (table 1). The column was heated at 40°C and the injection volume was 10µL. Under these conditions, the run time for resveratrol was 22.8±0.5 min. Calibration curves in ethanol 75% were designed over the range of 1-100 µg/mL (R^2=0.999).

Table 1. Resveratrol HPLC gradient (A: water, B: methanol, C: acetic acid).

Time (min)	A (%)	B (%)	C (%)
0	80	15	5
15	70	25	5
20	10	85	5
30	10	85	5
35	80	15	5
40	80	15	5

For analysis, 10 mg of nanoparticles were dispersed in 1 mL of water and centrifuged. After centrifugation at 17,000 rpm for 20 min at 4°C, the supernatants were analyzed in order to determine the amount of free resveratrol (not encapsulated). The amount of resveratrol loaded in the nanoparticles was calculated by subtracting from the theoretical total amount of

resveratrol, the amount of drug found in the supernatant. Each sample was assayed by triplicate and the results were expressed as the amount of resveratrol (in µg) per mg of nanoparticles.
The encapsulation efficiency (E.E.) was calculated as follows:

$$E.E.(\%) = \frac{(Rsv_t - Rsv_s)}{Rsv_t} \times 100 \quad \text{(Eq. 1)}$$

in which Rsv-t is the total theoretical amount of resveratrol in the formulations and Rsv-s corresponds to the amount of resveratrol quantified in the supernatants.

2.3.3. *In vitro* release studies

*In vitro*release experiments were conducted under sink conditionsat 37°C using simulated gastric (SGF) and intestinal fluids (SIF), containing 0.5% tween 20 as surfactant to increase resveratrol solubility.The studies were performed under agitation in a slide-A-Lyzer® Dialysis cassete 10.000 MWCO (Thermo scientific, Rockford, IL, USA). For this purpose, the cassette was filled with 3 mg of resveratrol loaded in casein nanoparticles previously dispersed in 5 mL and, then, introduced in a vessel containing 500 mL of SGF (pH 1.2: 37°C) under magnetic agitation. After 2 hours in SGF, the cassette was introduced in another vessel containing 500 mL of thermostatzed SIF (pH 6.8; 37°C, under agitation). At different time points, samples tubes were collected and filtered with 0.45 µm filters (Thermo, USA) before quantification.
The amount of resveratrol released from the formulations was quantified by HPLC. Calibration curves of free resveratrol in water containing 0.5% tween 20 at pH 1.2 and 6.8 were performed, over the range 0.05-6 µg/mL ($R^2 > 0.999$) in both cases.
In order to ascertain the drug release mechanism the obtained data were fitted to the Korsmeyer-Peppas and the zero-order models.
The Korsmeyer–Peppas model [33] is a simple semi-empirical approach which exponentially relates drug release with the elapsed time (Eq. 2).

$$\frac{M_t}{M_\infty} = \mathrm{K}_{KP} \cdot \mathrm{t}^{\mathrm{n}} \text{ (Eq 2.)}$$

where Mt/M∞ is the drug release fraction at time t, K_{KP} is a constant incorporating the structural and geometric characteristics of the matrix and n is the release exponent indicative of the drug release mechanism. The value of n indicates the mechanism of the release [33]. If the value is around 0.5, the mechanism is Case I (Fickian) diffusion, a value between 0.5 and 0.89 indicates anomalous (non-Fickian) diffusion suggesting a combination of mechanisms diffusion and erosion. Values of n between 0.89 and 1 indicate Case II transport, which involves a release mechanism ruled by erosion/relaxation of the matrix.

Additionally, the zero-order kinetics equation (Eq. 3) was also used in order to evaluate the type of release mechanism. This model is used for systems where the matrix releases the same amount of drug by unit of time [34].

$$\frac{M_t}{M_\infty} = \mathrm{K}_{ZO} \cdot \mathrm{t} \text{ (Eq 3.)}$$

where Mt/M∞ is the drug release fraction at time t, and K_{ZO} is the zero order release constant.
To fit the experimental data to the previous models, only the first portion of the release profile was used (Mt/M∞ ≤ 0.6) [34].

2.4. Labelling of casein nanoparticles

2.4.1. Radiolabelling of casein nanoparticles (gallium-67-citrate-NP)

Casein nanoparticles were radiolabelled with ^{67}Gallium (^{67}Ga). Briefly, casein molecules were first tagged with p-SCN-Bn-NOTA (NOTA). Thus, 50 mg of sodium caseinate and 5 mg of NOTA were incubated for 24 hours in a 5 mL of sodium bicarbonate solution (pH 9.5). After this reaction, the protein was purified by dialysis to remove the inorganic salts presented in the buffered medium and the free NOTA. After this purification process, the protein derivative (casein-NOTA) was lyophilized. Tagged (50 mg) and untagged protein (450 mg) were used to prepare casein nanoparticles following the same procedure described above. Finally, NOTA nanoparticles (NOTA-NP) were labelled by citrate-NOTA transquelation with gallium-67 citrate [35].

2.4.2. Fluorescently labelling of casein nanoparticles (LR-NP)

Lumogen red-loaded nanoparticles were prepared by adding 2.5 mg Lumogen® F Red 305 in acetone (5 mL) to the solution of sodium caseinate and lysine. Then, casein nanoparticles were formed by the addition of a calcium chloride water solution. The resulting nanoparticles were purified and dried in the Spray Drier apparatus under the same conditions described above.

2.4.3. *In vivo* biodistribution studies

All of these studies were performed in male Wistar rats (200-250 g) obtained from Harlan (Barcelona, Spain) and the protocols were approved by the Ethical Committee for Animal Experimentation of the University of Navarra (protocol numbers 117-12 and 059-13). Prior to the experiments, animals were placed in metabolic cages and drink was provided *ad libitum*.
For radiolabelled nanoparticles, animals received a 1 mL single dose of an aqueous suspension of nanoparticles (10 mg gallium-67-citrate-NP). Animals were anesthetized with isofluorane and placed in prone position on the gammacamera. The SPECT-CT images were performed in a Symbiagammacamera (Siemens Medical Systems, USA). The images were obtained 2 and 24 hours after the administration of the radiolabelled nanoparticles.
For fluorescently labelled nanoparticles, animals received orally a single dose of 1 mL of an aqueous suspension containing 30 mg of LR-NP. Two hours later, the animals were sacrificed and their gastrointestinal tract was removed. Jejunum portions of 1 cm were collected, stored in the tissue proceeding medium O.C.T. and frozen at -80°C. Each portion was then cut into 5-µm sections on a cryostat and attached to glass slides. Finally, these samples were fixed with formaldehyde and incubated with DAPI (4',6-diamidino-2-phenylindole) for 15 minutes before the cover assembly. The presence of fluorescently loaded nanoparticles in the intestinal mucosa and the cell nuclei dyed with DAPI were visualized in a fluorescence microscope (Axioimager M1, Zeiss) with a coupled camera (Axiocam ICc3, Zeiss) and fluorescent source (HBO 100, Zeiss).

2.5. *In vivo* pharmacokinetic studies in Wistar rats

Pharmacokinetic studies were performed in male Wistar rats (200-250 g) obtained from Harlan (Barcelona, Spain). Studies were approved by the Ethical Committee for Animal Experimentation of the University of Navarra (protocol number 014-10) in accordance with the European legislation on animal experiments.Previous to the oral administration of the formulations, animals were fasted overnight to avoid interference with the absorption, allowing free access to water.

For the pharmacokinetic study, rats were randomly divided into 4 groups (n=6). The experimental groups that received the resveratrol formulations orally were: (i) resveratrol aqueous suspension, (ii) resveratrol solution in PEG 400:water (1:1 by vol.) and (iii) resveratrol-loaded casein nanoparticles (Rsv-NP-C). As control, a group of animals received the resveratrol solution intravenously. Each animal received the amount of resveratrol equivalent to a dose of 15 mg/kg body weight either orally with a blunt needle via the esophagus into the stomach or intravenously via tail vein.

Blood samples were collected at set times after administration (0, 10 min, 30 min, 1, 2, 4, 6, 8, 24 and 48 hours) in specific plasma tubes (Microvette® 500K3E,ref 20.1341. SARSTEDT, Germany). Blood volume was recovered intraperitoneally with an equal volume of normal saline solution pre-heated at body temperature. Samples were immediately centrifuged at 10,000 rpm for 10 min. Plasma was separated into clean tubes and kept frozen at -80 °C until analysis of both resveratrol and resveratrol-3-O-D-glucuronide.

2.5.1. Determination of resveratrol and Rsv-3-o-D-glucuronide plasma concentration by HPLC

The amount of resveratrol was determined by high pressure liquid chromatography with UV detection (HPLC-UV), following an analytical method previously published with minor modifications [36]. Analysis were carried out in an Agilent model 1100 series LC and diode-array detector set at 306 nm. The data were analyzedChemstation G2171 program (B.01.03). The chromatographic system was equipped with a reversed-phase 250 mm x 2.1 mm C18 Kromasil (particle size 5 µm) column and a Gemini C18 support AJO-7596 precolumn. The mobile phase, pumped at 0.5 mL/min, was a mixture of water, methanol and acetic acid (50:45:5 by vol.) in isocratic conditions. The column was placed at 30°C and the injection volume was 30 µL. Under these conditions, the run time for resveratrol-3-O-D-glucuronide and resveratrol was 6.2 ± 0.5 min and 12.6 ± 0.5 min, respectively.

For analysis, an aliquot of plasma (100 µL) was mixed with 50 µL of HCl (0.1 N) and 500 µL of acetonitrile in order to precipitate proteins. The mixture was shaken vigorously at 2500 rpm (Hettichzentrifugen, Tuttlingen, Germany) for 10 min. Then, the samples were centrifuged at 4000 rpm for 10 min and the supernatant was recovered and evaporated to dryness at 25°C for 30 min in an Automatic environmental Speed vac® system (Savant apparatus, Holbrook, NY). Finally, 100 µL of an acetonitrile water mixture (1:1 by vol.) were added to reconstitute the extract. The resulting solution was filtered with 0.45 µm filters (Thermo,USA) and injected in the HPLC system.

For quantification, calibration curves were designed over the range between 2 and 70 µg/mL, for the metabolite, and between 50 and 3000 ng/mL for resveratrol (R^2> 0.99). The standards were

prepared by adding (resveratrol or resveratrol-3-O-D-glucuronide) in 500 µL acetonitrile to 100 µL free plasma following the same extraction method described above.
Under these experimental conditions, the limit of quantification for resveratrol was calculated to be 70 ng/mL. For the metabolite, the limit of quantitation of this technique was established as 4 µg/mL. Linearity, accuracy and precision values during the same day (intraday assay) at low, medium and high concentrations of resveratrol and resveratrol-3-O-D-glucuronide were always within the acceptable limits (less than 15%).

2.5.2. Pharmacokinetic data analysis

Resveratrol plasma concentration was plotted against time, and pharmacokinetic analysis was performed using a non-compartmental model with the WinNonlin 5.2 software (Pharsight Corporation, USA). The following parameters were estimated: maximal serum concentration (C_{max}), time in which C_{max} is reached (T_{max}), area under the concentration-time curve from time 0 to the last time analyzed (AUC), mean residence time (MRT), clearance (Cl), volume of distribution (V) and half-life in the terminal phase ($t_{1/2}$). Furthermore, the relative oral bioavailability (Fr %) of resveratrol was estimated by the following equation:

$$Fr\ (\%) = (\frac{AUC\ oral}{AUC\ iv}) \times 100 \quad \text{(Eq. 4)}$$

Where $AUC_{i.v.}$andAUC_{oral} were the areas under the curve for the iv and oral administrations, respectively.

2.6. *In vitro*/*In vivo* correlation (INVIC)

In order to evaluate a possible relationship between *in vivo* and *in vitro* data, the correlation by representing a point-to-point between in vitro amounts of resveratrol released and *in vivo* percent of resveratrol absorbed was studied. The fraction of resveratrol absorbed (FRA) was calculated from the mean plasma concentration-time inputs using the Wagner-Nelson equation [37].

$$FRA = \frac{C_t + k \times AUC_{0-t}}{k \times AUC_{0-\infty}} \quad \text{(Eq. 5)}$$

where Ct is the plasma concentration at a time t, k is the elimination rate constant, $AUC_{0\text{-}t}$ is the area under the curve from 0 to time t and $AUC_{0\text{-}\infty}$ is the area under the curve from 0 to infinity.

The fraction of resveratrol absorbed (FRA) *in vivo* was plotted versus the fraction of resveratrol released (FRD) *in vitro*. Linear regression analysis was applied to the in-vitro–in-vivo correlation plot and regression coefficient (R^2) was calculated [38].

2.7. Statistical analysis

Data are expressed as the mean ± standard deviation (SD). The non-parametric Kruskall-Wallis followed by Mann-Whitney U-test was used to investigate statistical differences. In all cases, $p < 0.05$ was considered to be statistically significant. All data processing was performed using Graph Pad® Prism statistical software.

3. Results

Table 2 shows the physico-chemical characteristics of casein nanoparticles used in this study. For empty nanoparticles, the mean size was around 140 nm and the zeta potential was negative. When resveratrol was encapsulated into casein nanoparticles, the resulting average size significantly increased (210 nm vs 140 nm) whereas the negative zeta potential was slightly more negative than for empty nanoparticles (-19 mV vs. -12 mV). The resveratrol loading was calculated to be 31 µg/mg NP, with encapsulation efficiency close to 70%.

Table 2.Physico-chemical characterization of casein nanoparticles. NP-C, Empty nanoparticles; Rsv-NP-C, Resveratrol loaded in casein nanoparticles. Data expressed as mean ± SD, n=3.

	Size (nm)[a]	PDI (nm)	Zeta potential (mV)[b]	Rsv loading (µg/mg NP)[c]	E.E. (%)[d]
NP-C	138 ± 13	0.19 ± 0.02	-12 ± 1		
Rsv-NP-C	210 ± 3	0.20 ± 0.02	-19 ± 1	31 ± 1	68 ± 3

[a] Determination of the nanoparticle size (nm) by photon correlation spectroscopy
[b] Determination of the zeta potential (mV) by electrophoretic laser Doppler anemometry
[c] Amount of drug loaded in the nanoparticles (µg Rsv/mg NP)
[d] Encapsulation efficiency (%)

The morphological analysis by scanning electron microscopy (Figure 1) showed that resveratrol-loaded casein nanoparticles consisted of homogeneous populations of polyhedral nanoparticles with rough surface and apparent size similar to that obtained by photon correlation spectroscopy.

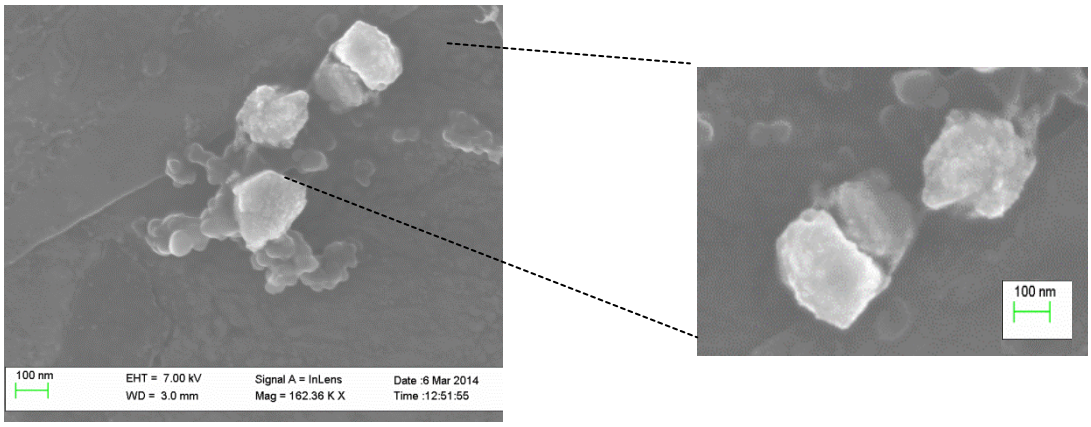

Figure 1. Scanning Electron Microscopy (SEM) microphotographs obtained from resveratrol-loaded casein nanoparticles.

3.1. *In vitro* release study

Resveratrol release kinetics from casein nanoparticles were evaluated in simulated physiological fluids. For this purpose, nanoparticles were initially incubated during the first 2 hours in simulated gastric fluid (SGF) and, then, in simulated intestinal fluid (SIF). Figure 2 represents the release profile of resveratrol from casein nanoparticles as the cumulative percentage of the cargo released *versus* time. Interestingly, the release of resveratrol from casein nanoparticles was found to be independent of the pH conditions. During the first 2 h, under SGF (pH 1.2), about 30% of the loaded resveratrol was released. Then, four hours later (in SIF) the amount released was close to 80% of the total content of resveratrol. Nine hours after the beginning of the experiment, almost the total amount of the encapsulated resveratrol was released from nanoparticles.

The resveratrol release data from casein nanoparticles fitted well to both the Korsmeyer-Peppas model (K_{KT} = 0.14 ± 0.01 $\mathbf{h^{-n}}$; n = 1.02 ± 0.04; R^2> 0.99) and the zero-order kinetics equation (K = 0.14 ± 0.00 $\mathbf{h^{-1}}$; R^2> 0.99). These results suggest that the release mechanism of resveratrol from casein nanoparticles would be ruled by the erosion of the nanoparticulate matrix.

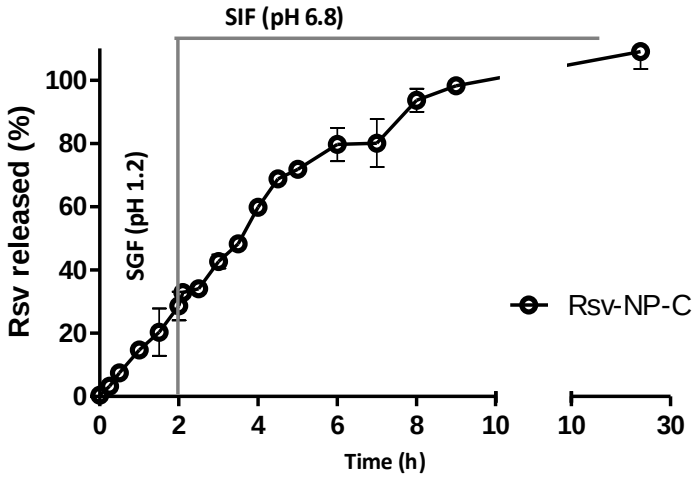

Figure 2.Resveratrol release profile from casein nanoparticles after incubation in simulated gastric (SGI, pH 1.2; 0-2 h) and simulated intestinal fluids (SIF, pH 6.8; 2-24 h) under sink conditions. Data expressed as mean ±SD, n=3.

3.2. *In vivo*biodistribution study of casein nanoparticles

Figure 3 shows the biodistribution of casein nanoparticles, at different times after their oral administration to rats. Two hours after their oral administration, casein nanoparticles were visualized in the stomach. Twenty-two hours later, the radioactivity was found in the distal part of gastrointestinal tract; whereas, 2 days post-administration, the radioactivity had disappeared. For the control formulation of gallium-67, during the 48-h in which the experiment took place, the radiolabelled agent was always visualized in the stomach.

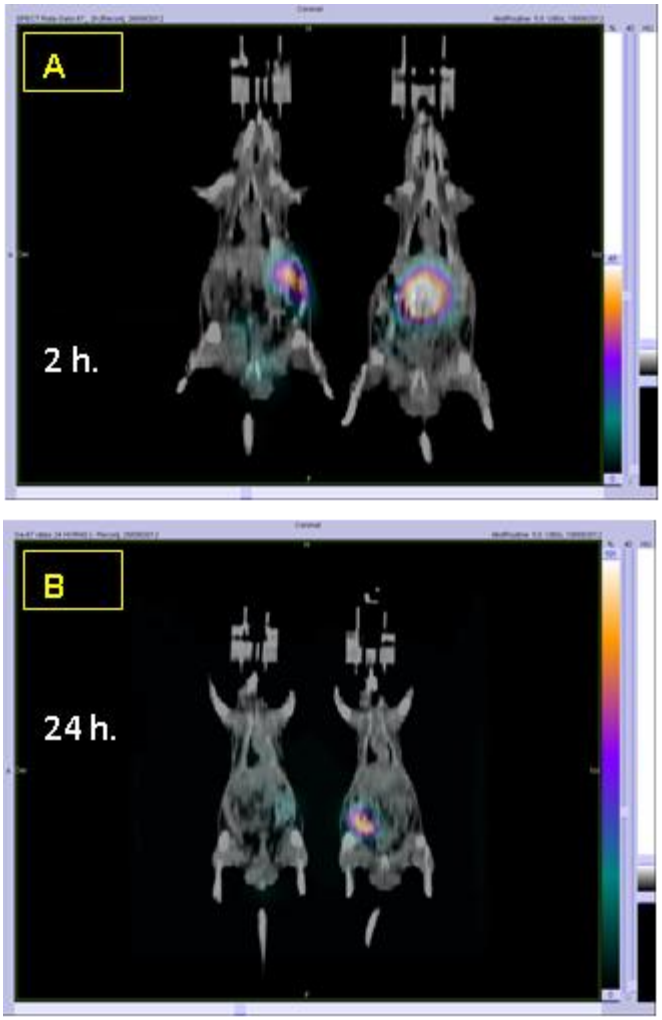

Figure 3.Comparison of the biodistribution of casein nanoparticles radiolabelled with 67-Gallium (NP-NOTA-Ga) and the radiomarker used as control (Gallio-citrate). Panels A and B show gammacamera images after oral administration of NP-NOTA-Ga (rat on the right) and control (rat on the left) at 2 and 24 hours post administration.

Figure 4 shows fluorescence microscopy images of jejunum samples, 2 hours after the oral administration to animals of fluorescently labelled nanoparticles. The control, an aqueous suspension of Lumogen® red, was observed as large aggregates in the lumen of animals or in contact with the external mucus layer (Figures 4A and 4B). On the contrary, casein nanoparticles (at least in part) were found in the mucus layer and in close contact with the surface of the gut epithelium (Figures 4C and 4D).

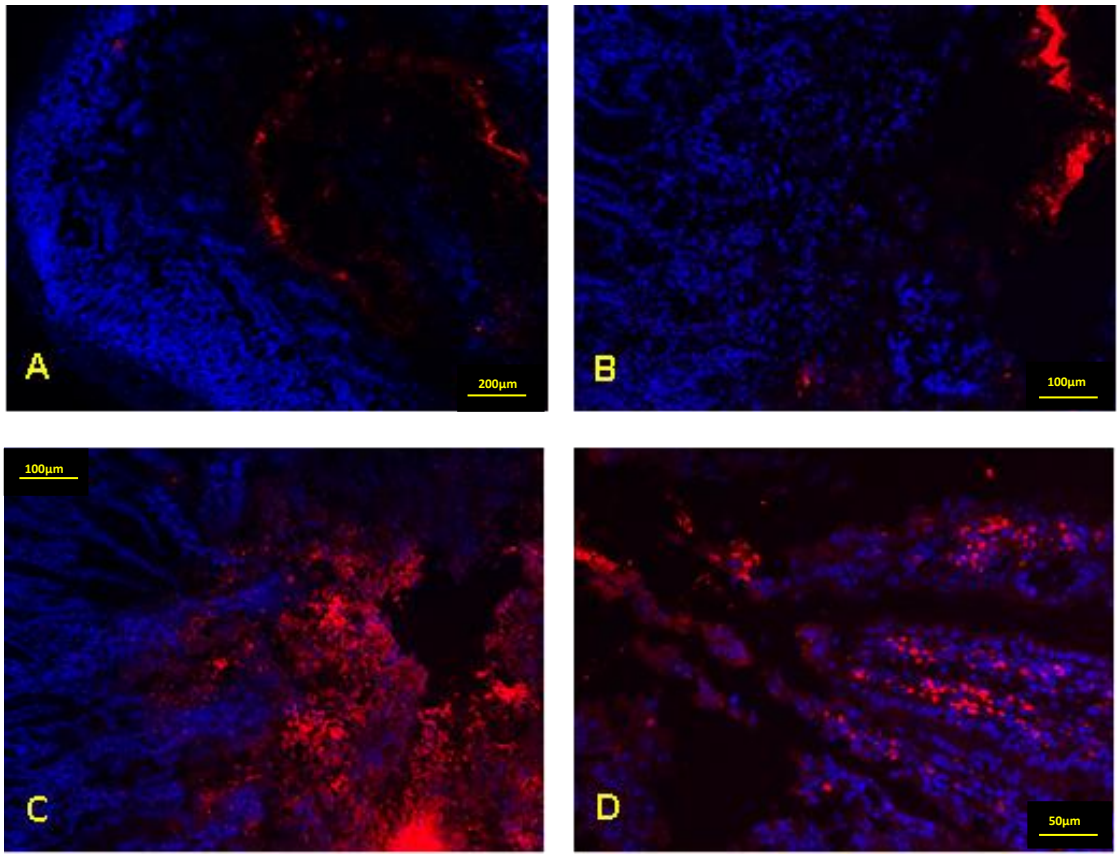

Figure 4. Fluorescence microscopy images of jejunum samples 2 hours after the oral administration of either a Lumogen® red suspension (A and B) or casein nanoparticles fluorescently labelled with Lumogen® red. Nuclei of cells were stained blue with DAPI.

1.1. Pharmacokinetic studies in Wistar rats

The plasma concentration-time profile of a resveratrol solution in PEG-400:water (1:1 by vol.) after its intravenous administration of a single dose (15 mg/kg) to rats is shown in Figure 5. Data were adjusted to a non-compartmental model. As it can be seen, the resveratrol plasma concentration decreased rapidly in a biphasic way, and no quantifiable levels were detected 8 hours post administration. The peak plasma concentration (C_{max}) of resveratrol was around 15µg/mL. Values obtained for AUC and half-life ($t_{1/2}$) were 11.4 µg h/ml and 2.0 hours, respectively. The resveratrol clearance and its distribution volume were calculated to be 0.2 L/h and 0.6 L, respectively (Table 3).

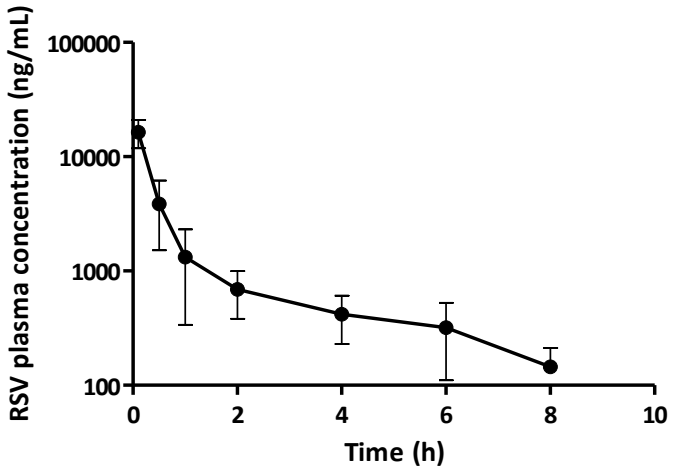

Figure 5.Resveratrol plasma concentration *vs.* time after a single i.v. administration of a resveratrol solution (dose 15 mg/kg).Data expressed as mean± SD, (n= 6).

Figure 6 shows the plasma concentration levels of resveratrol as a function of time after a single oral administration of 15 mg/kg to male Wistar rats of the different formulations tested (solution, suspension and casein nanoparticles). When the aqueous suspension of resveratrol was administered orally, no quantifiable levels of the polyphenol were detected in the plasma of laboratory animals. For the solution of resveratrol in a mixture PEG400:water (1:1 by vol.), the polyphenol plasma levels were only quantifiable during the first 4 hours post administration. Interestingly, when resveratrol was loaded in casein nanoparticles, the polyphenol plasma levels were quantified during 24 hours. In addition, at least during the first 8 hours, casein nanoparticles provided sustained levels of resveratrol in plasma.

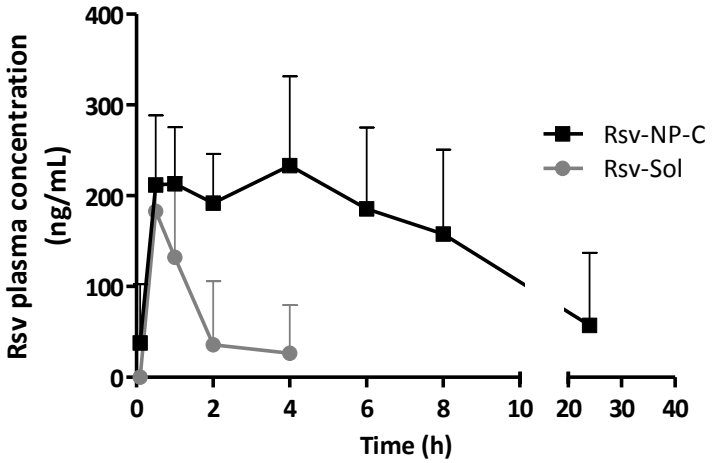

Figure 6. Resveratrol plasma concentration *vs.* time after a single oral administration of 15 mg/kg for the different formulations tested. i) Resveratrol PEG400:water solution (●), ii) Resveratrol-loaded casein nanoparticles (■). Data expressed as mean± SD, (n= 6).

Table 3 summarizes the main pharmacokinetic parameters estimated with a non-compartmental analysis of the experimental data obtained after the administration of the different formulations to rats. When resveratrol was administrated as a PEG400:water solution by the oral route, the AUC was around 0.29 μg h/mL. In the case of resveratrol encapsulated in casein nanoparticles, the AUC was found to be significantly higher than for the conventional formulation ($p<0.01$). In addition, both MRT and $t_{1/2}$ values of resveratrol in plasma after the administration of the nanoparticles was found to be around 6-fold higher than when resveratrol was administered as oral solution. On the other hand, the volume of distribution of the polyphenol as well as the resveratrol clearance and $t_{1/2}$ when administered in casein nanoparticles were similar to the values calculated after its administration by the intravenous route. Finally, the relative oral bioavailability of resveratrol when incorporated into nanoparticles achieves 27%, about 10-times higher than the value obtained when the polyphenol was formulated as oral solution.

Figure 7 shows the concentration of one of the main metabolites of resveratrol (resveratrol-O-3-glucuronide) in plasma as a function of time, after the administration of a single dose of resveratrol encapsulated in nanoparticles (oral) or dissolved in a PEG400:water solution (oral and intravenous). As expected, the metabolite plasma levels were higher than those observed for the polyphenol (Figure 6). However, the profiles of the curves were similar for both compounds, irrespective of the route of administration.

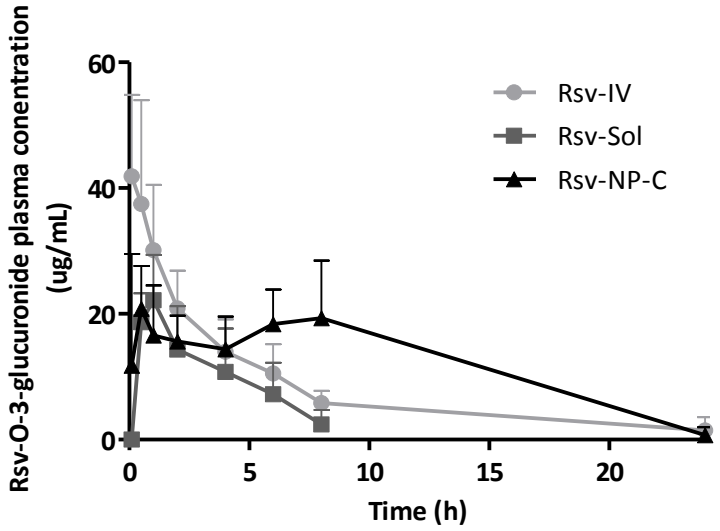

Figure 7. Resveratrol-O-3-glucuronide plasma concentration *vs* time after the administration of a single dose of resveratrol (15 mg/kg) in casein nanoparticles (oral) or dissolved in a PEG400:water mixture (oral and intravenously). i) Resveratrol solution intravenously administered (Rsv-IV) (●); ii) resveratrol solution orally administered (Rsv-Sol); (■), iii) resveratrol-loaded casein nanoparticles orally administered (Rsv-NP-C) (▲). Data expressed as mean ± SD, (n= 6).

When resveratrol was administered intravenously, its metabolite concentration reached 41.9µg/mL (C_{max}) and, then, its levels decreased rapidly reaching a very low amount in plasma only 8 hours post-administration. The AUC value was calculated to be 196.9 µg h/mL.
For the solution of resveratrol orally administered, the Cmax of the metabolite in plasma was found to be 2-times lower (22.1 µg/mL) than when administered by the iv route. In this case, the metabolite was only quantified in plasma during the first 8 hours post-administration. The AUC value was calculated to be 104.3 µg h/mL.
Concerning Rsv-NP-C, the profile of the curve representing the concentration of resveratrol-O-3-glucuronide in plasma vs time was characterized by increasing levels of the metabolite in plasma until reaching a plateau (around 20 µg/mL). Then, the plateau was maintained for at least 8 hours. Twenty-four hours after the administration of casein nanoparticles, quantifiable but low levels of the resveratrol metabolite were found. The AUC of resveratrol-O-3-glucuronide, when the polyphenol was administered orally after its encapsulation in casein nanoparticles (295.0 µg h/mL), was found to be around 2-times higher than when the resveratrol was iv administered ($p<0.05$) and 3-times higher than when the drug was orally administered as a PEG400:water solution ($p<0.01$).

Table 3. Pharmacokinetic parameters of resveratrol estimated after the i.v. and oral administration of a solution, a suspension and nanoparticles encapsulating the polyphenol at a single dose of 15 mg/kg bw to Wistar rats. Data are expressed as mean ± S.D (n=6).

	Route	C max (µg/mL)	T max (h)	AUC (µg h/mL)	t ½ (h)	Cl (mL/h)	Vd (mL)	MRT (h)	Fr (%)
Rsv iv.	iv	15.22 ± 5.18	0.1 ± 0	10.39 ± 3.80	2.0 ± 0.5	199.40 ± 89.81	569.17 ± 221.37	2.4±1.0	100
Rsv-sol.	po	0.20 ± 0.017**†	0.6 ± 0.2	0.28 ± 0.13**††	0.3 ± 0.2	386.71 ± 224.87	112.25 ±103.56	1.3±0.8*††	2.6
Rsv-susp.	po	-	-	-	-	-	-	-	-
Rsv-NP-C	po	0.29 ± 0.07**	1.8±1.3	2.76 ± 1.64**	2.7±0.7	161.81 ± 69.86	661.66 ± 242.92	8.2±3.7**	26.5

C_{max}: peak plasma concentration; T_{max}: time to reach plasma concentration; AUC: Area under the curve; t ½: half life of the terminal phase; Cl: Clearance; MRT: mean residence time Fr: relative oral bioavailability

*Significant differences *vs*Rsv iv ($p<0.05$) (Mann-Whitney-U)

**Significant differences *vs*Rsv iv ($p<0.01$) (Mann-Whitney-U)

† Significant differences *vs*Rsv Sol ($p<0.05$) (Mann-Whitney-U)

3.4. *In vitro-in vivo* correlation

The relationship between the *in vitro* dissolution data and the *in vivo* pharmacokinetic data was examined by plotting the percent of drug dissolved till 8 hours *vs*. the percent of intact resveratrol absorbed during the same period of time (Figure 8). A good linear regression relationship was observed between the amount of resveratrol released and the percents of the polyphenol absorbed (R^2 = 0.996).

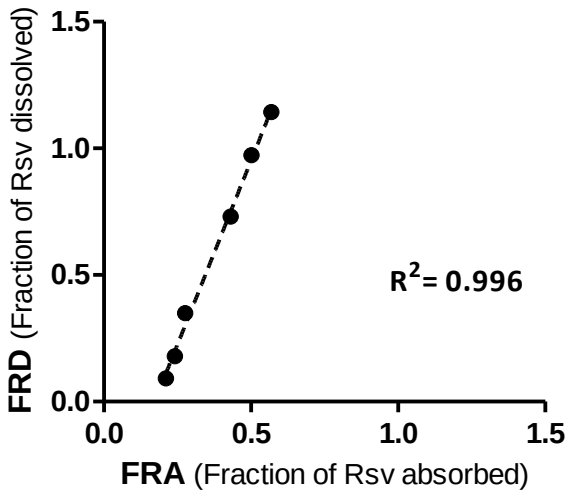

Figure 8. Relationship between fractions dissolved *in vitrovs.* fraction absorbed *in vivo.*

4. Discussion

This work reports the preparation and evaluation of casein nanoparticles as carriers for resveratrol. The use of casein may offer some advantages such as the capability of this food protein to be easily transformed into nanoparticles under mild conditions in an aqueous environment. In addition, milk caseins display a high affinity for antioxidant polyphenols, including resveratrol [39,40], and can bind these type of molecules via hydrophilic and hydrophobic interactions. Further, in the presence of proteins, resveratrol would be more protected from trans-to-cis isomerization than when it is in the free form [41-43].

The resulting resveratrol loaded casein nanoparticles were polyhedral (Figure1) and displayed a size of around 200 nm with resveratrol content close to 31 µg/mg nanoparticle. This result is at least similar to that reported by Jose and collaborators that used solid lipid nanoparticles for the delivery of this polyphenol [44]. Other recent works, using other types of nanoparticles reported between 2 and 3-times lower resveratrol loading than our casein nanoparticles [45-47].

Interestingly, the release of resveratrol from casein nanoparticles was found to be independent of the pH conditions. Moreover, the cumulative amount of resveratrol released from nanoparticles was found to be in accordance with zero-order kinetics (Figure 2). Thus, it is possible to speculate that the entry of water inside the casein nanoparticles would induce a

relaxation and/or erosion of the nanoparticles matrix that would favor the resveratrol diffusion [48]. A similar explanation was proposed by Bajpal*et all.*[49] and Fieelan*et all*.[50]that describe a release of the drug loaded mechanism based on the degradation of the sodium caseinate matrix through the entry of water inside the nanoparticles.
Interestingly, the presence of glutaraldehyde crosslinking casein microspheres modifies the release mechanism of theophylline to Higuchi diffusion model [51].

In the present study, the plasma concentrations of resveratrol provided by a conventional oral solution of the polyphenol in a mixture of PEG400 and water were low. With this solution, the oral bioavailability of resveratrol was calculated to be 2.6%. The highest recorded concentrations of resveratrol in plasma occurred 30 min after administration, and values returned to baseline within 4h (Figure 6).These results are in line with previous data reported in the literature by other research groups [52-54].
This low oral bioavailability might be explained by the effect of UDP-glucuronosyltransferase and sulphotransferases, localized in the liver [55,56] and intestine [27], that transform resveratrol in its glucuronides and sulphates derivatives [57].

On the other hand, casein nanoparticles provided higher and more prolonged resveratrol plasma levels than the oral solution. More important, the resveratrol plasma levels were sustained for at least 8 hours post-administration and significant amounts of the polyphenol was also quantified 24 h after the administration of nanoparticles to rats (Figure 6). As a consequence, the relative oral bioavailability of resveratrol when administered after its encapsulation in casein nanoparticles was found to be 10-times higher than when formulated as oral solution (Table 3). This improvement in the relative oral bioavailability of resveratrol observed for casein nanoparticles was higher than other increases reported in the literature. Thus, using SNEDDS, the resveratrol bioavailability was found to be 5-fold higher than the control formulation [58]. In a similar way, solid lipid nanoparticles have also been proposed as carriers for improving the oral bioavailability of resveratrol [59]. In this particular case, these lipid nanoparticles offered to resveratrol a bioavailability 8 times higher than the control formulation. On the other hand, in another work, Oganesyan and coworkers defined an oral bioavailability close to 30% with Eudragit RL nanoparticles and about 60% with lecithin/chitosan nanoparticles [60]. However, in this work, the control formulation of resveratrol displayed a bioavailability of 19%, in the fact that no levels of resveratrol were quantified 8 hours after administration [60].
Another important aspect of these nanoparticles is related to their effect on the primary pharmacokinetic parameters of resveratrol. Thus, with Rsv-NP-C, the values of the polyphenol half-life in plasma (t ½), clearance (Cl) and volume of distribution (Vd) were similar to those obtained after its intravenous administration as solution. These findings would be evidence that nanoparticles remain within the gut of animals and just the released resveratrol was absorbed. This fact was confirmed by the biodistribution studies. Thus, radiolabelled casein nanoparticles, after their administration to rats, remained in the gastrointestinal tract and no proofs of nanoparticle “translocation” or absorption was observed (absence of signals in the liver, spleen, lungs or kidneys of animals; Figure 3). Furthermore, the fluorescently labelling of casein nanoparticles with Lumogen® red allow to visualize a fluorescent signal in the area in which the epitlium cells are located (Figures 4C and 4D). All of this permits to hypothetize that casein nanoparticles showed muco-permeating properties and were able to reach the surface of the

enterocytes in which the cargo (resveratrol) was released. This would be in line with the idea proposed by Elzoghby and collaborators [61] who suggested that casein nanoparticles display a certain capability to cross the mucus layer and reach the surface of the enterocytes [62].
After the release of resveratrol from casein nanoparticles, it would be absorbed through the enterocytes and rapidly metabolized by enzymes. In rats, the major metabolite of resveratrol would be the glucuronide conjugate [63]. In our work, resveratrol-O-3-Glucuronide was quantified in plasma. Interestingly, for different formulations tested, the profile of the plasma curves for the metabolite (Figure 7) was similar to that observed for resveratrol (Figure 6). In any case, the highest AUC for the metabolite was found when resveratrol was administered encapsulated in casein nanoparticles. This fact confirms the controlled release properties of these carriers that are capable to sustain the plasma concentration of the polyphenol for at least 8 hours.
In the present study, the possibility of developing a level A correlation between the in vitro percentage released and the in vivo percentage absorbed for resveratrol when encapsulated in casein nanoparticles was investigated. A good correlation coefficient was obtained (R^2 =0.993). This finding would corroborate the capability of casein nanoparticles to carry resveratrol till the surface of the absorptive membrane and, once there, to control its release at a rate that would favor its absorption and entry in the circulation.

Conclusions

Resveratrol can be successfully encapsulated into casein nanoparticles. These carriers displayed interesting properties for the oral administration of this polyphenol. First, casein nanoparticles released resveratrol following a zero-order kinetic and the release rate was not affected by pH conditions. Second, casein nanoparticles promoted the absorption of resveratrol offering sustained levels of the polyphenol in plasma for at least 8 hours. As a consequence, the oral bioavailability of resveratrol when encapsulated in casein nanoparticles was calculated to be close to 26.5%. Last but not least, a level A*in vitro-in vivo* correlation was found between in the amount of resveratrol released from nanoparticles and the percentage orally absorbed. This fact would be related with the capability of casein nanoparticles to both reach the surface of the gut epithelium and control the release rate of resveratrol.

Acknowledgements

This work was supported by the Regional Government of Navarra (Alimentos funcionales, Euroinnova call) and the Spanish Ministry of Science and Innovation and Gobierno de Navarra (ADICAP; ref. IPT-2011-1717-900000). Rebeca Penalvaacknowledgesthe “Asociación de Amigos Universidad de Navarra” forthefinancialsupport.

References

[1] G.J. Soleas, E.P. Diamandis, D.M. Goldberg, Resveratrol: a molecule whose time has come? And gone?, Clin. Biochem. 30 (1997) 91-113.

[2] R.F. Guerrero, M.C. Garcia-Parrilla, B. Puertas, E. Cantos-Villar, Wine, resveratrol and health: a review, Nat. Prod. Commun. 4 (2009) 635-658.

[3] J.A. Baur, D.A. Sinclair, Therapeutic potential of resveratrol: the in vivo evidence, Nature Reviews Drug Discovery 5 (2006) 493-506.

[4] S.d. Renaud, M. de Lorgeril, Wine, alcohol, platelets, and the French paradox for coronary heart disease, The Lancet 339 (1992) 1523-1526.

[5] R. Pangeni, J.K. Sahni, J. Ali, S. Sharma, S. Baboota, Resveratrol: review on therapeutic potential and recent advances in drug delivery, Expert Opinion on Drug Delivery (2014) 1-14.

[6] M. Jang, L. Cai, G.O. Udeani, K.V. Slowing, C.F. Thomas, C.W. Beecher, H.H. Fong, N.R. Farnsworth, A.D. Kinghorn, R.G. Mehta, R.C. Moon, J.M. Pezzuto, Cancer chemopreventive activity of resveratrol, a natural product derived from grapes, Science 275 (1997) 218-220.

[7] G. Davidov-Pardo, D.J. McClements, Resveratrol encapsulation: Designing delivery systems to overcome solubility, stability and bioavailability issues, Trends Food Sci. Technol. 38 (2014) 88-103.

[8] H. Li, N. Xia, U. Förstermann, Cardiovascular effects and molecular targets of resveratrol, Nitric Oxide 26 (2012) 102-110.

[9] Z. Wang, J. Zou, Y. Huang, K. Cao, Y. Xu, J.M. Wu, Effect of resveratrol on platelet aggregation in vivo and in vitro, Chin. Med. J. (Engl) 115 (2002) 378-380.

[10] M. Hamberg, J. Svensson, B. Samuelsson, Thromboxanes: a new group of biologically active compounds derived from prostaglandin endoperoxides, Proc. Natl. Acad. Sci. U. S. A. 72 (1975) 2994-2998.

[11] Y. Yang, J. Chen, X. Wang, S. Wang, H. Hu, H. Wang, Resveratrol attenuates thromboxane A2 receptor agonist-induced platelet activation by reducing phospholipase C activity, Eur. J. Pharmacol. 583 (2008) 148-155.

[12] F. Orallo, E. Alvarez, M. Camina, J.M. Leiro, E. Gomez, P. Fernandez, The possible implication of trans-Resveratrol in the cardioprotective effects of long-term moderate wine consumption, Mol. Pharmacol. 61 (2002) 294-302.

[13] S. Das, V.K. Alagappan, D. Bagchi, H.S. Sharma, N. Maulik, D.K. Das, Coordinated induction of iNOS–VEGF–KDR–eNOS after resveratrol consumption: A potential mechanism for resveratrol preconditioning of the heart, Vascular Pharmacology 42 (2005) 281-289.

[14] M. Athar, J.H. Back, X. Tang, K.H. Kim, L. Kopelovich, D.R. Bickers, A.L. Kim, Resveratrol: A review of preclinical studies for human cancer prevention, Toxicol. Appl. Pharmacol. 224 (2007) 274-283.

[15] O. Kang, H. Jang, H. Chae, Y. Oh, J. Choi, Y. Lee, J. Kim, Y.C. Kim, D.H. Sohn, H. Park, D. Kwon, Anti-inflammatory mechanisms of resveratrol in activated HMC-1 cells: Pivotal roles of NF-κB and MAPK, Pharmacological Research 59 (2009) 330-337.

[16] S.J. Slater, J.L. Seiz, A.C. Cook, B.A. Stagliano, C.J. Buzas, Inhibition of protein kinase C by resveratrol, Biochimica Et Biophysica Acta (BBA) - Molecular Basis of Disease 1637 (2003) 59-69.

[17] S. Pervaiz, Chemotherapeutic potential of the chemopreventive phytoalexin resveratrol, Drug Resistance Updates 7 (2004) 333-344.

[18] M. Athar, J.H. Back, X. Tang, K.H. Kim, L. Kopelovich, D.R. Bickers, A.L. Kim, Resveratrol: A review of preclinical studies for human cancer prevention, Toxicol. Appl. Pharmacol. 224 (2007) 274-283.

[19] S.H. Tseng, S.M. Lin, J.C. Chen, Y.H. Su, H.Y. Huang, C.K. Chen, P.Y. Lin, Y. Chen, Resveratrol suppresses the angiogenesis and tumor growth of gliomas in rats, Clin. Cancer Res. 10 (2004) 2190-2202.

[20] A. Amri, J.C. Chaumeil, S. Sfar, C. Charrueau, Administration of resveratrol: What formulation solutions to bioavailability limitations?, J. Controlled Release 158 (2012) 182-193.

[21] G. Davidov-Pardo, D.J. McClements, Resveratrol encapsulation: Designing delivery systems to overcome solubility, stability and bioavailability issues, Trends Food Sci. Technol. 38 (2014) 88-103.

[22] A.C. Santos, F. Veiga, A.J. Ribeiro, New delivery systems to improve the bioavailability of resveratrol, Expert Opinion on Drug Delivery 8 (2011) 973-990.

[23] L. Camont, C. Cottart, Y. Rhayem, V. Nivet-Antoine, R. Djelidi, F. Collin, J. Beaudeux, D. Bonnefont-Rousselot, Simple spectrophotometric assessment of the trans-/cis-resveratrol ratio in aqueous solutions, Anal. Chim. Acta 634 (2009) 121-128.

[24] F. Orallo, Comparative studies of the antioxidant effects of cis-and trans-resveratrol, Curr. Med. Chem. 13 (2006) 87-98.

[25] C. Rius, M. Abu-Taha, C. Hermenegildo, L. Piqueras, J. Cerda-Nicolas, A.C. Issekutz, L. Estañ, J. Cortijo, E.J. Morcillo, F. Orallo, M. Sanz, Trans- but Not Cis-Resveratrol Impairs Angiotensin-II–Mediated Vascular Inflammation through Inhibition of NF-κB Activation and Peroxisome Proliferator-Activated Receptor-γ Upregulation, The Journal of Immunology 185 (2010) 3718-3727.

[26] C.G. Silva, J. Monteiro, R.R. Marques, A.M. Silva, C. Martínez, M. Canle, J.L. Faria, Photochemical and photocatalytic degradation of trans-resveratrol, Photochemical & Photobiological Sciences 12 (2013) 638-644.

[27] J.M. Planas, I. Alfaras, H. Colom, M.E. Juan, The bioavailability and distribution of< i> trans-resveratrol are constrained by ABC transporters, Arch. Biochem. Biophys. 527 (2012) 67-73.

[28] G. Davidov-Pardo, D.J. McClements, Resveratrol encapsulation: Designing delivery systems to overcome solubility, stability and bioavailability issues, Trends Food Sci. Technol. 38 (2014) 88-103.

[29] Y. Radko, K.B. Christensen, L.P. Christensen, Semi-preparative isolation of dihydroresveratrol-3-O-β-d-glucuronide and four resveratrol conjugates from human urine after oral intake of a resveratrol-containing dietary supplement, Journal of Chromatography B 930 (2013) 54-61.

[30] R. Ruotolo, L. Calani, E. Fietta, F. Brighenti, A. Crozier, C. Meda, A. Maggi, S. Ottonello, D. Del Rio, Anti-estrogenic activity of a human resveratrol metabolite, Nutrition, Metabolism and Cardiovascular Diseases 23 (2013) 1086-1092.

[31] R. Penalva, I. Esparza, M. Agüeros, C.J. Gonzalez-Navarro, C. Gonzalez-Ferrero, J.M. Irache, Casein nanoparticles as carriers for the oral delivery of folic acid, Food Hydrocolloids (In press).

[32] P. Arbós, M.A. Campanero, M.A. Arangoa, M.J. Renedo, J.M. Irache, Influence of the surface characteristics of PVM/MA nanoparticles on their bioadhesive properties, J. Controlled Release 89 (2003) 19-30.

[33] P.L. Ritger, N.A. Peppas, A simple equation for description of solute release I. Fickian and non-Fickian release from non-swellable devices in the form of slabs, spheres, cylinders or discs, J. Controlled Release 5 (1987) 23-36.

[34] P. Costa, J.M. Sousa Lobo, Modeling and comparison of dissolution profiles, European Journal of Pharmaceutical Sciences 13 (2001) 123-133.

[35] J. Morfin, É Tóth, Kinetics of Ga (NOTA) formation from weak Ga-citrate complexes, Inorg. Chem. 50 (2011) 10371-10378.

[36] D.J. Boocock, K.R. Patel, G.E.S. Faust, D.P. Normolle, T.H. Marczylo, J.A. Crowell, D.E. Brenner, T.D. Booth, A. Gescher, W.P. Steward, Quantitation of trans-resveratrol and detection of its metabolites in human plasma and urine by high performance liquid chromatography, Journal of Chromatography B 848 (2007) 182-187.

[37] M.A. Kassem, A.N. ElMeshad, A.R. Fares, Enhanced bioavailability of buspirone hydrochloride via cup and core buccal tablets: Formulation and< i> in vitro/in vivo evaluation, Int. J. Pharm. 463 (2014) 68-80.

[38] M.A.A. Kassem, A.N. ElMeshad, A.R. Fares, Enhanced bioavailability of buspirone hydrochloride via cup and core buccal tablets: Formulation and in vitro/in vivo evaluation, Int. J. Pharm. 463 (2014) 68-80.

[39] D.P. Acharya, L. Sanguansri, M.A. Augustin, Binding of resveratrol with sodium caseinate in aqueous solutions, Food Chem. 141 (2013) 1050-1054.

[40] P. Bourassa, J. Bariyanga, H. Tajmir-Riahi, Binding sites of resveratrol, genistein, and curcumin with milk α-and β-caseins, The Journal of Physical Chemistry B 117 (2013) 1287-1295.

[41] J. Zhang, Q. Mi, M. Shen, Resveratrol binding to collagen and its biological implication, Food Chem. 131 (2012) 879-884.

[42] J. Zhang, X. Dai, J. Huang, Resveratrol binding to fibrinogen and its biological implication, Food Biophysics 7 (2012) 35-42.

[43] Li Liang, H. A. Tajmir-Riahi and Muriel Subirade, Interaction of β-Lactoglobulin with Resveratrol and its Biological Implications, Biomacromolecules 9 (2008) 50-56.

[44] S. Jose, S.S. Anju, T.A. Cinu, N.A. Aleykutty, S. Thomas, E.B. Souto, In vivo pharmacokinetics and biodistribution of resveratrol-loaded solid lipid nanoparticles for brain delivery, Int. J. Pharm. 474 (2014) 6-13.

[45] A.R. Neves, M. Lúcio, S. Martins, J.L.C. Lima, S. Reis, Novel resveratrol nanodelivery systems based on lipid nanoparticles to enhance its oral bioavailability, International Journal of Nanomedicine 8 (2013) 177.

[46] A.R. Cho, Y.G. Chun, B.K. Kim, D.J. Park, Preparation of Chitosan–TPP Microspheres as Resveratrol Carriers, J. Food Sci. 79 (2014) E568-E576.

[47] D. Pando, G. Gutiérrez, J. Coca, C. Pazos, Preparation and characterization of niosomes containing resveratrol, J. Food Eng. 117 (2013) 227-234.

[48] G.W. Sinclair, N.A. Peppas, Analysis of non-Fickian transport in polymers using simplified exponential expressions, J. Membr. Sci. 17 (1984) 329-331.

[49] S. Bajpai, Casein cross-linked polyacrylamide hydrogels: study of swelling and drug release behaviour, Iranian Polymer Journal 8 (1999) 231-240.

[50] B. Fieelan, O. Corrigant, In vitro analysis of the release of incorporated agents from sodium caseinate microspheres, J. Microencapsul. 14 (1997) 63-78.

[51] M. Latha, A. Jayakrishnan, Glutaraldehyde Cross-linked Bovine Casein Microspheres as a Matrix for the Controlled Release of Theophylline: In-vitro Studies, J. Pharm. Pharmacol. 46 (1994) 8-13.

[52] H. Colom, I. Alfaras, M. Maijó, M.E. Juan, J.M. Planas, Population pharmacokinetic modeling of trans-resveratrol and its glucuronide and sulfate conjugates after oral and intravenous administration in rats, Pharm. Res. 28 (2011) 1606-1621.

[53] C. Cottart, V. Nivet-Antoine, C. Laguillier-Morizot, J. Beaudeux, Resveratrol bioavailability and toxicity in humans, Molecular Nutrition & Food Research 54 (2010) 7-16.

[54] M. Emília Juan, J. Buenafuente, I. Casals, J.M. Planas, Plasmatic levels of< i> trans-resveratrol in rats, Food Res. Int. 35 (2002) 195-199.

[55] C. De Santi, A. Pietrabissa, F. Mosca, G. Pacifici, Glucuronidation of resveratrol, a natural product present in grape and wine, in the human liver, Xenobiotica 30 (2000) 1047-1054.

[56] A. Maier-Salamon, B. Hagenauer, G. Reznicek, T. Szekeres, T. Thalhammer, W. Jäger, Metabolism and disposition of resveratrol in the isolated perfused rat liver: role of Mrp2 in the biliary excretion of glucuronides, J. Pharm. Sci. 97 (2008) 1615-1628.

[57] T. Walle, Bioavailability of resveratrol, Ann. N. Y. Acad. Sci. 1215 (2011) 9-15.

[58] G. Singh, R.S. Pai, Trans-resveratrol self-nano-emulsifying drug delivery system (SNEDDS) with enhanced bioavailability potential: optimization, pharmacokinetics and in situ single pass intestinal perfusion (SPIP) studies, Drug Deliv. (2014) 1-9.

[59] D. Pandita, S. Kumar, N. Poonia, V. Lather, Solid lipid nanoparticles enhance oral bioavailability of resveratrol, a natural polyphenol, Food Res. Int. 62 (2014) 1165-1174.

[60] E. Oganesyan, I. Miroshnichenko, N. Vikhrieva, A. Lyashenko, S.Y. Leshkov, Use of nanoparticles to increase the systemic bioavailability of trans-resveratrol, Pharmaceutical Chemistry Journal 44 (2010) 74-76.

[61] A.O. Elzoghby, W.S. Abo El-Fotoh, N.A. Elgindy, Casein-based formulations as promising controlled release drug delivery systems, J. Controlled Release 153 (2011) 206-216.

[62] A.O. Elzoghby, W.S. Abo El-Fotoh, N.A. Elgindy, Casein-based formulations as promising controlled release drug delivery systems, J. Controlled Release 153 (2011) 206-216.

[63] G. Kuhnle, J.P. Spencer, G. Chowrimootoo, H. Schroeter, E.S. Debnam, S.K.S. Srai, C. Rice-Evans, U. Hahn, Resveratrol is absorbed in the small intestine as resveratrol glucuronide, Biochem. Biophys. Res. Commun. 272 (2000) 212-217.

Chapter 5

Casein nanoparticles in combination with 2-hydroxypropyl-β-cyclodextrin improves the oral bioavailability of quercetin

Abstract

The aim of this work was to optimize the preparative process of quercetin loaded casein nanoparticles as well as to evaluate the pharmacokinetics of this flavonoid when administered orally in Wistar rats. Nanoparticles were obtained by coacervation after the incubation of casein, 2-hydroxypropyl-β-cyclodextrin (HP-β-CD) and quercetin in aqueous environment. Then, nanoparticles were purified by ultrafiltration and dried in a Spray-drying apparatus. The resulting nanoparticles displayed a size of about 200 nm with a negative zeta potential and a quercetin loading of about 32 μg/mg nanoparticles. From these devices, quercetin was released following a zero-order kinetic, suggesting a mechanism based on erosion of the nanoparticle matrix, and it was found to be independent of the pH of the medium. For the pharmacokinetic study, quercetin was orally administered to rats as a single dose of 25 mg/kg. Animals treated with quercetin-loaded casein nanoparticles displayed higher plasma levels than those observed in animals receiving the solution of the flavonoid (control). Thus, the relative oral bioavailability of quercetin when administered as casein nanoparticles (close to 37%) was found to be about 9-times higher than the oral solution of the flavonoid in a mixture of PEG 400 and water. In summary, the combination of casein and 2-hydroxypropyl-β-cyclodextrin produces nanoparticles that may be a good option to load quercetin for both nutraceutical and pharmaceutical purposes.

1. Introduction.

Quercetin(3,3',4',5,7-pentahydroxyflavone) is a naturally occurring flavonoid and one of the most potent antioxidants of plant origin [1,2]. Chronic intake of quercetin may be associated with a decreased risk of coronary heart disease [3,4] and other degenerative diseases [5-7], as well as with a reduction in the hepatic fat accumulation associated with consumption of a western-style diet [8]. The daily intake of quercetin with a typical western diet was estimated to be about 10 mg and the major sources of this flavonoid would be tea, red wine, fruits, and vegetables [9]. In some countries, quercetin is available as a dietary supplement with daily manufacturer recommendations of 200–1200 mg quercetin[9]. In addition, quercetin has been proven safe as a dietary supplement [10] and may be used as a nutraceutical for functional foods within a concentration range of 0.008–0.5% or 10–125 mg/serving[11].

However, when orally administered, quercetin shows a very low bioavailability (less than 10% in rats and even 1% in humans)[12,13]. This drawback would be related to the low solubility of the aglycone form (around 10 mg/L in water) [14]] as well as to the intense presystemic metabolism that suffer this flavonoid in the gut mucosa. In fact, quercetin would be substrate of the efflux pumps (e.g. P-glycoprotein) found in the enterocytes in the gut and cytochrome P-450 (CYP) isoenzymes and transferases located both in the gastrointestinal tract and in the liver [15-18]. As a result of this metabolism, the major circulating compounds in the plasma would be the glucoronide and sulphate derivatives of quercetin[19]. Apart from its considerable metabolism, quercetin is chemo- and thermo-labile and rapidly degraded when exposed to alkaline media, light and warm temperature [20,21].

In order to enhance the oral bioavailability of quercetin, different strategies have been tested. In this context, analogues of quercetin (e.g. quercetin-glutamic acid conjugates) have been developed, showing remarkable increases in water solubility, stability and cell permeability [22]. Another interesting approach was the administration of quercetin in association with a P-gp inhibitor. Thus, the co-administration of piperine with quercetin significantly potentiated the protective effect of the flavonoid against chronic unpredictable stress-induced cognitive dysfunction in mice [23].

Recently, several nanotechnology based strategies have been also proposed to increase the oral bioavailability of quercetin including the use of nanosuspensions[24], selft-emulsifying delivery systems [25][26], microemulsions[27], nanoemulsions[28], polymeric nanoparticles [29] and lipid nanocapsules[30,31].

Based on previous results [32], casein nanoparticles could also provide an alternative formulation for the oral delivery of quercetin. Casein nanoparticles can be prepared by a coacervation process in an aqueous environment without using any type of organic solvent or toxic reagent. In addition, whenorally administered, these nanoparticles show a certain capability to reach the epithelium surface of the gut mucosa [Chapter 4]. In this particular case, and due to the metabolism of quercetin within the gut, casein nanoparticles were combined with 2-hydroxylpropyl-β-cyclodextrin in order to improve the oral bioavailability of quercetin. The main reason for this combination is related with the inhibitory properties in the effect of both the intestinal efflux pumps and the cytochrome P450 enzymatic complex [33-35].

Therefore, the aim of this work was to optimize the preparative process of quercetin-loaded casein nanoparticles as well as to evaluate their capabilities to promote the oral absorption and bioavailability of quercetin in Wistar rats.

2. Materials and methods.

2.1. Reagents.

Sodium caseinate was obtained from ANVISA (Madrid, Spain). Quercetin, lysine, 2-hydroxy-propyl-β-cyclodextrine (HP-β-CD), mannitol, chlorzoxazone, calcium chloride, poly(ethylene glycol) 400 (PEG 400), and tween 20 were from Sigma-Aldrich (Germany). Ethanol, methanol, acetic acid and acetonitrile (HPLC grade) were from Merck (Darmstadt, Germany). Deionised reagent water (18.2 MΩ resistivity) was prepared by a water purification system (Wasserlab, Spain). All reagents and chemicals used were of analytical grade.

2.2. Preparation of quercetin-loaded casein nanoparticles.

Nanoparticles were prepared by simple coacervation procedure followed by a purification step by ultrafiltration and subsequent drying by Spray-drying [36].
Briefly, 1 g of sodium caseinate, 90 mg of lysine and a variable amount of HP-β-CD were dissolved in 75 mL purified water. In parallel, 35 mg quercetin were dissolved in 3 mL absolute ethanol and added under magnetic stirring to the casein solution. Under magnetic stirring, nanoparticles were formed by the addition of 40 mL of an aqueous solution of $CaCl_2$ 0.8% w/v. The resulting nanoparticles suspension was purified by ultrafiltration through a polysulfone membrane cartridge of 50kDa pore size (Medica SPA, Italy). Finally, 30 mL of an aqueous solution of mannitol (100 mg/mL) were added to the suspension of casein nanoparticles and the suspension was dried in a Buchi Mini Spray Drier B-290 apparatus (BuchiLabortechnik AG, Switzerland) under the following experimental conditions: (i) inlet temperature: 90°C, (ii) outlet temperature: 45-50°C, (iii) air pressure: 2-5 bar, (iv) pumping rate: 2-6 mL/min, (v) aspirator: 100% and (vi) air flow: 900 L/h. The resulting nanoparticles were named Que-HPCD-NP-C.
On the other hand, nanoparticles in the absence of the cyclodextrin were also prepared (Que-NP-C). In this case, sodium caseinate (1 g), lysine (90 mg) and quercetin (35 mg) in 3 mL of ethanol were incubated in 75 mL purified water. Then, nanoparticles were formed by the addition of 40 mL of a solution of calcium chloride in purified water (0.8% w/v). The resulting nanosuspensions were purified and dried as described above.
Empty nanoparticles were prepared as described above but in the absence of the oligosaccharide and quercetin (NP-C) or in the absence of the flavonoid (HPCD-NP-C).

2.3. Preparation of quercetin conventional formulations.

For *in vivo* studies, two conventional formulations of quercetin were used. The first one consisted on a solution of the polyphenol in a mixture of PEG 400 and water (6:4 by vol.). For this purpose, 62.5 mg of quercetin were dissolved in 6 mL of PEG 400 under magnetic stirring. Then 4 mL of purified water were added and the final mixture was agitated in darkness conditions for 10 min. This formulation was named Que-sol.
The second one was an extemporary suspension of quercetin in purified water (Que-susp). Briefly, 62.5 mg quercetin was dispersed in 10 mL of purified water under magnetic agitation for

10 min. The size of the resulting suspension was 15.5 ± 4.3 µm. The suspension was used after inspection for absence of aggregates.

2.4. Characterization of nanoparticles.

2.4.1. Size, zeta potential and morphology.

The mean hydrodynamic diameter and the zeta potential of nanoparticles were determined by photon correlation spectroscopy (PCS) and electrophoretic laser Doppler anemometry, respectively, using a Zetaplus apparatus (Brookhaven Instrument Corporation, USA). The diameter of the nanoparticles was determined after dispersion in ultrapure water (1:10) and measured at 25°C with a scattering angle of 90°. The zeta potential was measured after dispersion of the dried nanoparticles in 1 mMKCl solution.
The morphology and shape of nanoparticles was examined using a field emission scanning electron microscope (FE-SEM) in a Zeiss DSM940 digital scanning electron microscope (Oberkochen, Germany) coupled with a digital image system (Point Electronic GmBh, Germany).
Prior to analysis, particles were washed to remove mannitol. For this purpose, spray-dried nanoparticles were resuspendedin distilled water and centrifuged at 27,000xg for 10 min. Then, the supernatants were discarded and the obtained pellets were mounted on copper grids. Finally, the pellet was shaded with an amalgam of gold/palladium for fifteen seconds using a sputter coater (K550X Emitech, Ashford, UK).
The yield of the process was calculated by gravimetry as described previously [32,37].

2.4.2. Quercetin analysis.

The amount of quercetin loaded into the nanoparticles was quantified by HPLC-UV following an analytical method previously published with minor modifications [38]. Analysis were carried out in an Agilent model 1100 series LC and a diode-array detector set at 370 nm. The chromatographic system was equipped with a reversed-phase 150 mm x 2.1 mm C18 Alltima column (particle size 5 µm; Altech, USA) and a Gemini C18 precolumn (particle size 5 µm; Phenomenex, CA, USA). The mobile phase, pumped at 0.25 mL/min, consisted of a mixture of methanol, water and acetic acid in gradient conditions. The column was placed at 40°C and the injection volume was 10 uL. Calibration curves were designed over the range of 0.3-100 µg/mL. The limit of quantification was calculated to be 0.35 µg/mL.
For analysis, 10 mg of nanoparticles were dispersed in 1 mL of water and centrifuged. After a centrifugation at 30,500 xg for 20 min, the supernatants were analyzed in order to determine the amount of free quercetin (not encapsulated).The amount of quercetin loaded in the nanoparticles was calculated by subtracting from the theoretical amount of quercetin, the amount of drug found in the supernatant.
Each sample was assayed by triplicate and the results were expressed as the amount of quercetin (in µg) per mg of nanoparticles.

$$Quercetin\ loaded\ (\mu g/mgNP) = \frac{Que\ t - Que\ s}{Wp} \quad \text{(Eq. 1)}$$

The encapsulation efficiency (E.E.) was calculated as follows:

$$E.E.(\%) = \frac{(Que\ t - Que\ s)}{Que\ t} \times 100 \quad \text{(Eq.2)}$$

in which Que_t is the total theoretical amount of quercetin in the formulations, Que_s corresponds to the amount of quercetin quantified in the supernatants and Wp the amount of protein quantified as described above.

2.5. In vitro release studies.

Release experiments were conducted at 37°C using simulated gastric (SGF, pH 1.2) and intestinal (SIF, pH 6.8) fluids. In order to fulfil sink conditions, Tween® 20 (0.5% w/v) was added to both media.The studies were performed under agitation in a slide-A-Lyzer® Dialysis cassette 10.000 MWCO (Thermo scientific, Rockford, IL, USA).
For the study, 2 mg of quercetin loaded in casein nanoparticles were dispersed in 5 mL of purified water and introduce in the cassette, which was then placed into a vessel containing 500 mL of SGF for 2 hours. After this time, the same cassette was removed from the SGF and introduced in a second vessel with 500 mL of SIF until the end of the experiment. At different time points, samples of 1 mL were collected and filtered to 0.45 µm (Filter nylon, 0.45µL, Thermo scientific, Rockford, USA) before quantification. At each sampling time, the withdrawn volume was replaced with fresh fluid (gastric or intestinal simulated fluids).
The amount of quercetin released from the formulations was quantified by HPLC. Calibration curves of quercetin were prepared in both release media over the range of 0.16-6 µg /mL (R^2 > 0.99).

2.5.1. Analysis of release data.

In order to ascertain the drug release mechanism, data obtained from the *in vitro* release experiments were fitted to Korsmeyer-Peppas and zero-order models. The Korsmeyer–Peppas model [39] is a simple semi-empirical model which exponentially relates drug release with the elapsed time (Eq. 3).

$$\frac{M_t}{M_\infty} = \mathrm{K}_{KP} \cdot \mathrm{t}^{\mathrm{n}} \quad \text{(Eq. 3)}$$

whereMt/M_∞ is the drug release fraction at time *t*, K_{KP} is a constant incorporating the structural and geometric characteristics of the matrix and *n* is the release exponent indicative of the drug release mechanism. The value of *n* indicates the mechanism of the release [39]. If the value is around 0.5, the mechanism is Case I (Fickian) diffusion, and a value between 0.5 and 0.89 indicates anomalous (non-Fickian) diffusion suggesting a combination of mechanisms diffusion and erosion. Values of n between 0.89 and 1 indicate Case II transport, which involves a release mechanism ruled by erosion/relaxation of the matrix.

Data obtained from the *in vitro* release experiments were also fitted to a zero-order kinetic equation (Eq 4). This model is used for systems where the matrix releases the same amount of drug by unit of time [40].

$$\frac{M_t}{M_\infty} = \mathrm{K}_{\mathrm{ZO}} \cdot \mathrm{t} \quad \text{(Eq. 4)}$$

Where Mt/M_∞ is the drug release fraction at time *t*, and K_{ZO} is the zero order release constant.
To fit the experimental data to the previous equation, only one portion of the release profile was used, that is Mt/M∞ ≤ 0.6 [40].

2.6. In vivo pharmacokinetic studies in Wistar rats.

Pharmacokinetic studies were performed in male Wistar rats (200-250 g) obtained from Harlan (Barcelona, Spain). Studies were approved by the Ethical Committee for Animal Experimentation of the University of Navarra (protocol number 028-11) in accordance with the European legislation on animal experiments. Previous to the oral administration of the formulations, animals were fasted overnight to avoid interference with the absorption, allowing free access to water.
For the pharmacokinetic study, rats were randomly divided into 5 groups (n=6). The experimental groups were as follows: (i) quercetin aqueous suspension (Que-susp), (ii) quercetin solution in PEG 400:water (60:40 v/v) (Que-sol) (iii) quercetin-loaded casein nanoparticles (Que-NP-C) and (iv) quercetin-loaded casein nanoparticles containing HP-β-CD (Que-HPCD-NP-C). All of these formulations were orally administered with a blunt needle via the esophagus into the stomach. As control, a group of animals received intravenously the solution of quercetin in the mixture of PEG 400 and water. In all cases, the dose of quercetin (orally or intravenously) was 25 mg/kg body weight.
Blood samples were collected at set times after administration (0, 10 min, 30 min, 1, 2, 4, 6, 8, 24 and 48 hours) in Microvette® 500K3E plasma tubes (SARSTEDT, Germany). Blood volume was recovered intraperitoneally with an equal volume of normal saline solution pre-heated at body temperature. Samples were immediately centrifuged at 9,400 xg for 10 min and plasma aliquots were frozen at -80 °C until analysis.

2.6.1. Determination of quercetin plasma concentration.

The amount of quercetin was determined in plasma by HPLC as described above using chlorzoxazone as internal standard. Prior the analysis, quercetin was extracted from plasma samples following a protocol previously described by Li and co-workers [31] with minor modifications. For sample preparation, an aliquot of 100 µL of plasma sample was mixed with 25 µL of internal standard solution (chlorzoxazone, 50 µg/mL in methanol), 125 µL of methanol and 50 µL of HCl (25% by vol.) for protein precipitation followed by vigorous shaking at 2500 rpm for 10 min. Then, samples were hydrolyzed in a water bath at 50°C for 15 min and were centrifuged at 10,000 rpm for 10 min. The obtained supernatants were filtered (Filter nylon, 0.45µL, Thermo scientific, Rockford, USA) and a 50 µL aliquot of each sample were injected onto the HPLC column.

The same protocol was used for calibration and quality control standards preparation, using blank plasma and different solutions of quercetin in methanol. Calibration curves were designed over the range 70-5000 ng/mL (R^2>0.999). Under these experimental conditions, the run time of quercetin was 13.9 min (detected at 370 nm) and the internal standard 12.6 min (detected at 303 nm). The limit of quantification was calculated as 200 ng/mL. Linearity, accuracy and precision values during the same day (intraday assay) at low, medium and high concentrations of quercetin were within the acceptable limits (relative error and coefficient of variation less than 15%).

2.6.2. Pharmacokinetic data analysis.

Quercetin plasma concentration was plotted against time, and pharmacokinetic analysis, was performed using a non-compartmental model with the WinNonlin 5.2 software (Pharsight Corporation, USA). The following parameters were estimated: maximal serum concentration (C_{max}), time in which C_{max} is reached (T_{max}), area under the concentration-time curve from time 0 to last time (AUC), mean residence time (MRT), clearance (Cl), volume of distribution (V) and half-life in the terminal phase ($t_{1/2}$). Furthermore, the relative bioavailability (Fr) of quercetin was estimated by the following equation:

$$Fr\ (\%) = \frac{AUC\ oral}{AUC\ iv} \times 100 \quad \text{(Eq. 5)}$$

Where $AUC_{i.v.}$andAUC_{oral} are the areas under the curve for the iv and oral administrations, respectively.

2.7. Statistical analysis.

Data are expressed as the mean ± standard deviation (SD) of at least three experiments. The non-parametric Kruskall-Wallis followed by Mann-Whitney U-test was used to investigate statistical differences. In all cases, p< 0.05 was considered to be statistically significant. All data processing was performed using Graph Pad® Prism statistical software.

3. Results

For the optimization of the preparative process of quercetin-loaded nanoparticles, the flavonoid/oligosaccharide ratio and the time of incubation between the main components of the formulation (sodium caseinate, quercetin and HP-β-CD) before the formation of nanoparticles were evaluated. Figure 1 shows the influence of the incubation time and the quercetin/HP-β-CD ratio (1:1, 1:2, 1:3 by mol) on the encapsulation efficiency and payload of the resulting nanoparticles. Surprisingly, the best results were obtained when nanoparticles were formed with a quercetin/HP-β-CD ratio of 1:1 by mol and after 30 min of incubation. Under these experimental conditions, the payload of the resulting nanoparticles was 31.5 µg of quercetin per mg nanoparticles with an encapsulation efficiency close to 83%. As a consequence, a quercetin/cyclodextrin ratio of 1:1 by mol, and a time of incubation of 30 minutes were selected.

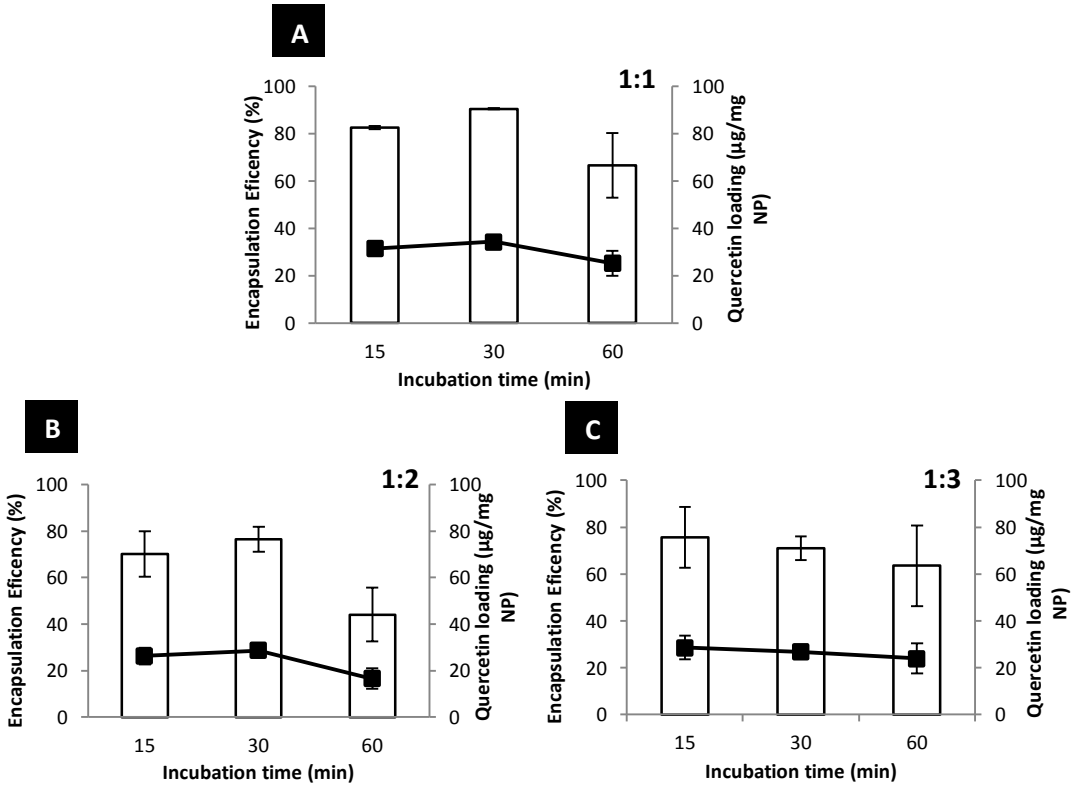

Figure 1. Influence of the incubation time (15, 30 and 60 min) and the quercetin/HP-β-CD ratio (1:1, 1:2 and 1:3 by mol) on the flavonoid loading (line, right axis) and its encapsulation efficiency (bars, left axis). Experimental conditions : (A) quercetin/ HP-β-CD ratio 1:1 by mol; (B) quercetin/ HP-β-CD ratio 1:2 by mol and (C) quercetin/ HP-β-CD ratio 1:3 by mol. Data expressed as mean ± SD, n=3.

Table 1 shows the physico-chemical characteristics of the nanoparticles used in this study. The mean diameter of empty casein nanoparticles was smaller than those loaded with quercetin. Interestingly, the incorporation of HP-β-CD to casein nanoparticles decreased the mean diameter of the resulting nanoparticles. This was particularly significative for quercetin-loaded

nanoparticles, in which the presence of HP-β-CD decreased the mean size from 251 nm (for Que-NP-C) to 171 nm (for Que-HPCD-NP-C). In all cases the polydispersity index was below 0.3, indicating homogeneous nanoparticle formulations, and the zeta potential was negative. This negative charge was slightly higher when quercetin was loaded in casein nanoparticles. Another important aspect to highlight was that the incorporation of HP-β-CD increased 40% the quercetin loading in casein nanoparticles (22.3 until 31.5 µg/mg nanoparticles).

Table 1.Physico-chemical characteristics of empty casein nanoparticles (NP-C), quercetin-loaded casein nanoparticles (Que-NP-C) and quercetin-loaded 2-hydroxypropyl-β-cyclodextrin casein nanoparticles (Que-HPCD-NP -C). Data expressed as mean ± SD, (n=3).

Formulation	Size (nm)[a]	PDI (nm)	Zeta potential (mV)	E.E. (%)[c]	Que loading (µg/mg NP)[b]
NP-C	138±13	0.19±0.02	-11.9±0.9	-	-
HPCD-NP-C	141±3	0.17±0.01	-12.3±2.1	-	-
Que-NP-C	251±9	0.26±0.02	-14.3±1.1	75.4±0.9	22.3±0.3
Que-HPCD-NP-C	171±5	0.19±0.01	-15.2±1.1	82.9±6.6	31.5±3.8

[a]Determination of volumen mean diameter by photon correlation spectroscopy.
[b] Determination of quercetin content by HPLC-UV.
[c] Encapsulation Efficiency (%)by HPLC-UV.

The morphological analysis by scanning electron microscopy (Figure 2) showed that quercetin-loaded casein nanoparticles consisted of homogeneous population of irregular shaped nanoparticles, with a mean size similar to that obtained by photon correlation spectroscopy. Que-NP-C (Figure 2A) displayed a smooth surface; however, the formulation containing the cyclodextrin displayed nanoparticles with a rough surface (Figure 2B).

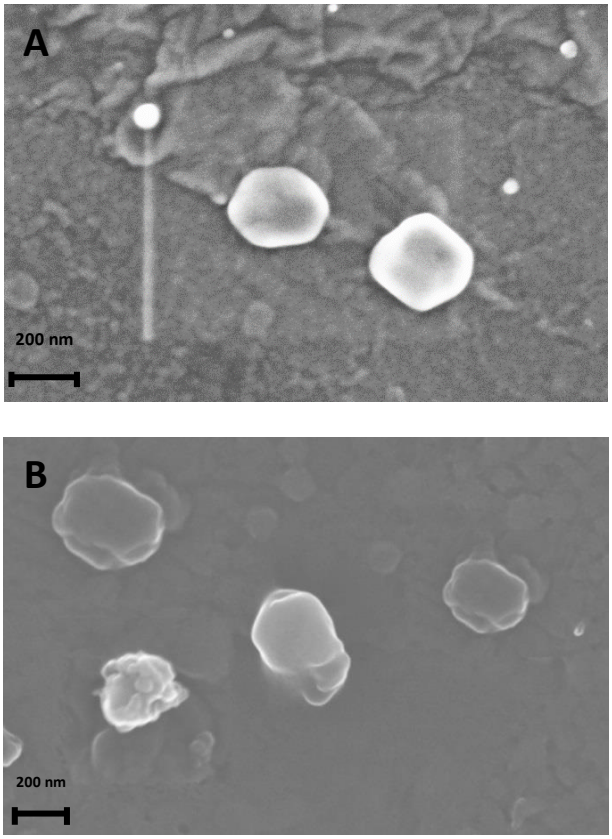

Figure 2.Scanning electron microscopy (SEM) of casein nanoparticles. (A) Que-NP-C: quercetin loaded in casein nanoparticles; (B) Que-HPCD-NP-C: quercetin loaded in casein nanoparticles containing hydroxypropyl-β-cyclodextrin.

3.1. *In vitro* release profile.

The release of quercetin from casein nanoparticles was evaluated in simulated gastric and intestinal fluids (Figure 3). Overall, the release of quercetin appeared to be independent of the pH conditions and slightly more rapid when released from control nanoparticles than from Que-HPCD-NP-C. During the first 2 hours, under SGF, about 20% of the loaded quercetin was released from both nanoparticle formulations. Then, after 4 hours of incubation in SIF, the amount of quercetin released was around 80% of the total content in Que-NP-C and close to 60% from Que-HPCD-NP-C. In any way, from both nanoparticle formulations, 24 hours after the beginning of the experiment, almost the total amount of the encapsulated quercetin was released from casein nanoparticles.

The quercetin release data from both nanoparticles were fitted to the Korsmeyer-Peppas model, obtaining “n” values close to 1 (Table 2). These data suggested that the quercetin release from nanoparticles involves a release mechanism ruled by an erosion/relaxation phenomenon of the matrix. Therefore the release data were fitted to the zero-order model, obtaining good

regression coefficients (R^2> 0.98). In all cases, the release constants were slightly higher when quercetin was released from nanoparticles prepared in the absence of HP-β-CD than for Que-HPCD-NP-C.

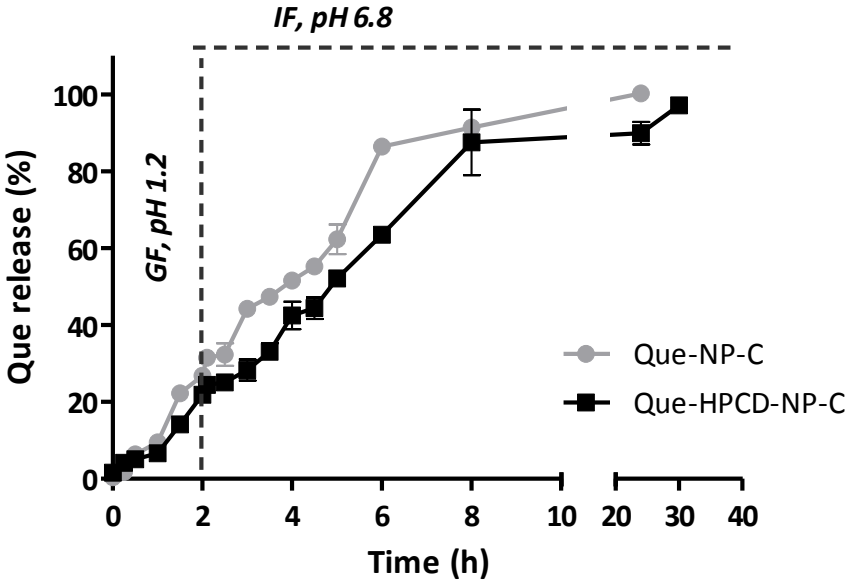

Figure 3.In vitro release studies of quercetin loaded in nanoparticles. Que-NP-C: quercetin-loaded casein nanoparticles (●); Que-HPCD-NP-C: quercetin-loaded in casein nanoparticles containing HP-β-CD (▪). Data represented as mean ± SD, (n=3).

Table 2.Analysis of quercetin release from casein nanoparticles incubated during the first two hours in SGF and, then, in SIF.

	Korsmeyer-Peppas			Zero-Order	
	K_{KP} (h^{-n})	**n**	**R^2**	**K_{ZO} (h^{-1})**	**R^2**
Que-NP-C	0.14±0.01	0.94±0.06	0.98	0.13±0.01	0.98
Que-HPCD-NP-C	0.10±0.01	1.02±0.06	0.98	0.10±0.01	0.99

3.2. Pharmacokinetic studies.

Figure 4 shows the plasma concentration-time profile of quercetin intravenously administered as single dose (25 mg/kg) in a solution of PEG400 and water (60:40 by vol.). Data were adjusted to a non-compartimental model. The quercetin plasma concentration decreased rapidly in a biphasic way, not being detectable 8 hours after the administration. The peak plasma concentration (C_{max}) of quercetin was 175 µg/mL. Values obtained for AUC and half-life ($t_{1/2}$) were around 167 µg h/ml and 0.60 hours, respectively. The mean residence time (MRT) was 1.57 hours; whereas the quercetin clearance and its distribution volume were calculated to be 30 mL/h and 26 mL respectively (Table 3).

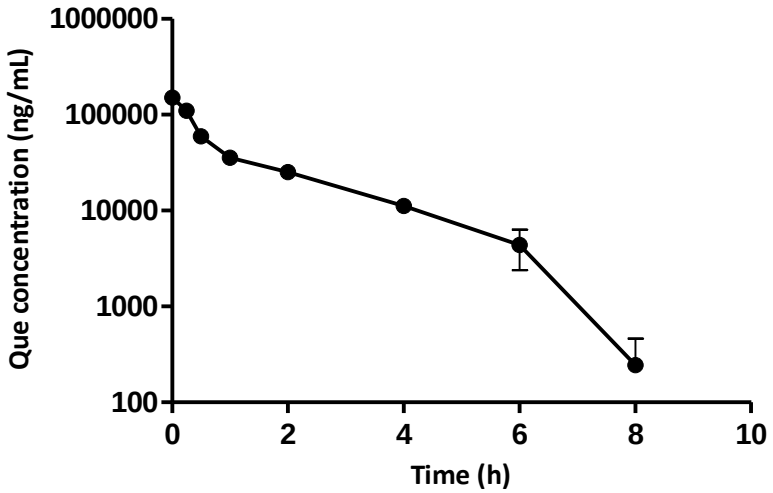

Figure 4. Plasma quercetin concentration *vs.* time profile after the intravenous administration of a single dose of the flavonoid (25 mg/kg) formulated as solution in a mixture of PEG400 and distilled water. Data are expressed as mean ± SD, (n=6).

Figure 5 shows the plasma concentration profile versus time of quercetin after a single oral dose of 25 mg/kg to rats when administered as quercetin solution, suspension or encapsulated in nanoparticles. From the oral administration of aqueous solution, the quercetin levels in the plasma of animals increased rapidly during the first 1 hour post administration when Cmaxwas reached. Then, the amount of quercetin in plasma decreased slowly during the following hours. However, in the case of the administration of quercetin as a suspension, drug levels found in the plasma of animals were significantly lower than after the solution administration and only quantifiable during the first 4 hours.

For nanoparticle formulations, quercetin plasma levels vs. time displayed different profiles than those observed when the conventional formulations of the flavonoid (Que-sol and Que-susp). In both cases, the profile of quercetin in plasma were characterized by high, sustained and prolonged levels of the flavonoid. For Que-NP-C, these high levels of the flavonoid in plasma were quantified up to 24 hours post-administration, whereas, for Que-HPCD-NP-C, plasma levels were observed up to 72 hours post-adminsitration.

Table 3 summarizes the pharmacokinetic parameters estimated during the analysis of the experimental data obtained after the administration of the different quercetin formulations to rats. The oral solution of quercetin provided an AUC value 10-times higher than that observed for the suspension of the flavonoid (Que-susp). For classical casein nanoparticles (Que-NP-C), the AUC value was about 3 times higher than for the oral solution of the flavonoid. Moreover, for Que-HPCD-NP-C, the AUC was the highest and represented 61 µg h/mL, about 10 fold higher than the value calculated for the oral solution of quercetin. The half-life and the mean residence time of quercetin in plasma were significantly higher when the flavonoid was administered in casein nanoparticles than formulated as solution or suspension. In a similar way, the volume of distribution of quercetin also increased when the flavonoid was encapsulated in casein nanoparticles, whereas its clearance was of the same order in all cases. Finally, the relative oral bioavailability of quercetin when incorporated in casein nanoparticles ranged from 11% to 36% (for Que-NP-C and Que-HPCD-NP-C, respectively). However, for the oral solution, the oral bioavailability of the flavonoid was only of about 4%.

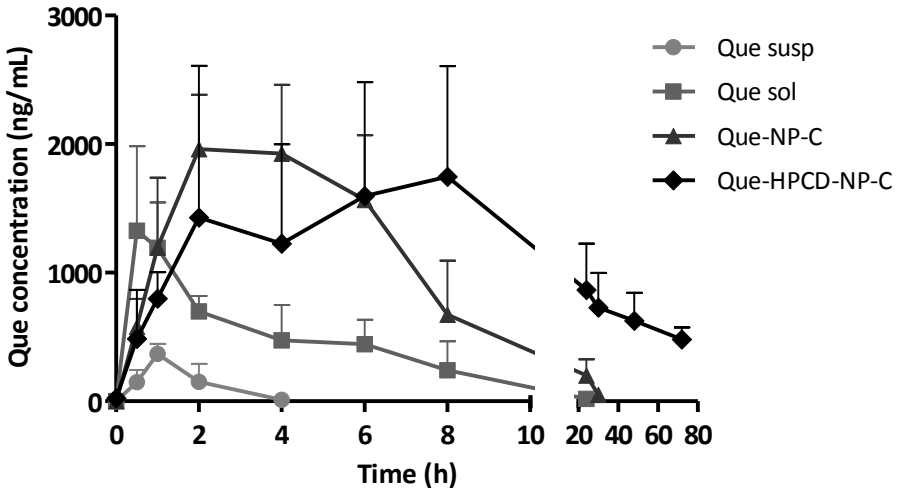

Figure 5.Quercetin plasma concentration *vs.* time after the oral administration of the different formulations at a dose of 25 mg/kg.i) quercetin suspension (Que-Susp, ●), ii) quercetin solution (Que,-Sol, ■), iii) quercetin loaded in casein nanoparticles (Que-NP-C, ▲) and iv) quercetin loaded in casein nanoparticles in the presence of HP-β-CD (Que-HPCD-NP-C, ♦). Data expressed as mean ± SD (n=6).

Table 3. Pharmacokinetic parameters of quercetin calculated from either the intravenous or oral administration of a single dose of the flavonoid (25 mg/Kg) formulated as a solution, suspension or encapsulated in nanoparticles. Que-NP-C: quercetin-loaded casein nanoparticles; Que-HPCD-NP-C: quercetin-loaded casein nanoparticles in the presence of HP-β-CD. Data expressed as mean ± SD; (n=6).

	Tmax (h)	Cmax (µg/mL)	t 1/2 (h)	AUC (µg h/mL)	Vz (mL)	Cl (mL/h)	MRT (h)	F (%)
Que-IV	0.00±0.00	175.87±13.39	0.60±0.35	166.74±8.21	26.28±16.13	30.17±1.35	1.57±0.12	100.00
Que-Susp	1.00±0.00	0.37±0.08**	0.54±0.49**	0.55±0.25**	29.08±24.50**	45.33±18.97	1.22±0.35**	0.33
Que-Sol (Peg 400-H_2O)	0.60±0.22	1.40±0.41	3.51±1.97	6.77±2.20	146.20±78.91	29.19±0.91	4.86±0.55	4.10
Que-NP-C	3.67±1.51**	2.20±0.40*	6.28±1.51*	19.60±4.12**	261.67±60.86**	28.95±0.92	7.78±1.68**	11.75
Que-NP-HPCD-C	6.33±2.65**	1.89±1.05	28.41±7.35^{**+}	61.40±24.48^{**+}	893.46±137.32^{**+}	22.34±2.61	28.47±3.01^{**+}	36.83

C_{max}: peak plasma concentration; T_{max}: time to reach plasma concentration; AUC: Area under the curve; t ½: half life of the terminal phase; Cl: Clearance; MRT: mean residence time Fr: relative oral bioavailability

* Significant differences *vs*Que-Sol ($p<0.05$) Mann-Whitney-U

** Significant differences *vs*Que-Sol ($p<0.01$) Mann-Whitney-U

$^{+}$ Significant differences *vs* Que-NP-C ($p<0.01$) Mann-Whitney-U

4. Discusion

Quercetin (aglycone) has been classified as a class IV compound within the biopharmaceutical classification system (BCS) [41]. In fact, when orally administered, the presence of quercetin in plasma can only be detected during short periods of time and the flavonoid has a poor bioavailability [42]. Thus, quercetin would be extensively metabolized before its entry into blood and internal organs, suggesting biotransformation in gastrointestinal tissues and liver. Within the gut, quercetin is metabolized by different enzymes (e.g. UDP-glucuronyltransferases, catechol-O-methyltransferases and phenol sulfotransferases), resulting in the formation of glucuronated, sulfated, and methylated quercetin conjugates [43,44]. Subsequently, the resulting quercetin derivatives and any remaining unmetabolizedquercetin are released into the circulation via the hepatic portal vein. In the liver, quercetin and its derivatives are further subject to conjugation, resulting in the formation of sulfate and/or glucuronide derivatives [45,46]. Additionally, the unabsorbed fraction of the flavonoid may be degraded to one of several different phenolic acids (e.g., 3,4-dihydroxyphenylacetic acid) and carbon dioxide (CO_2) by the colonic microflora [47,48].

In the present study, casein nanoparticles in combination with 2-hydroxyl-propyl-β-cyclodextrin (HP-β-CD) have been evaluated as a carrier for the oral delivery of quercetin. Nanoparticles were prepared by a simple coacervation method followed by a purification step and a subsequently drying process in order to minimize the physico-chemical degradation of the flavonoid.
The mean size of the quercetin-loaded casein nanoparticles was about 170 nm with a zeta potential of -15 mV. Interestingly, the incorporation of HP-β-CD produced more homogeneous (decreased PDI, Table 1) and smaller nanoparticles, without affecting their surface negative charge properties. Furthermore, the incorporation of the oligosaccharide permitted to significantly increase the quercetin loading (31 µg/mg vs. 22 µg/mg, in the absence of the cyclodextrin). This payload is in line with other previous results reported by other authors using similar devices such as Eudragit® L (acrylic polymer) nanoparticles [29], PLGA nanocapsules[49] or solid lipid nanoparticles [31].

On the other hand, the release of quercetin from casein nanoparticles appeared to be independent of the pH conditions and followed a zero-order kinetic. This fact could be explained by the entry of the aqueous medium inside the casein nanoparticles that induced the diffusion of quercetin by a release mechanism ruled by erosion/relaxation of the matrix. Surprinsingly, the incorporation of the cyclodextrin to the casein nanoparticles slightly decreased the release rate of quercetin from the resulting nanocarriers. This finding would suggest that the oligosaccharide interacts with casein to form a more compact matrix that would delay the release of quercetin from nanoparticles. Some years ago, it was reported that β-cyclodextrin is capable of forming inclusion complex with β-casein [50], and, thus, prevent its aggregation when warmed. In the same line, cyclodextrins have been proposed as stabilizers of therapeutic proteins in order to minimize aggregation phenomena [51]. However, in this case, the interaction between the oligosaccharide molecules and the protein would yield to a more resistant matrix to the erosion and/or relaxation that would occur in an aqueous environment.

In any case, further investigations are necessary to elucidate the real mechanism of the interaction between cyclodextrin and casein in the nanoparticulate form.

When quercetin was administered by the intravenous route as a solution of PEG400 and water, the profile of the curve was biphasic (Figure 4) and similar to that published previously [18]. The terminal half-life ($t_{1/2}$) of the quercetin was 0.6 h and the MRT was calculated to be 1.57 h. The oral administration of the same solution of quercetin induced discrete plasma levels that were only quantified during the first 8 hours post-administration. For this solution, the bioavailability of quercetin was calculated to be about 4%. This result is in line with the data obtained by Chen and co-workers, who described a quercetin bioavailability of 5% with a 15% HP-β-CD aqueous solution of the flavonoid in male Sprague-Dawley rats [18].

When quercetin was loaded in nanoparticles and orally administered to rats, the plasma levels of the flavonoid were higher than those observed for the control oral formulations (Figure 5). The incorporation of HP-β-CD in casein nanoparticles produced a significant prolongation of the quercetin plasma levels up to 72 h. This result was also evidenced by the high half-life ($t_{1/2}$) and MRT of the flavonoid when administered in the casein nanoparticles (see Table 3). Under these circumstances, the relative oral bioavailability of quercetin was calculated to be close to 37% (nine times higher than for the control solution of the flavonoid).

These prolonged and high levels of quercetin in plasma would be related to a combination of two phenomena. First, casein nanoparticles would conduct the cargo until the surface of the gut epithelium. The mucus-permeating properties of these carriers (see Chapter 4) would facilitate both their arrival to the surface of the enterocytes and an increased residence time in close contact with the absorptive membrane. Second, the cargo would be released and the presence of HP-β-CD would disarm the intestinal efflux pumps and the enzymatic complex associated to the cytochrome P450 [33-35]. All together would permit the absorption of quercetin and its improved bioavailability when encapsulated in these casein nanoparticles.
Alternatively, lymphatic absorption may be a supplementary factor that can also contribute to this improved bioavailability observed for quercetin (aglycone) when loaded in casein nanoparticles. Recently, it has been demonstrated that quercetin may be absorbed by both intestinal capillaries and lymphatic ducts [43,52]. This is important because absorption via the lymphatic system avoids hepatic first-pass metabolism and would prolong the presence of the flavonoid in the body.

Conclusions

In summary, the preparation of casein nanoparticles in the presence of HP-β-CD appears to be a good option to load quercetin for both nutraceutical and pharmaceutical purposes. The resulting nanoparticles offer a zero-order release rate of the flavonoid when incubated in simulated fluids. *In vivo*, these casein nanoparticles produced high and sustained levels of quercetin for periods up to 72 hours and an oral relative bioavailability close to 37%.

Acknowledgements

This work was supported by the Regional Government of Navarra (Alimentos funcionales, Euroinnova call) and the Spanish Ministry of Science and Innovation and Gobierno de Navarra (ADICAP; ref. IPT-2011-1717-900000). Rebeca Penalvaacknowledgesthe “Asociación de Amigos Universidad de Navarra” forthefinancialsupport.

References

[1] J. Czepas, K. Gwoździński, The flavonoid quercetin: Possible solution for anthracycline-induced cardiotoxicity and multidrug resistance, Biomedicine & Pharmacotherapy (in press).

[2] Agnes W. Boots, Review: Health effects of quercetin: From antioxidant to nutraceutical, Eur. J. Pharmacol. 585 (2008) 325.

[3] J.W. Erdman Jr, D. Balentine, L. Arab, G. Beecher, J.T. Dwyer, J. Folts, J. Harnly, P. Hollman, C.L. Keen, G. Mazza, M. Messina, A. Scalbert, J. Vita, G. Williamson, J. Burrowes, Flavonoids and heart health: proceedings of the ILSI North America Flavonoids Workshop, May 31-June 1, 2005, Washington, DC, J. Nutr. 137 (2007) 718S-737S.

[4] F. Perez-Vizcaino, J. Duarte, R. Andriantsitohaina, Endothelial function and cardiovascular disease: effects of quercetin and wine polyphenols, Free Radic. Res. 40 (2006) 1054-1065.

[5] M. Comalada, D. Camuesco, S. Sierra, I. Ballester, J. Xaus, J. Gálvez, A. Zarzuelo, In vivo quercitrin anti-inflammatory effect involves release of quercetin, which inhibits inflammation through down-regulation of the NF-κB pathway, Eur. J. Immunol. 35 (2005) 584-592.

[6] R.L. Edwards, T. Lyon, S.E. Litwin, A. Rabovsky, J.D. Symons, T. Jalili, Quercetin reduces blood pressure in hypertensive subjects, J. Nutr. 137 (2007) 2405-2411.

[7] C. Manach, G. Williamson, C. Morand, A. Scalbert, C. Remesy, Bioavailability and bioefficacy of polyphenols in humans. I. Review of 97 bioavailability studies, Am. J. Clin. Nutr. 81 (2005) 230S-242S.

[8] M. Kobori, S. Masumoto, Y. Akimoto, H. Oike, Chronic dietary intake of quercetin alleviates hepatic fat accumulation associated with consumption of a Western-style diet in C57/BL6J mice, Molecular Nutrition & Food Research 55 (2011) 530-540.

[9] S. Egert, S. Wolffram, A. Bosy-Westphal, C. Boesch-Saadatmandi, A.E. Wagner, J. Frank, G. Rimbach, M.J. Mueller, Daily quercetin supplementation dose-dependently increases plasma quercetin concentrations in healthy humans, J. Nutr. 138 (2008) 1615-1621.

[10] T. Okamoto, Safety of quercetin for clinical application (Review), Int. J. Mol. Med. 16 (2005) 275-278.

[11] M. Harwood, B. Danielewska-Nikiel, J. Borzelleca, G. Flamm, G. Williams, T. Lines, A critical review of the data related to the safety of quercetin and lack of evidence of< i> in vivo toxicity, including lack of genotoxic/carcinogenic properties, Food and Chemical Toxicology 45 (2007) 2179-2205.

[12] M.M. Chan, D. Fong, K.J. Soprano, W.F. Holmes, H. Heverling, Inhibition of growth and sensitization to cisplatin-mediated killing of ovarian cancer cells by polyphenolic chemopreventive agents, J. Cell. Physiol. 194 (2003) 63-70.

[13] K.A. Khaled, Y.M. El-Sayed, B.M. Al-Hadiya, Disposition of the flavonoid quercetin in rats after single intravenous and oral doses, Drug Dev. Ind. Pharm. 29 (2003) 397-403.

[14] V. Atul Bhattaram, U. Graefe, C. Kohlert, M. Veit, H. Derendorf, Pharmacokinetics and bioavailability of herbal medicinal products, Phytomedicine 9 (2002) 1-33.

[15] P.R. Babu, K.N. Babu, P.H. Peter, K. Rajesh, P.J. Babu, Influence of quercetin on the pharmacokinetics of ranolazine in rats and in vitro models, Drug Dev. Ind. Pharm. 39 (2013) 873-879.

[16] P. Limtrakul, O. Khantamat, K. Pintha, Inhibition of P-glycoprotein function and expression by kaempferol and quercetin (2013).

[17] T. Bansal, A. Awasthi, M. Jaggi, R.K. Khar, S. Talegaonkar, Pre-clinical evidence for altered absorption and biliary excretion of irinotecan (CPT-11) in combination with quercetin: possible contribution of P-glycoprotein, Life Sci. 83 (2008) 250-259.

[18] X. Chen, O.Q. Yin, Z. Zuo, M.S. Chow, Pharmacokinetics and modeling of quercetin and metabolites, Pharm. Res. 22 (2005) 892-901.

[19] Y. Guo, R.S. Bruno, Endogenous and exogenous mediators of quercetin bioavailability, J. Nutr. Biochem. (in press).

[20] S. Scalia, M. Mezzena, Incorporation of quercetin in lipid microparticles: Effect on photo-and chemical-stability, J. Pharm. Biomed. Anal. 49 (2009) 90-94.

[21] M. Calabrò, S. Tommasini, P. Donato, D. Raneri, R. Stancanelli, P. Ficarra, R. Ficarra, C. Costa, S. Catania, C. Rustichelli, Effects of α-and β-cyclodextrin complexation on the physico-chemical properties and antioxidant activity of some 3-hydroxyflavones, J. Pharm. Biomed. Anal. 35 (2004) 365-377.

[22] M.K. Kim, K. Park, W. Yeo, H. Choo, Y. Chong, In vitro solubility, stability and permeability of novel quercetin–amino acid conjugates, Bioorg. Med. Chem. 17 (2009) 1164-1171.

[23] P. Rinwa, L. Machawal, A. Kumar, Piperine potentiates the protective effect of quercetin against chronic unpredictable stress-induced cognitive dysfunction in mice, Alzheimer's & Dementia 8 (2012) P198-P199.

[24] L. Gao, G. Liu, X. Wang, F. Liu, Y. Xu, J. Ma, Preparation of a chemically stable quercetin formulation using nanosuspension technology, Int. J. Pharm. 404 (2011) 231-237.

[25] J. Tang, J. Sun, Z. He, Self-emulsifying drug delivery systems: strategy for improving oral delivery of poorly soluble drugs, Current Drug Therapy 2 (2007) 85-93.

[26] G.L. Li, Y.T. Fan, Y.H. Zhang, Y.F. Li, X.R. Li, Y. Liu, M. Li, In vitro and in vivo evaluation of total flavones of Hippophae rhamnoides self-microemulsifying drug delivery system, Yao Xue Xue Bao 47 (2012) 1055-1062.

[27] A.P. Rogerio, C.L. Dora, E.L. Andrade, J.S. Chaves, L.F. Silva, E. Lemos-Senna, J.B. Calixto, Anti-inflammatory effect of quercetin-loaded microemulsion in the airways allergic inflammatory model in mice, Pharmacological Research 61 (2010) 288-297.

[28] A. Karadag, X. Yang, B. Ozcelik, Q. Huang, Optimization of Preparation Conditions for Quercetin Nanoemulsions Using Response Surface Methodology, J. Agric. Food Chem. 61 (2013) 2130-2139.

[29] H. Pool, D. Quintanar, J. de Dios Figueroa, J.E.H. Bechara, D.J. McClements, S. Mendoza, Polymeric nanoparticles as oral delivery systems for encapsulation and release of polyphenolic compounds: impact on quercetin antioxidant activity & bioaccessibility, Food Biophysics 7 (2012) 276-288.

[30] A. Barras, A. Mezzetti, A. Richard, S. Lazzaroni, S. Roux, P. Melnyk, D. Betbeder, N. Monfilliette-Dupont, Formulation and characterization of polyphenol-loaded lipid nanocapsules, Int. J. Pharm. 379 (2009) 270-277.

[31] H. Li, X. Zhao, Y. Ma, G. Zhai, L. Li, H. Lou, Enhancement of gastrointestinal absorption of quercetin by solid lipid nanoparticles, J. Controlled Release 133 (2009) 238-244.

[32] R. Penalva, I. Esparza, M. Agüeros, C.J. Gonzalez-Navarro, C. Gonzalez-Ferrero, J.M. Irache, Casein nanoparticles as carriers for the oral delivery of folic acid, Food Hydrocolloids 44 (2015) 399–406.

[33] M. Ishikawa, H. Yoshii, T. Furuta, Interaction of modified cyclodextrins with cytochrome P-450, Biosci. Biotechnol. Biochem. 69 (2005) 246-248.

[34] K. Uekama, Design and evaluation of cyclodextrin-based drug formulation, Chemical and Pharmaceutical Bulletin 52 (2004) 900-915.

[35] T.R. Buggins, P.A. Dickinson, G. Taylor, The effects of pharmaceutical excipients on drug disposition, Adv. Drug Deliv. Rev. 59 (2007) 1482-1503.

[36] Agüeros, M., Esparza,, I., González-Ferrero, C., González-Navarro, C.J., Irache, J.M., Romo, A, Nanoparticles for encapsulating compounds, preparation thereof and use of same. (2011).

[37] P. Arbós, M.A. Campanero, M.A. Arangoa, M.J. Renedo, J.M. Irache, Influence of the surface characteristics of PVM/MA nanoparticles on their bioadhesive properties, J. Controlled Release 89 (2003) 19-30.

[38] P. Iacopini, M. Baldi, P. Storchi, L. Sebastiani, Catechin, epicatechin, quercetin, rutin and resveratrol in red grape: Content,< i> in vitro antioxidant activity and interactions, Journal of Food Composition and Analysis 21 (2008) 589-598.

[39] P.L. Ritger, N.A. Peppas, A simple equation for description of solute release I. Fickian and non-Fickian release from non-swellable devices in the form of slabs, spheres, cylinders or discs, J. Controlled Release 5 (1987) 23-36.

[40] P. Costa, J.M. Sousa Lobo, Modeling and comparison of dissolution profiles, European Journal of Pharmaceutical Sciences 13 (2001) 123-133.

[41] S. Waldmann, M. Almukainzi, N.A. Bou-Chacra, G.L. Amidon, B. Lee, J. Feng, I. Kanfer, J.Z. Zuo, H. Wei, M.B. Bolger, Provisional biopharmaceutical classification of some common herbs used in western medicine, Molecular Pharmaceutics 9 (2012) 815-822.

[42] X. Cai, Z. Fang, J. Dou, A. Yu, G. Zhai, Bioavailability of quercetin: Problems and promises, Curr. Med. Chem. 20 (2013) 2572-2582.

[43] K. Murota, J. Terao, Quercetin appears in the lymph of unanesthetized rats as its phase II metabolites after administered into the stomach, FEBS Lett. 579 (2005) 5343-5346.

[44] B.A. Graf, C. Ameho, G.G. Dolnikowski, P.E. Milbury, C.Y. Chen, J.B. Blumberg, Rat gastrointestinal tissues metabolize quercetin, J. Nutr. 136 (2006) 39-44.

[45] E. Oliveira, D. Watson, In vitro glucuronidation of kaempferol and quercetin by human UGT-1A9 microsomes, FEBS Lett. 471 (2000) 1-6.

[46] M.G. Boersma, H. van der Woude, J. Bogaards, S. Boeren, J. Vervoort, N.H. Cnubben, M.L. van Iersel, P.J. van Bladeren, I.M. Rietjens, Regioselectivity of phase II metabolism of luteolin and quercetin by UDP-glucuronosyl transferases, Chem. Res. Toxicol. 15 (2002) 662-670.

[47] X. Chen, O.Q. Yin, Z. Zuo, M.S. Chow, Pharmacokinetics and modeling of quercetin and metabolites, Pharm. Res. 22 (2005) 892-901.

[48] M.R. Olthof, P.C. Hollman, M.N. Buijsman, J.M. van Amelsvoort, M.B. Katan, Chlorogenic acid, quercetin-3-rutinoside and black tea phenols are extensively metabolized in humans, J. Nutr. 133 (2003) 1806-1814.

[49] S. Ghosh, S.R. Dungdung, S.T. Chowdhury, A.K. Mandal, S. Sarkar, D. Ghosh, N. Das, Encapsulation of the flavonoid quercetin with an arsenic chelator into nanocapsules enables the simultaneous delivery of hydrophobic and hydrophilic drugs with a synergistic effect against chronic arsenic accumulation and oxidative stress, Free Radical Biology and Medicine 51 (2011) 1893-1902.

[50] M. Lee, O.R. Fennema, Ability of cyclodextrins to inhibit aggregation of. beta.-casein, J. Agric. Food Chem. 39 (1991) 17-21.

[51] T. Serno, R. Geidobler, G. Winter, Protein stabilization by cyclodextrins in the liquid and dried state, Adv. Drug Deliv. Rev. 63 (2011) 1086-1106.

[52] I. Chen, Y. Tsai, C. Huang, T. Tsai, Lymphatic absorption of quercetin and rutin in rat and their pharmacokinetics in systemic plasma, J. Agric. Food Chem. 58 (2009) 546-551.

Chapter 6

Zein nanoparticles as carriers for the oral delivery of folic acid

Abstract

The application of plant proteins in controlled release is a good option since they are very accessible materials, cheap, found in naturally vegetal matrixes, and have a good capacity to interact with a wide variety of compounds and nutrients. The aim of this work was to prepare and characterize zein nanoparticle of folic acid. These nanoparticles were prepared by desolvation process, stabilized with lysine, purified and finally dried by spray drying. The resulting nanoparticles displayed a mean size close to 200 nm with negative zeta potential and a folic acid content around 54 µg per mg nanoparticle. The in vitro studies showed no release of the drug under simulated gastric conditions by the carrier while *ex vivo* imaging demonstrated their mucopenetrating abilities in the proximal jejunum of the rats. Finally, a pharmacokinetic study after the oral administration of the folic acid loaded zein nanoparticles to Wistar rats revealed that this formulation was able to enhance the folic acid oral bioabailability up to 70%.

1. Introduction

Zein, a major storage protein of corn, is located in "zein-bodies" of ~1 μm distributed uniformly throughout the cytoplasm of corn endosperm cells between starch granules of 5–35 μm [1]. From a physico-chemical point of view, the key characteristic of zein is its insolubility in water except at extreme pH conditions (e.g. pH 11 or above) or in presence of high concentrations of urea, alcohol or anionic detergents [2]. This characteristic is directly related with its composition in aminoacids. Thus, zein is particularly rich in glutamic acid (21–26%) and non-polar aminoacids such as leucine (20%), proline (10%) and alanine (10%), but deficient in basic and acidic aminoacids[3].

Zein is actually a mixture of different peptides. In accordance with the nomenclature developed by Esen, zein polypeptides are classified as α, β, γ, and δ-zeins on the basis of differencesin solubility and sequence [4]. Alpha-zein is the most abundant (around 80% of total zein) and includes two prolamin groups with apparent molecular weights of 24 and 27 kDa. Beta-zein consists of a methionine-rich polypeptide of 17 kDa and constitutes up to 10% of the total zein; whereas γ-zein is also composed of two peptides of 27 and 18 kDa. Finally, δ-zein is a minor fraction and has a molecular weight of about 10 kDa[5,6].

Because of its hydrophobic character and deficiency in essential aminoacids (e.g. lysine and tryptophan), the use of this corn protein in human food products is limited. However, zein has been proposed as material for the manufacture of a wide variety of products, including textile fibers for clothes [7], biodegradable films andplastics used for packaging [8], coatings for food and pharmaceutical dosage forms [9-11] and scaffolds for tissue engineering [12].

In the last years, microparticles and nanoparticles from zein have also been studied as carriers of non-polar compounds including vitamin D3 [13], curcumin[14] or tymol[15]. Such devices were capable of protecting the loaded compounds from stomach harsh conditions and providing a mechanism for constant release of drugs [16-18].

Folic acid (pteroyl-L-glutamic acid, vitamin B9) is a water soluble vitamin that is essential during periods of rapid cell division and growth. It is implicated in cell replication and has an important role in one-carbon metabolism, essential for cardiovascular and neurological functions [19].

During periods of inadequate folate intake or malabsorption, biochemical changes due to this lack of folic acid/folate may result in deleterious consequences, including increased risk for certain types of chronic diseases [20] and developmental disorders (e.g., neural tube defects) [21]. In this way, previous studies have shown that folate deficiency is associated with higher incidence of mental symptoms in general population and poor cognitive performance that may increase the risk of dementia in old age [22-24]. Particularly in major depression, low folic acid levels are frequently described in clinical studies [25,26]. Corroborating these findings, a variety of controlled and open-label studies have shown that the efficacy of antidepressants is influenced by folatestatus and may be enhanced by folic acid supplementation [27]. On the other hand, low folate intake or low plasma folate concentration has also been associated with increased cardiovascular and cerebrovascular risks [28]. All of these effects would be related with high plasma levels of homocysteine, a cytotoxic sulfur-containing aminoacid that can induce DNA strand breakage, oxidative stress and apoptosis [28,29].

Interestingly, folic acid supplementation might reduce the hyperhomocysteinaemia[30,31]. However, the supply of folate coenzymes *in vivo* depends primarily on the quantity and

bioavailability of ingested folic acid/folate and the rate of loss by urinary and fecal routes and through catabolism.Additionally, folate is highly susceptible to oxidative destruction. In fact, 50–95% of folate content in food is estimated to be lost during storage, preparation, or manufacturing processes [32,33].

The aim of this work was to design and evaluate zein nanoparticles as carriers capable of improving the bioavailability of folic acid when orally administered. For this purpose, these zein nanoparticles were prepared by an original procedure and their capability to improve the oral bioavailability of folic acid was evaluated and compared with a conventional aqueous solution of the vitamin in rats.

2. Materials and methods

2.1. Materials

Zein, folic acid, lysine, arginine, pepsin, pancreatin, mannitol and sodium chloride were from Sigma-Aldrich (Germany). Ethanol, acetonitrile and o-phosphoric acid (HPLC grade) were from Merck (Darmstadt, Germany). Lumogen® F red 305 was from Kremer (Aichstetten, Germany). Tissue-Tek® OCT compound was obtained from Sakura (Alphen, Netherlands). Iodine 125 was from Perkin Elmer (USA). AccuDiag™ Folate-Folic acid ELISA Kit was purchased from Diagnostic Automation/Cortez Diagnostics Inc. (USA). Deionised water (18.2 MΩ resistivity) was prepared by a water purification system (Wasserlab, Spain). All reagents and chemicals used were of analytical grade.

2.2. Preparation of zein nanoparticles

Zein nanoparticles were prepared by a desolvation procedure followed by a purification step by ultrafiltration and subsequent drying in a Spray-drying apparatus [34]

2.2.1. Empty zein nanoparticles (NP-Z)

Briefly, 600 mg ofzein and 100 mg of lysine were firstly dissolved in 70 mL ethanol:water mixture (1:1 v/v) by magnetic stirring at room temperature. Then, nanoparticles were formed by the addition of 70 mL of water. The suspension was purified and concentrated by ultrafiltration through a polysulfone membrane cartridge of 50 kDa pore size (Medica SPA, Italy). Finally, 20 ml of an aqueous solution of mannitol (100 mg/mL) was added to the suspension of zein nanoparticles in order to prevent irreversible aggregation of nanoparticles during the drying step, and the mixture was dried in a Büchi Mini Spray Drier B-290 apparatus (BüchiLabortechnik AG, Switzerland) under the following experimental conditions: (i) inlet temperature of 90°C, (ii) outlet temperature 45-50°C, (iii) air pressure: 2-5 bar, (iv) pumping rate of 2-6 mL/min, (v) aspirator of 100% and (vi) air flow at 900 L/h.

2.2.2. Folic acid-loaded zein nanoparticles (FA-NP-Z)

The preparation of zein nanoparticles loaded with folic acid (FA-NP-Z) was similar to that of the empty particles, with some minor adjustments. For this purpose, 600 mg of zein and 100 mg of lysine were dissolved in 70 mL purified water. In parallel, 200 mg folic acid was dissolved in 50 mL of an aqueous solution of lysine (4 mg/mL). Then, 15 mL of the aqueous folic acid solution were added to the zein solution and the resulting mixture was incubated at room temperature for 10 min under magnetic stirring. Finally, zein nanoparticles were obtained by the addition of 70 mL of water. The suspension was purified and dried as described above.

2.3. Characterization of nanoparticles

2.3.1. Size, zeta potential and morphology

The particle size distribution and zeta potential of the above formulations were measured by photon correlation spectroscopy (PCS) and electrophoretic laser Doppler anemometry, respectively, using a Zetaplus apparatus (Brookhaven Instrument Corporation, USA). The diameter of the nanoparticles was determined after dispersion in distilled water (1:10) and measured at 25°C with a scattering angle of 90°. The zeta potential was measured after dispersion of the dried nanoparticles in 1 mM pH 6 KCl solutions.

The morphology and shape of nanoparticles were examined using a field emission scanning electron microscope FE-SEM (ULTRA Plus, Zeiss, The Netherlands). Prior to analysis, particles were washed to remove mannitol. For this purpose, spray-dried nanoparticles were suspended in distilled water and centrifuged at 17,000 xg for 10 min. Then, the supernatants were discarded and the obtained pellets were mounted on copper grids. Finally, the pellet was shaded with an amalgam of gold/palladium during fifteen seconds using a sputter coater (K550X Emitech, Ashford, UK).

2.3.2. Yield of the preparative process

In order to quantify the amount of protein transformed into nanoparticles, 10 mg of the nanoparticle formulation were dispersed in water and centrifuged at 17,000 xg for 20 min. Supernatants were discarded and the pellets were digested with ethanol 75%. Then, the amount of protein was quantified by UV spectrophotometry at 278 nm in an Agilent 8453 system (Agilent Technologies, USA). For analysis, calibration curves were constructed between 90 and 1200 µg/mL (R^2> 0.999; quantification limit = 143 µg/mL).

The amount of protein forming nanoparticles in the formulation was estimated as the ratio between the amount of the protein quantified in the pellet of the centrifuged samples and the total amount of protein used for the preparation of nanoparticles and expressed as follows:

$$Yield\ (\%) = \frac{(Protein\ in\ pellet)}{(Total\ protein\ )} \times 100 \quad \text{[Eq. 1]}$$

2.4. Folic acid analysis

The amount of folic acid loaded into the nanoparticles was quantified by HPLC-UV following an analytical method previously published by Sierra and collaborators [35] with minor modifications. Analysis was carried out in an Agilent model 1100 series LC and a diode-array detector set at 290 nm. The chromatographic system was equipped with a reversed-phase 150 mm x 2.1 mm C18 Alltima column (particle size 5 µm; Altech, USA) and a Gemini C18 precolumn (particle size 5 µm; Phenomenex, CA, USA). The mobile phase, pumped at 0.25 mL/min, was a mixture of phosphoric acid (33 mM, pH 2.3) and acetonitrile in a gradient condition (Table 1). The column was placed at 40ºC and the injection volume was 10 µL. Under these conditions, folic acid eluted at 21.2 ± 0.5 min. For calculations, calibration curves were designed over the range of 2 and 200 µg/mL ($R^2 > 0.999$). The limit of quantification was calculated to be 4.3 µg/mL. For analysis, 10 mg of nanoparticles were dispersed in 1 mL of water and centrifuged. In order to determine the amount of folic acid loaded inside the nanoparticles, the pellets were digested with ethanol 75%. In parallel, the total amount of folic acid in the dry formulations was quantified by direct digestion of 10 mg of formulation with 1 mL of ethanol 75%. In all cases the samples were filtered through 0.45 µm membranes before analysis. Each sample was assayed in triplicate and results were expressed as follows:

$$\text{Folic acid loading } (\mu g/\text{ mg NP}) = \frac{\text{FA p}}{\text{W p}} \times 100 \quad \text{(Eq. 2)}$$

$$\text{Encapsulation efficency } (\%) = \frac{\text{FA p}}{\text{FA t}} \times 100 \quad \text{[Eq. 3]}$$

in which FAp corresponds to the amount of folic acid quantified in the pellets; FAt is the total amount of folic acid in the dry formulation and Wp is the amount of protein transformed into nanoparticles and quantified by spectrophotometry as described above.

2.5. *In vitro* release study

Release experiments were conducted under sink conditions at 37°C using simulated fluids for gastric (SGF; pH 1.2; pepsin 0.32% w/v) and intestinal (SIF; pH 6.8; pancreatin 1% w/v) conditions. The studies were performed under agitation in a Vortemp 56TM Shaking Incubator (Labnet International Inc., NJ USA) after the dispersion of the nanoparticles in the appropriate medium.

For each specific time interval, 20 µg of folic acid formulated in nanoparticles wereresuspended in 1 mL of the corresponding simulated fluid. The different formulations were kept in the SGF for 2 hours before being transferred to SIF for a subsequent 20 hours. At different intervals, samples were collected and centrifuged at 17,000 rpm for 20 minutes. The amount of folic acid released was quantified by HPLC from the supernatants as described above.

2.6. Zein nanoparticles labelling

2.6.1. Radiolabelling of zein nanoparticles (^{125}I-NP-Z)

Zein nanoparticles were radiolabelled with Iodine-125 (^{125}INa) by standard mild oxidative iodination. For this purpose, 10 mg zein nanoparticles were tagged with 2 iodobeads and 3.5 µL of ^{125}INa in 600µL of PBS:water for injection (1:2 by vol). After 15 min of incubation, iodine zein nanoparticles (^{125}I-NP-Z) were obtained. In order to check the stability of the labelling, ^{125}I-NP-Z were incubated in dialysis cassettes with simulated gastric or intestinal media and deiodination measured by TLC of samples for up to 48 h.

2.6.2. Lumogen red loaded in zein nanoparticles (LR-NP-Z)

Zein nanoparticles were fluorescently labelled with Lumogen® F Red 305 (LR-NP-Z). For that, 2 mg of Lumogen® red in acetone (5 mL) were added to the hydroalcoholic solution of zein and lysine. Then, zein nanoparticles were formed by the addition of 70 mL of water. The resulting nanoparticles were purified and dried in the spray-drier apparatus under the same conditions described above.
The amount of Lumogen® F Red 305 was determined by colorimetry at wavelength 540 nm in a spectrophotometer Agilent 8453 system (USA). The Lumogen loading was estimated as the difference between its initial concentration added and the concentration found in the supernatant after the centrifugation of the samples in water (17,000 rpm for 20 min). For quantification, standard curves of Lumogen red in ethanol 75% were used (concentration range of 5-30 µg/mL $R^2 \geq 0.999$).

2.7. *In vivo* distribution study

All of these studies were performed in male Wistar rats obtained from Harlan (Barcelona, Spain) and the protocols were approved by the Ethical Committee for Animal Experimentation of the University of Navarra (protocol numbers 117-12 and 059-13). Prior to the experiment, animals were placed in metabolic cages and drink provided *ad libitum*.
For radiolabelled nanoparticles, animals (200-250 g) received a 1 mL single dose of an aqueous suspension of nanoparticles (10 mg of ^{125}I-NP-Z). As control, an aqueous suspension of ^{125}I was administered by oral route. Animals were anesthetized with isofluorane and place in prone position on the gammacamera. The gammagraphic studies were performed in a E.cam Dual-Head-Variable-Angle System gammacamera (Siemens Medical Systems, USA) The images were obtained 2, 24, 48 and 72 hours after the administration of the radiolabelled nanoparticles.

For fluorescently labelled nanoparticles, animals received orally a single dose of 1 mL of an aqueous suspension containing 30 mg of LP-NP-Z. Two hours later, the animals were sacrificed and guts were removed. Jejunum portions of 1 cm were collected, stored in the tissue proceeding medium O.C.T. and frozen at -80°C. Each portion was then cut into 5-µm sections on a cryostat and attached to glass slides. Finally, these samples were fixed with formaldehyde and incubated with DAPI (4',6-diamidino-2-phenylindole) for 15 minutes before the cover assembly. The presence of fluorescently loaded nanoparticles in the intestinal mucosa and the cell nuclei

dyed with DAPI were visualized in a fluorescence microscope (Axioimager M1, Zeiss) with a coupled camera (Axiocam ICc3, Zeiss) and fluorescent source (HBO 100, Zeiss).

2.8. *In vivo* pharmacokinetic studies in male Wistar rats

2.8.1. Pharmacokinetic studies

Pharmacokinetic studies were performed in male Wistar rats (200-250 g) obtained from Harlan (Barcelona, Spain). Studies were approved by the Ethical Committee for Animal Experimentation of the University of Navarra (protocol number 014-10) in accordance with the European legislation on animal experiments. Prior to the experiment, animals were adaptively fed for 1 week with free access to a Folic Acid deficient diet (TD 95247, Harlan, USA) and drinking water (22±2°C; 12-h light and 12-h dark cycles; 50-60% relative humidity). Previous to the oral administration of the formulations, animals were fasted overnight to avoid interference with the absorption, allowing free access to water.

For the pharmacokinetic study, rats were randomly divided into 4 groups of 6 animals each. The experimental groups were an aqueous solution of folic acid (Folic acid dissolved in PBS) and folic acid-loaded zein nanoparticles (FA-NP-Z) dispersed in water. As controls, a group of animals was intravenously administered with a solution of folic acid in PBS and the last group of rats received PBS (without folic acid) orally. The single folic acid administered dose was 1 mg/kg body weight either orally with a blunt needle via the oesophagus into the stomach or intravenously via tail vein.

Blood samples were collected at set times after administration (0, 10 min, 30 min, 1, 2, 4, 6, 8 and 24 hours) in specific serum tubes (SARSTEDT Microtube 1,1 mL Z-Gel). Blood volume was recovered intraperitoneally with an equal volume of sterile saline solution pre-heated to body temperature. Samples were immediately centrifuged at 10,000 rpm for 10 min. Serum was separated into clean tubes and kept frozen at -80 °C until analysis.

2.8.2. Determination of Folic Acid in serum

The amount of folic acid in serum was determined by an Enzyme Immunoassay. Calibrator and quality control samples were prepared by adding appropriate volumes of standard folic acid solution in PBS to serum. Calibration curves were designed over the range 4-450 ng/mL (r^2> 0.996). For analysis, 100 µL of the serum samples were added to each well of the microtiter plate, followed by the addition of 50 µL of folic acid antibody. After incubation for 60 min at room temperature, the plate was washed three times with the washing solution (PBS-Tween 20 0.5%). Then, 100 µL of conjugate (anti-mouse-IgG-HRP) was added into each well and after 60 min at room temperature; the plate was washed again for three times with the washing solution. For the reaction, 100 µL of substrate was added into each well and incubated in darkness conditions for 20 min at room temperature. The reaction was stopped by the addition of 100 µLof sulphuric acid 0.5 M into each well. Finally, the absorbance was measured at 450 nm in an ELISA reader (LabsystemsiEMS Reader MF).

Under these experimental conditions, the limit of quantification of this method was calculated to be 4 ng/mL. The recovery of folic acid from serum samples was 90.1 ± 0.3 %. Accuracy values

during the same day (intraday assay) at low, medium and high concentrations of FA were always within the acceptable limits (less than 15%).

2.8.3. Pharmacokinetic data analysis

The pharmacokinetic analysis of serum concentration plotted against time datawas performed using a non-compartmental model with the WinNonlin 5.2 software (Pharsight Corporation, Mountain View, USA). The following parameters were estimated: maximal serum concentration (C_{max}), time taken to reach C_{max} (T_{max}), area under the concentration-time curve from time 0 to ∞ (AUC), mean residence time (MRT), clearance (Cl), volume of distribution (V) and half-life in the terminal phase ($t_{1/2}$). Furthermore, the relative oral bioavailability (Fr %) of folic acid was estimated using the following equation:

$$\mathrm{Fr}\ (\%) = \frac{\mathrm{AUC\ oral}}{\mathrm{AUC\ iv}} \times 100 \quad \text{[Eq. 4]}$$

where AUC iv and AUC oral are the areas under the curve for the iv and oral administrations, respectively.

2.9. Statistical analysis

Data are expressed as the mean ± standard deviation (SD) of at least three experiments. The non-parametric Kruskall-Wallis followed by Mann-Whitney U-test was used to investigate statistical differences. In all cases, $p< 0.05$ was considered to be statistically significant. All data processing was performed using SPSS® statistical software (SPSS® 15, Microsoft, USA).

3. Results

3.1. Folic acid loaded zein nanoparticles

Table 1 summarizes the main physico-chemical properties of folic acid-loaded nanoparticles. When folic acid was encapsulated into zein nanoparticles, a moderate increase in the mean size of the resulting carriers was observed (about 164 nm for empty nanoparticles *vs* 193 nm for FA-NP-Z); whereas the negative zeta potential decreased from -46 mV (control nanoparticles) to -30 mV (folic acid nanoparticles). The folic acid loading into the zein nanoparticles (FA-NP-Z) was calculated to be around 54 µg/mg nanoparticle with an encapsulation efficiency close to 57%.

The morphological analysis by scanning electron microscopy(Figure 1) showed than folic acid loaded zein nanoparticles consisted of homogeneous populations of spherical nanoparticles with a smooth surface and an apparent similar size to that obtained by photon correlation spectroscopy.

Table 1. Physico-chemical characterization of zein nanoparticles. NP-Z, Empty nanoparticles were manufactured without FA. FA-NP-Z, Folic acid loaded in zein nanoparticles. Data expressed as mean ± SD, n=3.

Formulations	Size (nm)[a]	PDI (nm)	Zeta Potential (mV)[b]	FA loading (µg FA/mg NP)[c]	E.E.(%)[d]
NP-Z	164 ± 2	0.07 ± 0.01	-46.0 ± 1.5	-	-
FA-NP-Z	193 ± 3	0.20 ± 0.06	-29.3 ± 3.1	54 ± 7	57±6

[a] Determination of the nanoparticle size (nm) by photon correlation spectroscopy

[b] Determination of the zeta potential (mV) by electrophoretic laser Doppler anemometry

[c] Amount of drug loaded in the nanoparticles (µg FA/mg NP)

[d] Encapsulation efficiency (%)

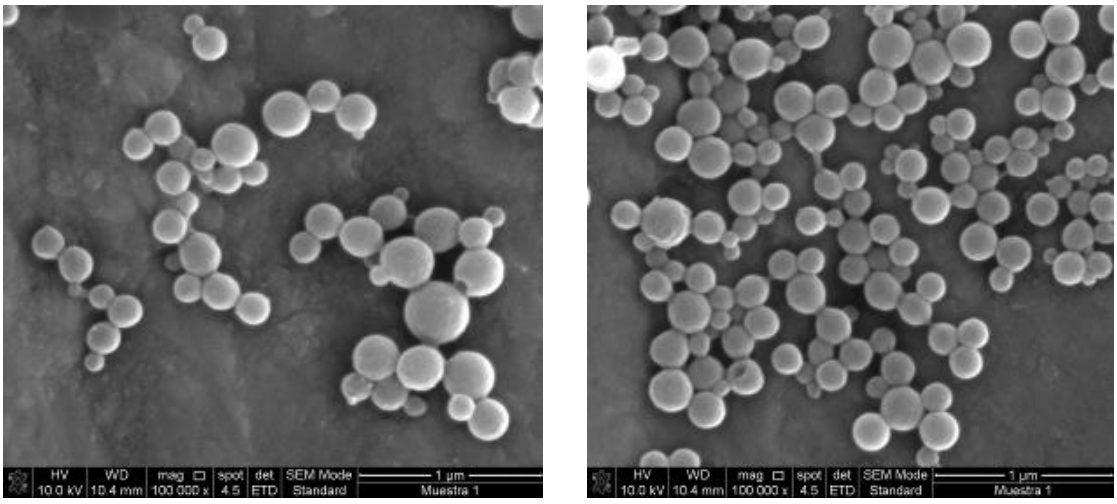

Figure 1. Scanning Electron Microscopy (SEM) microphotographs obtained from folic acid-loaded zein nanoparticles.

3.2. *In vitro* release study

Figure 2 represents the release profile of folic acid from the zein nanoparticles formulations as cumulative percentage of the vitamin released as a function of time. When nanoparticles were incubated in SGF, no release of folic acid was observed. On the contrary, when zein nanoparticles were assayed in SIF, two different steps in the release behavior of folic acid could be differentiated. First, a burst effect in which about 70% of the loaded vitamin was released from the nanoparticles in 30 min. Then, a second step characterized by a sustained and slow release of the remaining folic acid up to 24 hours.

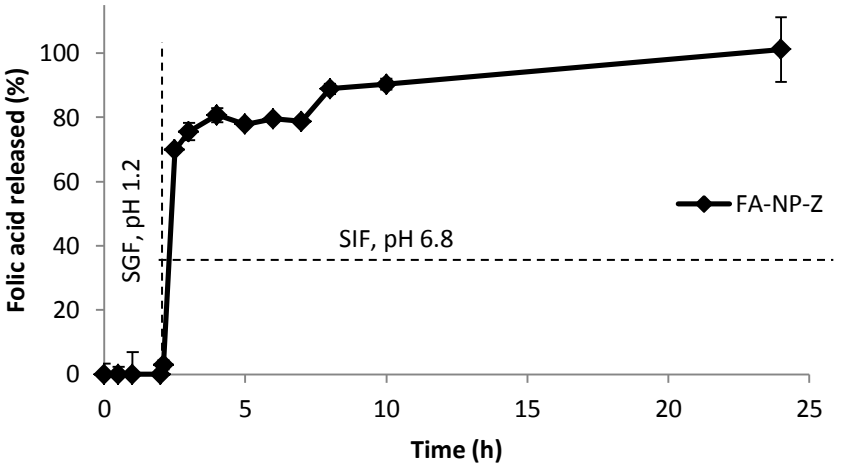

Figure 2. Folic acid release profile from zein nanoparticles after incubation in simulated gastric fluid (0-2 h) and intestinal fluid (2-48 h) under sink conditions. Data expressed as mean ±SD, n=3.

3.3. *In vivo* distribution study of ^{125}I-NP-Z and Lumogen-NP-Z in the gut mucosa

Figure 3 shows the biodistribution (SPECT-CT images) of free 125-iodine (figure 3A) and zein nanoparticles radiolabelled with 125-iodine (figure 3B) orally administered to rats.
For those animals treated orally with the control (free 125-iodine), the radioactivity was always found in their stomach and thyroid. On the other hand, the radioactivity associated to zein nanoparticles was visualized in the stomach 2 hours after administration; although, twenty two hours later the radioactive signal was also found at the thyroid and the distal areas of the colon. Finally, 48 hours after administration, the remaining activity was observed in the thyroid and stomach of animals, in which the signal was significantly lower than that observed at the previous times.

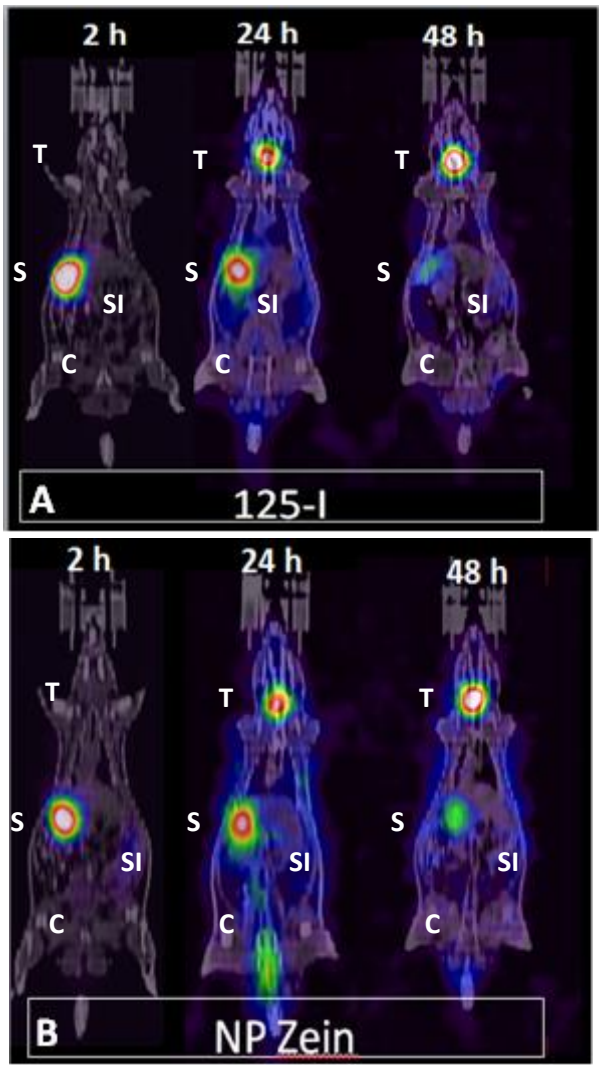

Figure 3. Biodistribution of ^{125}-Iodine control andradiolabelled zeinnanoparticles . Panels A and B show gammacamera images after oral administration of 10 mg of ^{125}-Iodine (3A) and ^{125}-Iodine-NP-Z (3B) at 2, 24 and 48 hours post administration. Thyroid (T), Stomach (S), Small intestine (SI), Colon (C).

Figure 4 shows fluorescence microscopy images of jejunum samples of animals treated with Lumogen® red formulations. Control formulation (an aqueous suspension of the fluorescent marker) was visualized as large aggregates in the lumen of animals or in contact with the external mucus layer (Figures 4A and 4B). Zein nanoparticles appeared to be able to reach and interact closely with the surface of the intestinal epithelium (Figure 4C and 4D).

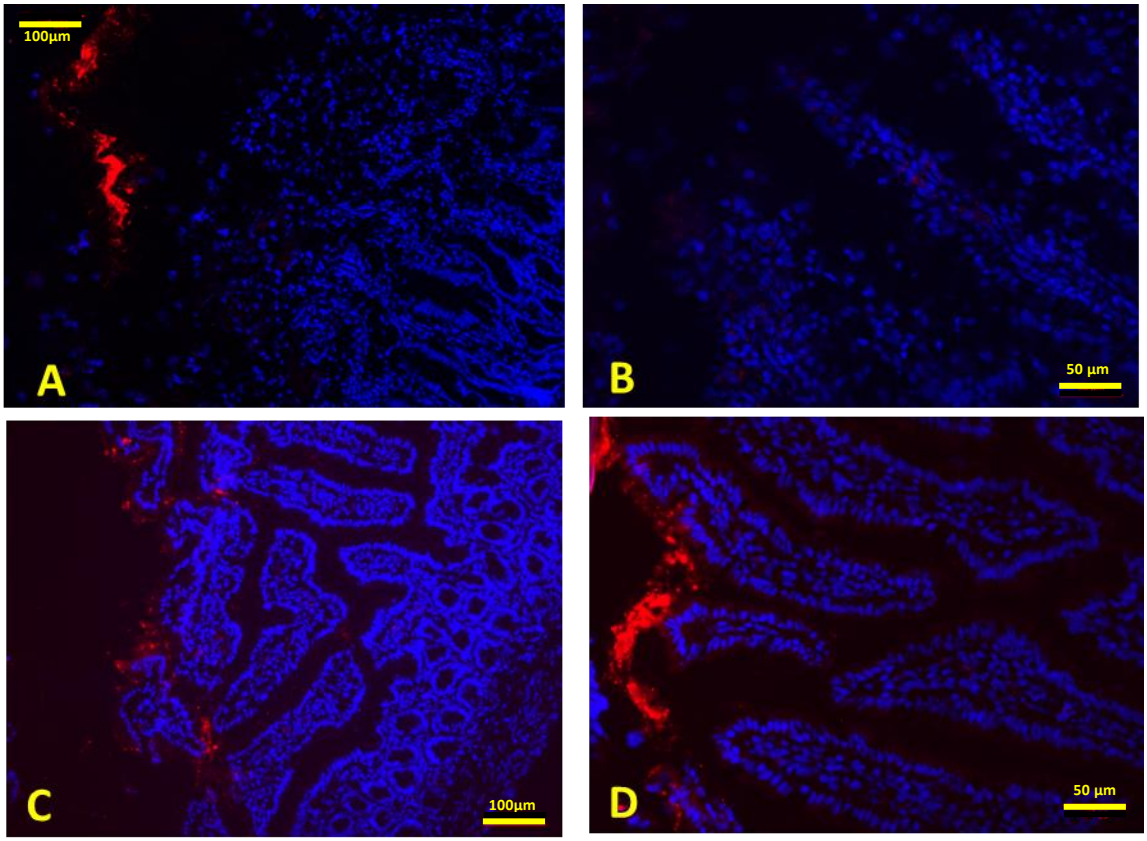

Figure 4. Fluorescence microscopy images of jejunum samples 2 hours after the oral administration of either a Lumogen® red suspension (A and B) or zein nanoparticles fluorescently labelled with Lumogen® red. Nuclei of cells were stained blue with DAPI.

3.4. Pharmacokinetic studies in Wistar rats

Figure 5 shows the folic acid levels in the serum of rats after the intravenous administration of a vitamin aqueous solution (dose 1 mg/kg) are presented in Figure 5. Data were adjusted to a non-compartmental model. The folic acid serum concentration decreased rapidly displaying a biphasic pattern that was adjusted to a non-compartmental model. The peak plasma concentration (C_{max}) and the AUC were 6 µg/mL and 3.7 µg h/mL, respectively. The folic acid half-life ($t_{1/2}$) in serum was calculated to be 1.1 hours; whereas its clearance and volume of distribution were calculated to be 0.06 L/h and 0.1 L, respectively (Table 5).

When folic acid was administered orally as aqueous solution, the levels of the vitamin in the sera of animals increased rapidly during the first 1 h post-administration, in which the C_{max} was reached (Figure 6). Then the vitamin levels decreased slowly until the end of the experiment (24 h post-administration). For the formulation based on zein nanoparticles, the levels of folic acid in the sera of animals displayed a similar profile to that observed for the free folic acid (FA solution). However, the serum levels of the vitamin from nanoparticles were significantly higher than those observed for the aqueous solution of folic acid.

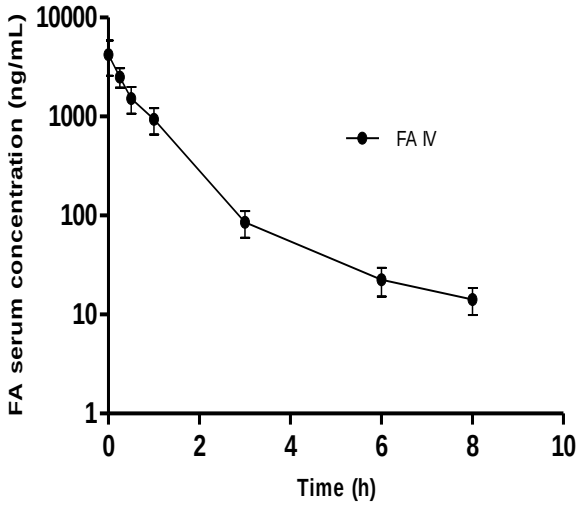

Figure 5. Folic acid concentration *vs* time after a single i.v. administration of a folic acid solution at a dose of 1 mg/kg. Data expressed as mean± SD; (n= 6).

Table 2 summarizes the pharmacokinetic parameters derived from the analysis of the data obtained after the administration of the different folic acid formulations to rats.When folic acid was administrated orally as aqueous solution, the AUC was 1.4 µg h/mL; whereas, this parameter was 3.0 µg h/mL when the vitamin was given after its encapsulation in zein nanoparticles. Similarly, the peak plasma concentration (C_{max}) of folic acid in the nanoparticles was around 2- times higher than for the vitamin aqueous solution. On the contrary, other important pharmacokinetic parameters of folic acid (eg. volume of distribution, clearance or half-life of the terminal phase) were similar when the vitamin was administered as aqueous solution or loaded in zein nanoparticles. Finally, the relative oral bioavailability of folic acid when incorporated in zein nanoparticles was of about 70%, whereas for the folic acid aqueous solution the oral bioavailability was only of 35%.

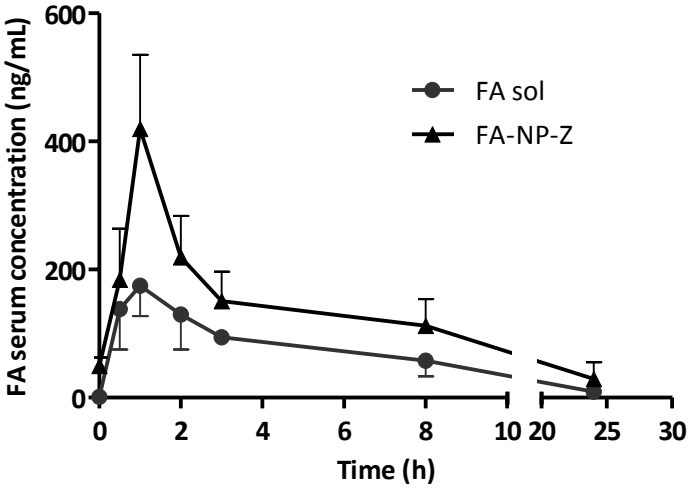

Figure 6. Folic acid serum concentration vs time after a single oral administration of 1 mg/kg for the different formulations tested. i) Folic acid solution in PBS (●; FA sol), ii) Folic acid loaded in zein nanoparticles (▲; FA-NP-Z). Data expressed as mean ± SD; (n= 6).

Table 2. Pharmacokinetic parameters of folic acid administered as single dose of 1 mg/kg by the intravenous or oral route as aqueous solution or loaded in zein nanoparticles. Data are expressed as mean ± S.D (n=6).

	Route	C_{max} (µg/mL)	T_{max} (h)	AUC (µgh/mL)	T½ (h)	Cl (L/h)	Vd (L)	MRT (h)	Fr (%)
PBS	p.o	-	-	-	-	-		-	-
FA i.v.	p.iv	5.5 ± 2.7**	0.0	3.7 ± 0.4**	1.2±0.6	0.06±0.01	0.10±0.05	0.9±0.2**	100**
FA sol	p.o.	0.2 ± 0.0	1.0 ± 0.6	1.3 ± 0.3	5.9±1.9	0.06±0.02	0.44±0.07	5.7±1.6	35
FA-NP-Z	p.o.	0.4 ± 0.1 *	1.0 ± 0.0	3.0 ± 1.0 *	7.1±2.6	0.05±0.01	0.49±0.11	6.5±1.3	70*

C_{max}: peak plasma concentration; T_{max}: time to reach plasma concentration; AUC: Area under the curve; t½: half-life of the terminal phase; Cl: Clearance; MRT: mean residence time Fr: relative oral bioavailability

*Significant differences ($p<0.05$) *vs* FA sol (Mann-Whitney-U)

**Significant differences ($p<0.01$) *vs* FA sol (Mann-Whitney-U)

4. Discusion

Folic acid, as other weak acid compounds, possesses a pH-dependent aqueous solubility, being insoluble in aqueous media below pH 5 [36]. *In vivo*, the pH of the stomach contents may induce the precipitation of the vitamin that, once in the small intestine (pH around 5-6), would be (at least in part) re-dissolved. However, in these pH conditions, and because of the hydrophilic nature of the charged molecule, specific transporters are required for folic acid absorption. These highly specific transporters (RFC and PCFT) are expressed at the apical brush-border membrane of the proximal jejunum [37] in which the absorption of the vitamin takes place [38].

On the other hand, zein is a biodegradable and biocompatible material, economic to use and with a "GRAS" status [39]. In addition, zein is an amphiphilic protein with an important ability to interact with solutes like drugs [40] or aminoacids[41,42]. Another important aspect of zein would be its resistance to digestive enzymes [3] which could be of interest to dosage froms with controlled release properties [16]. Furthermore, nanoparticles from this corn protein may be prepared easily under mild conditions by a desolvation technique after the addition of water to a hydroalcoholic solution of the protein. However, due to the biodegradable character of the resulting nanoparticles a drying step is necessary to improve their shelf-life during storage.
When zein nanoparticles were prepared in this way, the resulting dried powder was difficult to redispersed in aqueous media. In order to solve this drawback, zein nanoparticles were prepared in the presence of lysine to generate carriers capable of dispersing by simple hand-agitation. In fact, the incorporation of lysine turned the positive zeta potential (of zein nanoparticles in the absence of the basic amino acid) inside out a negative superficial charge of the resulting nanoparticles (Table 1).

In this context, folic acid-loaded zein nanoparticles displayed a size after reconstitution of about 200 nm with a negative zeta potential of -24mV and a low polydispersity index (Table 1). The folic acid content was close to 54 µg/mg nanoparticles. This result represents a 2-times higher vitamin content than in casein nanoparticles or more than 3-fold the folic acid loading when nano- and microcapsules from either whey protein or starch were used [43].
Interestingly, the release of folic acid from zein nanoparticles was found to be dependent of the pH conditions. Thus, under simulated gastric conditions, no folic acid release was observed from the zein nanoparticles, whereas, when nanoparticles were incubated in SIF, the release was almost immediate (Figure 2). These findings would be directly related with the behaviour of zein in aqueous media. In fact, under acidic pH conditions, glutamine residues of zein may be deamidated to yield glutamic acid; [44]. Due to the fact that the pKa of glutamic acid is around 4.1, under intestinal pH conditions, these residues would be deprotonated, resulting in a negative net charge [45] similar to that of the folic acid. Thus the repulsion between ionized folic acid and zein would result in a rapid release of the vitamin from the nanoparticles.

In the present study, the serum concentrations of folic acid provided by a conventional oral solution of the vitamin in PBS were almost zero. With this aqueous solution, the oral bioavailability of folic acid was calculated to be 35%. The highest concentrations of folic acid occurred 1 hour after the administration, and values returned to baseline after 24 hours. These results are in line with previous data reported in the literature by other research groups [46-48].
On the other hand, zein nanoparticles provided higher folic acid levels than the oral solution. As a consequence, the relative oral bioavailability of folic acid when administered after its encapsulation in zein nanoparticles was calculated to be close to 70% and 2-times higher than when administered as oral solution (Table 3). Another important aspect to highlight would be that the profile of the serum curve as well as the primary pharmacokinetic parameters of folic acid when encapsulated in zein nanoparticles were similar to those observed for the oral solution of the vitamin. Thus, the differences in the oral bioavailability of the vitamin might only be due to the capabilities of zein nanoparticles as carriers to transport the folic acid to the absorptive membrane.
When orally administered, zein nanoparticles remain within the gastrointestinal tract for a period of at least 24 h post-administration (Figure 3). Interestingly, the absence of signals in the liver, spleen, lungs and kidneys of animals suggested that zein nanoparticles were not capable of entering into the circulation from the gut (Figure 3). Within the gastrointestinal tract of animals, zein nanoparticles would be capable of conducting the vitamin and remaining in close contact with the intestinal microvilli, as observed by fluorescence microscopy (Figure 4). This last observation would be in line with previous data suggesting the mucoadhesive properties of zein[45,49,50].
To sum up, the encapsulation of folic acid in zein nanoparticles would not be only capable of preventing the vitamin precipitation in the acidic pH conditions of the stomach, but also of transporting the cargo in close proximity to the jejunum epithelium surface. Once there, the mucoadhesive properties of zein would be responsible for an increase of the residence time of these carriers in the upper region of the gastrointestinal tract, in which the absorption of folic acid is favored.

Conclusions

In summary, zein nanoparticles appeared to be more adequate than a conventional formulation for the oral delivery of folic acid. *In vitro*, zein nanoparticles prevented the release of the vitamin under acidic pH conditions and, thus, minimizing the possibilities for its precipitation. Orally administered, the profile of the vitamin serum curve as well as its primary pharmacokinetic parameters (volume of distribution, clearance, serum half-life) were found to be independent of the formulation tested (oral solution or zein nanoparticles). On the contrary, the oral bioavailability of folic acid when encapsulated in zein nanoparticles was calculated to be 2-times higher than when administered as oral solution. This fact would be related with the mucoadhesive properties of zein.

Acknowledgements

This work was supported by the Regional Government of Navarra (Alimentos funcionales, Euroinnova call) and the Spanish Ministry of Science and Innovation and Gobierno de Navarra (ADICAP; ref. IPT-2011-1717-900000). Rebeca Penalvaacknowledgesthe “Asociación de Amigos Universidad de Navarra” forthefinancialsupport.

References

[1] D. Duvick, Protein granules of maize endosperm cells, Cereal Chem. 38 (1961) 4-385.

[2] D. Fu, C.L. Weller, R.L. Wehling, Zein: properties, preparations, and applications, Food Science and Biotechnology 8 (1999) 1-10.

[3] R. Shukla, M. Cheryan, Zein: the industrial protein from corn, Industrial Crops and Products 13 (2001) 171-192.

[4] A. Esen, A proposed nomenclature for the alcohol-soluble proteins (zeins) of maize (< i> Zea mays L.), J. Cereal Sci. 5 (1987) 117-128.

[5] J. Wang, P.H. Geil, D.R. Kolling, G.W. Padua, Analysis of zein by matrix-assisted laser desorption/ionization mass spectrometry, J. Agric. Food Chem. 51 (2003) 5849-5854.

[6] F.A. Momany, D.J. Sessa, J.W. Lawton, G.W. Selling, S. Hamaker, J.L. Willett, Structural Characterization of α-Zein, Journal of Agricultural and Food Chemistry 54 (2006) 543 -7.

[7] G.W. Selling, A. Biswas, A. Patel, D.J. Walls, C. Dunlap, Y. Wei, Impact of solvent on electrospinning of zein and analysis of resulting fibers, Macromolecular Chemistry and Physics 208 (2007) 1002-1010.

[8] T. Padgett, I. Han, P. Dawson, Incorporation of food-grade antimicrobial compounds into biodegradable packaging films, Journal of Food Protection 61 (1998) 1330-1335.

[9] H. Guo, Y. Shi, A novel zein-based dry coating tablet design for zero-order release, Int. J. Pharm. 370 (2009) 81-86.

[10] A. Rakotonirainy, Q. Wang, G. Padua, Evaluation of zein films as modified atmosphere packaging for fresh broccoli, J. Food Sci. 66 (2001) 1108-1111.

[11] H.X. Guo, J. Heinämäki, J. Yliruusi, Stable aqueous film coating dispersion of zein, J. Colloid Interface Sci. 322 (2008) 478-484.

[12] J. Tu, H. Wang, H. Li, K. Dai, J. Wang, X. Zhang, The *in vivo* bone formation by mesenchymal stem cells in zein scaffolds, Biomaterials 30 (2009) 4369-4376.

[13] Y. Luo, Z. Teng, Q. Wang, Development of zein nanoparticles coated with carboxymethyl chitosan for encapsulation and controlled release of vitamin D3, J. Agric. Food Chem. 60 (2012) 836-843.

[14] A. Patel, Y. Hu, J.K. Tiwari, K.P. Velikov, Synthesis and characterisation of zein–curcumin colloidal particles, Soft Matter 6 (2010) 6192-6199.

[15] D. Xiao, P.M. Davidson, Q. Zhong, Spray-dried zein capsules with coencapsulated nisin and thymol as antimicrobial delivery system for enhanced antilisterial properties, J. Agric. Food Chem. 59 (2011) 7393-7404.

[16] R. Paliwal, S. Palakurthi, Zein in controlled drug delivery and tissue engineering, J. Controlled Release (2014).

[17] T. Zou, Z. Li, S.S. Percival, S. Bonard, L. Gu, Fabrication, characterization, and cytotoxicity evaluation of cranberry procyanidins-zein nanoparticles, Food Hydrocoll. 27 (2012) 293-300.

[18] E. Mathiowitz, H. Bernstein, E. Morrel, K. Schwaller, Method for producing protein microspheres (1991).

[19] G. Kronenberg, M. Colla, M. Endres, Folic acid, neurodegenerative and neuropsychiatric disease, Curr. Mol. Med. 9 (2009) 315-323.

[20] R. Iyer, S. Tomar, Folate: a functional food constituent, J. Food Sci. 74 (2009) R114-R122.

[21] J. Scott, P. Kirke, A. Molloy, L. Daly, D. Weir, The role of folate in the prevention of neural-tube defects, Proc. Nutr. Soc. 53 (1994) 631-636.

[22] M.P. Mattson, T.B. Shea, Folate and homocysteine metabolism in neural plasticity and neurodegenerative disorders, Trends Neurosci. 26 (2003) 137-146.

[23] E.H. Reynolds, The neurology of folic acid deficiency, Handb. Clin. Neurol. 120 (2014) 927-943.

[24] M. Lövdén, L. Bergman, R. Adolfsson, U. Lindenberger, L. Nilsson, Studying individual aging in an interindividual context: typical paths of age-related, dementia-related, and mortality-related cognitive development in old age., Psychol Aging 2 (2005) 303-16.

[25] M.T. Abou-Saleh, A. Coppen, Folic acid and the treatment of depression, J. Psychosom. Res. 61 (2006) 285-287.

[26] J. Sarris, N. Schoendorfer, D.J. Kavanagh, Major depressive disorder and nutritional medicine: a review of monotherapies and adjuvant treatments, Nutr. Rev. 67 (2009) 125-131.

[27] R.T. Owen, Folate augmentation of antidepressant response, Drugs Today (Barc) 49 (2013) 791-798.

[28] R. Zeng, C. Xu, Y. Xu, Y. Wang, M. Wang, The effect of folate fortification on folic acid-based homocysteine-lowering intervention and stroke risk: a meta-analysis, Public Health Nutr. (2014) 1-8.

[29] M. Curro, S. Condello, D. Caccamo, N. Ferlazzo, G. Parisi, R. Ientile, Homocysteine-induced toxicity increases TG2 expression in Neuro2a cells, Amino Acids 36 (2009) 725-730.

[30] A. de Bree, W.M. Verschuren, A.L. Bjorke-Monsen, N.M. van der Put, S.G. Heil, F.J. Trijbels, H.J. Blom, Effect of the methylenetetrahydrofolate reductase 677C-->T mutation on the relations among folate intake and plasma folate and homocysteine concentrations in a general population sample, Am. J. Clin. Nutr. 77 (2003) 687-693.

[31] S.E. Chiuve, E.L. Giovannucci, S.E. Hankinson, D.J. Hunter, M.J. Stampfer, W.C. Willett, E.B. Rimm, Alcohol intake and methylenetetrahydrofolate reductase polymorphism modify the relation of folate intake to plasma homocysteine, Am. J. Clin. Nutr. 82 (2005) 155-162.

[32] H.E. Sauberlich, Laboratory Tests for the Assessment of Nutritional Status, CrC Press, 1999.

[33] M.K. Off, A.E. Steindal, A.C. Porojnicu, A. Juzeniene, A. Vorobey, A. Johnsson, J. Moan, Ultraviolet photodegradation of folic acid, Journal of Photochemistry and Photobiology B: Biology 80 (2005) 47-55.

[34] M. Agüeros, I. Esparza, C. Gonzalez-Ferrero, C.J. Gonzalez-Navarro, J.M. Irache, A. Romo, Nanoparticles for encapsulation of compounds, the production and uses thereof. (2012).

[35] I. Sierra, C. Vidal-Valverde, A simple method to determine free and glycosylated vitamin B6 in legumes, J. Liq. Chromatogr. Rel. Technol. 20 (1997) 957-969.

[36] Z. Wu, X. Li, C. Hou, Y. Qian, Solubility of Folic Acid in Water at pH Values between 0 and 7 at Temperatures (298.15, 303.15, and 313.15) K, Journal of Chemical & Engineering Data 55 (2010) 3958-3961.

[37] R. Zhao, L.H. Matherly, I.D. Goldman, Membrane transporters and folate homeostasis: intestinal absorption and transport into systemic compartments and tissues, Expert Reviews in Molecular Medicine 11 (2009) e4.

[38] V.S. Subramanian, J.S. Marchant, H.M. Said, Apical membrane targeting and trafficking of the human proton-coupled transporter in polarized epithelia, Am. J. Physiol. Cell. Physiol. 294 (2008) C233-40.

[39] P. Hurtado-Lopez, S. Murdan, Formulation and characterisation of zein microspheres as delivery vehicles, Journal of Drug Delivery Science and Technology 15 (2005) 267-272.

[40] F. Sousa, A. Luzardo-Álvarez, J. Blanco-Méndez, M. Martín-Pastor, NMR techniques in drug delivery: Application to zein protein complexes, Int. J. Pharm. 439 (2012) 41-48.

[41] B. Hsu, Y. Weng, Y. Liao, W. Chen, Structural investigation of edible zein films/coatings and directly determining their thickness by FT-Raman spectroscopy, J. Agric. Food Chem. 53 (2005) 5089-5095.

[42] T. Cserhati, E. Forgacs, Effect of pH and salts on the binding of free amino acids to the corn protein zein studied by thin-layer chromatography, Amino Acids 28 (2005) 99-103.

[43] R. Pérez-Masiá, R. López-Nicolás, M.J. Periago, G. Ros, J.M. Lagaron, A. López-Rubio, Encapsulation of folic acid in food hydrocolloids through nanospray drying and electrospraying for nutraceutical applications, Food Chem. 168 (2015) 124-133.

[44] Y. Yong, S. Yamaguchi, Y. Gu, T. Mori, Y. Matsumura, Effects of enzymatic deamidation by protein-glutaminase on structure and functional properties of alpha-zein., J Agric Food Chem 23 (2004) 7094-100.

[45] B. Zhang, Y. Luo, Q. Wang, Effect of acid and base treatments on structural, rheological, and antioxidant properties of α-zein, Food Chem. 124 (2011) 210-220.

[46] R. Penalva, I. Esparza, M. Agüeros, C.J. Gonzalez-Navarro, C. Gonzalez-Ferrero, J.M. Irache, Casein nanoparticles as carriers for the oral delivery of folic acid, Food Hydrocolloids (In press).

[47] N.C. Alemdaroglu, U. Dietz, S. Wolffram, H. Spahn-Langguth, P. Langguth, Influence of green and black tea on folic acid pharmacokinetics in healthy volunteers: potential risk of diminished folic acid bioavailability, Biopharm. Drug Dispos. 29 (2008) 335-348.

[48] P. Nguyen, R. Boskovic, P. Yazdani, B. Kapur, H. Vandenberghe, G. Koren, Comparing folic acid pharmacokinetics among women of childbearing age: single dose ingestion of 1.1 versus 5 MG folic acid, Can. J. Clin. Pharmacol. 15 (2008) 314-22.

[49] A. Patel, Y. Hu, J.K. Tiwari, K.P. Velikov, Synthesis and characterisation of zein–curcumin colloidal particles, Soft Matter 6 (2010) 6192-6199.

[50] S. Wongsasulak, S. Pathumban, T. Yoovidhya, Effect of entrapped α-tocopherol on mucoadhesivity and evaluation of the release, degradation, and swelling characteristics of zein–chitosan composite electrospun fibers, J. Food Eng. 120 (2014) 110-117.

Chapter 7

Zein based nanoparticles improve the oral bioavailability of resveratrol and its anti-inflammatory effects in a mouse model of endotoxic shock

Journal of Agriculture Food Chemistry, Submited.

.

Abstract

Resveratrol offers pleiotropic health beneficial effects including its reported capability to inhibit lipopolysaccharide (LPS) induced cytokine production.The aim of this work was to prepare, characterize and evaluate a resveratrol nanoparticulate formulation based on zein. For this purpose, the oral bioavailability of the polyphenol when encapsulated in these nanoparticles as well as its anti-inflammatory effect in a mouse model of endotoxic shock were studied.

Resveratrol-loaded nanoparticles displayed sizes around 300 nm with a negative zeta potential and a polyphenol loading close to 90 μg/mg of NP. In vitro, the release of resveratrol from the nanoparticles was found to be pH-independent and adjusted well to the Peppas-Salin kinetic model, suggesting a mechanism based on the combination of diffusion and erosion of the nanoparticle matrix. Pharmacokinetic studies demonstrated that zein-based nanoparticles provided high and prolonged plasma levels of the polyphenol for at least 24 h. In addition, the oral bioavailability of resveratrol when administered in these nanoparticles was up to 50%. Furthermore, zein nanoparticles loaded with resveratrol administered daily during 7 days at 15 mg/kg, were able to diminish the endotoxic symptoms induced in mice by the intraperitoneal (ip) administration of LPS (i.e. hypothermia, piloerection and stillness) compared to resveratrol solution on daily basics. In addition, serum TNF-α also decreased in those animals receiving the polyphenol encapsulated in nanoparticles.

1. Introduction

Resveratrol (Rsv) (3,5,4'-trihydroxy-trans-stilbene), is a polyphenol molecule that was identified from the dried roots of *Polygonumcuspidatum*, a plant used in traditional Chinese and Japanese medicine[1] also called "Kojo-kon or Itadori" [2]. Resveratrol has been classified as a phytoalexin for being synthesized in spermatophytes in response to injury, UV irradiation and fungal attack [3]. It is mainly found in a wide variety of plant species such as peanuts, skins, plums and in red wine [4].

Resveratrol offers pleiotropic health beneficial effects, including antioxidant and anti-aging effects[5,6], cardioprotective[7], anticancer [8] and neuroprotective activities [9].

In the lasts years, it has been demonstrated the preventive effect of resveratrol against diabetes. Resveratrol would reduce hyperglycemia[10] and, in animals with hyperinsulinemia, it would reduce blood insulin [11]. Similarly, resveratrol was reported to reduce body weight and adiposity in obese recipients, including rodents [11-14], primates [15] and humans [16]. The action would involve the activation of sirtuin 1 (SIRT1) that inhibits inflammatory pathways in macrophages and modulates insulin sensitivity [17,18]. Furthermore, different studies have shown that resveratrol is capable of inhibiting lipopolysaccharide (LPS) induced cytokine production [19,20]. This effect, via modulation of NF-κB, would decrease the production and gene expression of, IL1 and TNF-α, important endogenous pyrogens[21].

In spite of these potential health benefits, the use of resveratrol is limited due to its high lipohilicity, short biological half-life, and chemical instability. In addition, when resveratrol is orally administered, only trace amounts of the unchanged polyphenol can be detected in plasma [22]. This low bioavailability is due to the polyphenol biotransformation by UDP-glucuronosyltransferase and sulphotransferases that produces resveratrol-3'-glucuronide and the sulphate derivative, respectively[4,23]. In rats, the major metabolite of resveratrol is the glucuronide conjugate [24], whereas, in humans, both the glucuronide and the sulphate derivatives have been described [25]. These metabolites have a longer plasma half-life, however, their efficacy are unknown[1]. Renal excretion is the major route of elimination of the polyphenol and its derivatives [4,23,26].

In order to solve these drawbacks different strategies have been pursued including its encapsulation in different oral delivery systems such as emulsions and nanoemulsions[27], self-nano emulsifying drug delivery systems [28], solid lipid nanoparticles [29] and polymeric nanoparticles [30] among others.

An alternative approach might be the use of zein nanoparticles. Zein is the major storage protein of maize and comprises aprox. 45-50% of the total protein content in corn [31].

Since zein is a natural protein, it is actually a heterogeneous mixture of different peptides than can be divided in three main fractions: α-zein (75-85% of total zein) with a MW of 21-25 kDa and 10kDa, β-zein (10-15%) of a MW of 17-18 kDa, and, γ-zein (5-10%) with a MW of 27 kDa[32,33]. Zein is an amphiphilic protein, possessing high percentages of leucine (20%), proline (10%), alanine (10%) and glutamine (21-26%) [34,35]. Due to its aminoacid composition, zeinis insoluble in water but soluble in an aqueous alcohol solution [36] and it can be processed to form films [37], fibers [38], microparticles[39] or nanoparticles [40].

Therefore, the aim of this work was to prepare, characterize and evaluate a resveratrol nanoparticulate formulation based on zein. The oral bioavailability of the polyphenol when

encapsulated in these nanoparticles, as well as its anti-inflammatory effect in a mouse model of induced endotoxicshock were studied.

2. Material and Methods

Zein, resveratrol, lysine, mannitol, sodium ascorbate, PEG 400 and Tween 20 were purchased from Sigma-Aldrich (Germany). Resveratrol-3-O-D-glucuronide was from @rtMolecule (Poitiers, France). Sodium caseinate was supplied from ANVISA (Madrid, Spain). Ethanol, methanol, acetic acid and acetonitrile HLPC grade were obtained from Merck (Darmastadt, Germany). Lipopolysaccharide (LPS) from *Salmonella enterica*serovar. Minnesota was from Sigma®, (St. Louis, USA). Deionised reagent water (18.2 MΩ resistivity) was prepared by a water purification system (Wasserlab, Spain). All reagents and chemicals used were of analytical grade.

2.1 Preparation of resveratrol-loaded nanoparticles

Resveratrol (Rsv) was encapsulated in either zein nanoparticles (Rsv-NP-Z) or in zein-casein nanoparticles (Rsv-NP-M). In both cases, zein nanoparticles were prepared by a desolvation method followed by a purification step by ultrafiltration and subsequent drying in a spray-drier apparatus as indicated below[41].
Briefly, 600 mg of zein and 100 mg of lysine were dissolved in 60 mL of an ethanol:water mixture (65% ethanol by vol.). In parallel, 100 mg resveratrol were dissolved in 10 mL of ethanol and 6 mL of this solution were transferred to the zein solution. In addition, 6 mg of sodium ascorbate were added to minimze the oxidation of the polyphenol. The mixture was magnetically stirred i darkness conditions for 10 min at room temperature. Nanoparticles were obtained by the continuous addition of 60 mL of purified water. The suspension was purified and concentrated by ultrafiltration using a polysulfone membrane cartridge of 50 kDa pore size (Medica SPA, Italy). Then, 15 mL of purified water containing 1.2 g mannitol were added to the resulting suspension of nanoparticles. Finally the suspension was dried in a Büchi Mini Spray Drier B-290 apparatus (BüchiLabortechnik AG, Switzerland) under the following experimental conditions: (i) inlet temperature: 90°C, (ii) outlet temperature: 45-50°C, (iii) air pressure: 4-6 bar, (iv) pumping rate: 5 mL/min, (v) aspirator: 100% and (vi) air flow: 400-500 L/h.

On the other hand, resveratrol-loaded in zein-casein nanoparticles (Rsv-NP-M) were prepared as described above with minor differences. In brief, 250 mg of zein, 50 mg of lysine, 52.5 mg of resveratrol and 6 mg of sodium ascorbate were dissolved in 30 mL of ethanol 65%. The mixture was magnetically stirred in darkness conditions for 10 min and the nanoparticles were obtained by the continuous addition of 30 mL of water containing 300 mg of sodium caseinate. Then, the purification and drying of nanoparticles were performed as described previously.
Control formulations (NP-Z and NP-M) were prepared as described above but in absence of resveratrol.

2.2 Preparation of resveratrol conventional formulations

Two different formulations of resveratrol were also prepared. The former consisted of a solution of the polyphenol in a mixture of PEG 400 and water (1:1 by vol.). For this purpose, 37.5 mg of resveratrol were dissolved in 5 mL of PEG 400 under magnetic stirring. Then, 5 mL of purified water were added and the final mixture was agitated in darkness conditions for 10 min (Rsv-sol).

The latter was an extemporary suspension of resveratrol (Rsv-susp) in purified water. Briefly, 37.5 mg of resveratrol were dispersed in 10 mL of purified water under magnetic agitation for 10 min. The suspension was used after visual inspection for absence of aggregates. (Size: 21439 ± 9240 nm; PDI: 0.51 ± 0.04)

2.3 Physicochemical characterization of nanoparticles

2.3.1 Size, zeta potential and morphology

The mean hydrodynamic diameter and the zeta potential of nanoparticles were determined by photon correlation spectroscopy (PCS) and electrophoretic laser Doppler anemometry, respectively, using a Zetamasteranalyzer system (Malvern Instruments Ltd., Worcestershire, UK). The diameter of the nanoparticles was determined after dispersion in ultrapure water (1:10) and measured at 25 °C with a scattering angle of 90°. The zeta potential was measured after dispersion of the dried nanoparticles in 1 mMKCl solution.

The morphology of the nanoparticles was studied using a field emission scanning electron microscopy (FE-SEM) in a Zeiss DSM940 digital scanning electron microscope (Oberkochen, Germany) coupled with a digital image system (Point Electronic GmBh, Germany). The yield of the process was calculated by gravimetry as described previously [42,43].

2.3.2 Resveratrol analysis

The amount of resveratrol loaded into the nanoparticles was quantified by HPLC-UV followed an analytical method previously described [44] with minor modifications. Analysis were carried out in an Agilent model 1100 series LC and diode-array detector set at 306 nm. Data were analysed in chemstation G2171 program (B.01.03). The chromatographic system was equipped with a reverse phase phase 150 mm x 2.1 mm C18 Alltima column (particle size 5 µm; Altech, USA) and a Gemini C18 support AJO-7596 precolumn. The mobile phase, pumped at 0.25 mL/min was a mixture of water/methanol/acetic acid in a gradient condition (Table 1). The column was heated at 40°C and the injection volume was 10 µL. Under these conditions, the run time for resveratrol was 22.8±0.5 min. Calibration curves in ethanol 75% were designed over the range of 1-100 µg/mL ($R^2 \geq 0.999$).

For analysis, 10 mg of nanoparticles were dispersed in 1 mL of water and centrifuged at 2,000 rpm for 5 min. The obtained supernatants were analyzed in order to determine the amount of resveratrol encapsulated. The amount of free resveratrol was calculated by digestion of the pellets with ethanol 75%. In parallel, the total amount of resveratrol in the dried formulations was quantified by direct digestion of 10 mg of formulation with 1 mL of ethanol 75%. Each

sample was assayed by triplicate and the results were expressed as the amount of resveratrol (µg) per mg of nanoparticles.
The encapsulation efficiency (E.E) was calculated as follows:

$$E.E.(\%) = \frac{Rsv_s}{Rsv_t} \times 100 \quad \text{(Eq. 1)}$$

in which Rsv-t is the total amount of resveratrol in the formulations and Rsv-p corresponds to the amount of resveratrol quantified in the pellet.

2.4 *In vitro* release study

Release experiments were conducted under sink conditionsat 37°C using simulated gastric (pH 1.2; SGF) and intestinal (pH 6.8; SIF) fluids (European Pharmacopeia), containing 0.5% Tween 20 as surfactant to increase the resveratrol aqueous solubility.The studies were performed under agitation in a slide-A-Lyzer® Dialysis cassete 10000 MWCO (Thermo scientific, Rockford, IL, USA). For this purpose, the cassette was filled with 3 mg of resveratrol loaded in zein nanoparticles previously dispersed in 5 mL water and, then, introduced in a vessel containing 500 mL of SGF (pH 1.2; 37°C) under magnetic agitation. After 2 h in SGF, the cassette was introduced in another vessel containing 500 mL of thermostat-zed SIF (pH 6.8; 37ºC, under agitation). At different time points, samples tubes were collected and filtered with 0.45 µm size-pore filters (Thermo scientific, Rockford, USA) before quantification.
The amount of resveratrol released from the formulations was quantified by HPLC. Calibration curves of free resveratrol in water containing 0.5% Tween 20 at pH 1.2 and 6.8 were performed, over the range 0.05-6 µg/mL ($R^2 \geq 0.999$) in both cases.
In order to ascertain the resveratrol release mechanism the obtained data were fitted to the Korsmeyer-Peppas and the Peppas-Sahlin models. The Korsmeyer–Peppas model [45] is a simple semi-empirical approach which exponentially relates drug release with the elapsed time as expressed in the following equation (Eq. 2).

$$\frac{M_t}{M_\infty} = \mathrm{K}_{KP} \cdot \mathrm{t}^{\mathrm{n}} \quad \text{(Eq. 2)}$$

In which Mt/M_∞ is the drug release fraction at time *t*, K_{KP} is a constant incorporating the structural and geometric characteristics of the matrix and *n* is the release exponent indicative of the drug release mechanism. The value of *n* indicates the mechanism of the release.[45]. Values close to 0.5 indicate a Case I (Fickian) diffusion mechanism; values between 0.5 and 0.89 indicate anomalous (non-Fickian) diffusion. Values of *n* between 0.89 and 1 indicate Case II transport, erosion of the matrix.

The contribution of Fickian and non-Fickian release was also evaluated by using the Peppas–Sahling model equation [46] (Eq. 3).

$$\frac{M_t}{M_\infty} = \mathrm{K}_{\mathrm{D}} \cdot \mathrm{t}^{1/2} + \mathrm{K}_{\mathrm{E}} \cdot \mathrm{t} \text{ (Eq. 3)}$$

where the first term of the right-hand side is the Fickian contribution (K_D is the diffusional constant) and the second term is the Case II erosional contribution (K_E is the erosional constant). K_D and K_E values were used to calculate the contribution percentage of diffusion (D) and erosion (E), with Eqs. 4 and 5 [47]:

$$D = \frac{1}{1+\frac{K_E}{K_D}t^{0.5}} \text{(Eq 4)}$$

$$\frac{E}{D} = \frac{K_E}{K_D}t^{0.5} \text{(Eq 5)}$$

To fit the experimental data to the previous equation, only one portion of the release profile was used, that is $M_t/M_\infty \leq 0.6$ [48].

2.5 *In vivo* pharmacokinetic studies in Wistar rats

Pharmacokinetic studies were performed in male Wistar rats (200-250 g) obtained from Harlan (Barcelona, Spain). Studies were approved by the Ethical Committee for Animal Experimentation of the University of Navarra (protocol number 028-11) in accordance with the European legislation on animal experiments.

Previous to the oral administration of the formulations, animals were fasted overnight to avoid interference with the absorption, allowing free access to water. For the pharmacokinetic study, rats were randomly divided into 5 groups of 6 animals each. The five experimental groups were: (i) resveratrol water suspension, (ii) resveratrol solution in a PEG 400:water mixture, (iii) resveratrol-loaded zein nanoparticles (Rsv-NP-Z) and (iv) resveratrol-loaded zein-casein nanoparticles (Rsv-NP-M). As controls a group of animals was treated intravenously with a PEG 400:water (1:1 by vol.) resveratrol solution. Each animal received the equivalent amount of resveratrol to a dose of 15 mg/kg body weight either orally with a blunt needle via the esophagus into the stomach or intravenously via tail vein.

Blood samples were collected at set times after administration (0, 10 min, 30 min, 1 h, 2 h, 4 h, 6 h, 8 h, 24h and 48 h) in specific plasma tubes (Microvette® 500K3E, SARSTEDT, Germany). Blood volume was recovered intraperitoneally with an equal volume of normal saline solution pre-heated at body temperature. Samples were immediately centrifuged at 10,000 rpm for 10 min and plasma aliquots were kept frozen at -80 ºC until HPLC analysis of both resveratrol and resveratrol-3-O-D-glucuronide.

2.5.1 Determination of resveratrol and resveratrol-3-O-D-glucuronide plasma concentration by HPLC

The amount of resveratrol was determined by high pressure liquid chromatography with UV detection (HPLC-UV), following an analytical method reported previously with minor modifications [49]. Analysis were carried out in an Agilent model 1100 series LC and diode-array detector set at 306 nm. Data were analysed in a Chemstation G2171 program (B.01.03). The chromatographic system was equipped with a reversed-phase 250 mm x 2.1 mm C18 Kromasil (particle size 5 µm) column and a Gemini C18 support AJO-7596 precolumn. The mobile phase, pumped at 0.5 mL/min, was a mixture of water, methanol and acetic acid (50:45:5 by vol.) in an isocratic condition. The column was placed at 30°C and the injection

volume was 30 µL. Under these conditions, the run times for resveratrol-3-o-D-glucuronide and resveratrol were 6.2 ± 0.5 min and 12.6 ± 0.5 min, respectively.

For analysis, an aliquot of 100 µL of plasma was mixed with 50 µL HCl 0.1 N and 500 µL acetonitrile (for protein precipitation) followed by vigorous shaking at 2500 rpm for 10 min. Then, samples were centrifuged at 4000 rpm for 10 min and the obtained supernatants were evaporated under vacuum in Automatic environmental Speed Vac® system (Holbrook, NY) at 25°C for 30 min. Finally, 100 µL of a mixture of acetonitrile and water (1:1 by vol.) was added and vigorously stirred in a vortex for 10 min. Then, and previously to the injection, samples were filtered through 0.45 µm pore-size filters (Thermo scientific, Rockford, IL, USA).

For quantification, calibration standards ranged from 2 to 70 µg/mL for the metabolite and from 50 to 3000 ng/mL for resveratrol ($R^2 \geq 0.99$) were prepared. All the calibration standards were obtained by adding either resveratrol or resveratrol-3-o-D-glucuronide in acetonitrile (500 µL) to 100 µL free plasma. Then the polyphenol or its metabolite was submitted to the same extraction protocol described above.

Under these experimental conditions, the limit of quantification was calculated to be 70 ng/mL, for resveratrol, and 4 µg/mL, for its metabolite. Linearity, accuracy and precision values during the same day (intraday assay) at low, medium and high concentrations of both resveratrol and the metabolite were always within the acceptable limits (relative error and coefficient of variation less than 15%).

2.5.2 Pharmacokinetic data analysis

Resveratrol plasma concentration was plotted against time, and pharmacokinetic analysis, was performed using a non-compartmental model with the WinNonlin 5.2 software (Pharsight Corporation, USA). The following parameters were estimated: maximal serum concentration (C_{max}), time in which C_{max} is reached (T_{max}), area under the concentration-time curve from time 0 to last time (AUC), mean residence time (MRT), clearance (Cl), volume of distribution (V) and half-life in the terminal phase ($t_{1/2}$). Furthermore, the relative bioavailability (Fr %) of resveratrol was estimated by the following equation:

$$Fr\ (\%) = \frac{AUC\ oral}{AUC\ iv} \times 100 \quad \text{(Eq. 6)}$$

where $AUC_{i.v.}$ and AUC_{oral} are the areas under the curve for the iv and oral administrations, respectively.

2.6 *In vitro/In vivo* correlation (INVIC)

The eventual correlation between *in vitro* and *in vivo* results was conducted by plotting a point-to-point between the amount of resveratrol released from nanoparticles and the fraction of resveratrol absorbed (FRA) calculated from the mean plasma concentration-time inputs using the Wagner-Nelson equation [50].

$$FRA = \frac{C_t + k \times AUC_{0-t}}{k \times AUC_{0-\infty}} \quad \text{(Eq. 7)}$$

where Ct is the plasma concentration of resveratrol at a time t, k is the elimination rate constant of the polyphenol, AUC_{0-t} is the area under the resveratrol concentration vs. time curve from 0 to time t, and $AUC_{0-\infty}$ is the area under the curve from 0 to infinity.

Linear regression analysis was applied to the *in vitro/in vivo* correlation plot and coefficient of determination (R^2) was calculated.

2.7 Anti-inflammatory efficacy study

2.7.1 Animal model

C57BL/6J female mice of 4 weeks-old (20-22 g) were purchased from Harlan (Barcelona, Spain), housed under standard animal facilities with 6 animals per cage and given free access to food and drinking water. Housing conditions were maintained by controlled temperature and humidity and with 12 h on/off light cycles. Animals were allowed to acclimate for one week before the experiments.

In vivo anti-inflammatory studies were evaluated in an endotoxic shock model set up by intraperitoneal administration of lipopolysaccharide (LPS) from *Salmonella enterica*serovar. Minnesota (Sigma®, St. Louis, USA) at dose of 40 µg per mouse. Before administration, LPS was dissolved in PBS and vortexed during 30 min to complete homogenization.

On day 1, mice were randomly distributed into four groups. The two experimental groups were (i) resveratrol oral solution in a PEG 400:water mixture, and (ii) resveratrol-loaded zein nanoparticles (Rsv-NP-Z). As control a group of animals did not receive any treatment (positive control group) and another one received neither LPS nor resveratrol (negative control group). Resveratrol groups received an oral dose of 15 mg/kg daily during 7 days.

Twenty four hours after the last dose of resveratrol (day 8) animals were challenged with 40 µg LPS by intraperitoneal route. Throughout the study, rectal temperature of mice was measured till 24 h after challenge. Similarly, animals were observed for any clinical signs or symptoms of toxicity daily and after the challenge. Reactions severity was classified in the following categories depending on their gravity: i) (-) absent; ii) (+) weak; iii) (++) moderate; and iv) (+++) strong, and the mobility was classified in i) very low, ii) low or iii) normal, depending on the activity of the animals.

In addition, 90 min after challenge, blood samples were collected from the retro-orbital cavity in EDTA-K vials (Microvette® 500K3E, SARSTEDT, Germany), centrifuged at 8,000 xg for 10 min and sera aliquots were conserved at -20 °C until use.

2.7.2 Measurement of plasma TNF-α

The concentration of circulating TNF-α in the serum was determined by an enzyme-linked immunosorbent assay kit (Quantikine® ELISA Mouse TNF-α, MTA00B, R&D Systems, Minneapolis, USA) according to manufacturer's instructions..

2.8 Statistical analysis

Data are expressed as the mean ± standard deviation (SD) of at least three experiments. The non-parametric Kruskall-Wallis followed by Mann-Whitney U-test was used to investigate statistical differences. In all cases, $p< 0.05$ was considered to be statistically significant. All data processing was performed using Graph Pad® Prism statistical software.

3. Results

3.1 Preparation and characterization of nanoparticles

Table 1 shows the physico-chemical characteristics of the nanoparticles used in this study. Overall, the mean diameter of empty nanoparticles was smaller than those loaded with resveratrol. Similarly, zein-casein nanoparticles were also found slightly smaller than zein ones. When resveratrol was encapsulated, zein nanoparticles displayed a mean size of about 310 nm, whereas nanoparticles based on zein and casein displayed a size of about 290 nm. In all cases, the polydispersity index was found to be lower than 0.2, indicating homogeneous nanoparticle formulations. Furthermore, the zeta potential of all nanoparticles was negative; however, when resveratrol was encapsulated the resulting nanoparticles were slightly more negative than for empty ones.

Additionally, the resveratrol loading was 80-90 μg/mg of nanoparticle, with encapsulation efficiencies close to 80%.

Table 1. .Physico-chemical characteristics of empty and resveratrol-loaded nanoparticles.NP-Z: empty zein nanoparticles; NP-M: empty zein-casein nanoparticles; Rsv-NP-Z: resveratrol-loaded zein nanoparticles; Rsv-NP-M: resveratrol-loaded casein-zein nanoparticles. Data expressed as mean ± SD, n=6.

	Size (nm)[a]	PDI (nm)	Zeta potential (mV)	Rsv loading (μg/mg NP)[b]	E.E. (%)[c]
NP-Z	264 ± 2	0.07 ± 0.01	-46 ± 2		
NP-M	228 ± 1	0.08 ± 0.04	-47 ± 1		
Rsv-NP-Z	307 ± 3	0.10 ± 0.01	-51 ± 0	80 ± 3	82 ± 4
Rsv-NP-M	288 ± 5	0.04 ± 0.02	-51 ± 1	91 ± 2	77 ± 2

[a] Determination of volumen mean diameter by photon correlation spectroscopy

[b] Determination of Resveratrol content by HPLC-UV

[c] Encapsulation Efficiency (%)

Figure 1 shows the morphology and shape of resveratrol-loaded nanoparticles. In all cases, nanoparticles consisted of homogeneous populations of spherical particles with a smooth surface. In addition, the size of nanoparticles as observed by SEM was similar to that calculated by photon correlation spectroscopy (Table 1).

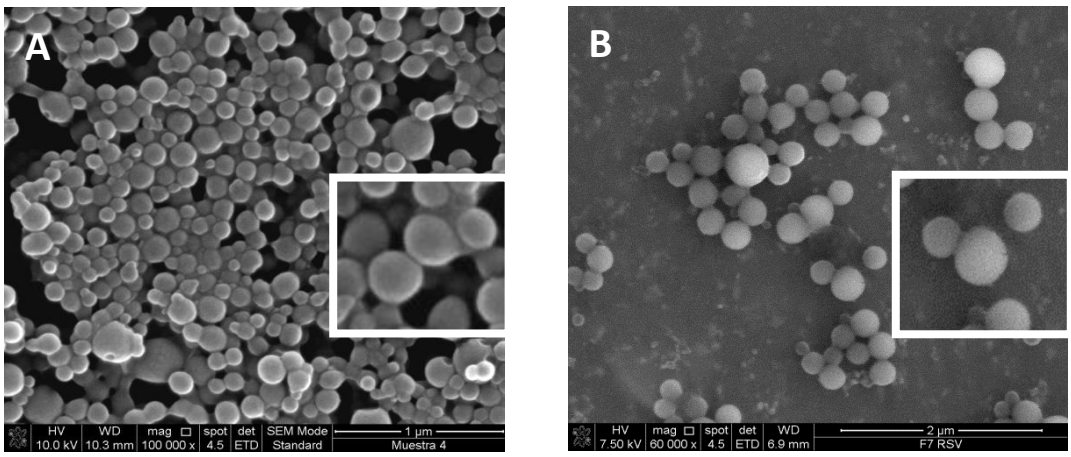

Figure 1. Scanning electron microscopy (SEM) microphotographs of resveratrol-loaded zein nanoparticles (A) and resveratrol-loaded in zein-casein nanoparticles (B).

3.2 *In vitro* release profile

Figure 2 represents the release profile of resveratrol from nanoparticles expressed as cumulative percentage of drug released *vs.* time. In all cases, the release of resveratrol from zein-based nanoparticles was found to be independent of the pH conditions. In addition, the release profile of both zein and zein-casein nanoparticles were similar and the incorporation of casein to the zein matrix did not significantly affect the release rate of resveratrol from these nanoparticles. During the first 2 h, under SGF conditions (pH 1.2), about 20% of the loaded resveratrol was released from zein and zein-casein nanoparticles. Then, 6 hours later (during SIF conditions) the amount released was close to 60% of the total content of resveratrol. From both types of nanoparticles, after 48 h, all the polyphenol content was released.

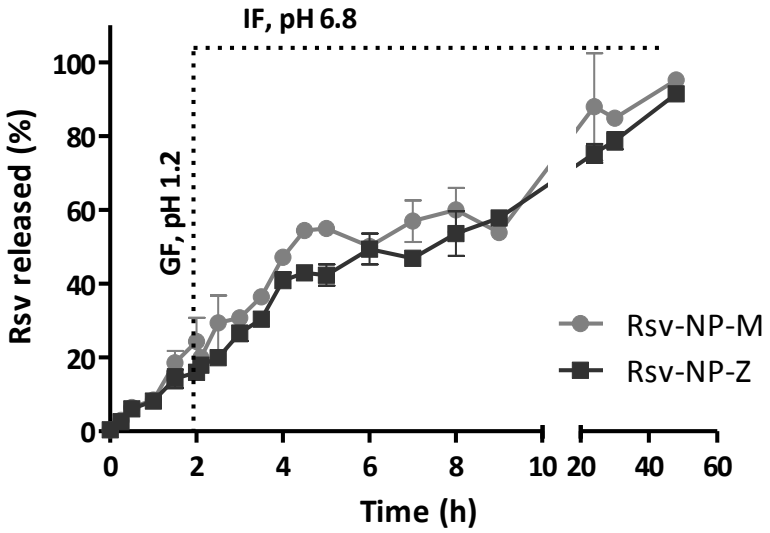

Figure 2. Resveratrol release from zein-based nanoparticles when incubated in simulated gastric (SGI, pH 1.2; 0-2 h) and simulated intestinal fluids (SIF, pH 6.8; 2-48 h) under sink conditions. Rsv-NP-M: resveratrol-loaded casein-zein nanoparticles (●); Rsv-NP-Z: resveratrol-loaded zein nanoparticles (■). Data represented as mean ± SD. (n=3).

The release profiles of resveratrol from both types of NPs were fitted to different mathematical release models (Table 2). Using the Korsmeyer-Peppas equation, R^2 values were quite high (R^2>0.94) and the exponent "n" values were between 0.50 and 0.89. These figures suggest that the release of resveratrol from nanoparticles would be a combination of Fickian diffusion and erosion of the nanoparticle matrix. Under these circumstances, the Peppas-Sahlin model was applied and the erosion (K_E) and diffusion (K_D) constants were calculated (Table 2).

For Rsv-NP-M, both constants were slightly higher than for Rsv-NP-Z, indicating a shightly quicker resveratrol release. K_D and K_E were also used to calculate the contribution percentage of diffusion and erosion as a function of time for both types of nanoparticles (Figure 3). Rsv-NP-Z and Rsv-NP-M presented a similar profile, characterized by a first step in which the release of resveratrol was conducted by a Fickian diffusion process and a second phase in which the polyphenol release was mainly driven by the erosion of the nanoparticle matrix. The time at which both mechanisms (diffusion and erosion) contributed in a similar amount to the release of resveratrol was calculated to be 3.5 h for Rsv-NP-Z and 5 h for Rsv-NP-M (Figure 3).

Table 2. Analysis of the resveratrol release mechanism from zein-casein nanoparticles and zein nanoparticles.

	Korsmeyer-Peppas			Peppas-Sahlin		
	K (h^{-n})	n	R^2	$k_D(h^{-1/2})$	$k_E(h^{-1})$	R^2
Rsv-NP-M	0.15±0.02	0.72±0.07	0.94	0.11±0.03	0.05±0.01	0.93
Rsv-NP-Z	0.12±0.01	0.75±0.06	0.96	0.08±0.02	0.04±0.01	0.95

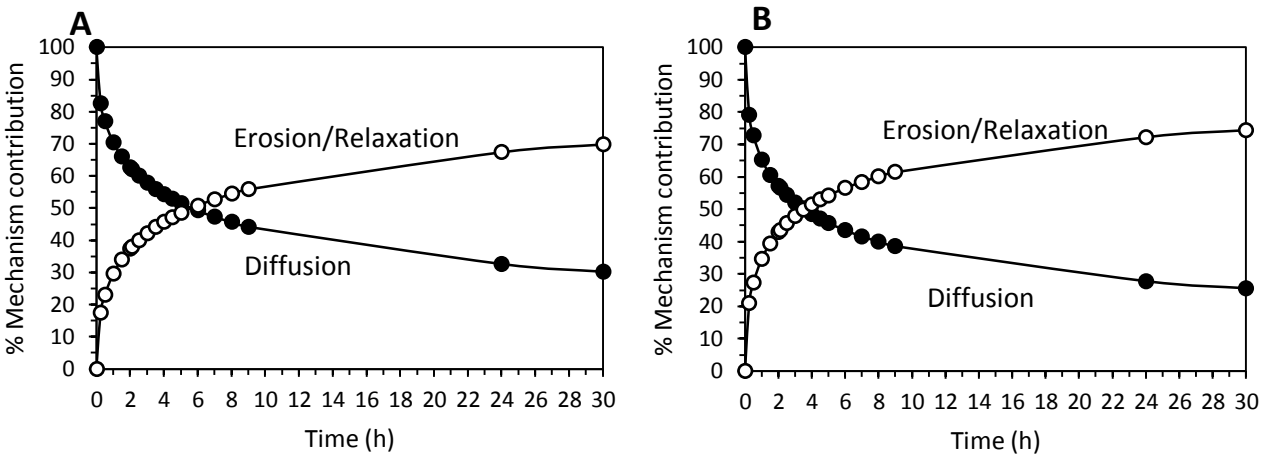

Figure 3. Fraction contribution of the Fickian diffusion (●) and the erosion/relaxation (○) mechanisms to resveratrol release from nanoparticles. Rsv-NP-M (A) and Rsv-NP-Z (B).

3.3 *In vivo* pharmacokinetics

Figure 4 shows the plasma concentration-time profile of a resveratrol solution in PEG-400:water (1:1 by vol.) after the intravenous administration to rats of a single dose of 15 mg/kg. The data were adjusted to a non-compartmental model. The resveratrol plasma concentration decreased rapidly in a biphasic way, and very low levels were quantified 8 h post administration. The peak plasma concentration (C_{max}) of resveratrol was around 15 µg/mL, whereas the AUC and half-life ($t_{1/2}$) were calculated to be 11.4 µg h/mL and 2.0 h, respectively. The resveratrol clearance and its volume of distribution were 200mL/h and 600mL, respectively (Table 3).

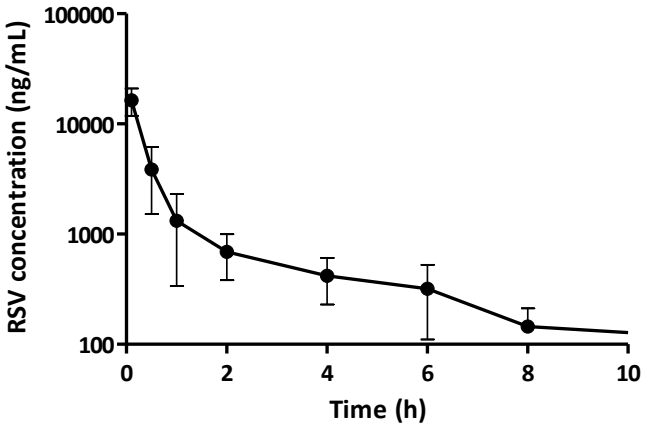

Figure 4. Resveratrol plasma concentration *vs* time after the intravenous administration of a single dose (15 mg/kg resveratrol) as solution in PEG 400 and water (1:1 by vol). Data are expressed as mean ± SD, n=6 per time point.

Figure 5 shows the plasma concentration levels of resveratrol when administered orally as a single dose of 15 mg/kg to rats, for the different formulations tested. Interestingly, when resveratrol was formulated as a suspension, no detectable levels of the polyphenol were

quantified in plasma. On the other hand, when resveratrol was administered as solution (Rsv-sol), the polyphenol plasma levels displayed an initial maximum concentration (C_{max}) of around 0.2 µg/mL, 30 min after the administration. Then, the plasma levels of resveratrol decreased rapidly and quantifiable levels were only detected during the first 4 h post-administration.

For resveratrol-loaded in zein nanoparticles (Rsv-NP-Z), the amount of the polyphenol in plasma increased during the first 4 h after administration till a maximum. Then, the resveratrol plasma levels decreased slowly during the following 20 h. Very low levels of resveratrol in plasma were quantified 48 h after its oral administration. When resveratrol was administered encapsulated in zein-casein nanoparticles (Rsv-NP-M), the profile of the curve was quite similar to that observed for zein nanoparticles. However the resveratrol C_{max} was reached before to that observed when loaded in zein nanoparticles and, except for plasma values quantified during the first times of the study, the mean plasma levels of resveratrol were lower than those observed with Rsv-NP-Z.

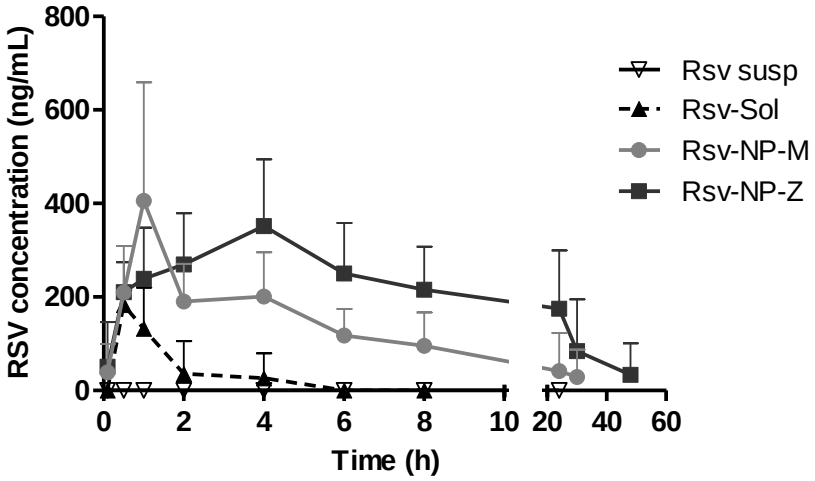

Figure 5. Resveratrol plasma concentration *vs* time after the oral administration of the different formulations at dose of 15 mg/kg. i) Resveratrol suspension (Rsv-susp▼), ii) resveratrol solution (Rsv-Sol ▲), iii) resveratrol-loaded zein-casein nanoparticles (Rsv-NP-M ●) and vi) resveratrol-loaded zein nanoparticles (Rsv-NP-Z ■). Data expressed as mean ± SD, (n=6).

Table 3 summarizes the main pharmacokinetic parameters estimated with a non-compartmental analysis of the experimental data obtained after the administration of the different formulations to rats. The resveratrol AUC values from nanoparticle formulations were significantly higher ($p< 0.01$) than those observed for the polyphenol solution. In addition, the AUC value of resveratrol loaded in zein nanoparticles was significantly higher ($p<0.05$) than that calculated for Rsv-NP-M. Similarly, the resveratrol MRT was 2 times higher when administered in the form of zein nanoparticles than when encapsulated in casein-zein nanoparticles. Finally, the relative oral bioavailability of resveratrol when incorporated in nanoparticles was calculated to be 28% with using zein-casein nanoparticles and 50% with using zein nanoparticles. These values were significantly higher than the bioavailability obtained with the PEG400-water solution (2.6%).

Figure 6 shows the plasma concentration *vs.* time profile of the resveratrol main metabolite (resveratrol-O-3-glucuronide) after the single administration of the polyphenol in the formulations tested. Interestingly, the profile of the plasma curves for both resveratrol and its metabolite were similar; however, the metabolite levels were always higher than for the polyphenol. When resveratrol was administered intravenously, the metabolite concentration reached 41.9 µg/mL (C_{max}) and, then, the metabolite levels decreased sharply. The AUC value was calculated to be 196.9 µg h/mL.

For the solution of resveratrol orally administered, the C_{max} of the metabolite in plasma was found to be 2-times lower (22.1 µg/mL) than when administered by the iv route. In this case, the metabolite was only quantified in plasma during the first 8 h post-administration. The AUC value was calculated to be 104.3 µg h/mL; 2 times lower than when the solution was given intravenously.

For nanoparticle formulations, the metabolite was quantified during the first 24 h after administration. In addition, for both types of nanoparticles the metabolite AUC data were similar (342.4 µg h/mL for Rsv-NP-Z, and 339.8 µg h/mL for Rsv-NP-M). These values were around 3 times higher than with the resveratrol solution iv administered.

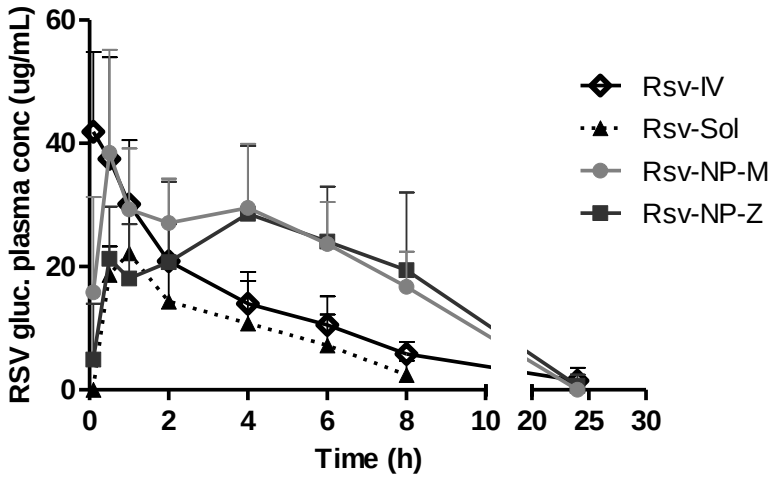

Figure 6. Resveratrol-O-3-glucuronide concentration *vs* time after a single administration (intravenous and oral) of the different formulations at dose of 15 mg/kg. i) Resveratrol intravenous (Rsv-IV, ◊) ii) resveratrol solution (Rsv-Sol, ▲), iii) resveratrol-loaded in zein-casein nanoparticles (Rsv-NP-M, ●) and iv) resveratrol loaded in zein nanoparticles (Rsv-NP-Z, ■). Data expressed as mean ± SD, n= 6.

Table 3. Pharmacokinetic parameters of resveratrol obtained after the administration of the different formulations tested at a dose of 15 mg/kg to Wistar male rats. i) Resveratrol intravenous (Rsv-iv.) ii) Rsv solution (Rsv-sol.), iii) Resveratrol suspension (Rsv-susp.) iv) Resveratrol loaded in zein-casein nanoparticles (Rsv-NP-M) and v) Resveratrol loaded in zein nanoparticles (Rsv-NP-Z). Data expressed as mean ± SD. (n=6)

	Route	C_{max} (µg/mL)	T_{max} (h)	AUC (µg h/mL)	T ½ (h)	Cl (mL/h)	Vd (mL)	MRT (h)	Fr (%)
Rsv iv.	p.iv	15.22± 5.18	0.1±0.0	10.39 ± 3.80	2.0±0.5	199.40 ± 89.81	569.17 ± 221.37	2.4±1.0	100
Rsv-sol.	p.o.	0.20 ± 0.02**	0.6±0.2	0.28 ± 0.13**	0.3±0.2	386.71 ± 224.87	112.25 ±103.56	1.3±0.8	2.6
Rsv-susp.	p.o.	ND	ND	ND	ND	ND	ND	ND	ND
Rsv-NP-M	p.o.	0.41 ± 0.26**†	1.8 ± 1.4	3.11 ± 2.00*†	3.7 ± 1.7	213.00 ± 95.00	991.25 ± 273.35	8.2 ± 5.5**†	28.0
Rsv-NP-Z	p.o.	0.39 ± 0.11**†	4.9 ± 3.1	5.17 ± 2.61$^{\dagger\bullet}$	5.5 ± 1.7	125.19 ± 40.58	909.30 ± 184.21	17.1 ± 7.1$^{**\dagger\bullet}$	50.0

C_{max}: peak plasma concentration; T_{max}: time to reach plasma concentration; AUC: Area under the curve; t ½: half life of the terminal phase; Cl: Clearance; MRT: mean residence time Fr: relative oral bioavailability

† Significant differences *vs*Rsv-Sol ($p<0.05$) Mann-Whitney-U

*Significant differences *vs* Rsv-i.v. ($p<0.01$) Mann-Whitney-U

$^{\bullet}$ Significant differences *vs*Rsv-NP-M ($p<0.05$) Mann-Whitney-U

3.4 *In vitro/in vivo* correlations

Figure 7 represents the relationship between the *in vitro* dissolution data (expressed as the cumulative percentage of the polyphenol released) and the fraction of resveratrol absorbed during the first 8 h post-administration.

A good linear regression was observed between the amount of resveratrol released and the percentages of polyphenol absorbed (R^2 = 0.8841 for Rsv-NP-M and R^2 = 0.8279 for Rsv-NP-Z).

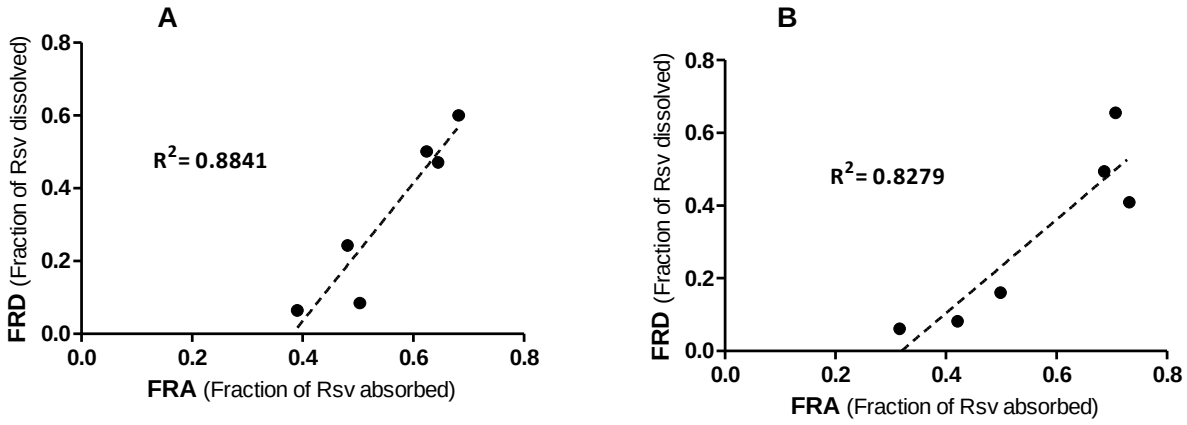

Figure 7. Relationship between fraction dissolved in vitro vs. fraction absorbed in vivo. Resveratrol loaded into zein-casein nanoparticles (A) (Rsv-NP-M) and resveratrol loaded into zein nanoparticles (B) (Rsv-NP-Z).

3.5 Anti-inflammatory efficacy study

We assessed the effect of resveratrol (15 mg/kg) on preventing an endotoxic shock in C57BL/6J mice induced by the i.p administration of 40 µg LPS. Rectal temperature of mice was measured during 24 h after challenge (Figure 8). Before challenge, the rectal temperature was unchanged in all the groups. Six hours after challenge, differences were observed between groups, in which, positive controls (without resveratrol pretreatment) suffer a great decrease in the rectal temperature in around 4°C. In addition, the animals pre-treated with resveratrol solution, decreased the rectal temperature in approx. 3°C. However, rectal temperature of animals treated with resveratrol loaded in zein nanoparticles, decreased only 0.5-1°C. No variations in the rectal temperature were observed in the control negative group. Twenty four hours after challenge animals treated with free resveratrol or encapsulated regained normal temperature.

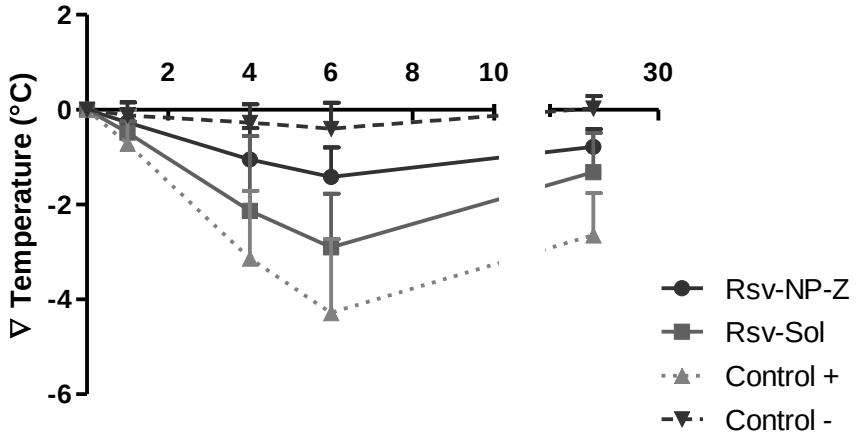

Figure 8: Comparative of decreased rectal temperature of mice after i.p. administration of LPS (40 µg) on time. Mice were pre-treated orally daily, for 7 days with resveratrol loaded in zein nanoparticles (Rsv-NP-Z) or resveratrol solubilized in PEG400-water (Rsv-sol). No-pretreated (control +) and negative controls were also included. Results expressed as mean ± SD (n=6).

Table 5 shows the overall endotoxic symptoms score including the number of animals displaying a temperature 2°C lower than the basal temperature, 6 h post-challenge. Animals of the positive control group that did not receive any resveratrol treatment, displayed a low mobility and signs of bristly hair and respiratory distress (Table II). On the contrary, animals treated with resveratrol-loaded zein nanoparticles displayed an almost normal behavior and an evident better symptomatology than those animals receiving resveratrol as oral solution, which appeared to be immobile or with high difficulty to coordinate any simple movement.

Table 4.Endotoxicsymtoms in the treated vs no treated LPS mice. Control -: No treated, no LPS; Control +: No treated, LPS; Rsv-Sol: administration of resveratrol solution daily during 7 days, LPS; Rsv-NP-Z: administration of resveratrol-loaded zein nanoparticles daily during 7 days, LPS. (n=6).

Treatment	Tª decreased >2°C	Piloerection	Mobility
Control -	0/6	-	Normal
Control +	6/6	+++	Very low
Rsv-Sol	4/6	++	Very Low
Rsv-NP-Z	1/6	+	Low

Severity of the symptoms: (-) None; (+) weak; (++) moderate; (+++) strong.
Decreased of temperature 6 hours after LPS injection.

Figure 9 shows the serum levels of TNF-α measured by ELISA before and 90 min after i.p. challenge withy LPS. Negligible levels of TNF-α were observed before LPS administration. The oral administration of resveratrol encapsulated in zein nanoparticles (Rsv-NP-Z) induced a

decrease in the levels of TNF-α with respect to mice pre-treated with resveratrol solution and the positive control group; however, these differences were not statistically significant. Significant differences ($p<0.01$) were observed between control negative and the rest of groups.

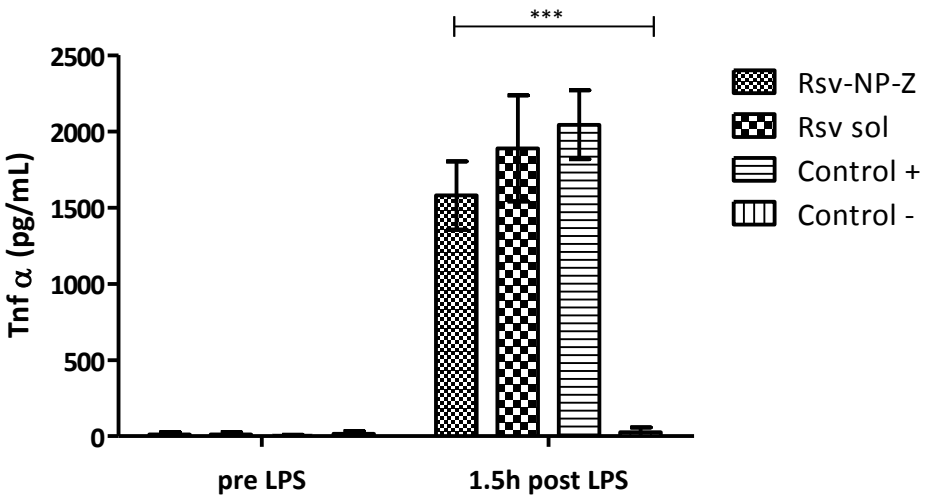

Figure 9. TNF-α serum levels after LPS intraperitoneal administration (40 μg) in untreated or treated with resveratrol C57BL/6J mice. Before challenge, mice were treated daily, during 7 days, with resveratrol loaded in zein nanoparticles (Rsv-NP-Z) or resveratrol solubilized in PEG-Water (50:50) (rsv-sol). No-pretreated (control +) and negative controls were also included. Data expressed as mean ± SD (n=6). $p<0.01$ Kruskal Wallis test.

4. Discussion

In this work we have encapsulated resveratrol in zein nanoparticles for the oral delivery of this polyphenol. The work also reports the pharmacokinetic profile of resveratrol as well as its antiinflammatory effect after its oral administration in these food-grade nanoparticles. Initially, resveratrol-loaded zein nanoparticles were prepared following a desolvation method and further purification by ultrafiltration and dying in a Spray-drier apparatus. However, due to the fact that zein nanoparticles possess abundant non-polar aminoacids, their dispersability in aqueous media is a challenge (Chen and Zhang, 2014). The use of citrate and phosphate salts has been recently proposed to minimize this problem [51]. The results presented here indicate that the incorporation of lysine could be also used in order to minimize the undesirable aggregation. Likely, this strategy was found adequate to obtain homogenous dispersions of the resulting nanoparticles. Only in the case in which drinking water was used, mechanical systems of agitation were required to generate a homogeneous suspension of zein nanoparticles. In order to solve this drawback, casein was selected. The use of this milk protein has recently suggested by Cheng and collaborators to prevent zein nanoparticles aggregation and increase their stability [52]. Interestingly, these nanoparticles (Rsv-NP-M) were rapidly redispersed in

water, with a simple hand agitation, and displayed a good stability (measured as absence of aggregation) in tap water for at least 10 days (data not shown).
The resulting Rsv-NP-Z and Rsv-NP-M nanoparticles displayed mean sizes close to 300 nm and negative zeta potentials. Previous studies showed that the encapsulation of resveratrol in SMEDDS [53], nanoemulsion[54], liposomes [55] and solid lipid nanoparticles [56], displayed sizes and surface charges in the same range than zein nanoparticles employed in this work (Rsv-NP-Z and Rsv-NP-M). The resveratrol loading ranged between 80 and 90 µg/mg nanoparticle respectively. This value is higher than other previously reported by other authors using solid lipid nanoparticles [56], PLGA [53] or nanoemulsions[54].

The release of resveratrol from both types of nanoparticles was found to be pH-independent. In fact, the release of resveratrol from nanoparticles would be a combination of both Fickian diffusion and erosion of the nanoparticle matrix (Peppas-Sahlin model). During the first hours of the release process, resveratrol molecules would diffuse from the nanoparticles to the aqueous media mainly controlled by Fickian diffusion. Later, the release of resveratrol would be mainly due to an erosion and/or relaxation process of the nanoparticle matrix. The time at which an erosion mechanism of the nanoparticles became the main phenomenon controlling the release of resveratrol was found to be 3.5 and 5 h, for Rsv-NP-Z and Rsv-NP-M, respectively. This surprising finding that would suggest that the incorporation of casein in zein nanoparticles results in more stable carriers, would be explained by the presence of a higher amount of resveratrol encapsulated close to the nanoparticle surface for Rsv-NP-M than for Rsv-NP-Z. This explanation would be in line with the finding that resveratrol was released slighty more rapidly from casein-zein nanoparticles than from zein ones. (Figure 2).

Pharmacokinetic studies were carried out at a single dose of 15 mg/kg, which is similar to that used in previous studies [53,57-59]. Intravenous administration of a single dose of resveratrol as a solution in PEG:water (1:1 by vol.) to rats produced an initial burst with high drug levels in plasma followed by a rapid biphasic decline over time (Figure 3). Eight hours after administration, the plasma drug levels were in the levels (below) of the quantification limit of the analytical technique. This typical profile for intravenous resveratrol [53,57,58,60], would be related with the rapid metabolism of the polyphenol *in vivo*.
When the solution of resveratrol was administered orally, low plasma values of the polyphenol were observed. This fact was consistent with previous findings described in the literature [53,58,59].
However, when resveratrol was administered after its encapsulation in zein nanoparticles, sustained and prolonged plasma levels of the polyphenol were observed for at least 30 h (Figure 5) and its relative oral bioavailability was of about 50% (Table 3). In addition, the resveratrol AUC when encapsulated in zein nanoparticles was found to be 10 times higher than when formulated as oral solution. On the other hand, for casein-zein nanoparticles, the resveratrol plasma levels were observed in plasma till 24-h after its administration (Figure 4); although, in general, these plasma levels were slightly lower than for zein nanoparticles. As a consequence, the relative oral bioavailability of resveratrol when loaded in casein-zein nanoparticles was of about 28%; 2-fold lower than for zein nanoparticles. This increasing capability to promote the absorption and bioavailability of resveratrol by using zein nanoparticles would be related with its high hydrophobic character [61], that would offer a

higher stability *in vivo* (as compared with casein) and to the capability of this corn protein to develop mucoadhesive interactions within the gut mucus layer [62]. Indeed, the hydrophobic character of zein nanoparticles would facilitate the development of interactions with hydrophobic domains of mucins in the mucus layer [61,63] and, thus, their mucoadhesiveproperties. On the contrary, for Rsv-NP-M, the incorporation of casein would disturb the mucoadhesive properties of zein nanoparticles, and, thus, the presence of casein would produce carriers with a lower residence time in the mucus layer covering the epithelium surface. As a result, the resveratrol bioavailability when encapsulated in casein-zein nanoparticles is lower than when loaded in zein nanoparticles.

Regarding the oral bioavailability of resveratrol, it is difficult to estabilish comparisons with other related works since the literature data are very scarce. In any case, the capability of zein nanoparticles to promote the oral bioavailability of resveratrol appears to be similar to that reported for Eudragit and chitosan/lecithin nanoparticles [64]. In that work, those nanoparticles administered as a single dose of 50 mg/kg in mice provided a relative oral bioavailability ranging from 39 to 61% respectively. More recently, Pandit and col. proposed a formulation of resveratrol loaded in solid lipid nanoparticles [65], reporting a ratio of 8 between the AUCs for resveratrol formulated in nanoparticles and a conventional solution. Here we report that, zein nanoparticles increased 18 times the AUC of resveratrol (compared to the PEG400:water solution).
Additionally, it has been reported that the administration of resveratrol loaded in nanoparticles does not affect its metabolism by ATP- binding cassette transporters [23]. However, under our experimental conditions, the plasma levels of resveratrol-O-3-glucuronide (measured as AUC) were higher than those observed when intravenously administered (about 1.7 times) or orally formulated in a PEG400-water solution (around 3.3 times). This fact would be related with the slow release of the polyphenol from the nanoparticles (in which it would be protected from degradation) and a prolonged residence of nanoparticles in the gut mucosa due to their mucoadhesive properties. In other words, by using nanoparticles, more resveratrol and during a longer period of time would reach the circulation, counterbalancing the natural rapid metabolism of the drug.
Interestingly, from both types of nanoparticles, the fraction of resveratrol absorbed from theses carriers correlated well with the percentage of the polyphenol released *in vitro* (see Figure 7).

Finally, we studied the biological activity of the resveratrol new fornulations*in vivo* as anti-inflammatory drug. The lipopolysaccharides (LPS) from most Gram negative bacteria induce in animals a pathophysiologic syndrome known as endotoxic shock, that is similar to sepsis shock syndrome that progress on multiple organ failure [66]. Symptoms such as piloerection, hypothermia, shivering, tachycardia and lethargy can be observed. These symptoms are related with large amounts of released inflammatory mediators, such as TNF-α, NO and PEG2,.where TNF-α play a central role as being the first one to be released [19,67]. Thus, we studied the efficacy of the resveratrol in an endotoxic shock model induced by LPS both in solution and loaded in zein nanoparticles. In this case, we selected zein nanoparticles because it showed the maximal level of oral bioavailability (50%). The positive control untreated group displayed the highest decrease in rectal temperature and the highest TNF-α serum level. In

contrast, the zein nanoparticles loaded with resveratrol administered daily during 7 days, were able to diminish the endotoxic symptoms like, hypothermia, piloerection and increase the movement of mice compared to Resveratrol solution on daily basics (Figure 7, Table 4). Besides, TNF-α diminish in serum, especially in those animals receiving resveratrol loaded in zein nanoparticles, although the individual values obtained were so variable that abolish the statistical significance. These results appear to indicate that the presence of sustained high levels of resveratrol in plasma could be efficient to reduce the inflammatory mediators in endotoxic shock induced by LPS.

Conclusions

Zein and zein-casein nanoparticles appear to be interesting carriers for the oral delivery of resveratrol. The polyphenol is released from these carriers by a combination of both diffusion and erosion of the nanoparticle matrix. The presence of casein in nanoparticles would increase the amount of resveratrol located in the peripheral areas of the nanoparticle matrix facilitating its release by diffusion as compared with pure zein nanoparticles. On the other hand, zein nanoparticles provided high and prolonged plasma levels of resveratrol up to 48%. As a consequence, these nanocarriers significantly increased the oral bioavailability of resveratrol reaching a value of close 50%. The oral administration of these nanoparticles during one week to mice challenged with LPS, protected them from the inflammatory symptoms of the endotoxic shock.

Acknowledgements

This work was supported by the Regional Government of Navarra (Alimentos funcionales, Euroinnova call) and the Spanish Ministry of Science and Innovation and Gobierno de Navarra (ADICAP; ref. IPT-2011-1717-900000). Rebeca Penalvaacknowledgesthe “Asociación de Amigos Universidad de Navarra” forthefinancialsupport.

References

[1] J.A. Baur, D.A. Sinclair, Therapeutic potential of resveratrol: the in vivo evidence, Nature Reviews Drug Discovery 5 (2006) 493-506.

[2] E. Wenzel, V. Somoza, Metabolism and bioavailability of trans-resveratrol, Molecular Nutrition & Food Research 49 (2005) 472-481.

[3] P. Saiko, A. Szakmary, W. Jaeger, T. Szekeres, Resveratrol and its analogs: defense against cancer, coronary disease and neurodegenerative maladies or just a fad?, Mutation Research/Reviews in Mutation Research 658 (2008) 68-94.

[4] A. Amri, J.C. Chaumeil, S. Sfar, C. Charrueau, Administration of resveratrol: What formulation solutions to bioavailability limitations?, J. Controlled Release 158 (2012) 182-193.

[5] K.M. Kasiotis, H. Pratsinis, D. Kletsas, S.A. Haroutounian, Resveratrol and related stilbenes: Their anti-aging and anti-angiogenic properties, Food and Chemical Toxicology 61 (2013) 112-120.

[6] C. Lucas-Abellán, M.T. Mercader-Ros, M.P. Zafrilla, J.A. Gabaldón, E. Núñez-Delicado, Comparative study of different methods to measure antioxidant activity of resveratrol in the presence of cyclodextrins, Food and Chemical Toxicology 49 (2011) 1255-1260.

[7] F. Orallo, E. Alvarez, M. Camina, J.M. Leiro, E. Gomez, P. Fernandez, The possible implication of trans-Resveratrol in the cardioprotective effects of long-term moderate wine consumption, Mol. Pharmacol. 61 (2002) 294-302.

[8] M. Athar, J.H. Back, X. Tang, K.H. Kim, L. Kopelovich, D.R. Bickers, A.L. Kim, Resveratrol: A review of preclinical studies for human cancer prevention, Toxicol. Appl. Pharmacol. 224 (2007) 274-283.

[9] S. Li, X. Wang, L. Kong, Design, synthesis and biological evaluation of imine resveratrol derivatives as multi-targeted agents against Alzheimer's disease, Eur. J. Med. Chem. 71 (2014) 36-45.

[10] P. Palsamy, S. Subramanian, Resveratrol protects diabetic kidney by attenuating hyperglycemia-mediated oxidative stress and renal inflammatory cytokines via Nrf2–Keap1 signaling, BiochimicaEtBiophysicaActa (BBA) - Molecular Basis of Disease 1812 (2011) 719-731.

[11] K. Szkudelska, T. Szkudelski, Resveratrol, obesity and diabetes, Eur. J. Pharmacol. 635 (2010) 1-8.

[12] J. Ahn, I. Cho, S. Kim, D. Kwon, T. Ha, Dietary resveratrol alters lipid metabolism-related gene expression of mice on an atherogenic diet, J. Hepatol. 49 (2008) 1019-1028.

[13] M. Lagouge, C. Argmann, Z. Gerhart-Hines, H. Meziane, C. Lerin, F. Daussin, N. Messadeq, J. Milne, P. Lambert, P. Elliott, B. Geny, M. Laakso, P. Puigserver, J. Auwerx, Resveratrol Improves Mitochondrial Function and Protects against Metabolic Disease by Activating SIRT1 and PGC-1α, Cell 127 (2006) 1109-1122.

[14] L. Rivera, R. Morón, A. Zarzuelo, M. Galisteo, Long-term resveratrol administration reduces metabolic disturbances and lowers blood pressure in obese Zucker rats, Biochem. Pharmacol. 77 (2009) 1053-1063.

[15] A. Dal-Pan, S. Blanc, F. Aujard, Resveratrol suppresses body mass gain in a seasonal non-human primate model of obesity, BMC Physiology 10 (2010) 11.

[16] S. Timmers, E. Konings, L. Bilet, R.H. Houtkooper, T. van de Weijer, G.H. Goossens, J. Hoeks, S. van der Krieken, D. Ryu, S. Kersten, Calorie restriction-like effects of 30 days of resveratrol supplementation on energy metabolism and metabolic profile in obese humans, Cell Metabolism 14 (2011) 612-622.

[17] K. Szkudelska, T. Szkudelski, Resveratrol, obesity and diabetes, Eur. J. Pharmacol. 635 (2010) 1-8.

[18] M.P. Gillum, M.E. Kotas, D.M. Erion, R. Kursawe, P. Chatterjee, K.T. Nead, E.S. Muise, J.J. Hsiao, D.W. Frederick, S. Yonemitsu, A.S. Banks, L. Qiang, S. Bhanot, J.M. Olefsky, D.D. Sears, S. Caprio, G.I. Shulman, SirT1 regulates adipose tissue inflammation, Diabetes 60 (2011) 3235-3245.

[19] K. Takahashi, A. Morikawa, Y. Kato, T. Sugiyama, N. Koide, M. Mu, T. Yoshida, T. Yokochi, Flavonoids protect mice from two types of lethal shock induced by endotoxin, FEMS Immunology & Medical Microbiology 31 (2001) 29-33.

[20] H. Farghali, D. Černý, L. Kameníková, J. Martínek, A. Hořínek, E. Kmoníčková, Z. Zídek, Resveratrol attenuates lipopolysaccharide-induced hepatitis in D-galactosamine sensitized rats: role of nitric oxide synthase 2 and heme oxygenase-1, Nitric Oxide 21 (2009) 216-225.

[21] Alarcón de la Lastra, Catalina, I. Villegas, Resveratrol as an anti-inflammatory and anti-aging agent: Mechanisms and clinical implications, Molecular Nutrition & Food Research 49 (2005) 405-430.

[22] T. Walle, Absorption and metabolism of flavonoids, Free Radical Biology Medicine 36 (2004) 829-837.

[23] J.M. Planas, I. Alfaras, H. Colom, M.E. Juan, The bioavailability and distribution of<i> trans-resveratrol are constrained by ABC transporters, Arch. Biochem. Biophys. 527 (2012) 67-73.

[24] G. Kuhnle, J.P. Spencer, G. Chowrimootoo, H. Schroeter, E.S. Debnam, S.K.S. Srai, C. Rice-Evans, U. Hahn, Resveratrol is absorbed in the small intestine as resveratrol glucuronide, Biochem. Biophys. Res. Commun. 272 (2000) 212-217.

[25] T. Walle, F. Hsieh, M.H. DeLegge, J.E. Oatis Jr, U.K. Walle, High absorption but very low bioavailability of oral resveratrol in humans, Drug Metab. Dispos. 32 (2004) 1377-1382.

[26] A.C. Santos, F. Veiga, A.J. Ribeiro, New delivery systems to improve the bioavailability of resveratrol, Expert Opinion on Drug Delivery 8 (2011) 973-990.

[27] K. Teskač, J. Kristl, The evidence for solid lipid nanoparticles mediated cell uptake of resveratrol, Int. J. Pharm. 390 (2010) 61-69.

[28] K. Bolko, A. Zvonar, M. Gašperlin, Mixed lipid phase SMEDDS as an innovative approach to enhance resveratrol solubility, Drug Dev. Ind. Pharm. 40 (2013) 102-109.

[29] G. Davidov-Pardo, D.J. McClements, Nutraceutical delivery systems: Resveratrol encapsulation in grape seed oil nanoemulsions formed by spontaneous emulsification, Food Chem. 167 (2015) 205-212.

[30] G. Singh, R.S. Pai, Optimized PLGA nanoparticle platform for orally dosed trans-resveratrol with enhanced bioavailability potential, Expert Opinion on Drug Delivery 11 (2014) 647-659.

[31] R. Shukla, M. Cheryan, Zein: the industrial protein from corn, Industrial Crops and Products 13 (2001) 171-192.

[32] A. Esen, A proposed nomenclature for the alcohol-soluble proteins (zeins) of maize (<i>Zea mays L.), J. Cereal Sci. 5 (1987) 117-128.

[33] T.J. Anderson, B.P. Lamsal, Review: Zein extraction from corn, corn products, and coproducts and modifications for various applications: A review, Cereal Chem. 88 (2011) 159-173.

[34] A. Pomes, Zein, Encyclopedia of Polymer Science and Technology 15 (1971) 125-132.

[35] G.W. Padua, Q. Wang, Controlled self-organization of zein nanostructures for encapsulation of food ingredients, Micro/Nanoencapsulation of Active Food Ingredients 1007 (2009) 143-155.

[36] R. Paliwal, S. Palakurthi, Zein in controlled drug delivery and tissue engineering, J. Controlled Release 189 (2014) 108-122.

[37] N. Singh, D.M. Georget, P.S. Belton, S.A. Barker, Physical properties of zein films containing salicylic acid and acetyl salicylic acid, J. Cereal Sci. 52 (2010) 282-287.

[38] Y. Li, L. Lim, Y. Kakuda, ElectrospunZein Fibers as Carriers to Stabilize (−)-EpigallocatechinGallate, J. Food Sci. 74 (2009) C233-C240.

[39] E.T. Lau, S.K. Johnson, D. Mikkelsen, P.J. Halley, K.J. Steadman, Preparation and in vitro release of zeinmicroparticles loaded with prednisolone for oral delivery, J. Microencapsul. 29 (2012) 706-712.

[40] M.C. Regier, J.D. Taylor, T. Borcyk, Y. Yang, A.K. Pannier, Fabrication and characterization of DNA-loaded zeinnanospheres, J. Nanobiotechnology 10 (2012) 44-3155-10-44.

[41] M. Agüeros, I. Esparza, C. Gonzalez-Ferrero, C.J. Gonzalez-Navarro, J.M. Irache, A. Romo, Nanoparticles for encapsulation of compounds, the production and uses thereof. (2012).

[42] R. Penalva, I. Esparza, M. Agüeros, C.J. Gonzalez-Navarro, C. Gonzalez-Ferrero, J.M. Irache, Casein nanoparticles as carriers for the oral delivery of folic acid, Food Hydrocolloids 44 (2015) 399–406.

[43] P. Arbós, M.A. Campanero, M.A. Arangoa, M.J. Renedo, J.M. Irache, Influence of the surface characteristics of PVM/MA nanoparticles on their bioadhesive properties, J. Controlled Release 89 (2003) 19-30.

[44] P. Iacopini, M. Baldi, P. Storchi, L. Sebastiani, Catechin, epicatechin, quercetin, rutin and resveratrol in red grape: Content,<i> in vitro antioxidant activity and interactions, Journal of Food Composition and Analysis 21 (2008) 589-598.

[45] P.L. Ritger, N.A. Peppas, A simple equation for description of solute release I. Fickian and non-Fickian release from non-swellable devices in the form of slabs, spheres, cylinders or discs, J. Controlled Release 5 (1987) 23-36.

[46] J. Sujja-areevath, D.L. Munday, P.J. Cox, K.A. Khan, Relationship between swelling, erosion and drug release in hydrophillic natural gum mini-matrix formulations, European Journal of Pharmaceutical Sciences 6 (1998) 207-217.

[47] N.A. Peppas, J.J. Sahlin, A simple equation for the description of solute release. III. Coupling of diffusion and relaxation, Int. J. Pharm. 57 (1989) 169-172.

[48] P. Costa, J.M. Sousa Lobo, Modeling and comparison of dissolution profiles, European Journal of Pharmaceutical Sciences 13 (2001) 123-133.

[49] D.J. Boocock, K.R. Patel, G.E.S. Faust, D.P. Normolle, T.H. Marczylo, J.A. Crowell, D.E. Brenner, T.D. Booth, A. Gescher, W.P. Steward, Quantitation of trans-resveratrol and detection of its metabolites in human plasma and urine by high performance liquid chromatography, Journal of Chromatography B 848 (2007) 182-187.

[50] M.A. Kassem, A.N. ElMeshad, A.R. Fares, Enhanced bioavailability of buspirone hydrochloride via cup and core buccal tablets: Formulation and<i> in vitro/in vivo evaluation, Int. J. Pharm. 463 (2014) 68-80.

[51] M.I. Molina, J.R. Wagner, The effects of divalent cations in the presence of phosphate, citrate and chloride on the aggregation of soy protein isolate, Food Res. Int. 32 (1999) 135-143.

[52] H. Chen, Q. Zhong, A novel method of preparing stable zein nanoparticle dispersions for encapsulation of peppermint oil, Food Hydrocoll.

[53] G. Singh, R.S. Pai, Trans-resveratrol self-nano-emulsifying drug delivery system (SNEDDS) with enhanced bioavailability potential: optimization, pharmacokinetics and in situ single pass intestinal perfusion (SPIP) studies, Drug Deliv. (2014) 1-9.

[54] M. Sessa, M.L. Balestrieri, G. Ferrari, L. Servillo, D. Castaldo, N. D'Onofrio, F. Donsì, R. Tsao, Bioavailability of encapsulated resveratrol into nanoemulsion-based delivery systems, Food Chem. 147 (2014) 42-50.

[55] C. Caddeo, M. Manconi, A.M. Fadda, F. Lai, S. Lampis, O. Diez-Sales, C. Sinico, Nanocarriers for antioxidant resveratrol: Formulation approach, vesicle self-assembly and stability evaluation, Colloids and Surfaces B: Biointerfaces 111 (2013) 327-332.

[56] S. Jose, S.S. Anju, T.A. Cinu, N.A. Aleykutty, S. Thomas, E.B. Souto, In vivo pharmacokinetics and biodistribution of resveratrol-loaded solid lipid nanoparticles for brain delivery, Int. J. Pharm. 474 (2014) 6-13.

[57] M.E. Juan, M. Maijó, J.M. Planas, Quantification of trans-resveratrol and its metabolites in rat plasma and tissues by HPLC, J. Pharm. Biomed. Anal. 51 (2010) 391-398.

[58] H. Colom, I. Alfaras, M. Maijó, M.E. Juan, J.M. Planas, Population pharmacokinetic modeling of trans-resveratrol and its glucuronide and sulfate conjugates after oral and intravenous administration in rats, Pharm. Res. 28 (2011) 1606-1621.

[59] S. Das, H. Lin, P.C. Ho, K. Ng, The impact of aqueous solubility and dose on the pharmacokinetic profiles of resveratrol, Pharm. Res. 25 (2008) 2593-2600.

[60] H. He, X. Chen, G. Wang, J. Wang, A.K. Davey, High-performance liquid chromatography spectrometric analysis of<i> trans-resveratrol in rat plasma, Journal of Chromatography B 832 (2006) 177-180.

[61] A.R. Patel, K.P. Velikov, Zein as a source of functional colloidal nano- and microstructures, Current Opinion in Colloid & Interface Science (2014) in press.

[62] Y. Yin, S. Yin, X. Yang, C. Tang, S. Wen, Z. Chen, B. Xiao, L. Wu, Surface modification of sodium caseinate films by zein coatings, Food Hydrocoll. 36 (2014) 1-8.

[63] A. Patel, Y. Hu, J.K. Tiwari, K.P. Velikov, Synthesis and characterisation of zein–curcumin colloidal particles, Soft Matter 6 (2010) 6192-6199.

[64] E. Oganesyan, I. Miroshnichenko, N. Vikhrieva, A. Lyashenko, S.Y. Leshkov, Use of nanoparticles to increase the systemic bioavailability of trans-resveratrol, Pharmaceutical Chemistry Journal 44 (2010) 74-76.

[65] D. Pandita, S. Kumar, N. Poonia, V. Lather, Solid lipid nanoparticles enhance oral bioavailability of resveratrol, a natural polyphenol, Food Res. Int. 62 (2014) 1165-1174.

[66] M.A. Freudenberg, T. Merlin, M. Gumenscheimer, C. Kalis, R. Landmann, C. Galanos, Role of lipopolysaccharide susceptibility in the innate immune response to Salmonella typhimurium infection: LPS, a primary target for recognition of Gram-negative bacteria, Microb. Infect. 3 (2001) 1213-1222.

[67] W. Li, H. Li, Q. Mu, H. Zhang, H. Yao, J. Li, X. Niu, Protective effect of sanguinarine on LPS-induced endotoxic shock in mice and its effect on LPS-induced COX-2 expression and COX-2 associated PGE2 release from peritoneal macrophages, Int. Immunopharmacol. 22 (2014) 311-317.

Chapter 8

Increased oral bioavailability and preventive anti-inflammatory effect of quercetin when loaded in zein nanoparticles

Abstract

Quercetin is a flavonoid abundant in plants, fruits and vegetables. It has been shown a high antioxidant, anti-inflammatory and anticancer activity. However, due to its poor water solubility and metabolism, the oral bioavailability of this flavonoid is too low, which limits its utilization. In order to promote the oral absorption and anti-inflammatory effect of quercetin, the flavonoid and 2-hydroxypropyl-β-cyclodextrin (HP-β-CD) were encapsulated in zein nanoparticles. The resulting nanoparticles displayed a mean size of size was close to 300 nm and the payload was calculated to be close to 70 μg/mg nanoparticle. The release of quercetin from zein nanoparticles followed a zero-order kinetic. In rats, the oral administration of quercetin-loaded nanoparticles, provided high and sustained levels of the flavonoid in plasma up to 72 h. Under these circumstances, the relative oral bioavailability was close to 60%, 14-times higher than for the control oral solution of the flavonoid. The anti-inflammatory effect of quercetin was measured in mice intraperitoneally challenged with lipopolysaccharide. Animals treated with quercetin-loaded nanoparticles (one dose 25 mg/kg every two days during 1 week) presented endotoxic symptoms less severe and TNF-α levels significantly lower than those observed in animals treated with the oral solution of the flavonoid (one dose 25 mg/kg every day during 1 week).

In summary, the encapsulation of quercetin in zein nanoparticles in the presence of HP-β-CD offer an important increase of its oral bioavailability and, thus, of its efficacy as antiinflammatory agent.

1. Introduction

Flavonoids consist of a large group of natural polyphenolic compounds having a benzo-γ-pyrone structure. More than 4000 varieties of flavonoids have been identified, many of which possess several pharmacological activities [1]. Quercetin(3,5,7,3,4-pentahydroxylflavone) is one of the most abundant flavonoids ubiquitously distributed in fruits, vegetables and herbs or related products [2]. In food, quercetinis usually glycosylated (mainly bound to glucose, rutinose, rhamnose, xylose or other sugars), with high concentrations found in capers, onions, cranberries or black plums [3].
Quercetin is considered to be a strong antioxidant due to its ability to scavenge free oxygen radicals and bind transition metal ions [4,5]. These properties of quercetin allow it to prevent the oxidation of low-density lipoproteins [6,7]. Apart from the antioxidant activity, quercetin shows antiviral [8]antiatherosclerotic[9], antitumor [10], and cardioprotective properties[11,12].
It is important to note that when the glycosylated forms of quercetin are assayed, there is usually a loss of activity in these effects in comparison with those obtained with the aglycone(without a sugar group)[13,14].

Moreover, quercetin is known to possess strong anti-inflammatory activity. *In vitro* studies have shown that this flavonoid is capable of inhibiting LPS induced cytokine production (e.g. TNF-α) [15]. This effect would be mediated via modulation of NF-κB pathway and a decrease in the gene expression and synthesis of TNF-α[3,16-18]. In line with these effects, it has been reported thatquercetin exhibited an antiinflammatory activity similar to that of indomethacin [19].
However, when administered orally, the bioavailability of quercetin is low (less than 10%) [1,3]. This fact would be mainly related to its high affinity for both intestinal efflux pumps (e.g. P-gp and MRP2) [20,21]and the cytochrome P450 (CYP3A), which are all abundantly present in the epithelium of the gastrointestinal tract[22].
In this context, the development of an oral quercetin formulation has therefore been a challenge, and many approaches have been tested or are under investigation. Thus, in order to promote the oral bioavailability of quercetin different strategies have been proposed including the use of poly-D-lactide nanoparticles [23], [24], microemulsions and self-emulsifying systems [25], [26], and lipid particulates [27-29].

Another possibility to promote the oral bioavailability of quercetin may be its encapsulation in zein nanoparticles. Zein is the major storage protein of corn with a hydrophobic character as a result of its aminoacid composition (high contents of leucine, proline and alanine) [30][31,32]. In addition, zein is known for its high thermal resistance and great oxygen barrier properties, which maybe of interest for the encapsulation or incorporation of compounds sensitive to oxidation or temperature [30].

The aim of this work was to design and evaluate the capability of zein nanoparticles to promote the oral absorption of quercetin. For this purpose, quercetin was encapsulated in zein nanoparticles with 2-hydroxypropyl-β-cyclodextrin, which has been identified as inhibitor of both the intestinal efflux pumps and the cytochrome P450 (e.g. CYP3A4) [33,34].

2. Materials and methods

2.1 Materials

Zein, quercetin, lysine, 2-*hydroxypropyl*-β-*cyclodextrin* (HP-β-CD), mannitol, chlorzoxazone, PEG 400, Tween 20 and sodium chloride were from Sigma-Aldrich (Germany). Ethanol, methanol, acetic acid and acetonitrile (HPLC grade) were from Merck (Darmstadt, Germany). PBS (Phosphate-Buffered saline) was from Gibco by Life Technologies Corp. (New York, USA). Lipopolysaccharide (LPS) from *Salmonella enterica*serovar. Minnesota was from Sigma (St. Louis, USA). Deionised reagent water (18.2 MO resistivity) was prepared by a water purification system (Wasserlab, Spain). All reagents and chemicals used were of analytical grade. Kit TNF-α was supplied from

2.2 Preparation of quercetin-loadednanoparticles

Zein nanoparticles were prepared by a desolvation procedure followed by a purification step by ultrafiltration and subsequent drying in a Spray-drying apparatus [35].

Briefly, 600 mg zein and 60 mg lysine were dissolved in 88 mL of ethanol 60%. In parallel, 50 mg quercetin and a variable amount of hydroxypropyl-β-cyclodextrin were dissolved in 10 mL absolute ethanol and added under magnetic stirring to the zein solution. After a time of incubation, nanoparticles were formed by the addition of 88 mL of purified water. The resulting suspension of nanoparticles was purified and concentrated by ultrafiltration through a polysulfone membrane cartridge of 50 kDa pore size (Medica SPA, Italy). Then, 30 mL of an aqueous solution of mannitol (100 mg/mL) were added and, finally, the suspension of zein nanoparticles was dried in a Buchi Mini Spray Drier B-290 apparatus (BuchiLabortechnik AG, Switzerland) under the following experimental conditions: (i) inlet temperature:90°C, (ii) outlet temperature: 45-50°C, (iii) air pressure: 2-5 bar, (iv) pumping rate: 2-6 mL/min, (v) aspirator: 100% and (vi) air flow:900 l/h.

On the other hand, nanoparticles in the absence of the cyclodextrin were also prepared (Que-NP-Z). In this case, zein (600 mg), quercetin (50 mg) and lysine (60 mg) were incubated in 88 mL of ethanol 60%. Then, nanoparticles were formed by the addition of water and the resulting nanosuspensions were purified and dried as described above.

Empty nanoparticleswere prepared as described above but in the absence of the oligosaccharide and quercetin (NP-Z) or in the absence of the flavonoid (HPCD-NP-Z).

2.3 Preparation of quercetin conventional formulations

For in vivo studies, two conventional formulations of quercetin were used. The first one consisted on a solution of the polyphenol in a mixture of PEG 400 and water (6:4 by vol.). For this purpose, 62.5 mg of quercetin were dissolved in 6 mL of PEG 400 under magnetic stirring. Then 4 mL of purified water were added and the final mixture was agitated in the dark for 10 min. This formulation was named Que-sol.

The second one was an extemporary suspension of quercetin in purified water (Que-susp). Briefly, 62.5mg quercetin was dispersed in 10 mL of purified water under magnetic agitation for 10 min. The size of the resulting suspension was 15.5 ± 4.3µm. The suspension was used after inspection for absence of aggregates.

2.4 Characterization of nanoparticles

2.4.1 Size, zeta potential and morphology

The mean hydrodynamic diameter and the zeta potential of nanoparticles were determined by photon correlation spectroscopy (PCS) and electrophoretic laser Doppler anemometry, respectively, using a Zetaplus apparatus (Brookhaven Instrument Corporation, USA). The diameter of the nanoparticles was determined after dispersion in ultrapure water (1:10) and measured at 25ºC with a scattering angle of 90°C. The zeta potential was measured after dispersion of the dried nanoparticles in 1 mMKClsolution (pH 6).

The morphology and shape of nanoparticles was examined using a field emission scanning electron microscope FE-SEM (ULTRA Plus, Zeiss, The Netherlands). Prior to analysis, particles were washed to remove mannitol. For this purpose, spray-dried nanoparticles were resuspended in ultrapure water and centrifuged at 27,000xg for 10 min. Then, the supernatants were discarded and the obtained pellets were mounted on copper grids. Finally, the pellet was shaded with an amalgam of gold/palladium during fifteen seconds using a sputter coater (K550X Emitech, Ashford, UK).

2.4.2 Yield of the preparative process

In order to quantify the amount of protein transformed into nanoparticles, 10 mg of empty nanoparticles were dispersed in water and centrifuged at 17,000 x g for 20 min. Supernatants were discarded and the pellets were digested with ethanol 75%. Then, the amount of protein was quantified by UV spectrophotometry at 278 nm in an Agilent 8453 system (Agilent Technologies, USA). For analysis, calibration curves were constructed between 90 and 1200 µg/mL (R^2> 0.999; quantitation limit = 143 µg/mL).

The amount of protein transformed into nanoparticles was estimated as the ratio between the amount of the zein quantified in the pellet of the centrifuged samples and the total amount of protein used for the preparation of nanoparticles and expressed as follows:

$$Yield(\%) = \frac{(Proteininpellet)}{(Totalprotein\ )} \times 100 \quad \text{(Eq. 1)}$$

2.4.3 Quercetin quantification

The amount of quercetin loaded into the nanoparticles was quantified by HPLC-UV following a method previously described [36]. Analysis were carried out in an Agilent model 1100 series LC and a diode-array detector set at 370 nm. The chromatographic system was equipped with a reversed-phase 150 mm x 2.1 mm C18 Alltima column (particle size 5 µm; Altech, USA) and a Gemini C18 precolumn (particle size 5 µm; Phenomenex, CA, USA). The mobile phase, pumped at 0.25 mL/min, consisted of a mixture of methanol, water and acetic acid in gradient condition.

The column was placed at 40°C and the injection volume was 10 µL. Calibration curves were designed over the range of 0.3-100 µg/mL (R^2> 0.99). The limit of quantification was calculated to be 0.35 µg/mL.

For analysis, 10 mg of nanoparticles were dispersed in 1 mL water and centrifuged 30,500 g for 20 min. The amount of quercetin encapsulated was calculated by dissolution of the pellets with 1 mL of ethanol 75%. In addition, the total content of quercetin in the formulation was quantified. Thus, 10 mg of the formulation were dissolved in 1 mL of ethanol 75% (Que t). Each sample was assayed in triplicate and the results were expressed as the amount of quercetin (in µg) per mg of nanoparticles.

The encapsulation efficiency (E.E.) and quercetin loaded were calculated as follows:

$$E.E.(\%) = \frac{(Que\ p)}{(Que\ t)} \times 100 \text{ (Eq.2)}$$

$$Quercetin\ loaded\ (\mu g/mgNP) = \frac{(Que\ p)}{Wp} \text{(Eq. 3)}$$

in which (Que t) is the total experimental amount of quercetin in the formulations and (Que p) corresponds to the amount of quercetin quantified in the pellets and Wp the amount of protein quantified as described above.

2.5 In vitro releasestudies

Release experiments were conducted at 37°C using simulated gastric (SGF, pH 1.2) and intestinal (SIF, pH 6.8) fluids. In order to fulfil sink conditions, Tween® 20 (0.5% w/v) was added to both media.The studies were performed under agitation in a slide-A-Lyzer® Dialysis cassette 10.000 MWCO (Thermo scientific, Rockford, IL, USA). For the study, 2 mg of quercetin loaded in zein nanoparticles were dispersed in 5 mL of water and introduced in the cassette, which was then placed into a vessel containing 500 mL of SGF for 2 hours. After this time, the same cassette was removed from the SGF and introduced in a second vessel with 500 mL of SIF until the end of the experiment. At different time points, samples of 1 mL were collected and filtered to 0.45 µm (Filter nylon, 0.45µL, Thermo scientific, Rockford, USA) before quantification. The volume was recovered by the addition of an equal volume of gastric or intestinal simulated fluids.

The amount of quercetin released from the formulations was quantified by HPLC. Calibration curves of quercetin were prepared in both release media over the range of 0.16-6 µg /mL (R^2 > 0.99).

Data obtained from the *in vitro* release experiments were fitted to a Zero-Order kinetic equation (Eq 4). This model is used for systems where the matrix releases the same amount of drug by unit of time [37].

$$\frac{M_t}{M_\infty} = \mathrm{K}_{\mathrm{ZO}} \cdot \mathrm{t} \text{ (Eq 4)}$$

Where Mt/M_∞ is the drug release fraction at time *t*, and K_{ZO} is the zero order release constant.

To fit the experimental data to the previous equation, only one portion of the release profile was used, that is $M_t/M_\infty \leq 0.6$ [37].

2.6 In vivo pharmacokinetic studies in Wistar rats

2.6.1 Pharmacokinetic studies

Pharmacokinetic studies were performed in male Wistar rats (200-250 g) obtained from Harlan (Barcelona, Spain). Studies were approved by the Ethical Committee for Animal Experimentation of the University of Navarra (protocol number 128-11) in accordance with the European legislation on animal experiments.

Previous to the oral administration of the formulations, animals were fasted overnight to avoid interference with the absorption, allowing free access to water. For the pharmacokinetic study, rats were randomly divided into 5 groups (n=6). The experimental groups were: (i) quercetin water suspension, (ii) quercetin solution in PEG 400:water (60:40 v/v) (iii) quercetin-loaded zein nanoparticles (Que-NP-Z) and (iv) quercetin-loaded in zein nanoparticles containing HP-β-CD (Que-HPCD-NP-Z). As control, a group of animals received intravenously the solution of quercetin in the mixture of PEG 400 and water. In all case, the dose of quercetin (orally or intravenously) was 25 mg/kg body weight.

Blood samples were collected at set times after administration (0, 10 min, 30 min, 1, 2, 4, 6, 8, 24 and 48 hours) in Microvette® 500K3E plasma tubes (SARSTEDT, Germany). Blood volume was recovered intraperitoneally with an equal volume of normal saline solution pre-heated at body temperature. Samples were immediately centrifuged at 9,400 xg for 10 min and plasma aliquots were frozen at -80 °C until analysis.

2.6.2 Determination of quercetin plasma concentration by HPLC

The amount of quercetin was determined in plasma by HPLC as described above using chlorzoxazone as internal standard. Prior the analysis, quercetin was extracted from plasma samples following a protocol previously described by Li and co-workers [27] with minor modifications. Thus, aliquots of 100 µL plasma were mixed with 25 µL internal standard solution (chlorzoxazone 50 µg/mL in methanol). To this mixture, 125 µL methanol and 50 µL HCl (25% by vol.) were added under vigorous shaking for 10 min in order to induce protein precipitation. Then, samples were hydrolyzed in a water bath at 50°C for 15 min and, finally, centrifuged at at9,400 xg for 10 min. The resulting supernatants were filtered (Filter nylon, 0.45µL, Thermo scientific, Rockford, USA) and 50 µL was injected onto the HPLC column.

The same protocol was followed for the preparation of calibration curves and quality control standards, using blank plasma and different solutions of quercetin in methanol. Calibration curves were designed over the range between 70 and 5000 ng/mL (R^2=0.999). Under these experimental conditions the run time of quercetin was 13.9 ± 0.2 min (detected at 370 nm) and the internal standard 12.6 ± 0.2 min (detected at 303 nm). The limit of quantification was calculated as 200 ng/mL.Linearity, accuracy and precision values during the same day (intraday

assay) at low, medium and high concentrations of quercetin were within the acceptable limits (relative error and coefficient of variation less than 15%).

2.6.3 Pharmacokinetic data analysis

Quercetin plasma concentration was plotted against time, and pharmacokinetic analysis was performed using a non-compartmental model with the WinNonlin 5.2 software (Pharsight Corporation, USA). The following parameters were estimated: maximal serum concentration (C_{max}), time in which C_{max} is reached (T_{max}), area under the concentration-time curve from time 0 to last time (AUC), mean residence time (MRT), clearance (Cl), volume of distribution (V) and half-life in the terminal phase ($t_{1/2}$). Furthermore, the relative bioavailability (Fr %) of quercetin was estimated by the following equation:

$$Fr\ (\%) = \frac{AUC\ oral}{AUC\ iv} \times 100 \quad \text{(Eq. 5)}$$

In which $AUC_{i.v.}$andAUC_{oral} are the areas under the curve for the iv and oral administrations, respectively.

2.7 Anti-inflammatoryefficacystudy

2.7.1 Animal model

C57BL/6J female mice, 4 weeks-old (20-22 g), were purchased from Harlan (Barcelona, Spain) and housed under standard animal facilities with free access to food and drinking water. Housing conditions were maintained by controlled temperature and humidity and with 12 h on/off light cycles. Animals were allowed to acclimate for one week before the experiment.

In vivo anti-inflammatory studies were evaluated in an endotoxic shock model set up by intraperitoneal administration of lipopolysaccharide (LPS) from *Salmonella enterica* (serovar. Minnesota) at dose of 40 µg per animal. Before administration, LPS was dissolved in PBS and vortexed during 30 min to complete homogenization.

On day 1, mice were randomly distributed into the four following groups of 6 animals each: i) negative control group (animals received neither LPS nor quercetin), ii) positive control group (animals received LPS but were not treated with any quercetin formulation), iii) quercetin oral solution in a mixture of PEG400 and water (Rsv-sol), and iv) quercetin-loaded in zein nanoparticles containing HP-β-CD (Que-HPCD-NP-Z). Quercetin groups received an oral dose of 25 mg/Kg. According to pharmacokinetic studies, the animals treated with the quercetin solution, received the dose daily for 7 days. However, animals treated with nanoparticles (Que-HPCD-NP-Z) received the same dose (25 mg/kg) but every two days.

Twenty four hours after the last dose of quercetin, animals were challenged intraperitoneally with LPS (40 µg). Throughout the study, rectal temperature of mice was measured until 24 h after challenge. Similarly, animals were observed for any clinical signs or symptoms of toxicity daily and after the challenge. Reactions severity was classified in the following categories depending on their gravity: i) (-) absent; ii) (+) weak; iii) (++) moderate; andiv) (+++) strong.

Depending on the activity of the animals, their mobility was classified as follows: very low, low or normal.

In addition, 90 min after challenge, blood samples were collected from the retro-orbital cavity in EDTA-K vials, centrifuged at 8,000 xg for 10 min for sera collection that were conserved at -20 °C until use.

2.7.2 Measurement of plasma TNF-α.

The concentration of circulating TNF-α in the serum of animals was determined by an enzyme-linked immunosorbent assay kit (Quantikine® ELISA Mouse TNF-α, MTA00B, R&D Systems, Minneapolis, USA) according to manufacturer's instructions.

2.8 Statisticalanalysis.

Data are expressed as the mean ± standard deviation (SD) of at least three experiments. The non-parametric Kruskall-Wallis followed by Mann-Whitney U-test was used to investigate statistical differences. In all cases, $p < 0.05$ was considered to be statistically significant. All data processing was performed using Graph Pad® Prism statistical software.

3. Results

3.1 Physico-chemicalcharacteristics

For the optimization of the preparative process of quercetin-loaded nanoparticles in the presence of cyclodextrin, two parameters were studied: (i) the quercetin/2-hydroxypropyl-β-cyclodextrin ratio and (ii) the incubation time between the components of the formulation (quercetin, cyclodextrin and zein) before the formation of nanoparticles.

Figure 1 shows the influence of the incubation time and the quercetin/HP-β-CD ratio (1:1, 1:2, 1:3 by mol) on the encapsulation efficiency and payload of the resulting nanoparticles. By increasing the amount of cyclodextrin (reduction of the quercetin/HP-β-CD ratio), small differences in the payload and encapsulation efficiency of the flavonoid in zein nanoparticles were found. Regarding the incubation time between the components of the formulation, a minimum time of 30 min were required to obtain a maximum amount of quercetin loading. In consequence, a quercetin/cyclodextrin ratio of 1:1 by mol, and a time of incubation of 30 minutes were selected.

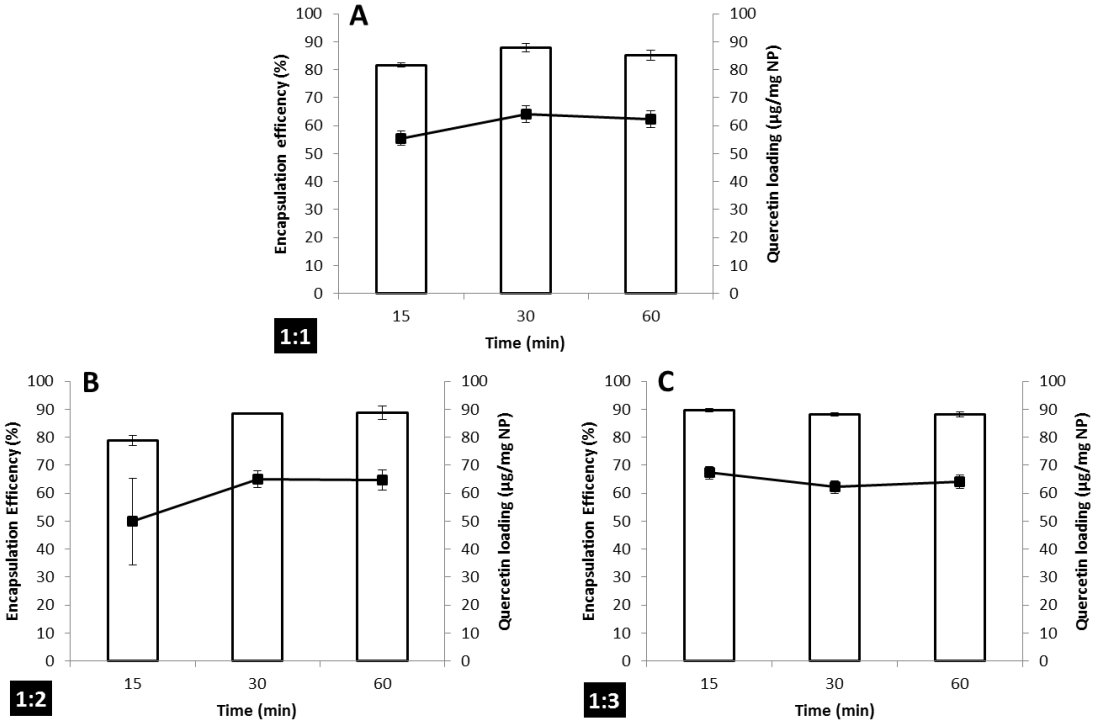

Figure 1: Influence of the incubation time (15, 30 and 60 min) and the quercetin/HP-β-CD ratio (1:1, 1:2 and 1:3 by mol) on the flavonoid loading (line, right axis) and its encapsulation efficiency (bars, left axis) in the resulting nanoparticles. Data expressed as mean ± SD, n=3.

The physic-chemical characteristics of quercetin-loaded nanoparticles are summarized in Table 1. In the absence of quercetin, nanoparticles displayed a mean size of around 220-250 nm and a negative zeta potential close to -50 mV.

Comparing with empty nanoparticles (NP), the encapsulation of quercetin significantly increased the size of the resulting nanoparticles nanoparticles($p<0.05$). Thus, for Que-HPCD-NP-Z the size was close to 300 nm, whereas for quercetin loaded nanoparticles prepared in the absence of HP-β-CD, the mean diameter was even higher and close to 360 nm. Interestingly, the polydispersity index (PDI) was found to be always lower and evidenced that nanoparticle formulations were homogeneous. In addition, the zeta potential of the quercetin-loaded nanoparticles was found to be slightly less negative than for empty ones (Table 1).

Another important point was that the use of HP-β-CD enabled us to increase the quercetin payload in zein nanoparticles. However this increase was modest, from 62 µg/mg for Que-NP-Z until 69 µg/mg for nanoparticles prepared in the presence of the oligosaccharide (Que-HPCD-NP-Z).

Table 1.Physico-chemical characteristics of empty zein nanoparticles (NP-Z and HPCD-NP-Z), quercetin-loaded zein nanoparticles (Que-NP-Z and Que-HPCD-NP-Z). Data expressed as mean ± SD, n=3.

Formulation	Size (nm)[a]	PDI (nm)	Zeta potential (mV)	Quercetin loading (µg/mg NP)[b]	E.E. (%)[c]
NP-Z	254 ± 2	0.07 ± 0.01	-46.0 ± 1.5	-	-
HPCD-NP-Z	222 ± 1	0.11 ± 0.02	-51.6 ± 0.5	**-**	**-**
Que-NP-Z	358 ± 7	0.21 ± 0.01	-45.2 ± 2.1	62.4 ± 1.2	74.4 ± 2.9
Que-HPCD-NP-Z	294 ± 1	0.25 ± 0.01	-43.8 ± 4.1	68.7 ± 1.1	80.7 ± 2.8

[a]Determination of volumen mean diameter by photon correlation spectroscopy.
[b] Determination of quercetin content by HPLC-UV.
[c] Encapsulation Efficiency.

Figure 2 shows the morphology and shape of quercetin-loaded nanoparticles. The microphotographs show homogeneous populations of spherical nanoparticles with an apparent size similar to that calculated by photon correlation spectroscopy (Table 1). Interestingly, the use of HP-β-CD affected neither the shape nor the surface aspect of the resulting nanoparticles.

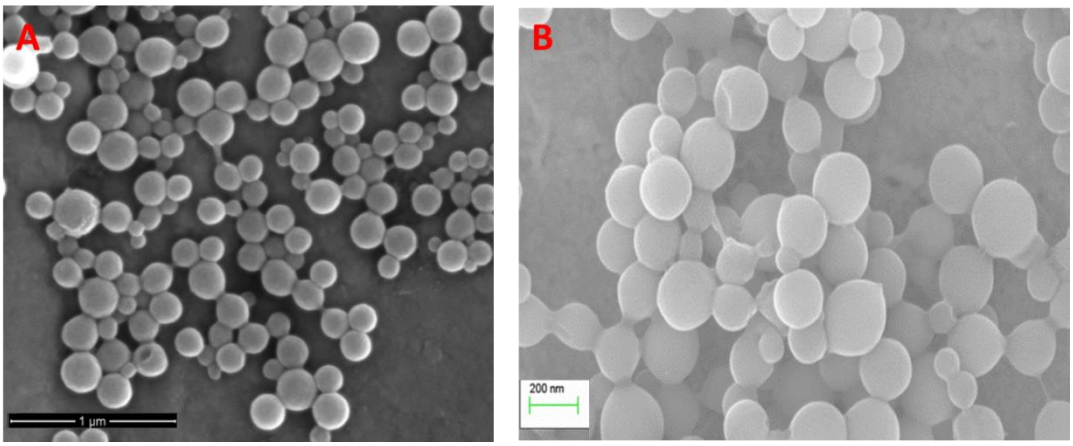

Figure 2. Scanning electron microscopy (SEM) of: quercetin-loaded zein nanoparticles (Que-NP-Z) (A) and quercetin-hydroxypropil-β-cyclodextrin-loaded in zein nanoparticles (Que-HPCD-NP-Z) (B).

3.2 In vitro release profile

The release profile of quercetin from zein nanoparticles was evaluated in simulated gastric and intestinal fluids (Figure 3). When nanoparticles were dispersed in simulated gastric fluid, quercetin was released following a zero order kinetic (Table 3). In 2 hours, around 15% of the loaded quercetin was released in both kinds of nanoparticles. When nanoparticles were moved to SIF, again, a similar release profile of quercetin from both kinds of nanoparticle formulations was observed. Nevertheless, after 3 h in SIF, quercetin appears to be released more rapidly from nanoparticles prepared in the absence of HP-β-CD than from those prepared with the oligosaccharide. Thus, at the end of the experiment, more than 80% of the quercetin loaded in Que-NP-Z was released, whereas only 70% of the flavonoid payload from Que-HPCD-NP-Z.

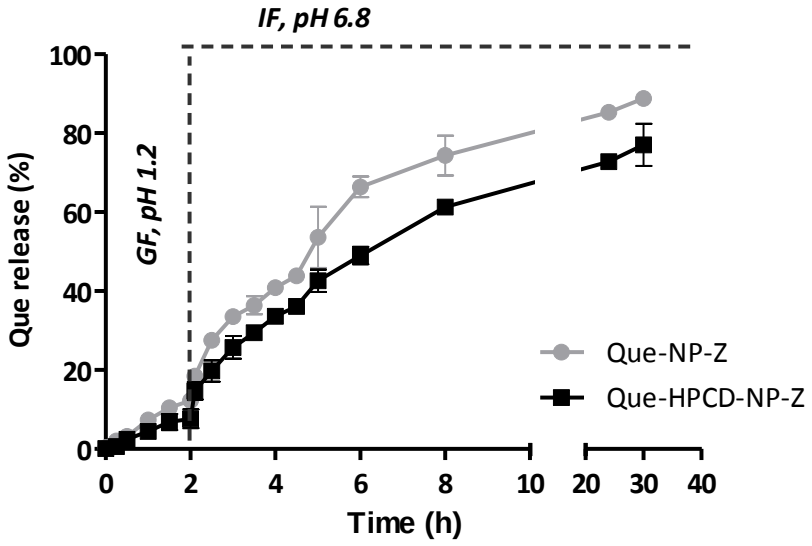

Figure 3.In vitro release studies of quercetin loaded in nanoparticles. Que-NP-Z: quercetin-loaded zein nanoparticles (●); Que-HPCD-NP-Z: quercetin-loaded zein nanoparticles containing HP-β-CD (▪). Data represented as mean ± SD, (n=3).

In order to confirm the zero-order release rate of quercetin from zein nanoparticles, equation [4] was applied. Table 2 summarises the release constants and the regression coefficients (R^2). Interestingly, for both types of zein nanoparticle formulations, the release constants of quercetin were about two-fold higher in SIF than in SGF. In addition, irrespective of the release medium, the release constants were slightly lower when quercetin was released from nanoparticles prepared with HP-β-CD.

Table 2.Analysis of the quercetin release from zein nanoparticles when incubated in simulated gastric and intestinal fluids.

	SGF		SIF	
	K_{zo}(h^{-1})	R^2	K_{zo} (h^{-1})	R^2
Que-NP-Z	0.06±0.01	0.99	0.11±0.01	0.95
Que-HPCD-NP-Z	0.04±0.01	0.97	0.09±0.01	0.99

3.3 In vivo pharmacokinetic

The plasma concentration profile of quercetin, after a single intravenous administration at 25 μg/kg formulated as solution in a mixture of PEG400 and water (6:4 by vol.), is shown in Figure 4. Under these conditions, the quercetin plasma concentration decreased rapidly, not being detectable 8 hours after its administration. The data were adjusted by non-compartmental model. The peak plasma concentration (C_{max}) of quercetin was around 175 μg/mL. The mean values for obtained for AUC and half-life ($t_{1/2}$) were 167 μg h ml^{-1} and 0.6 hours, respectively. The mean residence time (MRT) was 1.6 hours, whereas the quercetin clearance and its distribution volume were calculated to be 30 mL/h and 26 mL respectively (Table 3).

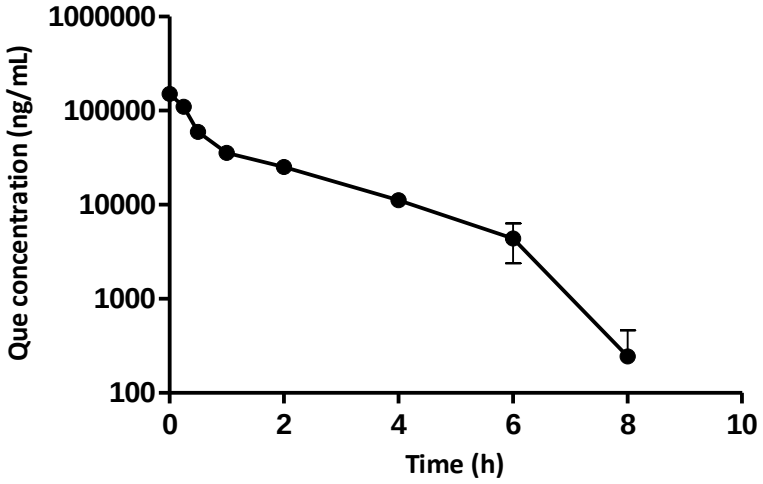

Figure 4.Pharmacokinetics of quercetin in rat when administered by the intravenous route. Animals received a single dose of 25 μg/Kg of the flavonoid formulated in a solution of PEG400 and water. Data expressed as mean ± SD. N=6 per time point.

Figure 5 shows the plasma concentration profiles of quercetin after a single oral dose of 25 mg/kg to rats when formulated as solution, suspension or encapsulated in nanoparticles. The aqueous suspension of quercetin offered low levels of the flavonoid in plasma. In addition, 4 hours post-administration, the quercetin plasma levels were below the quantification limit of the HPLC technique. For the oral solution of quercetin, the plasma levels of this flavonoid were higher than for the suspension. Thus, quercetin levels increased rapidly during the first 1 hour post administration, when C_{max} was reached. Then, the amount of quercetin in plasma decreased slowly during the following hours. Interestingly, when quercetin was loaded into zein nanoparticles, the plasma levels of the flavonoid in rats were significantly higher and more prolonged in time than for conventional formulations (solution and suspension). In addition, the presence of HP-β-CD provided high quercetin concentrations in plasma for a more prolonged time. Thus, for Que-HPCD-NP-Z, the quercetin levels were observed up to 72 hours post-administration. For zein nanoparticles prepared in the absence of HP-β-CD, the quercetin levels were also quantifiable during the first 48 h post-administration.

Table 3 summarizes the pharmacokinetic parameters obtained after the analysis of the experimental data. The peak plasma concentration (C_{max}) of quercetin in nanoparticles was

around 2.5-times higher than when formulated in the PEG400/water solution. Moreover, the clearance of quercetin was similar in all cases, independently of the formulation tested or the route of administration. On the contrary, the half-life and volume of distribution of the flavonoid in plasma were significantly higher when encapsulated in nanoparticles than when formulated in conventional dosage forms. Finally, the relative oral bioavailability of quercetin when incorporated in zein nanoparticles ranged from 35% to 57%. However, for the aqueous solution, the oral bioavailability of the flavonoid was only of 4%.

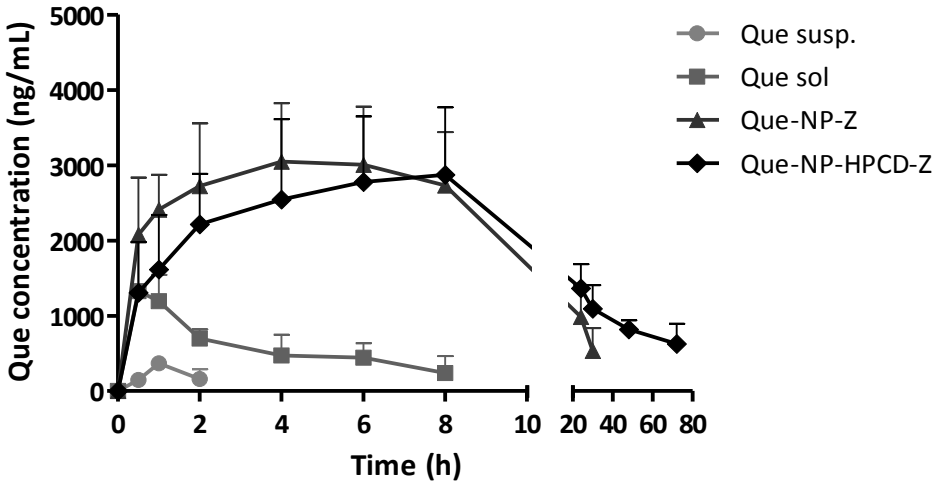

Figure 5.Quercetin plasma concentration *vs.* time after the oral administration of the different formulations at dose of 25 mg/kg.i) quercetin suspension (Que-Susp, ●), ii) quercetin solution (Que-Sol, ■), iii) quercetin loaded in zein nanoparticles (Que-NP-C, ▲) and iv) quercetin loaded in zein nanoparticles in the presence of HP-β-CD (Que-HPCD-NP-Z ♦). Data expressed as mean ± SD (n=6).

Table 3. Pharmacokinetic parameters of quercetin obtained after the administration of the different formulations tested at a dose of 25 mg/kg to Wistar male rats. i) quercetin intravenous (Que-IV) ii) quercetin solution (Que-Sol), iii) quercetin suspension (Que-susp) iv) quercetin loaded in zein nanoparticles (Que-NP-Z) and v) quercetin loaded in zein nanoparticles in the presence of HP-β-CD (Que-HPCD-NP-Z). Data expressed as mean ± SD; (n=6).

	Tmax (h)	Cmax (µg/mL)	t 1/2 (h)	AUC (µg h/mL)	Vz (mL)	Cl (mL/h)	MRT (h)	F (%)
Que-IV	0.00±0.00	175.87±13.39	0.60±0.35	166.74±8.21	26.28±16.13	30.17±1.35	1.57±0.12	100.00
Que-Susp	1.00±0.00	0.37±0.08	0.54±0.49†	0.55±0.25†	29.08±24.50†	45.33±18.97	1.22±0.35†	0.33
Que-Sol (PEG 400-H_2O)	0.60±0.22	1.40±0.41	3.51±1.97	6.77±2.20	146.20±78.91	29.19±0.91	4.86±0.55	4.10
Que-NP-Z	5.00±2.76	3.57±0.52†	5.40±3.97	60.54±10.42†	211.86±137.54	28.54±2.31	12.18±2.78†	34.59
Que-HPCD-NP-Z	5.50±2.66	3.38±0.59†	24.63±8.41†**	94.51±18.71†*	837.00±158.60†**	24.42±3.55	25.37±2.99†**	57.00

C_{max}: peak plasma concentration; T_{max}: time to reach plasma concentration; AUC: Area under the curve; t ½: half life of the terminal phase; Cl: Clearance; MRT: mean residence time Fr: relative oral bioavailability

† Significant differences *vs*Que-Sol ($p<0.01$) Mann-Whitney-U

*Significant differences *vs* Que-NP-Z ($p<0.05$) Mann-Whitney-U

** Significant differences *vs* Que-NP-Z ($p<0.01$) Mann-Whitney-U

3.4 Anti-inflammatoryefficacystudy

We investigated the effect of quercetin (25 mg/kg) in the prevention of an endotoxic shock induced in C57BL/6J mice by the intraperitoneal injection of 40 µg LPS. Rectal temperature of mice was measured during 24 h after challenge (Figure 6). Before challenge, the rectal temperature of animals was the same in all the groups. However, 6 hours after challenge, important differences were observed between groups. Thus, for positive controls (animals without quercetin pre-treatment) suffered an important decrease of their rectal temperature (around 4°C). For animals pre-treated with the quercetin solution in PEG400 and water, a 3°C decreased in rectal temperature was measured. Finally, rectal temperature of animals treated with quercetin loaded in zein nanoparticles (Que-HPCD-NP-Z) decreased only 0.5-1°C. Twenty four hours after challenge, all the animals regained their normal temperature.

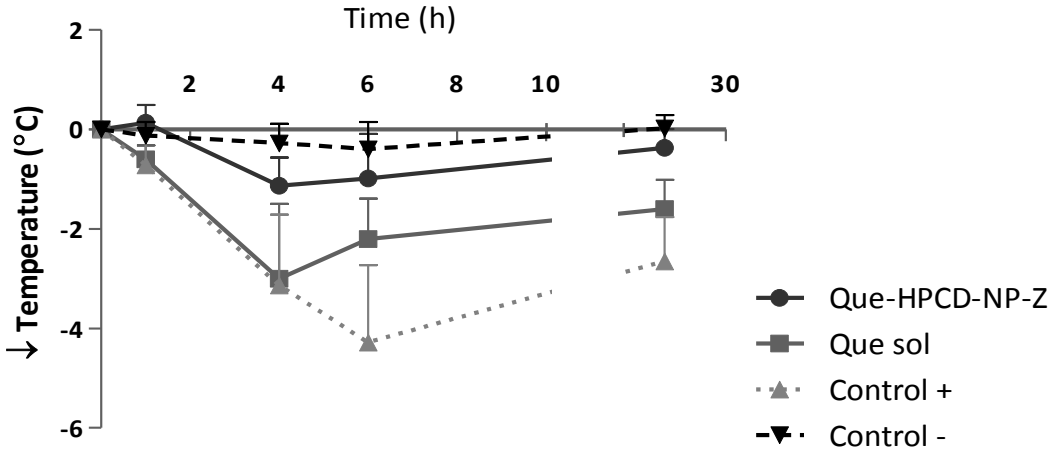

Figure 6: Evolution of the body temperature of mice after i.p. administration of LPS (40 µg). Mice were pre-treated orally daily for one week with: (i) quercetin loaded in zein2-hydroxypropil-β-cyclodextrin nanoparticles (Que-HPCD-NP-Z), at dose of 25mg/kg, one administration each 2 days or (ii) with a quercetin solution in PEG400/water (Que-sol), at 25 mg/kg, daily for seven days. Control (+) includes the group of animals challenged with LPS but that did not received quercetin. Control (–) represents animals that were neither challenged nor pre-treated with a quercetin formulation. Results expressed as mean ± SD (n=6).

Table 4 shows the overall symptoms score of mice after the ip administration of LPS. Animals of the positive control group displayed a low mobility and signs of bristly hair and respiratory distress. In addition, all of these animals displayed a decrease in their basal temperature higher than 2°C. On the other hand, animals treated with quercetin-loaded zein nanoparticles displayed an almost normal behavior and an evident better symptomatology than those animals receiving resveratrol as oral solution, which displayed important difficulties to move.

Table 4. Endotoxic symptoms in mice after the intraperitoneal administration of LPS. Control -: No treated, no LPS. Control +: No treated, LPS. Que-Sol: administration of quercetin solution daily during 7 days (25 mg/Kg per dose), LPS. Que-HPCD-NP-Z: administration of quercetin-loaded zein nanoparticles in the presence of HP-β-CD every two days during 7 days (25 mg/Kg), LPS. (n=6).

Treatment	Number of animals with Tªdecreased >2°C	Piloerection	Mobility
Control -	0/6	-	-
Control +	6/6	+++	+++
Que-Sol	3/6	++	++
Que-HPCD-NP-Z	0/6	+	+

Severity of the symptoms: (-) None; (+) weak; (++) moderate; (+++) strong.

Figure 7 summarizes the serum levels of TNF-α before and 90 min after LPS i.p. administration. Before the challenge, all the animals displayed no significant levels of the cytokine. On the contrary, after the ip administration of LPS, the serum levels of TNF-α increased dramatically. Likely, animals orally treated with quercetin encapsulated in zein nanoparticles (Que-HPCD-NP-Z) displayed significantly lower levels of the cytokine than those treated daily with the oral solution of the flavonoid ($p<0.05$). Significant differences ($p<0.01$) were observed between control positive and animals treated with Que-HPCD-NP-Z.

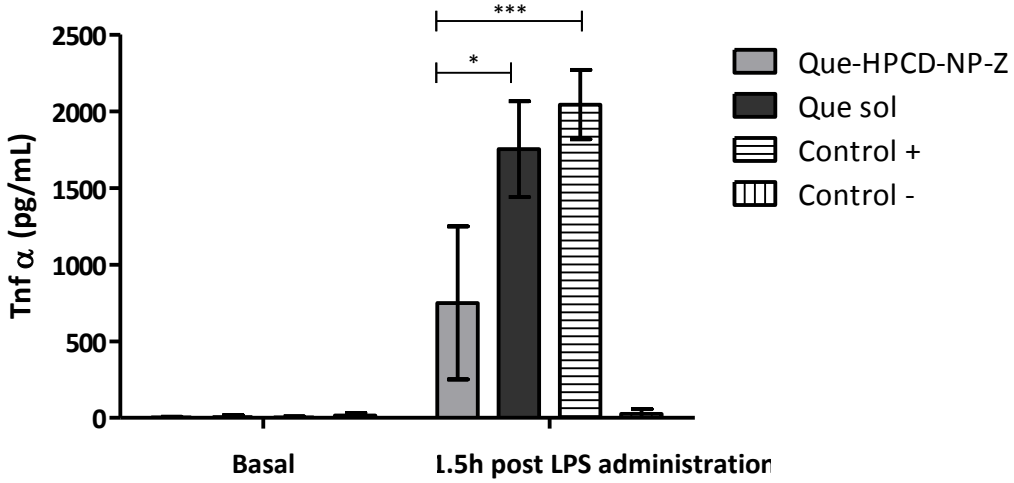

Figure 7. TNF-α serum levels after LPS intraperitoneal administration (40 µg) in untreated or treated with quercetinC57BL/6J mice. Before challenge, mice received either a quercetin solution (Que-sol; 25 mg/kg, 1 daily dose during 7 days) or quercetin loaded nanoparticles (Que-HPCD-NP-Z; 25 mg/Kg, 1 dose every two days during 7 days). Not-pretreated (control +) and negative controls were also included. Data expressed as mean ± SD, (n=6). *$p<0.05$ and ***$p<0.01$ Kruskal Wallis test.

4. Discussion

Quercetin is a flavonoid that has been reported to offer protection against a variety of chronic diseases such as inflammation, obesity, infections, cancer and cardiovascular diseases [8,14,16,38-41]. However its use as preventive agent is hampered by its poor water solubility, chemical instability and a low bioavailability. In this work, we evaluated the capability of zein nanoparticles to promote the oral bioavailability of quercetin and, thus, improve its efficacy in a model of inflammation induced by the administration of LPS in mice.

Zein nanoparticles were prepared by desolvation after the incubation of the protein with quercetin in the presence of HP-β-CD. This cyclodextrin was selected in order to promote the encapsulation of the lipophilic compounds in the core of nanoparticles as well as to inhibit the reported presystemic metabolism of the flavonoid[42,43]. After reconstitution of the dry powder obtained in the Spray-drier apparatus, quercetin-loaded nanoparticles displayed a spherical shape (Figure 2) with a size close to 300 nm and a negative surface charge of about -44 mV (Table 1). The payload was calculated to be around 69 µgquercetin per mg nanoparticle. Interestingly, the presence of HP-β-CD during the encapsulation and formation of zein nanoparticles decreased the mean size with a parallel significant increase ($p<0.05$) of the quercetin loading of the resulting carriers (Table 1). The capability of zein nanoparticles to load quercetin was found to be similar than the reported value for poly(ethylene glycol)-β-oligo(ε-caprolactone) micelles but lower than for self-nanoemulsifying drug delivery systems [44] or solid lipid nanoparticles [27].

On the other hand, it is noteworthy that quercetin was released from zein nanoparticles following a zero-order kinetic (Figure 3, Table 2). Surprisingly, the release rate of quercetin from zein nanoparticles decreased when the nanocarriers were prepared in the presence of HP-β-CD, which is well known excipient for its solubilizing properties. The only plausible explanation would be that the presence of the oligosaccharide would confer a higher stability to the resulting nanocarriers, decreasing the permeability of the nanoparticle matrix to the diffusion of aqueous media. This hypothesis would be in line with the finding that cyclodextrins may be used to cross-link nanofibers [45]. Thus, the addition of cyclodextrins in the zein nanofibers would increasetheirTgvalues,whichhas been related with a decrease in the zein chain mobility due to the presence of the oligosaccharide [46].

On the other hand, the release rate of quercetin was about 2-times higher under simulated intestinal conditions than in simulated gastric fluid. This fact would be due to the ionization of glutamic residues under neutral pH conditions [47], that would increase the permeability of the zein nanoparticles and, thus, the release rate of quercetin.

The oral administration of quercetin after its encapsulation into the zein nanoparticles offered prolonged and sustained plasma levels of the flavonoid for at least 30 hours (Figure 5). As a consequence, these nanoparticles offered higher quercetin plasma levels than those found with the administration of conventional formulations of the flavonoid (e.g. the oral solution and the suspension). Comparing with the oral solution, Que-HPCD-NP-Z improved 14-times the oral bioavailability of the flavonoid (Table 3). This finding would be directly related with the combined effect of the mucoadhesive properties of zein[48,49] and the inhibitory effect of HP-β-CD in the activity of both the intestinal efflux pumps [50] and the cytochrome P450 [51].

The capability of the developed nanoparticles to promote the oral bioavailability of quercetin appears to be in line with a nanoemulsion of the flavonoid, described by Sun and co-workers[52]. The oral administration of a single dose of 50 mg/kg quercetin formulated in the nanoemulsion yielded to an AUC 15 times higher than that observed for a suspension of the flavonoid used as control [52].

In the same way, similar bioavailability results have been described by the use of quercetin: caffeinecocrystals[53]. In this case, the cocrystals would offer a relative oral bioavailability of quercetin of about 9-fold compared with the control oral solution.

Bacterial LPS, as a constituent of the cell wall of Gram-negative bacteria, is a major causative agent of septic shock. LPS triggers the secretion of a variety of inflammatory products, such as tumor necrosis factor-α(TNF-α), interleukin-6, as well as excessive amounts of nitric oxide (NO) [54]. All of this contributes to the pathophysiology of septic shock including the tissue damage that precedes multiple organ dysfunctions [55]. It is interesting to highlight that, to date, it is very difficult to identify effective therapies for the Gram-negative shock syndrome [56]. TNF-α would play a central role in the effect induced by LPS as suggested by the neutralizing effect induced by the administration of antibodies against TNF-α[57,58].

In our case, as expected, animals challenged intraperitoneally with LPS displayed a sharp and fast increase of their TNF-α serum levels (Figure 7). The untreated animals (positive control group) showed the highest levels of the cytokine. On the contrary, animals treated with quercetin-loaded nanoparticles (Que-HPCD-NP-Z) presented TNF-α levels significantly lower than observed for the controls ($p<0.05$) or quantified in animals treated with the oral solution of the flavonoid. These findings correlated well with the evolution of the body temperature of animals (Figure 6) and their symptoms score (Table 4). Thus, animals treated with every 2 days with quercetin-loaded nanoparticles (25 mg/kg) presented endotoxic symptoms less severe than those observed for the other groups of animals. All of these results are in line with those reported very recently by Liao and Lin, who found that quercetin decreased the secretion of the pro-/antiinflammatory cytokine by peritoneal macrophages *ex vivo* in the presence of LPS. Interestingly, in the same work, the authors demonstrated that the main metabolite of quercetin, quercetin-3-glucuronide, was not effective [59]. In our work, we demonstrated that the encapsulation of quercetin in zein nanoparticles in the presence of HP-β-CD offer an important increase of its oral bioavailability and, thus, of its efficacy as antiinflammatory agent.

Conclusions

In summary, zein nanoparticles (in combination with HP-β-CD) appear to be adequate carriers for the oral delivery of quercetin. These carriers released the loaded flavonoid following a zero-order kinetic. In vivo, quercetin plasma levels provided by the oral administration of zein nanoparticles were high and sustained in time up to 48 h. Under these circumstances, the relative oral bioavailability of quercetin was calculated to be close to 60% in rat. In addition, the present study demonstrated that the developed quercetin-loaded nanoparticles attenuated the severity of LPS induced endotoxic shock in mice. In particular we demonstrated that quercetin (when encapsulated in the developed nanoparticles) significantly reduced the TNF-α levels and the symptomatology associated to the endotoxic shock.

Acknowledgements

This work was supported by the Regional Government of Navarra (Alimentos funcionales, Euroinnova call) and the Spanish Ministry of Science and Innovation and Gobierno de Navarra (ADICAP; ref. IPT-2011-1717-900000). Rebeca Penalvaacknowledgesthe “Asociación de Amigos Universidad de Navarra” forthefinancialsupport

References

[1] I. Erlund, Review of the flavonoids quercetin, hesperetin, and naringenin. Dietary sources, bioactivities, bioavailability, and epidemiology, Nutr. Res. 24 (2004) 851-874.

[2] A.B. Hendrich, Flavonoid-membrane interactions: possible consequences for biological effects of some polyphenolic compounds1, Acta Pharmacol. Sin. 27 (2006) 27-40.

[3] Agnes W. Boots, Review: Health effects of quercetin: From antioxidant to nutraceutical, Eur. J. Pharmacol. 585 (2008) 325.

[4] P. Hollman, M. Katan, Absorption, metabolism and health effects of dietary flavonoids in man, Biomedicine & Pharmacotherapy 51 (1997) 305-310.

[5] G.A. Naderi, S. Asgary, N. Sarraf-Zadegan, H. Shirvany, Anti-oxidant effect of flavonoids on the susceptibility of LDL oxidation, Mol. Cell. Biochem. 246 (2003) 193-196.

[6] A. Kumari, S.K. Yadav, Y.B. Pakade, B. Singh, S.C. Yadav, Development of biodegradable nanoparticles for delivery of quercetin, Colloids and Surfaces B: Biointerfaces 80 (2010) 184-192.

[7] C. Lin, Y. Leu, S.A. Al-Suwayeh, M. Ku, T. Hwang, J. Fang, Anti-inflammatory activity and percutaneous absorption of quercetin and its polymethoxylated compound and glycosides: The relationships to chemical structures, European Journal of Pharmaceutical Sciences 47 (2012) 857-864.

[8] H. Choi, J. Kim, C. Lee, Y. Ahn, J. Song, S. Baek, D. Kwon, Antiviral activity of quercetin 7-rhamnoside against porcine epidemic diarrhea virus, Antiviral Res. 81 (2009) 77-81.

[9] D.A. Pashevin, L.V. Tumanovska, V.E. Dosenko, V.S. Nagibin, V.L. Gurianova, A.A. Moibenko, Antiatherogenic effect of quercetin is mediated by proteasome inhibition in the aorta and circulating leukocytes, Pharmacological Reports 63 (2011) 1009-1018.

[10] H. Zhang, M. Zhang, L. Yu, Y. Zhao, N. He, X. Yang, Antitumor activities of quercetin and quercetin-5’,8-disulfonate in human colon and breast cancer cell lines, Food and Chemical Toxicology 50 (2012) 1589-1599.

[11] A. Annapurna, C.S. Reddy, R.B. Akondi, S.R. Rao, Cardioprotective actions of two bioflavonoids, quercetin and rutin, in experimental myocardial infarction in both normal and streptozotocin-induced type I diabetic rats, J. Pharm. Pharmacol. 61 (2009) 1365-1374.

[12] P.S. Brookes, S.B. Digerness, D.A. Parks, V. Darley-Usmar, Mitochondrial function in response to cardiac ischemia-reperfusion after oral treatment with quercetin, Free Radical Biology and Medicine 32 (2002) 1220-1228.

[13] S. Shen, Y. Chen, F. Hsu, W. Lee, Differential apoptosis-inducing effect of quercetin and its glycosides in human promyeloleukemic HL-60 cells by alternative activation of the caspase 3 cascade, J. Cell. Biochem. 89 (2003) 1044-1055.

[14] M. Comalada, D. Camuesco, S. Sierra, I. Ballester, J. Xaus, J. Gálvez, A. Zarzuelo, In vivo quercitrin anti-inflammatory effect involves release of quercetin, which inhibits inflammation through down-regulation of the NF-κB pathway, Eur. J. Immunol. 35 (2005) 584-592.

[15] P. Yu, Q. Zhou, W. Zhu, Y. Wu, L. Wu, X. Lin, M. Chen, B. Qiu, Effects of quercetin on LPS-induced disseminated intravascular coagulation (DIC) in rabbits, Thromb. Res. 131 (2013) e270-e273.

[16] R. Vidya Priyadarsini, R. Senthil Murugan, S. Maitreyi, K. Ramalingam, D. Karunagaran, S. Nagini, The flavonoid quercetin induces cell cycle arrest and mitochondria-mediated apoptosis in human cervical cancer (HeLa) cells through p53 induction and NF-κB inhibition, Eur. J. Pharmacol. 649 (2010) 84-91.

[17] C.S. Lee, E.B. Jeong, Y.J. Kim, M.S. Lee, S.J. Seo, K.H. Park, M.W. Lee, Quercetin-3-O-(2″-galloyl)-α-l-rhamnopyranoside inhibits TNF-α-activated NF-κB-induced inflammatory mediator production by suppressing ERK activation, Int. Immunopharmacol. 16 (2013) 481-487.

[18] T.L. Wadsworth, T.L. McDonald, D.R. Koop, Effects of Ginkgo biloba extract (EGb 761) and quercetin on lipopolysaccharide-induced signaling pathways involved in the release of tumor necrosis factor-α, Biochem. Pharmacol. 62 (2001) 963-974.

[19] G. Zdunić, D. Gođevac, M. Milenković, D. Vučićević, K. Šavikin, N. Menković, S. Petrović, Evaluation of Hypericum perforatum oil extracts for an antiinflammatory and gastroprotective activity in rats, Phytotherapy Research 23 (2009) 1559-1564.

[20] Ajazuddin, A. Alexander, A. Qureshi, L. Kumari, P. Vaishnav, M. Sharma, S. Saraf, S. Saraf, Role of herbal bioactives as a potential bioavailability enhancer for Active Pharmaceutical Ingredients, Fitoterapia 97 (2014) 1-14.

[21] M.N. Chabane, A.A. Ahmad, J. Peluso, C.D. Muller, G. Ubeaud-Séquier, Quercetin and naringenin transport across human intestinal Caco-2 cells, J. Pharm. Pharmacol. 61 (2009) 1473-1483.

[22] J. Choi, Y. Piao, K.W. Kang, Effects of quercetin on the bioavailability of doxorubicin in rats: role of CYP3A4 and P-gp inhibition by quercetin, Arch. Pharm. Res. 34 (2011) 607-613.

[23] A. Kumari, S.K. Yadav, Y.B. Pakade, B. Singh, S.C. Yadav, Development of biodegradable nanoparticles for delivery of quercetin, Colloids and Surfaces B: Biointerfaces 80 (2010) 184-192.

[24] H. Pool, D. Quintanar, J. de Dios Figueroa, J.E.H. Bechara, D.J. McClements, S. Mendoza, Polymeric nanoparticles as oral delivery systems for encapsulation and release of polyphenolic compounds: impact on quercetin antioxidant activity & bioaccessibility, Food Biophysics 7 (2012) 276-288.

[25] L. Gao, G. Liu, X. Wang, F. Liu, Y. Xu, J. Ma, Preparation of a chemically stable quercetin formulation using nanosuspension technology, Int. J. Pharm. 404 (2011) 231-237.

[26] S. Jain, A.K. Jain, M. Pohekar, K. Thanki, Novel self-emulsifying formulation of quercetin for improved in vivo antioxidant potential: Implications for drug-induced cardiotoxicity and nephrotoxicity, Free Radical Biology and Medicine 65 (2013) 117-130.

[27] H. Li, X. Zhao, Y. Ma, G. Zhai, L. Li, H. Lou, Enhancement of gastrointestinal absorption of quercetin by solid lipid nanoparticles, J. Controlled Release 133 (2009) 238-244.

[28] S. Scalia, M. Mezzena, Incorporation of quercetin in lipid microparticles: Effect on photo-and chemical-stability, J. Pharm. Biomed. Anal. 49 (2009) 90-94.

[29] S. Scalia, M. Haghi, V. Losi, V. Trotta, P.M. Young, D. Traini, Quercetin solid lipid microparticles: A flavonoid for inhalation lung delivery, European Journal of Pharmaceutical Sciences 49 (2013) 278-285.

[30] R. Shukla, M. Cheryan, Zein: the industrial protein from corn, Industrial Crops and Products 13 (2001) 171-192.

[31] A. Pomes, Zein, Encyclopedia of Polymer Science and Technology 15 (1971) 125-132.

[32] G.W. Padua, Q. Wang, Controlled self-organization of zein nanostructures for encapsulation of food ingredients, Micro/Nanoencapsulation of Active Food Ingredients 1007 (2009) 143-155.

[33] M. Ishikawa, H. Yoshii, T. Furuta, Interaction of modified cyclodextrins with cytochrome P-450, Biosci. Biotechnol. Biochem. 69 (2005) 246-248.

[34] P. Calleja, J. Huarte, M. Agüeros, L. Ruiz-Gatón, S. Espuelas, J.M. Irache, Molecular buckets: cyclodextrins for oral cancer therapy, Therapeutic Delivery 3 (2012) 43-57.

[35] M. Agüeros, I. Esparza, C. Gonzalez-Ferrero, C.J. Gonzalez-Navarro, J.M. Irache, A. Romo, Nanoparticles for encapsulation of compounds, the production and uses thereof. (2012).

[36] P. Iacopini, M. Baldi, P. Storchi, L. Sebastiani, Catechin, epicatechin, quercetin, rutin and resveratrol in red grape: Content,< i> in vitro antioxidant activity and interactions, Journal of Food Composition and Analysis 21 (2008) 589-598.

[37] P. Costa, J.M. Sousa Lobo, Modeling and comparison of dissolution profiles, European Journal of Pharmaceutical Sciences 13 (2001) 123-133.

[38] F. Dajas, Life or death: neuroprotective and anticancer effects of quercetin, J. Ethnopharmacol. 143 (2012) 383-396.

[39] S. Egert, A. Bosy-Westphal, J. Seiberl, C. Kürbitz, U. Settler, S. Plachta-Danielzik, A.E. Wagner, J. Frank, J. Schrezenmeir, G. Rimbach, Quercetin reduces systolic blood pressure and plasma oxidised low-density lipoprotein concentrations in overweight subjects with a high-cardiovascular disease risk phenotype: a double-blinded, placebo-controlled cross-over study, Br. J. Nutr. 102 (2009) 1065-1074.

[40] A. Perez, S. Gonzalez-Manzano, R. Jimenez, R. Perez-Abud, J.M. Haro, A. Osuna, C. Santos-Buelga, J. Duarte, F. Perez-Vizcaino, The flavonoid quercetin induces acute vasodilator effects in healthy volunteers: Correlation with beta-glucuronidase activity, Pharmacological Research 89 (2014) 11-18.

[41] F. Wang, Y. Yang, Quercetin suppresses insulin receptor signaling through inhibition of the insulin ligand–receptor binding and therefore impairs cancer cell proliferation, Biochem. Biophys. Res. Commun. 452 (2014) 1028-1033.

[42] M. Agüeros, V. Zabaleta, S. Espuelas, M.A. Campanero, J.M. Irache, Increased oral bioavailability of paclitaxel by its encapsulation through complex formation with cyclodextrins in poly(anhydride) nanoparticles, J. Controlled Release 145 (2010) 2-8.

[43] J. Calvo, J.L. Lavandera, M. Agüeros, J.M. Irache, Cyclodextrin/poly (anhydride) nanoparticles as drug carriers for the oral delivery of atovaquone, Biomed. Microdevices 13 (2011) 1015-1025.

[44] W. Li, S. Yi, Z. Wang, S. Chen, S. Xin, J. Xie, C. Zhao, Self-nanoemulsifying drug delivery system of persimmon leaf extract: optimization and bioavailability studies, Int. J. Pharm. 420 (2011) 161-171.

[45] L. Li, Y. Hsieh, Ultra-fine polyelectrolyte fibers from electrospinning of poly (acrylic acid), Polymer 46 (2005) 5133-5139.

[46] F. Kayaci, T. Uyar, Electrospun zein nanofibers incorporating cyclodextrins, Carbohydr. Polym. 90 (2012) 558-568.

[47] B. Zhang, Y. Luo, Q. Wang, Effect of acid and base treatments on structural, rheological, and antioxidant properties of α-zein, Food Chem. 124 (2011) 210-220.

[48] R. Paliwal, S. Palakurthi, Zein in controlled drug delivery and tissue engineering, J. Controlled Release 189 (2014) 108-122.

[49] Y. Han, Q. Xu, Z. Lu, J. Wang, Cell adhesion on zein films under shear stress field, Colloids and Surfaces B: Biointerfaces 111 (2013) 479-485.

[50] Y. Zhang, F. Meng, Y. Cui, Y. Song, Enhancing Effect of Hydroxypropyl-β-cyclodextrin on the Intestinal Absorption Process of Genipin, J. Agric. Food Chem. 59 (2011) 10919-10926.

[51] M. Ishikawa, H. Yoshii, T. Furuta, Interaction of modified cyclodextrins with cytochrome P-450, Biosci. Biotechnol. Biochem. 69 (2005) 246-248.

[52] M. Sun, Y. Gao, Y. Pei, C. Guo, H. Li, F. Cao, A. Yu, G. Zhai, Development of nanosuspension formulation for oral delivery of quercetin, Journal of Biomedical Nanotechnology 6 (2010) 325-332.

[53] A.J. Smith, P. Kavuru, L. Wojtas, M.J. Zaworotko, R.D. Shytle, Cocrystals of quercetin with improved solubility and oral bioavailability, Molecular Pharmaceutics 8 (2011) 1867-1876.

[54] L. Shapira, W.A. Soskolne, Y. Houri, V. Barak, A. Halabi, A. Stabholz, Protection against endotoxic shock and lipopolysaccharide-induced local inflammation by tetracycline: correlation with inhibition of cytokine secretion, Infect. Immun. 64 (1996) 825-828.

[55] E.A. Deitch, Multiple organ failure. Pathophysiology and potential future therapy, Ann. Surg. 216 (1992) 117-134.

[56] Y. Ren, Y. Xie, G. Jiang, J. Fan, J. Yeung, W. Li, P.K. Tam, J. Savill, Apoptotic cells protect mice against lipopolysaccharide-induced shock, J. Immunol. 180 (2008) 4978-4985.

[57] K.J. Tracey, Y. Fong, D.G. Hesse, K.R. Manogue, A.T. Lee, G.C. Kuo, S.F. Lowry, A. Cerami, Anti-cachectin/TNF monoclonal antibodies prevent septic shock during lethal bacteraemia, Nature 330 (1987) 662-664.

[58] F. Tsuji, K. Oki, A. Okahara, H. Suhara, T. Yamanouchi, M. Sasano, S. Mita, M. Horiuchi, DIFFERENTIAL EFFECTS BETWEEN MARIMASTAT, A TNF-α CONVERTING ENZYME INHIBITOR, AND ANTI-TNF-α ANTIBODY ON MURINE MODELS FOR SEPSIS AND ARTHRITIS, Cytokine 17 (2002) 294-300.

[59] Y. Liao, J. Lin, Quercetin, but Not Its Metabolite Quercetin-3-glucuronide, Exerts Prophylactic Immunostimulatory Activity and Therapeutic Antiinflammatory Effects on Lipopolysaccharide-Treated Mouse Peritoneal Macrophages Ex Vivo, J. Agric. Food Chem. 62 (2014) 2872-2880.

Chapter 9

General discussion

Discusión

El presente trabajo se ha centrado en el desarrollo de nuevas formulaciones a base de nanopartículas preparadas a partir de polímeros de origen natural capaces de vehiculizar distintos tipos de moléculas activas e incrementar significativamente su biodisponibilidad oral y eficacia, empleando para ello métodos sencillos de preparación, fácilmente escalables y aplicables en el ámbito farmacéutico y nutracéutico. Para ello, se han utilizado dos tipos de proteínas (caseína y zeína) como polímeros para la obtención de nanopartículas, en combinación con un aminoácido (lisina), para la encapsulación de tres tipos de activos diferentes: ácido fólico, quercetina y resveratrol.

¿Por qué caseína y zeína?

La mayor parte de los sistemas particulares diseñados para el sector alimentario o nutracéutico se basa en el empleo de carbohidratos mediante secado por spray dryer[1], técnicas de gelificación iónica [2] y coacervación por cambio de pH [3]. Las partículas obtenidas mediante spray dryer presentan tamaños elevados (micropartículas) y poseen características hidrosolubles, por lo que no son capaces de retener los activos en medios acuosos [4]. Por otra parte, los sistemas obtenidos mediante gelificaciones iónicas son de aplicación limitada, ya que dan lugar a la obtención de partículas de tamaños elevados (micro y milipartículas) [3] y el incremento de biodisponibilidad oral no es una de las ventajas más significativas que aportan [5]. El caso del quitosano podría considerarse excepcional ya que este polímero permite obtener partículas de diversas características, con elevado potencial para incrementar la biodisponibilidad oral de diferentes tipos de moléculas [6,7]. Sin embargo, los métodos de preparación son complejos y poco reproducibles, lo que dificultaría su aplicación o escalado a nivel industrial [8].

Por otra parte, el empleo de lípidos en el desarrollo de sistemas particulares requiere el empleo de técnicas de emulsificación y métodos complejos de cara a su escalado a nivel industrial [2].

Sin embargo, el empleo de proteínas de distintas características para el diseño de nanopartículas es todavía incipiente y presenta un elevado potencial para obtener, mediante métodos sencillos, nanopartículas de diferentes características fisicoquímicas[9-11].

Por este motivo, en el presente trabajo se han escogido dos tipos diferentes de proteínas. Una de ellas de origen animal (caseína) y la otra de origen vegetal (zeína). Se trata de proteínas de fácil acceso en el mercado, purificadas y a precios bajos, lo que garantizaría la disponibilidad de materia prima de cara a su producción a nivel industrial. Las características fisicoquímicas de ambas proteínas son diferentes, lo que dará lugar a la obtención de nanopartículas con distintas propiedades, permitiendo incrementar el espectro de aplicación:

En el caso de la caseína, se trata de un polímero hidrosoluble capaz de formar micelas de forma natural en la leche, lo que la convierte en un vehículo seguro. Además, posee unas características estructurales y propiedades físico-químicas muy adecuadas para la obtención

de “drugdeliverysystems”, como son: propiedades emulsificantes, estabilizante superficial, complejante de metales y pequeñas moléculas, etc. Asimismo, son reconocidas sus propiedades como sistemas de liberación controlada, capaces de incrementar labiodsisponibilidad de activos encapsulados [12]. Es importante destacar que no requiere el empleo de agentes reticulantes que podrían encarecer los procesos productivos y/o generar problemas de toxicidad en el producto final [12,13]. En el caso de la zeína, es una proteína liposoluble con características formadoras de films y fibras[14], empleada el sector farmacéutico como agente de recubrimiento [15] y también en el sector alimentario para la elaboración de recubrimientos comestibles. Dadas sus propiedades gastro-resistentes y mucoadhesivas, es muy apropiada para la liberación de compuestos en medio intestinal [16]. Además, no requiere la utilización de agentes reticulantes que podrían dificultar los procesos productivos y/o generar problemas de toxicidad en el producto final. Su empleo en el ámbito de la nanotecnología es todavía incipiente, pero hasta el momento ha demostrado un elevado potencial para la vehiculización de sustancias activas [17,18].

Por todo ello, se considera que el empleo de estos polímeros, solos o en combinación, es una estrategia adecuada para el diseño de nanopartículas poliméricas capaces de incrementar la biodisponibilidad oral de moléculas activas.

¿Cuál es el papel de la lisina en estas nanopartículas?

A lo largo del presente trabajo se ha demostrado que el empleo de lisina (aminoácido básico) para la preparación de nanopartículas tanto de caseína como de zeína aporta ventajas fundamentales:

En primer lugar, las interacciones electrostáticas que tienen lugar entre el aminoácido y los grupos carboxilo de las proteínas dan lugar a la obtención de cargas superficiales negativas en ambos tipos de nanopartículas, lo cual evita su agregación [19,20]. De hecho, la ausencia de la lisina, daría lugar a la obtención de sistemas con cargas superficiales neutras favoreciendo la agregación de las partículas [18,21]. Así, el aminoácido permite incrementar la estabilidad de los sistemas en suspensión acuosa y favorece su resuspensión una vez secos [22].

Del mismo modo, en ausencia de lisina, el proceso de secado mediante spray drier incrementaría considerablemente el tamaño de partícula debido al mismo fenómeno de agregación entre partículas. Todo ello dificultaría la introducción de este tipo de sistemasen el mercado, ya que el método de obtención no sería reproducible ni escalable.

Los métodos de fabricación empleados, ¿son los adecuados para su escalado a nivel industrial?

Los métodos de preparación diseñados para el presente trabajo fueron: coacervación (caseína)ódesolvatación (zeinas), ambos acompañados de un proceso adicional de purificación y secado mediante spray drier. Teniendo en cuenta que los dos primeros procesos (coacervación y desolvatación) son sencillos y escalables y que la purificación por ultrafiltración

y el secado por pulverización están implementados en diferentes sectores (farmacéutico, cosmético y alimentario), la elección de estas tecnologías para la preparación de nanopartículas puede ser considerada adecuada.

En general, estos métodos de fabricación de nanopartículas de caseína y de zeína se caracterizan por su sencillez tanto en el desarrollo y el equipamiento utilizado como en su bajo coste.

¿Cómo actúan estos sistemas en el organismo?

Tanto las nanopartículas de caseína (NP-C) como las de zeína(NP-Z) se caracterizan por su carácter gastroresistente, lo que las convierte en sistemas adecuados de liberación de activos a nivel intestinal [12,16].

Los estudios de biodistribución*ex vivo* con lumogen encapsulado y nanopartículas marcadas con radiofármacos (NOTA y Iodo) (Capítulo 2, figuras 3 y 4; Capítulo 4, figuras 3 y 4) permitieron confirmar que las nanopartículas alcanzan el intestino, donde permanecen alrededor de 24 horas. Adicionalmente se comprobó, mediante técnicas microscópicas, que las partículas poseen propiedades mucopenetrantes (NP caseínas) [12] o mucoadhesivas (NP zeina) [25]. Esto permite que, una vez en el intestino, las nanopartículas favorezcan que el activo encapsulado alcance la superficie del enterocito, lo que facilita su absorción.

Además, estudios complementarios de liberación *in vitro* demostraron que las partículas evitan la liberación en medio gástrico protegiendo el activo hasta su llegada al medio intestinal, donde lo liberan siguiendo una cinética de orden 0, mediante distintos mecanismos: erosión (NP caseinas) y erosión+ difusión (NP zeinas).

Estos resultados permitieron concluir que los sistemas diseñados son seguros y favorecen el incremento de absorción del activo encapsulado.

¿Por qué Ácido fólico, resveratrol y quercetina?

La elección de estos activos se realizó en base al modelo de clasificación biofarmacéutica (BCS). El objetivo fundamental residía en la elección de biomoléculas de distinta clasificación para evaluar el potencial de estos sistemas diseñados en la encapsulación e incremento de biodisponibilidad oral en cada caso. Por ello se eligió un activo modelo hidrosoluble como es el ácido fólico, otro activo modelo liposoluble (BCS II:baja solubilidad en agua y alta permeabilidad), como es el resveratrol[26], y un tercer activo, también con características liposolubles (BCS IV:baja solubilidad en agua, baja permeabilidad gastrointestinal), la quercetina[27].

Dentro de cada clase, la elección de estos activos se realizó en base su potencial interés en los sectores farmacéutico, nutracéuticoy alimentario, con propiedades beneficiosas reconocidas para la salud:

El ácido fólico, es una vitamina esencial [28]. Su carencia está asociada a la presencia de anemia megaloblástica y enfermedades como Alzheimer, síndrome de Down, etc. No puede ser sintetizada por el organismo[29]. La biodisponibilidad de los folatos presentes en los alimentos es baja, y cuando se administra en forma de cápsulas o comprimidos, precipita en las condiciones ácidas del estómago, limitando así su absorción en el intestino delgado. Además, es altamente sensible al oxígeno, luz, calor y cambios de pH[30,31].

El resveratrol,es un flavonoide que exhibe numerosas actividades farmacológicas como: antioxidante [32], efectos protectores cardiovasculares[33], acción antiinflamatoria [34] o actividad anticancerígena [35]. **La quercetina,** es un flavonol con beneficiosas propiedades farmacológicas como cardioprotector[36], antiinflamatorio [37] y anticanceroso [38]. Ambos flavonoides poseen una corta vida media, alta labilidad y baja biodisponibilidad [39,40].

Por todo ello, se consideró que el empleo de la nanotecnología para la vehiculización de estos activos podría aportar grandes beneficios como evitar su degradación, favorecer su liberación en el intestino, incrementar su biodisponibilidad y potenciar su eficacia.

¿Qué resultados se han obtenido?

A lo largo de este trabajo se diseñaron 6 tipos diferentes de nanopartículas: nanopartículas de caseína (NP-C), nanopartículas de caseína tratadas con altas presiones (NP-C-P_3), nanopartículas de caseína combinadas con hidroxipropil-β-ciclodextrina (NP-HPCD-C), nanopartículas de zeína (NP-Z), nanopartículaszeína-caseína (NP-M) y nanopartículas de zeína combinadas conhidroxipropil-β-ciclodextrina (HPCD-Z).

En términos generales, las características fisicoquímicas de las nanopartículas de zeína (con y sin HP-β-CD) permitieron encapsular entre 1,2 y 3 veces más cantidad de activo por mg de nanopartículaque las nanopartículas de caseína con y sin HP-β-CD y altas presiones (2 veces más en caso de ácido fólico, 1,2 en el caso de resveratrol y 3 en el caso de quercetina). Del mismo modo, la carga superficial encontrada en las partículas de caseína fue negativa (entre -11 mV y -19 mV) siendo entre 3 y 4 veces superior a los valores encontrados para las partículas de zeína (entre -29 mV y -52 mV). Por su parte, las nanopartículas de zeína-caseina presentaron valores similares a los obtenidos para las nanopartículas de zeína. En todos los casos, los resultados de encapsulación obtenidos fueron similares o incluso superiores a los obtenidos por otros autores para estos activos con otros sistemas nanoparticulados[41-45].

Adicionalmente, en estudios de liberación *in* vitro (en medios gástrico e intestinal simulados) se encontró que todos los sistemas liberaron una cantidad de activo inferior al 20 % en medio gástrico simulado, llegando al 100% en medio intestinal. En el caso de ácido fólico (Capítulo 3, figura 2; Capítulo 6, figura 2) a la entrada de medio intestinal se encontró un efecto burst que dio lugar a una liberación de hasta un 80% del activo. Esto es debido a que, en condiciones intestinales, el ácido fólico se encuentra cargado negativamente y de la misma forma que los residuos glutámicos de la zeina[46] y la caseína (fosfoproteína con pI 4,6) [47]. Ello genera una repulsión entre cargas que da lugar a la rápida liberación del ácido fólico en el medio intestinal.

En el caso del resveratrol el perfil de liberación encontrado correspondió a una cinética de orden 0, mediada por un mecanismo de difusión en el caso de las nanopartículas de caseína (Capítulo 4; figura 2), y un mecanismo conjunto de erosión y difusión en el caso de nanopartículas de zeína y zeína-casina (Capítulo 7, figura 2-3).

En el caso de quercetina, todos los tipos de nanopartículas se comportaron del mismo modo dando lugar a un perfil de liberación de orden 0 mediado por un mecanismo de difusión (Capítulo 5, figura 3; Capítulo 8, figura 3).

Una vez concluidos los estudios de liberación *in vitro*, se realizaron ensayos de farmacociética oral *in vivo* en ratas wistar macho. Los resultados obtenidos para cada molécula fueron:

Ácido fólico: para estudios de farmacocinética, se administró la dosis de 1 mg/kg por vía oral. En todos los casos la biodisponibilidad oral relativa del activo encapsulado fue entre 1,5 (NP caseína: Capítulo 3, tabla 5) y 2 (NP zeína: Capítulo 6, tabla 3) veces superior a la encontrada para el activo administrado en su forma libre. Entre nanopartículas de caseína y zeína, estas últimas presentaron una biodisponibilidad relativa 1,3 veces superior a la de las caseínas.

Los resultados obtenidos permitieron comprobar que la aplicación de altas presiones en las nanopartículas de caseína no incidió en un incremento de la biodisponibilidad oral relativa. En vista de los resultados, y teniendo en cuenta que la aplicación de altas presiones dificulta y encarece el proceso productivo, este tipo de sistema fue descartado para posteriores estudios.

Resveratrol: para los estudios de farmacocinética se administró por vía oral una dosis de 15 mg/kg. En todos los casos la biodisponibilidad oral relativa del resveratrol incrementó entre 10 (NP caseína (Capítulo 4; tabla 3) y NP zeina-caseína (Capítulo 7; tabla 3)) y 19 veces (NP zeína) (Capítulo 7; tabla 3) respecto a su administración en solución acuosa, siendo las partículas de zeína las que presentaron los resultados de biodisponibilidad superiores

En términos generales, los niveles de biodisponibilidad oral relativa alcanzados con estos sistemas superaron los obtenidos por otros autores mediante el empleo de SNEDDS [42] o nanopartículas lipídicas [48] (biodisponibilidades orales relativas solamente entre 5 y 8 veces superiores a la de la solución oral de activo). En otros casos se obtuvieron resultados de biodisponibilidad oral de resveratrol similares a los alcanzados en el presente estudio, pero empleando polímeros de origen sintético como el PLGA. [49].

Quercetina: para los estudios de farmacocinética se administró una dosis de 25mg/kg. En todos los casos la biodisponibilidad oral de quercetina aumentó entre 3 (NP caseína: Capítulo 5, tabla 2) y 14 (NP zeina: Capítulo 8, tabla 3) veces respecto a la administración del flavonoide en solución acuosa. En todos los casos la biodisponibilidad relativa del activo administrado en la formulación de zeína fue 1,5 veces superior a la de las formulaciones de nanopartículas de caseína. Otros autores, tras la administración oral de quercetina encapsulada en nanopartículas lipídicas [50], co-cristales [51] o nanosuspensiones[52], lograron incrementos de biodisponibilidad del activo similares a los obtenidos en el presente estudio (entre 5 y 14 veces respecto a la administración de quercetina en solución).

En base a todos los resultados anteriores, se concluyó lo siguiente:

- Todas las nanopartículas diseñadas permitieron obtener incrementos significativos de biodisponibilidad oral de los distintos tipos de activos encapsulados.
- El empleo de altas presiones para la reticulación de nanopartículas de caseína no aportó ventajas respecto a la biodisponibilidad.
- Las nanopartículas de zeína demostraron mayor potencial que las NP de caseína para incrementar la biodisponibilidad de todos los tipos de activos encapsulados.
- Las NP mixtas de zeína y de caseina presentaron características físico químicas similares a las de las zeínas y biodisponibilidades relativas similares a las nanopartículas de caseína.

Finalmente, y en base a los citados resultados, se seleccionaron las formulaciones que permitieron obtener mayores incrementos en la biodisponibilidad relativa (Rsv-NP-Z y Que-HPCD-NP-Z) con objeto de evaluar su capacidad para potenciar el efecto antiinflamatorio de quercetina y resveratrol en un modelo animal de shock endotóxico producido por LPS.

Para ello se administraron previamente durante 1 semana las siguientes formulaciones: Resveratrol en solución y resveratrol encapsulado en nanopartículas de zeina, diariamente a dosis de 15 mg/kg; Quercetina en solución y quercetina encapsulada en nanopartículas de zeina conteniendo HP-β-CD a dosis de 25 mg/kg, siendo en este caso la pauta de administración de la solución diaria y la de la formulación encapsulada en nanopartículas cada dos días. Siete días después del tratamiento con los flavonoides se les inyectó a los ratones LPS induciéndoles shock endotóxico. La realización de dicho estudio permitió observar una mayor eficacia antiinflamatoria (en base a resultados de temperatura corporal, síntomas endotóxicos y nivel de TNF-α) de los grupos tratados con nanopartículas.Además, la eficacia fue significativamente mayor en el grupo pretratado con quercetina encapsulada en nanopartículas de zeína conteniendo HP-β-CD.

Todos estos resultados revelaron que los sistemas diseñados son adecuados y ofrecen un potencial elevado para incrementar la biodisponibilidad oral de diversos activos en el ámbito farmacéutico, nutracéutico y alimentario.

Perspectivas futuras

Dados los resultados obtenidos durante este trabajo, los posibles pasos para el futuro deberían ser los siguientes:

Escalado de las formulaciones.

Estas formulaciones han sido desarrolladas a escala de laboratorio. Los procesos de preparación empleados (coacervación, desolvatación, purificación y secado) son sencillos y emplean técnicas habitualmente utilizadas en el sector (farmacéutico, cosmético, nutracéutico y alimentario). Por este motivo se considera que deberían ser fácilmente preparadas a nivel industrial. Para ello, sería necesario realizar una fase previa de escalado que permita conocer los puntos críticos de la fabricación que deben ser controlados durante el proceso productivo para garantizar que las formulaciones resultantes de la preparación a gran escala mantienen las mismas propiedades y características fisicoquímicas que las partículas diseñadas originalmente. a

Evaluación de la estabilidad de las formulaciones en las condiciones que exige la regulación.

El objetivo de este ensayo residiría en el estudio de las características de las formulaciones en su envase final (parámetros fisicoquímicos, eficacias de encapsulación, parámetros macroscópicos, perfiles de liberación, etc) almacenadas a distintas condiciones (temperatura y humedad), a lo largo del tiempo, siguiendo las indicaciones establecidas en la guía ICH Q1A (R2): " "Stabilitytesting of new drugssubstances and prodrugs".

De este modo se podrían establecer las condiciones de almacenamiento más adecuadas para el producto final, así como su tiempo de vida útil.

Evaluación de la eficacia de las formulaciones en otros modelos animales.

Dado que los resultados de eficacia en el modelo animal de shock endotóxico inducido por LPS fueron positivos, sería interesante evaluar la eficacia de estas nanopartículas con quercetina y resveratrol encapsulado en otros modelos animales como por ejemplo en un modelo animal de alergia al cacahuete.

Ensayos clínicos y de intervención nutricional.

Referencias

[1] M. Fathi, Á Martín, D.J. McClements, Nanoencapsulation of food ingredients using carbohydrate based delivery systems, Trends Food Sci. Technol. 39 (2014) 18-39.

[2] M.A. Augustin, Y. Hemar, Nano-and micro-structured assemblies for encapsulation of food ingredients, Chem. Soc. Rev. 38 (2009) 902-912.

[3] L. Chen, G.E. Remondetto, M. Subirade, Food protein-based materials as nutraceutical delivery systems, Trends Food Sci. Technol. 17 (2006) 272-283.

[4] Z. Fang, B. Bhandari, Encapsulation of polyphenols – a review, Trends Food Sci. Technol. 21 (2010) 510-523.

[5] I.J. Joye, G. Davidov-Pardo, D.J. McClements, Nanotechnology for increased micronutrient bioavailability, Trends Food Sci. Technol. (2014).

[6] M.Z. Elsabee, E.S. Abdou, Chitosan based edible films and coatings: A review, Materials Science and Engineering: C 33 (2013) 1819-1841.

[7] N. Mati-Baouche, P. Elchinger, H. de Baynast, G. Pierre, C. Delattre, P. Michaud, Chitosan as an adhesive, European Polymer Journal 60 (2014) 198-212.

[8] S.A. Agnihotri, N.N. Mallikarjuna, T.M. Aminabhavi, Recent advances on chitosan-based micro- and nanoparticles in drug delivery, J. Controlled Release 100 (2004) 5-28.

[9] A. Matalanis, O.G. Jones, D.J. McClements, Structured biopolymer-based delivery systems for encapsulation, protection, and release of lipophilic compounds, Food Hydrocoll. 25 (2011) 1865-1880.

[10] A.O. Elzoghby, W.M. Samy, N.A. Elgindy, Protein-based nanocarriers as promising drug and gene delivery systems, J. Controlled Release 161 (2012) 38-49.

[11] A. Nesterenko, I. Alric, F. Violleau, F. Silvestre, V. Durrieu, The effect of vegetable protein modifications on the microencapsulation process, Food Hydrocoll. 41 (2014) 95-102.

[12] A.O. Elzoghby, W.S. Abo El-Fotoh, N.A. Elgindy, Casein-based formulations as promising controlled release drug delivery systems, J. Controlled Release 153 (2011) 206-216.

[13] A.M. Klibanov, Stabilization of enzymes against thermal inactivation, Adv. Appl. Microbiol. 29 (1983) 28.

[14] B. Ghanbarzadeh, M. Musavi, A.R. Oromiehie, K. Rezayi, E. Razmi Rad, J. Milani, Effect of plasticizing sugars on water vapor permeability, surface energy and microstructure properties of zein films, LWT - Food Science and Technology 40 (2007) 1191-1197.

[15] R. Shukla, M. Cheryan, Zein: the industrial protein from corn, Industrial Crops and Products 13 (2001) 171-192.

[16] R. Paliwal, S. Palakurthi, Zein in controlled drug delivery and tissue engineering, J. Controlled Release 189 (2014) 108-122.

[17] A.R. Patel, K.P. Velikov, Zein as a source of functional colloidal nano- and microstructures, Current Opinion in Colloid & Interface Science (2014) in press.

[18] R. Paliwal, S. Palakurthi, Zein in controlled drug delivery and tissue engineering, J. Controlled Release 189 (2014) 108-122.

[19] B. Wiman, P. Wallén, Structural Relationship between “Glutamic Acid” and “Lysine” Forms of Human Plasminogen and Their Interaction with the NH2-Terminal Activation Peptide as Studied by Affinity Chromatography, European Journal of Biochemistry 50 (1975) 489-494.

[20] J.M. Scholtz, H. Qian, V.H. Robbins, R.L. Baldwin, The energetics of ion-pair and hydrogen-bonding interactions in a helical peptide, Biochemistry (N. Y.) 32 (1993) 9668-9676.

[21] D.S. Horne, Casein Interactions: Casting Light on the Black Boxes, the Structure in Dairy Products, Int. Dairy J. 8 (1998) 171-177.

[22] R. Penalva, I. Esparza, M. Agüeros, C.J. Gonzalez-Navarro, C. Gonzalez-Ferrero, J.M. Irache, Casein nanoparticles as carriers for the oral delivery of folic acid, Food Hydrocolloids 44 (2015) 399–406.

[23] L. Chen, G.E. Remondetto, M. Subirade, Food protein-based materials as nutraceutical delivery systems, Trends Food Sci. Technol. 17 (2006) 272-283.

[24] M. Rossi, F. Cubadda, L. Dini, M.L. Terranova, F. Aureli, A. Sorbo, D. Passeri, Scientific basis of nanotechnology, implications for the food sector and future trends, Trends Food Sci. Technol. 40 (2014) 127-148.

[25] I.J. Joye, D.J. McClements, Biopolymer-based nanoparticles and microparticles: Fabrication, characterization, and application, Current Opinion in Colloid & Interface Science (2014).

[26] A. Amri, J.C. Chaumeil, S. Sfar, C. Charrueau, Administration of resveratrol: What formulation solutions to bioavailability limitations?, J. Controlled Release 158 (2012) 182-193.

[27] A.R. Patel, K.P. Velikov, Colloidal delivery systems in foods: A general comparison with oral drug delivery, LWT - Food Science and Technology 44 (2011) 1958-1964.

[28] I.A. Brouwer, M. van Dusseldorp, C.E. West, R.P. Steegers-Theunissen, Bioavailability and bioefficacy of folate and folic acid in man, Nutrition Research Reviews 14 (2001) 267-267.

[29] H. Heseker, Folic acid and other potential measures in the prevention of neural tube defects, Ann. Nutr. Metab. 59 (2011) 41-45.

[30] M.J. Akhtar, M.A. Khan, I. Ahmad, Photodegradation of folic acid in aqueous solution, J. Pharm. Biomed. Anal. 19 (1999) 269-275.

[31] M.K. Off, A.E. Steindal, A.C. Porojnicu, A. Juzeniene, A. Vorobey, A. Johnsson, J. Moan, Ultraviolet photodegradation of folic acid, Journal of Photochemistry and Photobiology B: Biology 80 (2005) 47-55.

[32] C. Lucas-Abellán, M.T. Mercader-Ros, M.P. Zafrilla, J.A. Gabaldón, E. Núñez-Delicado, Comparative study of different methods to measure antioxidant activity of resveratrol in the presence of cyclodextrins, Food and Chemical Toxicology 49 (2011) 1255-1260.

[33] F. Orallo, Comparative studies of the antioxidant effects of cis-and trans-resveratrol, Curr. Med. Chem. 13 (2006) 87-98.

[34] Alarcón de la Lastra, Catalina, I. Villegas, Resveratrol as an anti-inflammatory and anti-aging agent: Mechanisms and clinical implications, Molecular Nutrition & Food Research 49 (2005) 405-430.

[35] M. Athar, J.H. Back, X. Tang, K.H. Kim, L. Kopelovich, D.R. Bickers, A.L. Kim, Resveratrol: A review of preclinical studies for human cancer prevention, Toxicol. Appl. Pharmacol. 224 (2007) 274-283.

[36] F. Perez-Vizcaino, J. Duarte, R. Andriantsitohaina, Endothelial function and cardiovascular disease: effects of quercetin and wine polyphenols, Free Radic. Res. 40 (2006) 1054-1065.

[37] M. Comalada, D. Camuesco, S. Sierra, I. Ballester, J. Xaus, J. Gálvez, A. Zarzuelo, In vivo quercitrin anti-inflammatory effect involves release of quercetin, which inhibits inflammation through down-regulation of the NF-κB pathway, Eur. J. Immunol. 35 (2005) 584-592.

[38] F. Dajas, Life or death: neuroprotective and anticancer effects of quercetin, J. Ethnopharmacol. 143 (2012) 383-396.

[39] T. Walle, Absorption and metabolism of flavonoids, Free Radical Biology Medicine 36 (2004) 829-837.

[40] S. Scalia, M. Mezzena, Incorporation of quercetin in lipid microparticles: Effect on photo-and chemical-stability, J. Pharm. Biomed. Anal. 49 (2009) 90-94.

[41] S. Jose, S.S. Anju, T.A. Cinu, N.A. Aleykutty, S. Thomas, E.B. Souto, In vivo pharmacokinetics and biodistribution of resveratrol-loaded solid lipid nanoparticles for brain delivery, Int. J. Pharm. 474 (2014) 6-13.

[42] G. Singh, R.S. Pai, Trans-resveratrol self-nano-emulsifying drug delivery system (SNEDDS) with enhanced bioavailability potential: optimization, pharmacokinetics and in situ single pass intestinal perfusion (SPIP) studies, Drug Deliv. (2014) 1-9.

[43] M. Sessa, M.L. Balestrieri, G. Ferrari, L. Servillo, D. Castaldo, N. D'Onofrio, F. Donsì, R. Tsao, Bioavailability of encapsulated resveratrol into nanoemulsion-based delivery systems, Food Chem. 147 (2014) 42-50.

[44] C. Caddeo, M. Manconi, A.M. Fadda, F. Lai, S. Lampis, O. Diez-Sales, C. Sinico, Nanocarriers for antioxidant resveratrol: Formulation approach, vesicle self-assembly and stability evaluation, Colloids and Surfaces B: Biointerfaces 111 (2013) 327-332.

[45] H. Pool, D. Quintanar, J. de Dios Figueroa, J.E.H. Bechara, D.J. McClements, S. Mendoza, Polymeric nanoparticles as oral delivery systems for encapsulation and release of polyphenolic compounds: impact on quercetin antioxidant activity & bioaccessibility, Food Biophysics 7 (2012) 276-288.

[46] B. Zhang, Y. Luo, Q. Wang, Effect of acid and base treatments on structural, rheological, and antioxidant properties of α-zein, Food Chem. 124 (2011) 210-220.

[47] C. Holt, Structure and Stability of Bovine Casein Micelles, in: Structure and Stability of Bovine Casein MicellesAdvances in Protein Chemistry, Academic Press, 1992, pp. 63-151.

[48] D. Pandita, S. Kumar, N. Poonia, V. Lather, Solid lipid nanoparticles enhance oral bioavailability of resveratrol, a natural polyphenol, Food Res. Int. 62 (2014) 1165-1174.

[49] G. Singh, R.S. Pai, Optimized PLGA nanoparticle platform for orally dosed trans-resveratrol with enhanced bioavailability potential, Expert Opinion on Drug Delivery 11 (2014) 647-659.

[50] H. Li, X. Zhao, Y. Ma, G. Zhai, L. Li, H. Lou, Enhancement of gastrointestinal absorption of quercetin by solid lipid nanoparticles, J. Controlled Release 133 (2009) 238-244.

[51] A.J. Smith, P. Kavuru, L. Wojtas, M.J. Zaworotko, R.D. Shytle, Cocrystals of quercetin with improved solubility and oral bioavailability, Molecular Pharmaceutics 8 (2011) 1867-1876.

[52] M. Sun, Y. Gao, Y. Pei, C. Guo, H. Li, F. Cao, A. Yu, G. Zhai, Development of nanosuspension formulation for oral delivery of quercetin, Journal of Biomedical Nanotechnology 6 (2010) 325-332.

Chapter 10

Conclusions

Conclusiones

El desarrollo experimental recogido en este trabajo se basa en el diseño, evaluación y optimización de dos tipos de nanopartículas de origen natural (caseína y zeina) para incrementar la biodisponibilidad oral de tres activos (ácido fólico, resveratrol y quercetina) con potencial interés en los sectores farmacéutico y nutracéutico. Los resultados obtenidos en esta tesis doctoral nos han permitido concluir lo siguiente:

1.- Se diseñaron tres tipos de nanopartículas de caseína (C-NP, NP-C HP y NP-C-P_3) empleando un método de coacervación simple seguido de purificación y secado mediante spray-drying. El empleo de lisina en todos los casos permitió estabilizar las nanopartículas previniendo su agregación en suspensión.

a- Los estudios de biodistribución in vivo llevados a cabo tras la administración oral de las nanopartículas de caseína marcadas con Galio-67 demostraron que las nanopartículas permanecen en medio intestinal hasta 24 horas , no mostrando señal de translocación o absorción por otro órgano. Además, la visualización microscópica del intestino tras la administración de nanopartículas de caseína con lumogen encapsulado, relevó el carácter mucopenetrante de estas partículas, lo que explica su tiempo de permanencia en el medio intestinal.

b- Las nanopartículas de caseína permitieron encapsular ácido fólico como modelo de molécula hidrosoluble obteniendo cargas de hasta 30 µg de activo por mg de nanopartícula. Dichas nanopartículas protegieron al activo de su liberación en medio gástrico simulado, dando lugar a un marcado efecto burst tras la entrada en medio intestinal que liberó hasta un 80 % del ácido fólico. El estudio de farmacocinética llevado a cabo en ratas wistar a dosis de 1 mg/kg demostró incrementos de biodisponibilidad oral entre el 50 y el 53% para el ácido fólico encapsulado en nanopartículas de caseína comparado con su administración en solución acuosa. El empleo de altas presiones para la reticulación de nanopartículas de caseína no aportó ventajas respecto a la biodisponibilidad, ni a la cantidad de activo encapsulada.

c- Se encapsuló resveratrol como modelo de molécula liposoluble (clase II) en nanopartícuals de caseína, obteniendo cargas de hasta 30 µg por mg de nanopartícula. El perfil de liberación del activo desde las nanopartículas siguió una cinética de órden 0, siendo la erosión de la matriz lo que moduló la liberación del resveratrol. Del mismo modo, el estudio de farmacocinética oral a dosis de 15 mg/kg reveló que la biodisponilidad oral del activo es 10 veces superior cuando se administra encapsulado en nanopartículas que cuando es administrado disuelto en PEG 400:H_2O. Adicionalmente, se encontró una elevada correlación entre la cantidad de resveratrol liberada en el estudio “in vitro” y el porcentaje absorbido “in vivo”.

d- Se encapsuló quercetina como modelo de molécula liposoluble (clase IV) en nanopartículas de caseína. El uso de HP-β-CD en combinación con nanopartículas de caseína

permitió incrementar la cantidad de quercetina encapsulada en dichas naopartículas. El perfil de liberación in vitro de quercetina siguió una cinética de orden 0, siendo más lenta cuando la HP-β-CD se incorporó en la formulación. Asimismo, los estudios de farmacocinética, revelaron un incremento de la biodisponibilidad oral de quercetina encapsulada en nanopartículas de caseína de 9 veces respecto al activo en solución.

2.- Se diseñaron tres tipos de nanopartículas de zeína (Z-NP, M-NP y HPCD-Z-NP) empleando un método de desolvatación con agua seguido de purificación y secado mediante spray-drying. El empleo de lisina en ambos casos aportó una carga negativa a las nanopartículas resultantes, previniendo así los fenómenos de agregación durante la formación de las partículas y tras su secado.

a- Tras la administración por vía oral de nanopartículas de zeína marcadas con Iodo-125 a ratas wistar, se observó señal radioactiva a lo largo del tracto gastrointestinal durante 48 horas. A excepción del tiroides, donde el iodo tiene afinidad para acumularse, no se detectó ninguna señal en otros órganos, por lo que las nanopartículas de zeína no poseen capacidad para absorberse. Del mismo modo, la visualización microscópica del intestino tras la administración de las nanopartículas de zeína con lumogen rojo encapsulado, confirmó el carácter mucoadhesivo de estas formulaciones.

b- Tras la encapsulación de ácido fólico en nanopartículas de zeína se obtuvieron nanopartículas esféricas de 200 nm y potencial negativo. Dichas nanopartículas protegieron al activo de su liberación en medio gástrico simulado, dando lugar a un marcado efecto burst tras la entrada en medio intestinal, seguido de una liberación controlada hasta 24 horas. Los estudios de farmacocinética en rata Wistar macho, revelaron un incremento de la biodisponibilidad oral del ácido fólico de un 70% cuando éste fue administrado en nanopartículas de zeína, en comparación con el activo administrado en solución.

c- Se encapsuló resveratrol como modelo de molécula liposoluble (clase II) en dos tipos diferentes de nanopartículas: nanopartículas de zeina (NP-Z) y nanopartículas de zeina-caseina (NP-M). En ambos casos se obtuvieron partículas de tamaños en torno a 300 nm, con potencial negativo y cantidad de resveratrol encapsulado en torno a 80 µg por mg de nanopartícula. La liberación de resveratrol de estos sistemas en medio gástrico e intestinal simulado siguió una cinética mixta (Peppas-Sahlinmodel) entre erosión de la matriz y difusión del activo, llegando al 90% de liberación tras 48 horas de incubación. Tras la administración oral de estas formulaciones, se incrementó significativamente la biodisponibilidad oral del resveratrol (entre 10 y 19 veces) respecto a su administración en solución, siendo mayor el incremento correspondiente a las nanopartículas preparadas en ausencia de caseina.

d- Se encapsuló quercetina como modelo de molécula liposoluble (clase IV) en nanopartículas de zeína. El uso de HP-β-CD en combinación con nanopartículas de zeina,

permitió incrementar la cantidad de quercetina encapsulada en dichas naopartículas. La liberación de quercetina siguió una cinética de órden 0, siendo más lenta cuando la HP-β-CD se incorporó en la formulación. Del mismo modo, los estudios de farmacocinética revelaron un incremento de la biodisponibilidad oral de quercetina cercana a 14 veces tras su encapsulación en las nanopartículas de zeina.

e- Las formulaciones de quercetina y resveratrol que permitieron obtener mayor biodisponibilidad oral del activo, Rsv-NP-Z y Que-HPCD-NP-Z mostraron mayores efectos antiinflamatorios en un modelo de ratón de shock endotóxico inducido por LPS que los activos administrados en solución. Así, la administración previa de las formulaciones mejoró los síntomas endotóxicos tras la inyección de la toxina en comparación con la administración de los mismos flavonoides sin encapsular. Asimismo, los niveles de TNF-α fueron menores, siendo significativamente inferiores con la administración de quercetina encapsulada en nanopartículas de zeina combinada con HP-β-CD.

3.- Las nanopartículas de zeína demostraron mayor potencial para incrementar la biodisponibilidad oral de los activos encapsulados que las nanopartículas de caseína.

4.- La inclusión de HP-β-CD durante el proceso de encapsulación de los activos da lugar a nanopartículas capaces de aumentar significativamente la biodisponibilidad oral relativa de quercetina y resveratrol.

Chapter 11

Annex

Estudio de la eficacia de resveratrol encapsulado en nanopartículas de zeina (Rsv-NP-Z) en un modelo animal de alergia al cacahuete.

1- Material y métodos

Modelo animal (n=6);

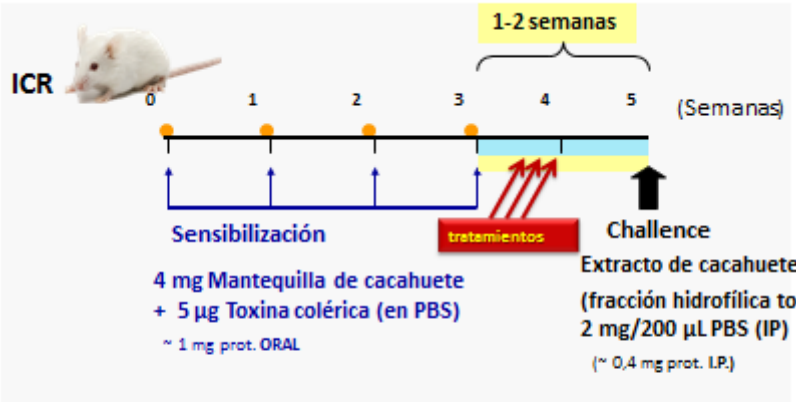

Determinación de
- **Citoquinas tras estimulación de sangre in vitro (Th1/Th2/Th17)**

en los tiempos: pre-tratamientos y pre-challenge

Tratamiento;

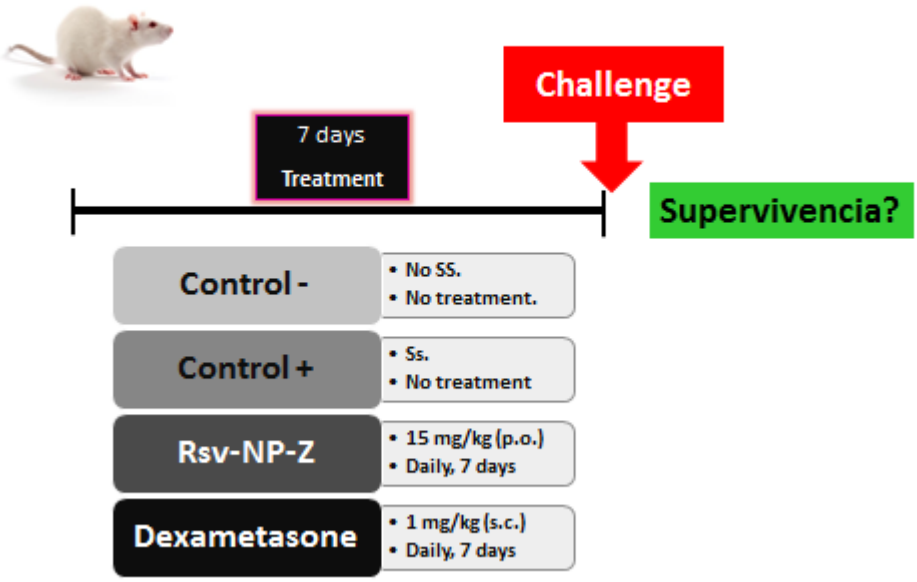

2- Resultados

Supervivenciadespuésdeldesafío

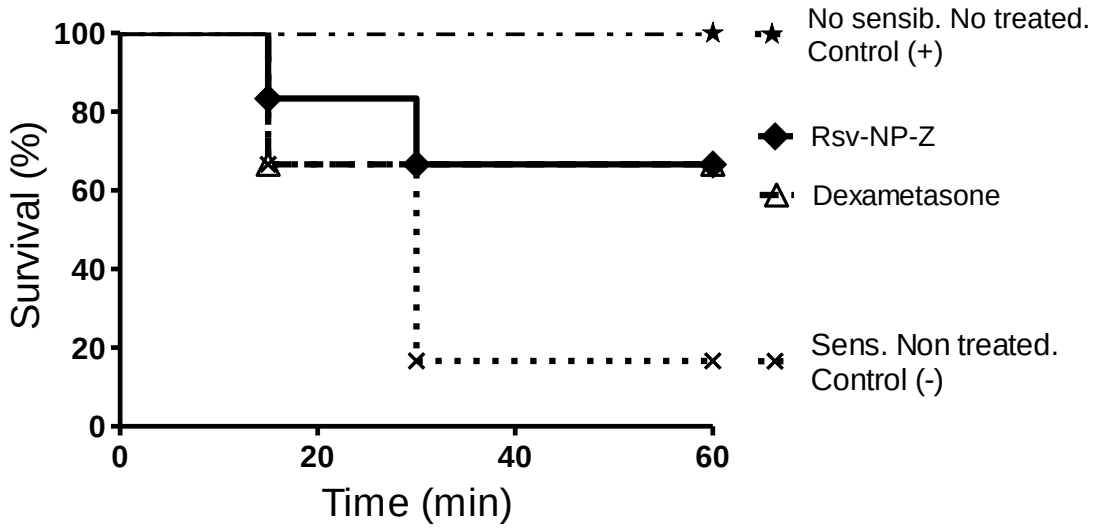

Cuantificación de citocinas

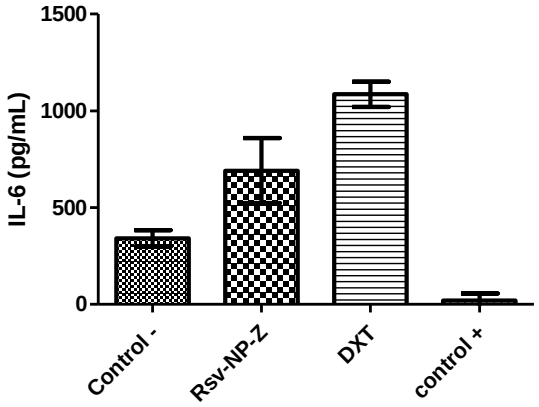

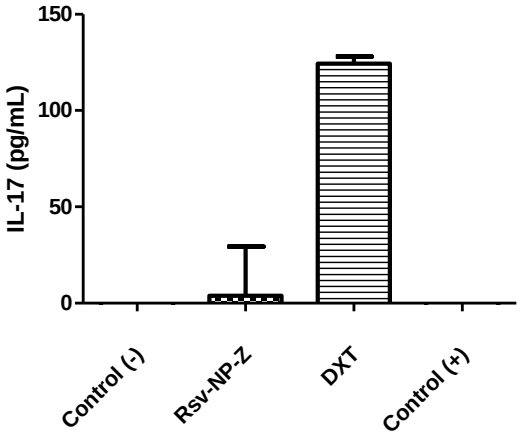

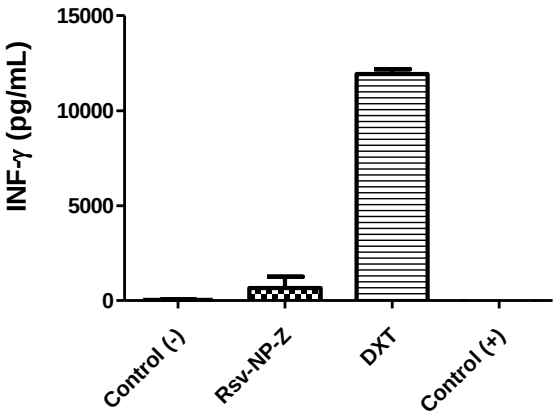

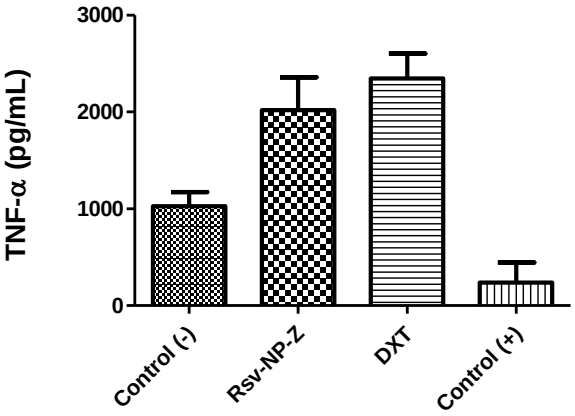

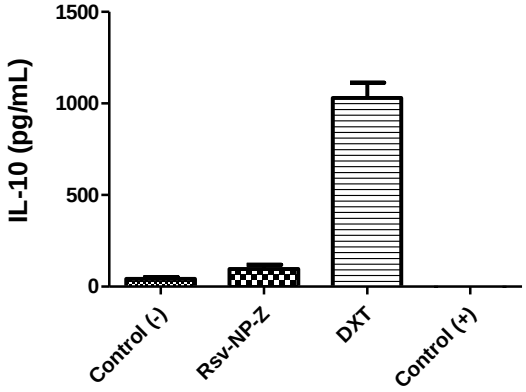

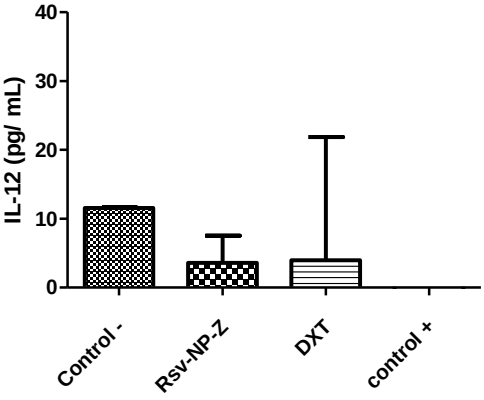

"La potencia intellectual de un hombre,
Se mide por la dosis de humor que es capaz de utilizar"

Friedrich Nietzsche